Advancing wildfire monitoring using multi-scale Earth observations

Morgan A. Crowley

Department of Natural Resource Sciences
Faculty of Agricultural and Environmental Sciences
McGill University
Montréal, Québec, Canada

January 2022

A thesis submitted to McGill University in partial fulfillment of the requirements of the degree of Doctor of Philosophy

Table of Contents

Abstract

As wildfire seasons become more extreme and less predictable across Canada and the world, satellite imagery and other Earth observations provide vital data for monitoring individual wildfires and supporting fire management decision-making. In this thesis, I explore multi-scale approaches and data sources used in landscape ecology and remote sensing research, apply data fusion methods to map wildfire progressions, and identify future opportunities for using Earth observations for wildfire monitoring. In the first research chapter of my thesis, I review and thematically analyze over 150 recently published manuscripts from the fields of remote sensing and landscape ecology to identify recent and future advances in the realm of multi-scale, multi-source ecological analyses. In the second chapter of my thesis, I create a prototype for mapping the fire progression of a single wildfire, Elephant Hill Fire, from the 2017 fire season in British Columbia. This prototype uses a Bayesian synthesis algorithm to fuse multi-sensor, multi-scale Earth observations on Google Earth Engine, a high-capacity and cloud-based processing platform. The third thesis chapter generates fire progression metrics from fused multi-source, multi-scale observations for all large fires from the 2017 fire season in British Columbia. This whole-fire-season study advances upon the previous chapter's fire progression mapping technique by integrating an object-based classification approach into the classification protocol. In the final chapter of my thesis, Chapter 4, I present a whole-systems conceptual framework to identify the data and information needs for all fire monitoring stages and analyze historical wildfire case studies. The ultimate target of this dissertation is to advance multi-source, multi-sensor, and multi-stage fire monitoring research by presenting novel data fusion methods, fire progression metric analyses, and conceptual framework development. The findings of this thesis

can be used to support wildland fire monitoring to improve our understanding of fires and fire seasons over space and time.

Résumé

Alors que les saisons des feux de forêt deviennent plus extrêmes et moins prévisibles au Canada et dans le monde, l'imagerie satellitaire et d'autres observations terrestres fournissent des données vitales pour surveiller les feux de forêt individuels et appuyer la prise de décision en matière de gestion des incendies. Dans cette thèse, j'explore les approches multi-échelles et les sources de données utilisées dans la recherche en écologie du paysage et en télédétection, j'applique des méthodes de fusion de données pour cartographier la progression des feux de forêt et j'identifie les futures opportunités d'utilisation des observations terrestres pour la surveillance des feux de forêt. Dans le premier chapitre de ma thèse, je passe en revue et analyse thématiquement plus de 150 manuscrits récemment publiés dans les domaines de la télédétection et de l'écologie du paysage, pour identifier les avancées récentes et futures dans le domaine des analyses écologiques multi-échelles et multi-sources. Dans le deuxième chapitre de ma thèse, je crée un prototype pour cartographier la progression du feu de forêt, Elephant Hill Fire, de la saison des incendies 2017 en Colombie-Britannique. Ce prototype utilise un algorithme de synthèse bayésien pour fusionner des observations terrestres multi-capteurs et multi-échelles sur Google Earth Engine, une plate-forme de traitement de grande capacité et basée sur le cloud. Le troisième chapitre de ma thèse génère des mesures de progression des incendies à partir d'observations multi-sources et multi-échelles fusionnées pour tous les grands incendies de la saison 2017 en Colombie-Britannique. Cette étude sur l'ensemble de la saison des feux de forêt fait avancer la technique de cartographie de la progression des incendies du chapitre précédent,

en intégrant une approche de classification basée sur les objets dans le protocole de classification. Dans le dernier chapitre de ma thèse, le chapitre 4, je présente un cadre conceptuel pour un système forestier complet identifiant les besoins en données et en informations à toutes les étapes de surveillance des incendies et pour analyser des études de cas historiques sur les incendies de forêt. L'objectif ultime de cette thèse est de faire avancer la recherche multi-sources, multi-capteurs et multi-étapes pour la surveillance des feux en présentant de nouvelles méthodes de fusion de données, d'analyses métriques de progression des incendies et le développement d'un cadre conceptuel. Les résultats de cette thèse peuvent être utilisés pour soutenir la surveillance des incendies forestiers afin d'améliorer notre compréhension des feux et des saisons des feux de forêt dans l'espace et le temps.

For my mom, for encouraging me to pursue what made me happy.

For my big sister, for modelling determination and achievement for me.

For my daughter, so you can determine and achieve your own happiness in life!

Acknowledgements

Since beginning my Ph.D. in September of 2017, I have grown not only as a scientist but also as a person. Many folks along the way have contributed to and supported my journey, most prominently my supervisor Dr. Jeffrey Cardille. It has been nearly ten years since I first approached you as an undergraduate student interested in your data-intensive research. Even though I had very little experience outside of my courses, you took the time to teach me valuable data-processing skills that initiated my geospatial and remote sensing curiosity. When I returned to Canada, you provided me with a new research opportunity that reignited my passion for Landsat-based research, exposed me to the novel Google Earth Engine platform, and rebuilt my self-confidence as a scientist. This Ph.D. would not have been possible without you seeing my potential and expanding my skill set (even when no one else would) and your continued support along the way through many life events. Thank you to Dr. Elena Bennett, who acted as a bonus-supervisor long before my Ph.D. when you connected me with Dr. Cardille way back in 2012. You have provided invaluable support and mentorship through the Bennett Lab, the MSSI Landscape Scholars program, and as a member of my Ph.D. committee. You have helped cultivate my interests in social-ecological systems and broad-scale synthesis. Thank you to my committee member and collaborator, Dr. Joanne White, for encouraging my excitement about forest monitoring using remote sensing through your innovative research, accessible mentorship, and inspiring feedback. Whenever I get stuck, mentally or data-wise, you always see the potential in my ideas and provide advice to help me dig out from my hole.

Thank you to my other collaborators. I look forward to continuing collaborations beyond my Ph.D. program, including folks from NRCan, Discoveries in Remote Sensing, the Google Earth Engine community, UBC Fire Discussion group and more. On the McGill campuses, thank you to the Bennett and Cardille Lab members, the MSSI Landscape Scholars and advisors, and the Macdonald Women+ in Science community members. My Ph.D. greatly benefitted from support from the Department of Natural Resource Sciences and the Graduate and Postdoctoral Studies offices through multiple GREAT and Graduate Mobility Awards, the Schulich Graduate Fellowship, and the Walter M. Stewart scholarship. Thank you for additional support for my degree from NSERC, NRCan, AGU, MDPI's Remote Sensing and Forests, and IALE-NA. Thank you also to the Ladies of Landsat and Sisters of SAR communities, especially Kate, Crista, Meghan, Flávia, Sheryl, and Gopika. Your mentorship, advice and friendships kept me going through it all, from my first conference to my comprehensive exams to becoming a mother in science. Thank you for teaching me how to believe in myself as a professional scientist!

Thank you to my family and friends. To my parents for supporting me through thick and thin. To my siblings and their families for making me laugh along the way. To my in-laws for cheerleading me throughout it all. To my Grammy and Boppa, who were two of the first people to inspire my inquiry and exploration and were also always the most excited by my academic and professional achievements. Thank you to all my friends and colleagues from UNH and McGill. To Athena, who always got me out of my head at the end of the day with her quirky, furry antics. To my daughter, Wiley, who has already taught me more in one year about myself and life than a thousand Ph.Ds. possibly could. Wiley, your joy and curiosity are incomparable! Lastly, to my pseudo-supervisor and 24/7 mentor, my husband Ian, who helped me see my own potential and provided advice at literally every stage of my program. Your love of science inspired me to pursue a Ph.D., and your support helped me actually stick with it. I would never have thought this Ph.D. was a possibility for me, but I am at the finish line because of the support from everyone around me.

List of Figures

List of Tables

Contribution to original knowledge

The four chapters in my dissertation contribute to original knowledge by addressing research gaps in landscape ecology, remote sensing, and fire science.

Chapter 2 identifies advances in the fields of Landscape Ecology and of Remote Sensing by synthesizing recently published papers that have integrated Earth observations into their research approaches. By reviewing recent advances in these fields, I identify future opportunities for multi-scale, multi-source Earth observations to support landscape ecology research. This work has been cited more than five times and accessed more than 3,000 times since its publication in *Current Landscape Ecology Reports* in June 2020.

Chapter 3 presents a prototype for mapping one fire's progression, using a multi-scale synthesis that draws upon the recent advances in landscape ecology and remote sensing presented in Chapter 2. Since its publication in *Remote Sensing Letters* in 2019, Chapter 3 is in the top 10 most read articles on the journal's webpage, and has been frequently cited over 19 times and accessed over 3,500 times by others in the field of remote sensing.

Chapter 4 builds upon Chapter 3's prototype by integrating object-based image analysis into the classification approach, applying the prototype methods to an entire fire season, and deriving and analyzing fire and fire season progression metrics. Published in remote sensing's top-rated journal, *Remote Sensing of Environment,* Chapter 4 has been frequently cited over 11 times since 2019. By creating novel classification and data-fusion methods to refine burned-area mapping in Chapters 3 and 4, my work improves upon previous methods vulnerable to atmospheric noise, production delays, observation gaps, and coarse spatial resolution. These research articles advance the fields of remote sensing and fire monitoring by implementing highly systematic methods for synthesizing data from multiple sources to improve near-term fire disturbance monitoring.

In Chapter 5, I present a conceptual framework to identify information needs and objectives for fire monitoring. Pre-fire inventorying, active fire monitoring, and post-fire impact assessments occur in stages, which are distinct subdomains and even overseen by different agencies. But when different stages of fire monitoring are considered independently from one another, there is potential for mismatches in objectives and data needs to create research gaps and decision-making limitations. I contribute a method for harmonizing these various objectives and data needs through this whole-system fire monitoring framework. This research results from multiple conversations with fire monitoring experts from across Canada and the USA. As such, it has benefitted from diverse coauthorship and collaborative feedback, making it an important contribution to remote sensing and fire science.

In addition to the formal contribution to original knowledge represented by publication of thesis chapters, the impact of my work has expanded well beyond the academic realm in several ways. I have spoken about my research on the Scene from Above and Down to Earth podcasts and as a guest contributor on CBC Radio Noon in Montreal. My research has been featured in seven news articles in both French and English publications like *La Terre de Chez Nous* and *CScience IA*. In 2019, my research was highlighted by Dr. Rebecca Moore's keynote talk at the Geo for Good summit. As a result of my doctoral research contributions, I was recognized as one of Geospatial World's 50 Rising Stars in 2021 and one of Radiant Earth Foundation's Women Leading the Machine-Learning for Earth Observations (ML4EO) community.

Contribution of authors

My thesis has been prepared in manuscript format and contains four chapters authored by myself, the candidate. Three chapters have been published, and one is in preparation to be submitted for publication, each of which has benefitted from the perspectives and feedback of coauthors. The following describes the contributions to each chapter from all coauthors:

Chapter 2 was published in *Current Landscape Ecology Reports* in collaboration with my supervisor, Dr. Jeffrey Cardille. As lead author I designed and organized the literature review, led the writing of the manuscript, drafted all figures, and spearheaded the publication revision process. Dr. Cardille provided feedback on the review themes, reviewed the findings, and provided revisions to the text and figures.

Chapter 3 was published in *Remote Sensing Letters* in collaboration with Drs. Joanne White and Michael Wulder of the Canadian Forest Service and my supervisor Dr. Cardille. As the lead author, I designed the prototype, carried out the data processing and analysis, drafted the initial text and figures, and led the publication revision process. Drs. Cardille, White and Wulder all contributed to the foundational knowledge of the study, discussed the findings, and provided feedback and revisions to the text and figures.

Chapter 4 was published in the Google Earth Engine special issue in Remote Sensing of Environment in collaboration with Dr. Jeffrey Cardille, and Drs. Joanne White and Michael Wulder of the Canadian Forest Service. As the lead author, I designed the study, carried out the data processing and analysis, drafted the initial text and figures, and led the publication revision process. Drs. Cardille, White and Wulder all contributed to the foundational knowledge of the study, discussed the findings, and provided feedback and revisions to the text and figures.

Chapter 5 is in preparation to submit for publication in collaboration with Drs. Christopher Stockdale, Joanne White, Joshua Johnston, Michael Wulder, Jeffrey Cardille, Jesse Rieb, Jessica McCarty, and Tianjia Liu. The first draft of the conceptual framework and case studies came out of initial discussions between 2019 and 2020 between me and Dr. Stockdale. As the lead author, I developed the whole-systems framework concept and drafted the initial manuscript and figures. Dr. White provided feedback on the initial and most recent framework and case studies, and all other coauthors provided feedback on the manuscript text and figures. Dr. Rieb will help design and draft the final versions of the figures for manuscript submission. I will continue to integrate coauthor feedback and lead the submission and revision process of the manuscript in 2022.

1. Introduction

In the past 40 years, fire incidence, size, and severity have been changing due to longer fire seasons, increasing fuel loads, and changing climate (Jolly et al., 2015; National Academies of Sciences, Engineering, and Medicine et al., 2017; Price et al., 2015). The increasing occurrences of extreme wildfires have regional and global implications (Jolly et al., 2015), including changes in critical ecosystem services delivered by these forests, including decreases in timber supply, wildlife habitat, carbon storage, and air quality, all of which have detrimental effects on human health and well-being (Fiore et al., 2015; Reid et al., 2016; Rittmaster et al., 2006; Thom and Seidl, 2016). “Self-regulating” fire regimes that were previously moderated only by fire history and ecozone attributes are becoming more severe due to increasing fuel loads from invading forest diseases/pests and changing human activities (Agee, 1999; Collins et al., 2009; Flannigan et al., 2000; Hanes et al., 2019; McKenzie et al., 2011; Parisien et al., 2014; Parks et al., 2016, 2015, 2014; Peterson, 2002). These altered, severe fire regimes create a perpetuating global system, where more extreme fire seasons impact climate by disturbing global carbon cycles, further exacerbating subsequent years’ fire seasons due to increasing climatic variability and global warming (Flannigan et al., 2000).

In Canada, lengthening fire seasons and changing fuel loads have resulted in more extreme fire seasons and active fire regimes with increasingly frequent burn intervals (Flannigan et al., 2005; Hanes et al., 2019; Wang et al., 2015). The annual burned area in Canada is predicted to escalate due to increasing severities, sizes of individual fires, and lightning ignition sources (Flannigan et al., 2005; Hanes et al., 2019; Wang et al., 2015), in contrast with decreasing global burned area trends (Andela et al., 2017; Arora and Melton, 2018). For example, in British Columbia (BC), the largest fire seasons in the province’s history with respect to area burned occurred in 2017 and 2018, each with more than a million hectares of burned area (BC Wildfire Service, 2017). After the 2017 extreme fire season, the BC government issued a report describing that fire season as “the new normal” for wildfire conditions and vulnerability for future fire seasons within the province (Abbott and Chapman, 2018). BC government officials called for increasing real-time, near-term and consistent mapping approaches to aid in wildfire planning and response (Abbott and Chapman, 2018), underscoring a need for systematic fire monitoring efforts using remote sensing technologies (Bowman, 2018).

As the need for innovative fire monitoring approaches increases, the field of remote sensing is making significant technological advances with increased accessibility of cloud-based and cyberinfrastructure platforms that have large processing and storage, such as those from Google, Microsoft, Amazon, ESRI and more. One such platform, Google Earth Engine, stores data from multiple sources and provides a programming interface for remote-sensing analysis (Gorelick et al., 2017). Fire monitoring datasets with large spatial and fine temporal scales are made even more attainable using the plethora of freely available data and advanced remote sensing algorithms offered by Google Earth Engine. Previously, the accessibility and availability of imagery were such that fine-scale near-real-time monitoring of fires was impractical due to high financial costs, large processing requirements and sparse frequencies of observations.

In this thesis, I build upon the recent developments made in the field of Earth observation science for cloud-based processing platforms and high-quality, open-access data sources to advance the mapping and analysis of fire progressions in Canada. I develop and apply a novel approach for reconstructing detailed fire progressions over large areas using observations from multiple sources in Google Earth Engine. I demonstrate how combining observations from multiple sensors can be used to map fire growth progressions for actively burning fires to inform managers and planners interested in fire risk, spread, and impact.

1.1 Thesis objectives

My thesis aims to analyze how fire monitoring using Earth observations can be advanced using multi-sensor, multi-scale, open-access data, and cloud-based processing platforms. The specific objectives for each of my four research chapters are:

- **Chapter 2:** Review recent theoretical and methodological contributions of remote sensing to landscape ecology and identify future opportunities for advances using Earth observations.
- **Chapter 3:** Create a classification approach and prototype for constructing fire progression maps using a Bayesian data-fusion algorithm in Google Earth Engine applied on a single, large 2017 fire in British Columbia.
- **Chapter 4:** Analyze fire characteristics of all stand-replacing 2017 fires in British Columbia using newly generated fire progression metrics derived from integrating object-based image analysis into the fire mapping methods from Chapter 3.
- **Chapter 5:** Conceptualize a whole-systems framework for identifying and synthesizing information needs and objectives for fire monitoring.

1.2 Literature review

1.2.1 Remote sensing of forests

Satellite remote sensing platforms provide landscape-level views of forest structure for observation, measurement, and inventory (Iverson et al., 1989; Lu, 2006; McRoberts and

Tomppo, 2007). Launched in 1972 by the National Aeronautics and Space Administration (NASA), the Earth Resources Technological Satellite (ERTS-1, later renamed Landsat-1) was the first imaging satellite to focus on analyzing Earth's resources (Boyd and Danson, 2005). At present, there is a growing constellation of imaging satellites orbiting the world, whether privately funded (e.g., PLANET Dove microsatellites, DigitalGlobe's WorldView-3) or publicly funded (e.g., NASA's Landsat program, the European Space Agency's Copernicus mission). Satellite-mounted sensors provide standardized measurements and observations of the earth's surface and different sensors collect observations with varying spatial, temporal, spectral, and radiometric resolutions (Boyd and Danson, 2005; Danson et al., 1995; Marceau et al., 1994). Once transmitted to Earth, satellite images undergo post-processing such as orbital, atmospheric, and orthorectification corrections (Hall et al., 1995). The repeated coverage provided by satellites enables large-scale Earth observations, readily available, cost-effective, and easier to post-process than imagery from earth-based imaging platforms (Lefsky et al., 2001). Each pixel corresponds with the absorption and transmission values of the objects imaged, such as vegetation type, structure, and health (Wulder, 1998). Changes in incoming solar radiation absorbed by forest vegetation are most prominently imaged in the near-infrared (NIR) band, but also can be measured using the visible red, middle infrared (MIR), and short-wave infrared (SWIR) wavelengths (Asner and Warner, 2003; Boyd and Danson, 2005; Chen et al., 2018; Steininger, 2000).

Empirical and correlative approaches between satellite imagery and ground-based measurements help identify forest structural features and changes, such as biomass, canopy cover, height, density etc. (Boyd and Danson, 2005; Cohen et al., 2001, 1995; Danson et al., 1995; Franklin et al., 2001; Luther et al., 2006; Nelson et al., 2002; Scarth et al., 2001; Wulder, 1998; Wulder et al., 2004). Spectral vegetation indices (e.g., normalized differenced vegetation index) accentuate spectral features which can be used to estimate features like leaf-area index, forest volume/basal area, and photosynthetic activities (Boyd and Danson, 2005; Cohen et al., 2001, 1995; Cohen and Goward, 2004; Curran, 1980; Danson et al., 1995; Eklundh et al., 2001; Gamon et al., 1995; Healey et al., 2006; Horler and Ahern, 1986; Li and Strahler, 1985; Wulder, 1998). High and very high spectral and spatial resolution satellite imagery can be used to identify fine-scale features such as tree crowns, ages, and ecosystem productivity (Franklin et al., 2001; Kayitakire et al., 2006; Martin and Aber, 1997; Palace et al., 2008; Wulder, 1998). Multi-temporal satellite imagery analyses are used to identify forest structure changes over time (Asner et al., 2000; Frolking et al., 2009; Garcia Millan and Sanchez-Azofeifa, 2018; Lefsky et al., 2001).

1.2.2 Canadian forest fires

Wildland fires are a primary driver of ecosystem services in the boreal regions of Canada (Pausas and Keeley, 2019; Pohjanmies et al., 2017). Often a result of natural causes like lightning, boreal forest fires are a vital ecological process that clear open space in forests, help control pest outbreaks and regulate extreme fires, all while supporting tree species succession and structural changes (Helbig et al., 2016; Pausas and Keeley, 2019). Historical fire regimes vary across boreal and taiga regions in the world. In North America, the fire regime is dominated by fewer but larger (>200 ha) high-intensity crown fires with a mean fire return interval of ~180 years (de Groot et al., 2013a, 2013b). Despite historical efforts to suppress all fire in some boreal regions like Canada, fire management has changed over time to balance natural regime fire processes with protecting human lives, infrastructure, and commodity production (Stocks et al., 2002). However, due to a changing climate, boreal forest fire regimes are becoming less predictable over time and are projected to continue to transform in the future (de Groot et al., 2013b; Stocks et al., 1998).

There are a multitude of drivers that impact Canadian boreal fires from the combustion of individual fires to overall fire season behaviours. Fire ignition is a product of a source, oxygen availability, and fuel load availability and flammability (Aldersley et al., 2011; Gralewicz et al., 2012b; Huang and Rein, 2016; Malamud et al., 2005; Morgan et al., 2001; Prestemon et al., 2013). Once ignited, a wildfire's intensity and spread in space and time is influenced by social and biophysical drivers like weather, fuel vegetation, and topography that influence conditions like fuel loads, fuel flammability and fuel continuity (Aldersley et al., 2011; Bessie and Johnson, 1995; Coughlan et al., 2018; Flannigan et al., 2005; Flannigan and Harrington, 1988; Gralewicz et al., 2012a; L. M. Johnston et al., 2020; Parisien et al., 2014; Remy et al., 2017; Romme, 1982; Turner and Romme, 1994). Drivers that affect fuel load availability include forest and vegetative conditions such as structure, age, type, species diversity, and management practices (Aldersley et al., 2011; Prestemon et al., 2013). Fuel flammability is caused by weather drivers such as daily rainfall, temperature, relative humidity, and climatic variables like drought (Aldersley et al., 2011; Meyn et al., 2007). Fuel loads and flammability together influence a fire's intensity, and the continued availability of flammable fuel primarily impacts fire spread and behaviour (Aldersley et al., 2011). Biophysical drivers like topography, wind speed and direction, and land cover pattern direct the fire to continue burning new and flammable fuel loads (Aldersley et al., 2011; Prestemon et al., 2013). Boreal fire regimes and fire seasons are becoming more variable and unpredictable due to the impacts of climate change and fire suppression on these drivers that influence fire combustion and behaviour (Gralewicz et al., 2012a; McCarty et al., 2021; Parks et al., 2012). As these drivers continue to be impacted by climate change, so do the ignition conditions and behaviours of individual fires, fire seasons, and long-term fire regimes.

1.2.3 Forest fire monitoring and change assessment using remote sensing data

To monitor conditions and changes across millions of square kilometers of fire-prone landscapes in Canada and the United States, agencies often rely on Earth observation data (Chuvieco et al., 2020, 2019; Giglio et al., 2018; J. M. Johnston et al., 2020; O'Connor, 2021; Schroeder et al., 2008; Wooster et al., 2021). Pre-fire conditions, including fuel load and vegetation type mapping, are primarily derived from optical sensors (e.g., Landsat, Sentinel-2, MODIS) and are available in monthly or annual data layers (Chuvieco et al., 2020; Gale et al., 2021). Once a fire occurs, satellite systems like GOES, VIIRS, MODIS and SLSTR provide large-area imagery with a moderate spatial resolution (375m to 2km) and sub-daily collection rates, beneficial for detecting ignitions across large regions (Roy et al., 2005). Fire impact assessments often rely on premade fire monitoring datasets readily available for monitoring global fire locations, extents, and progressions (Andela et al., 2019; Chuvieco et al., 2016; Giglio et al., 2016; Humber et al., 2018). Other research evaluates multi-scale components of fires and their impacts, such as a landscape's wildland fire risk or a fire's burn severity with spectral indices like the differenced normalized burn ratio (dNBR). These studies often integrate ground-based ecological data with remote sensing data to account for landscape changes due to fire impact (Bernier et al., 2016; L. M. Johnston et al., 2020; Parks et al., 2018, 2015; Whitman et al., 2018). Fire severity, for example, can be mapped from satellite-based imagery by estimating organic matter change using spectral indices after a fire has passed through to describe how that fire impacted the ecosystem where it occurred (Keeley, 2009; Parks et al., 2018, 2015; Whitman et al., 2018).

Remote-sensing derived fire datasets are used to reconstruct fire progressions and final burned areas because of their large-scale coverage and open-access availability. There are multiple datasets and mapping protocols available for monitoring fire occurrence and progressions in Canada, in particular. The National Burned Area Composite (NBAC) dataset identifies refined fire perimeters with unburned islands and water bodies removed from multiple sources, including the jurisdictionally produced Canadian National Fire Database (CNFDB) and satellite imagery from Landsat (Amiro et al., 2001; Burton et al., 2009; de Groot et al., 2007; Fraser et al., 2004; Parisien et al., 2006; Stinson et al., 2011; Stocks et al., 2002). The Composite-to-Change (C2C) protocol automates the monitoring and inventorying of forest disturbances like burned areas using the annual proxy best-available pixel (BAP) for the 30m Landsat record (Hermosilla et al., 2017, 2016; White et al., 2017, 2014). Satellite imagery from AVHRR, MODIS, and VIIRS is used by the Canadian Forest Service in the Fire Monitoring, Mapping and Modeling daily hotspot map used by fire agencies across Canada (Fraser et al., 2000). Additional spatial interpolation and data fusion methods have been used to downscale and refine MODIS active fire and burned area datasets with additional sources such as Landsat and Sentinel-2 (Crowley et al., 2019a, 2019b; de Groot et al., 2009, 2007; Hilker et al., 2009a, 2009b; Parks, 2014; Parks et al., 2012).

1.2.4 Advances in remote sensing

There have been major advances made in cloud-based computing in the last ten years that support large-scale ecological monitoring. For example, the development of the Google Earth

Engine (GEE) platform (https://earthengine.google.com) makes multi-temporal and large-scale analyses more feasible for the global land change research community (Hansen et al., 2013). GEE is a cloud-based platform used to access, process, and analyze satellite imagery and geospatial data at a global scale (Gorelick et al., 2017). In GEE, users can apply their algorithms to a multi-petabyte catalogue of open-access data on Google servers using parallel processing to increase processing time (Gorelick et al., 2017; Hansen and Loveland, 2012). Using a freely available platform for processing and classification of open-access imagery reduces computing costs, while dataset creation speeds can dramatically increase for disaster response (Hansen and Loveland, 2012).

Fusing Earth observations from multiple satellite sources further advances the possibility of monitoring near-real-time fire progressions (Li and Roy, 2017; Wulder et al., 2018). Recent developments suggest that information from multiple satellites can be combined at an increased temporal resolution for retrospective mapping and estimating fire growth while the fire is still active (Crowley et al., 2019a, 2019b). The Bayesian Updating of Land Cover (BULC) algorithm, for example, synthesizes classifications of individual images through time by weighing evidence from multiple classifications to produce a time series of land undergoing rapid change (Cardille et al., 2022; Cardille and Fortin, 2016; Crowley et al., 2019a, 2019b; Deines et al., 2019; Fortin et al., 2020; Lee et al., 2020, 2018). Data fusion algorithms like BULC combine complementary strengths of multiple data streams to map fire progressions retrospectively and eventually map fire progressions in near-real-time (Boschetti et al., 2015; Hilker et al., 2009a, 2009b; Korhonen et al., 2017; Mora et al., 2013; Roy et al., 2014; Wulder et al., 2010).

1.3 References

Abbott, G., Chapman, M., 2018. Addressing the new normal: 21st century disaster management in British Columbia. British Columbia Government.

Agee, J.K., 1999. Fire effects on landscape fragmentation in interior west forests. Forest fragmentation: wildlife and management implications. (Eds JA Rochelle, LA Lehmann, J Wisniewski) pp 43–60.

Aldersley, A., Murray, S.J., Cornell, S.E., 2011. Global and regional analysis of climate and human drivers of wildfire. Sci. Total Environ. 409, 3472–3481.

Amiro, B.D., Todd, J.B., Wotton, B.M., Logan, K.A., Flannigan, M.D., Stocks, B.J., Mason, J.A., Martell, D.L., Hirsch, K.G., 2001. Direct carbon emissions from Canadian forest fires, 1959-1999. Can. J. For. Res. 31, 512–525.

Andela, N., Morton, D.C., Giglio, L., Chen, Y., van der Werf, G.R., Kasibhatla, P.S., DeFries, R.S., Collatz, G.J., Hantson, S., Kloster, S., Bachelet, D., Forrest, M., Lasslop, G., Li, F., Mangeon, S., Melton, J.R., Yue, C., Randerson, J.T., 2017. A human-driven decline in global burned area. Science 356, 1356–1362.

Andela, N., Morton, D.C., Giglio, L., Paugam, R., Chen, Y., Hantson, S., van der Werf, G.R., Randerson, J.T., 2019. The Global Fire Atlas of individual fire size, duration, speed and direction. Earth Syst. Sci. Data 11, 529–552.

Arora, V.K., Melton, J.R., 2018. Reduction in global area burned and wildfire emissions since 1930s enhances carbon uptake by land. Nat. Commun. 9, 1326.

Asner, G.P., Townsend, A.R., Braswell, B.H., 2000. Satellite observation of El Niño effects on Amazon Forest phenology and productivity. Geophys. Res. Lett. 27, 981–984.

Asner, G.P., Warner, A.S., 2003. Canopy shadow in IKONOS satellite observations of tropical forests and savannas. Remote Sens. Environ. 87, 521–533.

BC Wildfire Service, 2017. Remembering 2017: Looking back a year later at the start of the 2017 wildfire season for the Cariboo Fire Centre [WWW Document]. Province of British Columbia. URL https://www2.gov.bc.ca/gov/content/safety/wildfire-status/about-bcws/wildfire-history/remembering-2017 (accessed 2.15.19).

Bernier, P.Y., Gauthier, S., Jean, P.-O., Manka, F., Boulanger, Y., Beaudoin, A., Guindon, L., 2016. Mapping Local Effects of Forest Properties on Fire Risk across Canada. For. Trees Livelihoods 7, 157.

Bessie, W.C., Johnson, E.A., 1995. The Relative Importance of Fuels and Weather on Fire Behavior in Subalpine Forests. Ecology 76, 747–762.

Boschetti, L., Roy, D.P., Justice, C.O., Humber, M.L., 2015. MODIS–Landsat fusion for large area 30m burned area mapping. Remote Sens. Environ. 161, 27–42.

Bowman, D., 2018. Wildfire science is at a loss for comprehensive data. Nature.

Boyd, D.S., Danson, F.M., 2005. Satellite remote sensing of forest resources: three decades of research development. Progress in Physical Geography: Earth and Environment. https://doi.org/10.1191/0309133305pp432ra

Burton, P.J., Parisien, M.-A., Hicke, J.A., Hall, R.J., Freeburn, J.T., 2009. Large fires as agents of ecological diversity in the North American boreal forest. Int. J. Wildland Fire 17, 754–767.

Cardille, J.A., Fortin, J.A., 2016. Bayesian updating of land-cover estimates in a data-rich environment. Remote Sens. Environ. 186, 234–249.

Cardille, J.A., Perez, E., Crowley, M.A., Wulder, M.A., White, J.C., Hermosilla, T., 2022. Multi-sensor change detection for within-year capture and labelling of forest disturbance. Remote

Sensing of Environment. https://doi.org/10.1016/j.rse.2021.112741

Chen, Y., Li, L., Lu, D., Li, D., 2018. Exploring Bamboo Forest Aboveground Biomass Estimation Using Sentinel-2 Data. Remote Sensing 11, 7.

Chuvieco, E., Aguado, I., Salas, J., García, M., Yebra, M., Oliva, P., 2020. Satellite Remote Sensing Contributions to Wildland Fire Science and Management. Current Forestry Reports 6, 81–96.

Chuvieco, E., Mouillot, F., van der Werf, G.R., San Miguel, J., Tanasse, M., Koutsias, N., García, M., Yebra, M., Padilla, M., Gitas, I., Heil, A., Hawbaker, T.J., Giglio, L., 2019. Historical background and current developments for mapping burned area from satellite Earth observation. Remote Sens. Environ. 225, 45–64.

Chuvieco, E., Yue, C., Heil, A., Mouillot, F., Alonso-Canas, I., Padilla, M., Pereira, J.M., Oom, D., Tansey, K., 2016. A new global burned area product for climate assessment of fire impacts. Glob. Ecol. Biogeogr. 25, 619–629.

Cohen, W.B., Goward, S.N., 2004. Landsat's Role in Ecological Applications of Remote Sensing. Bioscience 54, 535–545.

Cohen, W.B., Maiersperger, T.K., Spies, T.A., Oetter, D.R., 2001. Modelling forest cover attributes as continuous variables in a regional context with Thematic Mapper data. Int. J. Remote Sens. 22, 2279–2310.

Cohen, W.B., Spies, T.A., Fiorella, M., 1995. Estimating the age and structure of forests in a multi-ownership landscape of western Oregon, U.S.A. Int. J. Remote Sens. 16, 721–746.

Collins, B.M., Miller, J.D., Thode, A.E., Kelly, M., van Wagtendonk, J.W., Stephens, S.L., 2009. Interactions Among Wildland Fires in a Long-Established Sierra Nevada Natural Fire Area. Ecosystems 12, 114–128.

Coughlan, M.R., Magi, B.I., Derr, K.M., 2018. A Global Analysis of Hunter-Gatherers, Broadcast Fire Use, and Lightning-Fire-Prone Landscapes. Fire 1, 41.

Crowley, M.A., Cardille, J.A., White, J.C., Wulder, M.A., 2019a. Large-area synthesis of multiple remotely sensed data sources for mapping within-year wildfire progression. Remote Sens. Environ.

Crowley, M.A., Cardille, J.A., White, J.C., Wulder, M.A., 2019b. Multi-sensor, multi-scale, Bayesian data synthesis for mapping within-year wildfire progression. Remote Sens. Lett. 10, 302–311.

Curran, P., 1980. Multispectral remote sensing of vegetation amount. Progress in Physical Geography: Earth and Environment 4, 315–341.

Danson, F.M., Plummer, S.E., Briggs, S.A., 1995. Remote sensing and the information extraction problem.

de Groot, W.J., Cantin, A.S., Flannigan, Soja, A.J., Gowman, L.M., Newbery, A., 2013a. A comparison of Canadian and Russian boreal forest fire regimes. For. Ecol. Manage. 294, 23–34.

de Groot, W.J., Flannigan, Cantin, A.S., 2013b. Climate change impacts on future boreal fire regimes. For. Ecol. Manage. 294, 35–44.

de Groot, W.J., Landry, R., Kurz, W.A., Anderson, K.R., Englefield, P., Fraser, R.H., Hall, R.J., Banfield, E., Raymond, D.A., Decker, V., Others, 2007. Estimating direct carbon emissions from Canadian wildland fires. Int. J. Wildland Fire 16, 593–606.

de Groot, W.J., Pritchard, J.M., Lynham, T.J., 2009. Forest floor fuel consumption and carbon emissions in Canadian boreal forest fires. Can. J. For. Res. 39, 367–382.

Deines, J.M., Kendall, A.D., Crowley, M.A., Rapp, J., Cardille, J.A., Hyndman, D.W., 2019.

Mapping three decades of irrigation across the US High Plains Aquifer with Landsat. Remote Sensing of Environment 233, 111400.

Eklundh, L., Harrie, L., Kuusk, A., 2001. Investigating relationships between Landsat ETM+ sensor data and leaf area index in a boreal conifer forest. Remote Sens. Environ. 78, 239–251.

Fiore, A.M., Naik, V., Leibensperger, E.M., 2015. Air quality and climate connections. J. Air Waste Manag. Assoc. 65, 645–685.

Flannigan, M.D., Harrington, J.B., 1988. A Study of the Relation of Meteorological Variables to Monthly Provincial Area Burned by Wildfire in Canada (1953–80). J. Appl. Meteorol. 27, 441–452.

Flannigan, M.D., Logan, K.A., Amiro, B.D., Skinner, W.R., Stocks, B.J., 2005. Future Area Burned in Canada. Clim. Change 72, 1–16.

Flannigan, M.D., Stocks, B.J., Wotton, B.M., 2000. Climate change and forest fires. Sci. Total Environ. 262, 221–229.

Fortin, J.A., Cardille, J.A., Perez, E., 2020. Multi-sensor detection of forest-cover change across 45 years in Mato Grosso, Brazil. Remote Sensing of Environment. https://doi.org/10.1016/j.rse.2019.111266

Franklin, S.E., Wulder, M.A., Gerylo, G.R., 2001. Texture analysis of IKONOS panchromatic data for Douglas-fir forest age class separability in British Columbia. Int. J. Remote Sens. 22, 2627–2632.

Fraser, R.H., Hall, R.J., Landry, R., Lynham, T., Raymond, D., Lee, B., Li, Z., 2004. Validation and Calibration of Canada-Wide Coarse-Resolution Satellite Burned-Area Maps. Photogrammetric Engineering & Remote Sensing 70, 451–460.

Fraser, R.H., Li, Z., Cihlar, J., 2000. Hotspot and NDVI Differencing Synergy (HANDS): A New Technique for Burned Area Mapping over Boreal Forest. Remote Sens. Environ. 74, 362–376.

Frolking, S., Palace, M.W., Clark, D.B., Chambers, J.Q., Shugart, H.H., Hurtt, G.C., 2009. Forest disturbance and recovery: A general review in the context of spaceborne remote sensing of impacts on aboveground biomass and canopy structure. J. Geophys. Res. 114. https://doi.org/10.1029/2008jg000911

Gale, M.G., Cary, G.J., Van Dijk, A.I.J.M., Yebra, M., 2021. Forest fire fuel through the lens of remote sensing: Review of approaches, challenges and future directions in the remote sensing of biotic determinants of fire behaviour. Remote Sens. Environ. 255, 112282.

Gamon, J.A., Field, C.B., Goulden, M.L., Griffin, K.L., Hartley, A.E., Joel, G., Penuelas, J., Valentini, R., 1995. Relationships between NDVI, canopy structure, and photosynthesis in three Californian vegetation types. Ecol. Appl. 5, 28–41.

Garcia Millan, V., Sanchez-Azofeifa, A., 2018. Quantifying Changes on Forest Succession in a Dry Tropical Forest Using Angular-Hyperspectral Remote Sensing. Remote Sensing 10, 1865.

Giglio, L., Boschetti, L., Roy, D.P., Humber, M.L., Justice, C.O., 2018. The Collection 6 MODIS burned area mapping algorithm and product. Remote Sens. Environ. 217, 72–85.

Giglio, L., Schroeder, W., Justice, C.O., 2016. The collection 6 MODIS active fire detection algorithm and fire products. Remote Sens. Environ. 178, 31–41.

Gorelick, N., Hancher, M., Dixon, M., Ilyushchenko, S., Thau, D., Moore, R., 2017. Google Earth Engine: Planetary-scale geospatial analysis for everyone. Remote Sens. Environ. 202, 18–27.

Gralewicz, N.J., Nelson, T.A., Wulder, M.A., 2012a. Spatial and temporal patterns of wildfire ignitions in Canada from 1980 to 2006. Int. J. Wildland Fire 21, 230–242.

Gralewicz, N.J., Nelson, T.A., Wulder, M.A., 2012b. Factors influencing national scale wildfire susceptibility in Canada. For. Ecol. Manage. 265, 20–29.

Hall, F.G., Shimabukuro, Y.E., Huemmrich, K.F., 1995. Remote sensing of forest biophysical structure using mixture decomposition and geometric reflectance models. Ecol. Appl. 5, 993–1013.

Hanes, C.C., Wang, X., Jain, P., Parisien, M.-A., Little, J.M., Flannigan, M.D., 2019. Fire-regime changes in Canada over the last half century. Can. J. For. Res. 49, 256–269.

Hansen, M.C., Loveland, T.R., 2012. A review of large area monitoring of land cover change using Landsat data. Remote Sensing of Environment. https://doi.org/10.1016/j.rse.2011.08.024

Hansen, M.C., Potapov, P.V., Moore, R., Hancher, M., Turubanova, S.A., Tyukavina, A., Thau, D., Stehman, S.V., Goetz, S.J., Loveland, T.R., Kommareddy, A., Egorov, A., Chini, L., Justice, C.O., Townshend, J.R.G., 2013. High-resolution global maps of 21st-century forest cover change. Science 342, 850–853.

Healey, S.P., Yang, Z., Cohen, W.B., Pierce, D.J., 2006. Application of two regression-based methods to estimate the effects of partial harvest on forest structure using Landsat data. Remote Sens. Environ. 101, 115–126.

Helbig, M., Pappas, C., Sonnentag, O., 2016. Permafrost thaw and wildfire: Equally important drivers of boreal tree cover changes in the Taiga Plains, Canada. Geophysical Research Letters. https://doi.org/10.1002/2015gl067193

Hermosilla, T., Wulder, M.A., White, J.C., Coops, N.C., Hobart, G.W., 2017. Updating Landsat time series of surface-reflectance composites and forest change products with new observations. Int. J. Appl. Earth Obs. Geoinf. 63, 104–111.

Hermosilla, T., Wulder, M.A., White, J.C., Coops, N.C., Hobart, G.W., Campbell, L.B., 2016. Mass data processing of time series Landsat imagery: pixels to data products for forest monitoring. International Journal of Digital Earth 9, 1035–1054.

Hilker, T., Wulder, M.A., Coops, N.C., Linke, J., McDermid, G., Masek, J.G., Gao, F., White, J.C., 2009a. A new data fusion model for high spatial- and temporal-resolution mapping of forest disturbance based on Landsat and MODIS. Remote Sens. Environ. 113, 1613–1627.

Hilker, T., Wulder, M.A., Coops, N.C., Seitz, N., White, J.C., Gao, F., Masek, J.G., Stenhouse, G., 2009b. Generation of dense time series synthetic Landsat data through data blending with MODIS using a spatial and temporal adaptive reflectance fusion model. Remote Sens. Environ. 113, 1988–1999.

Horler, D.N.H., Ahern, F.J., 1986. Forestry information content of Thematic Mapper data. Int. J. Remote Sens. 7, 405–428.

Huang, X., Rein, G., 2016. Interactions of Earth's atmospheric oxygen and fuel moisture in smouldering wildfires. Sci. Total Environ. 572, 1440–1446.

Humber, M.L., Boschetti, L., Giglio, L., Justice, C.O., 2018. Spatial and temporal intercomparison of four global burned area products. Int J Digit Earth 2018. https://doi.org/10.1080/17538947.2018.1433727

Iverson, L.R., Graham, R.L., Cook, E.A., 1989. Applications of satellite remote sensing to forested ecosystems. Landsc. Ecol. 3, 131–143.

Johnston, J.M., Jackson, N., McFayden, C., Ngo Phong, L., Lawrence, B., Davignon, D., Wooster, M.J., van Mierlo, H., Thompson, D.K., Cantin, A.S., Johnston, D., Johnston, L.M., Sloane, M., Ramos, R., Lynham, T.J., 2020. Development of the User Requirements for the Canadian WildFireSat Satellite Mission. Sensors 20. https://doi.org/10.3390/s20185081

Johnston, L.M., Wang, X., Erni, S., Taylor, S.W., McFayden, C.B., Oliver, J.A., Stockdale, C., Christianson, A., Boulanger, Y., Gauthier, S., Arseneault, D., Mike Wotton, B., Parisien, M.-A., Flannigan, M.D., 2020. Wildland fire risk research in Canada. Environmental Reviews.

Jolly, W.M., Cochrane, M.A., Freeborn, P.H., Holden, Z.A., Brown, T.J., Williamson, G.J., Bowman, D.M.J.S., 2015. Climate-induced variations in global wildfire danger from 1979 to 2013. Nat. Commun. 6, 7537.

Kayitakire, F., Hamel, C., Defourny, P., 2006. Retrieving forest structure variables based on image texture analysis and IKONOS-2 imagery. Remote Sens. Environ. 102, 390–401.

Keeley, J.E., 2009. Fire intensity, fire severity and burn severity: a brief review and suggested usage. Int. J. Wildland Fire 18, 116.

Korhonen, L., Hadi, Packalen, P., Rautiainen, M., 2017. Comparison of Sentinel-2 and Landsat 8 in the estimation of boreal forest canopy cover and leaf area index. Remote Sens. Environ. 195, 259–274.

Lee, J., Cardille, J.A., Coe, M.T., 2020. Agricultural Expansion in Mato Grosso from 1986–2000: A Bayesian Time Series Approach to Tracking Past Land Cover Change. Remote Sensing. https://doi.org/10.3390/rs12040688

Lee, J., Cardille, J.A., Coe, M.T., 2018. BULC-U: Sharpening Resolution and Improving Accuracy of Land-Use/Land-Cover Classifications in Google Earth Engine. Remote Sensing 10, 1455.

Lefsky, M.A., Cohen, W.B., Spies, T.A., 2001. An evaluation of alternate remote sensing products for forest inventory, monitoring, and mapping of Douglas-fir forests in western Oregon. Can. J. For. Res. 31, 78–87.

Li, J., Roy, D.P., 2017. A Global Analysis of Sentinel-2A, Sentinel-2B and Landsat-8 Data Revisit Intervals and Implications for Terrestrial Monitoring. Remote Sensing 9, 902.

Li, X., Strahler, A.H., 1985. Geometric-Optical Modeling of a Conifer Forest Canopy. IEEE Trans. Geosci. Remote Sens. GE-23, 705–721.

Lu, D., 2006. The potential and challenge of remote sensing-based biomass estimation. Int. J. Remote Sens. 27, 1297–1328.

Luther, J.E., Fournier, R.A., Piercey, D.E., Guindon, L., Hall, R.J., 2006. Biomass mapping using forest type and structure derived from Landsat TM imagery. Int. J. Appl. Earth Obs. Geoinf. 8, 173–187.

Malamud, B.D., Morein, G., Turcotte, D.L., 2005. Log-periodic behavior in a forest-fire model. Nonlinear Process. Geophys. 12, 575–585.

Marceau, D.J., Howarth, P.J., Gratton, D.J., 1994. Remote sensing and the measurement of geographical entities in a forested environment. 1. The scale and spatial aggregation problem. Remote Sensing of Environment. https://doi.org/10.1016/0034-4257(94)90046-9

Martin, M.E., Aber, J.D., 1997. High spectral resolution remote sensing of forest canopy lignin, nitrogen, and ecosystem processes. Ecol. Appl. 7, 431–443.

McKenzie, D., Miller, C., Falk, D.A., 2011. Toward a Theory of Landscape Fire, in: McKenzie, D., Miller, C., Falk, D.A. (Eds.), The Landscape Ecology of Fire. Springer Netherlands, Dordrecht, pp. 3–25.

McRoberts, R.E., Tomppo, E.O., 2007. Remote sensing support for national forest inventories. Remote Sens. Environ. 110, 412–419.

Meyn, A., White, P.S., Buhk, C., Jentsch, A., 2007. Environmental drivers of large, infrequent wildfires: the emerging conceptual model. Progress in Physical Geography: Earth and Environment 31, 287–312.

Mora, B., Wulder, M.A., White, J.C., Hobart, G., 2013. Modeling Stand Height, Volume, and Biomass from Very High Spatial Resolution Satellite Imagery and Samples of Airborne LiDAR. Remote Sensing 5, 2308–2326.

Morgan, P., Hardy, C.C., Swetnam, T.W., Rollins, M.G., Long, D.G., 2001. Mapping fire regimes across time and space: Understanding coarse and fine-scale fire patterns. International Journal of Wildland Fire. https://doi.org/10.1071/wf01032

National Academies of Sciences, Engineering, and Medicine, Division on Earth and Life Studies, Board on Agriculture and Natural Resources, Board on Earth Sciences and Resources, Committee on Increasing Resilience to Wildland Fire: A Century of Wildland Fire Research, 2017. A Century of Wildland Fire Research: Contributions to Long-term Approaches for Wildland Fire Management: Proceedings of a Workshop. National Academies Press.

Nelson, T., Niemann, K.O., Wulder, M.A., 2002. Spatial statistical techniques for aggregating point objects extracted from high spatial resolution remotely sensed imagery. J. Geogr. Syst. 4, 423–433.

O'Connor, A., 2021. Effective Wildfire Management Using Remote Sensing Technology [WWW Document]. L3Harris Geospatial. URL https://www.l3harrisgeospatial.com/Learn/Whitepapers/Whitepaper-Detail/ArtMID/17811/ArticleID/24063/Effective-Wildfire-Management-Using-Remote-Sensing-Technology?utm_source=twitter&utm_medium=wildfire_management_whitepaper

(accessed 10.18.21).

Palace, M., Keller, M., Asner, G.P., Hagen, S., Braswell, B., 2008. Amazon forest structure from IKONOS satellite data and the automated characterization of forest canopy properties. Biotropica 40, 141–150.

Parisien, M.-A., Parks, S.A., Krawchuk, M.A., Little, J.M., Flannigan, M.D., Gowman, L.M., Moritz, M.A., 2014. An analysis of controls on fire activity in boreal Canada: comparing models built with different temporal resolutions. Ecol. Appl. 24, 1341–1356.

Parisien, M.-A., Peters, V.S., Wang, Y., Little, J.M., Bosch, E.M., Stocks, B.J., 2006. Spatial patterns of forest fires in Canada, 1980–1999. Int. J. Wildland Fire 15, 361–374.

Parks, S.A., 2014. Mapping day-of-burning with coarse-resolution satellite fire-detection data. Int. J. Wildland Fire 23, 215–223.

Parks, S.A., Holsinger, L.M., Miller, C., Nelson, C.R., 2015. Wildland fire as a self-regulating mechanism: the role of previous burns and weather in limiting fire progression. Ecol. Appl. 25, 1478–1492.

Parks, S.A., Holsinger, L.M., Panunto, M.H., Matt Jolly, W., Dobrowski, S.Z., Dillon, G.K., 2018. High-severity fire: evaluating its key drivers and mapping its probability across western US forests. Environ. Res. Lett. 13, 044037.

Parks, S.A., Miller, C., Holsinger, L.M., Scott Baggett, L., Bird, B.J., 2016. Wildland fire limits subsequent fire occurrence. Int. J. Wildland Fire 25, 182–190.

Parks, S.A., Miller, C., Nelson, C.R., Holden, Z.A., 2014. Previous Fires Moderate Burn Severity of Subsequent Wildland Fires in Two Large Western US Wilderness Areas. Ecosystems 17, 29–42.

Parks, S.A., Parisien, M.-A., Miller, C., 2012. Spatial bottom-up controls on fire likelihood vary across western North America. Ecosphere 3, 1–20.

Pausas, J.G., Keeley, J.E., 2019. Wildfires as an ecosystem service. Front. Ecol. Environ. 17, 289–295.

Peterson, G.D., 2002. Contagious Disturbance, Ecological Memory, and the Emergence of Landscape Pattern. Ecosystems 5, 329–338.

Pohjanmies, T., Triviño, M., Le Tortorec, E., Mazziotta, A., Snäll, T., Mönkkönen, M., 2017. Impacts of forestry on boreal forests: An ecosystem services perspective. Ambio 46, 743–755.

Prestemon, J.P., Hawbaker, T.J., Bowden, M., Carpenter, J., Brooks, M.T., Abt, K.L., Sutphen, R., Scranton, S., 2013. Wildfire ignitions: a review of the science and recommendations for empirical modeling. Gen. Tech. Rep. SRS-GTR-171. Asheville, NC: USDA-Forest Service, Southern Research Station. 20 p. 171, 1–20.

Price, O.F., Pausas, J.G., Govender, N., Flannigan, M., Fernandes, P.M., Brooks, M.L., Bird, R.B., 2015. Global patterns in fire leverage: the response of annual area burnt to previous fire. Int. J. Wildland Fire 24, 297–306.

Reid, C.E., Brauer, M., Johnston, F.H., Jerrett, M., Balmes, J.R., Elliott, C.T., 2016. Critical Review of Health Impacts of Wildfire Smoke Exposure. Environ. Health Perspect. 124, 1334–1343.

Remy, C.C., Hély, C., Blarquez, O., Magnan, G., Bergeron, Y., Lavoie, M., Ali, A.A., 2017. Different regional climatic drivers of Holocene large wildfires in boreal forests of northeastern America. Environmental Research Letters. https://doi.org/10.1088/1748-9326/aa5aff

Rittmaster, R., Adamowicz, W.L., Amiro, B., Pelletier, R.T., 2006. Economic analysis of health effects from forest fires. Can. J. For. Res. 36, 868–877.

Romme, W.H., 1982. Fire and Landscape Diversity in Subalpine Forests of Yellowstone National Park. Ecol. Monogr. 52, 199–221.

Roy, D.P., Jin, Y., Lewis, P.E., Justice, C.O., 2005. Prototyping a global algorithm for systematic fire-affected area mapping using MODIS time series data. Remote Sens. Environ. 97, 137–162.

Roy, D.P., Wulder, M.A., Loveland, T.R., C. E., W., Allen, R.G., Anderson, M.C., Helder, D., Irons, J.R., Johnson, D.M., Kennedy, R., Scambos, T.A., Schaaf, C.B., Schott, J.R., Sheng, Y., Vermote, E.F., Belward, A.S., Bindschadler, R., Cohen, W.B., Gao, F., Hipple, J.D., Hostert, P., Huntington, J., Justice, C.O., Kilic, A., Kovalskyy, V., Lee, Z.P., Lymburner, L., Masek, J.G., McCorkel, J., Shuai, Y., Trezza, R., Vogelmann, J., Wynne, R.H., Zhu, Z., 2014. Landsat-8: Science and product vision for terrestrial global change research. Remote Sens. Environ. 145, 154–172.

Scarth, P., Phinn, S.R., McAlpine, C., 2001. Integrating High and Moderate Spatial Resolution Image Data to Estimate Forest Age Structure. Can. J. Remote Sens. 27, 129–142.

Schroeder, W., Prins, E., Giglio, L., Csiszar, I., Schmidt, C., Morisette, J., Morton, D., 2008. Validation of GOES and MODIS active fire detection products using ASTER and ETM+ data. Remote Sens. Environ. 112, 2711–2726.

Steininger, M.K., 2000. Satellite estimation of tropical secondary forest above-ground biomass: Data from Brazil and Bolivia. Int. J. Remote Sens. 21, 1139–1157.

Stinson, G., Kurz, W.A., Smyth, C.E., Neilson, E.T., Dymond, C.C., Metsaranta, J.M., Boisvenue, C., Rampley, G.J., Li, Q., White, T.M., Others, 2011. An inventory-based analysis of Canada's managed forest carbon dynamics, 1990 to 2008. Glob. Chang. Biol. 17, 2227–2244.

Stocks, B.J., Fosberg, M.A., Lynham, T.J., Mearns, L., Wotton, B.M., Yang, Q., Jin, J.Z., Lawrence, K., Hartley, G.R., Mason, J.A., Others, 1998. Climate change and forest fire potential in Russian and Canadian boreal forests. Clim. Change 38, 1–13.

Stocks, B.J., Mason, J.A., Todd, J.B., Bosch, E.M., Wotton, B.M., Amiro, B.D., Flannigan, M.D., Hirsch, K.G., Logan, K.A., Martell, D.L., Skinner, W.R., 2002. Large forest fires in Canada, 1959–1997. J. Geophys. Res. 108, 512.

Thom, D., Seidl, R., 2016. Natural disturbance impacts on ecosystem services and biodiversity in temperate and boreal forests. Biol. Rev. Camb. Philos. Soc. 91, 760–781.

Turner, M.G., Romme, W.H., 1994. Landscape dynamics in crown fire ecosystems. Landsc. Ecol. 9, 59–77.

Wang, X., Thompson, D.K., Marshall, G.A., Tymstra, C., Carr, R., Flannigan, M.D., 2015. Increasing frequency of extreme fire weather in Canada with climate change. Clim. Change 130, 573–586.

White, J.C., Wulder, M.A., Hermosilla, T., Coops, N.C., Hobart, G.W., 2017. A nationwide annual characterization of 25 years of forest disturbance and recovery for Canada using Landsat time series. Remote Sens. Environ. 194, 303–321.

White, J.C., Wulder, M.A., Hobart, G.W., Luther, J.E., Hermosilla, T., Griffiths, P., Coops, N.C., Hall, R.J., Hostert, P., Dyk, A., Guindon, L., 2014. Pixel-Based Image Compositing for Large-Area Dense Time Series Applications and Science. Can. J. Remote Sens. 40, 192–212.

Whitman, E., Parisien, M.-A., Thompson, D.K., Hall, R.J., Skakun, R.S., Flannigan, M.D., 2018. Variability and drivers of burn severity in the northwestern Canadian boreal forest.

Ecosphere. https://doi.org/10.1002/ecs2.2128

Wooster, M.J., Roberts, G.J., Giglio, L., Roy, D., Freeborn, P., Boschetti, L., Justice, C., Ichoku, C., Schroeder, W., Davies, D., Smith, A., Setzer, A., Csiszar, I., Strydom, T., Frost, P., Zhang, T., Xu, W., de Jong, M., Johnston, J., Ellison, L., Vadrevu, K., McCarty, J., Tanpipat, V., Schmidt, C., San-Miguel, J., 2021. Satellite remote sensing of active fires: History and current status, applications and future requirements. Remote Sens. Environ. 267, 112694.

Wulder, M.A., 1998. Optical remote-sensing techniques for the assessment of forest inventory and biophysical parameters. Progress in Physical Geography. https://doi.org/10.1191/030913398675385488

Wulder, M.A., Coops, N.C., Roy, D.P., White, J.C., Hermosilla, T., 2018. Land cover 2.0. Int. J. Remote Sens. 39, 4254–4284.

Wulder, M.A., Hall, R.J., Coops, N.C., Franklin, S.E., 2004. High Spatial Resolution Remotely Sensed Data for Ecosystem Characterization. Bioscience 54, 511–521.

Wulder, M.A., White, J.C., Gillis, Walsworth, N., Hansen, M.C., Potapov, P., 2010. Multiscale satellite and spatial information and analysis framework in support of a large-area forest monitoring and inventory update. Environ. Monit. Assess. 170, 417–433.

Preface to Chapter 2

As illustrated in the introduction and literature review in Chapter 1, Earth observations provide valuable insights for monitoring landscape changes and disturbances like forest fires. Recent advances have been made in remote sensing to support large-area disturbance monitoring, such as cloud-based processing, open data accessibility, increased data sources, and multi-source data fusion. In Chapter 2, I apply a systematic review to synthesize recent advances in remote sensing. By doing so, I identify how landscape ecologists use remote sensing techniques and project future opportunities for them to employ remote sensing in their research approaches based on recent and expected innovations being made in remote sensing. This study is a significant contribution to science because it provides a path forward for innovations in landscape ecology using remote sensing.

Chapter 2 was published in 2020 in *Current Landscape Ecology Reports* and uses the Springer Basic (numeric) citation style.

2. Remote Sensing's recent and future contributions to Landscape Ecology

Authors:

Morgan A. Crowley[a*]

Jeffrey A. Cardille[a]

[a]*Department of Natural Resource Sciences*

McGill University

21,111 Lakeshore Road

Ste.-Anne-de-Bellevue, Québec, Canada

*Corresponding Author: morgan.crowley@mail.mcgill.ca

Journal: Current Landscape Ecology Reports

Section: Methodological developments in landscape ecology and related fields

Publication date: 09 May, 2020

Full citation: Crowley, M.A., Cardille, J.A. Remote Sensing's Recent and Future Contributions to Landscape Ecology. *Curr Landscape Ecol Rep* 5, 45–57 (2020). https://doi.org/10.1007/s40823-020-00054-9

Keywords: landscape ecology, remote sensing, multi-scale, open access, data fusion, machine learning

Abstract

Purpose of Review: The purpose of this article is to review landscape ecology research from the past five years to identify past and future contributions from remote sensing to landscape ecology.

Recent Findings: Recent studies in landscape ecology have employed advances made in remote sensing. These include the use of reliable and open datasets derived from remote sensing, the availability of new sources for freely available satellite imagery, and machine-learning image classification techniques for classifying land cover types. Remote sensing data sources and methods have been used in landscape ecology to examine landscape structure. Additionally, these data sources and methods have been used to analyze landscape function including the effects of landscape structure and landscape change on biodiversity and population dynamics. Lastly, remote sensing data sources and methods have been used to analyze historical landscape changes and to simulate future landscape changes.

Summary: The ongoing integration of remote sensing analyses in landscape ecology will depend on continued accessibility of free imagery from satellite sources and open-access data-analysis software, analyses spanning multiple spatial and temporal scales, and novel land cover classification techniques that produce accurate and reliable land cover data. Continuing advances in remote sensing can help to address new landscape ecology research questions, enabling analyses that incorporate information that ranges from ground-based field samples of organisms to satellite-collected remote sensing data.

2.1 Introduction

In the last five years, landscape ecologists have continued their seminal focus on the relationships of pattern and process [1], addressing questions of landscape structure, landscape function, and landscape change [2]. For example, recent studies have analyzed landscape structure by examining urban green cover, rangeland distribution, wetland extent [3–6], fragmentation of forests [7], land cover and land use [8–10], and heterogeneity of urban and agricultural landscapes [11– 14]. For relating landscape structure to ecological processes, studies have focused on habitat and resource selection by plants and animals [15–18], forest dynamics and structure [19], and pollination on agricultural lands [20, 21]. For analyzing the movement across landscapes, analyses have explored movement related to corridors and connectivity [22–27] and movement of species populations related to metapopulation dynamics using genetics to track reproduction and population dispersal across generations [28, 29]. For quantifying landscape change, recent studies have used landscape history to analyze disturbances such as fire and their impacts on landscape structure over time [30–33]. By analyzing prior landscape changes, other landscape ecologists have also worked towards predicting changes in landscape structure and evaluating potential impacts through system feedbacks and potential changes in land planning by using simulation models [34–56].

Many of these studies in landscape ecology have relied on contributions from the field of remote sensing. Since the launch of the satellite Landsat-1 MSS in 1972, a variety of remote sensing platforms (e.g., satellite, aerial) have collected data in the form of image observations. Each sensor gathers imagery at a pre-defined spatial resolution, which denotes the ground measurement that each pixel represents in an image. Spectral resolutions vary based on the wavelength intervals that the sensors are collecting reflectance of the sun on the earth's surface.

The temporal resolution of a given remote sensing platform is derived from its orbital path and speed, which determines the satellite's revisit rate for collecting a new image in the same location. Sensors currently in operation include optical sensors from NASA's Landsat program, optical and synthetic-aperture radar (SAR) sensors from the European Space Agency Copernicus constellation, and many other public and privately owned airborne and spaceborne systems. Researchers are able to choose their remote sensing sources based on their research questions, whether they use sources such as unmanned aerial vehicles (UAVs), active sensors like light detection and ranging (lidar), field-based spectroscopy, cross-boundary satellites [38–41]. Users can pre-process images to correct for atmospheric interferences caused by haze, clouds, or angle of the sun [42–44]. By comparing imagery and ground-based measurements, users can classify land cover types (e.g., forests, wetlands, development) to analyze the landscape structure [45–48]. Freely available remote sensing data from satellite sensors with large spatial coverage has become available in the last ten years [49–53, 54•]. For example, in 2008, the free and open Landsat data policy was implemented and in 2014 the first sensor from the European Space Agency's open-access Copernicus mission was launched [49–53, 55]. With increasing data availability for large-area coverage and medium-spatial resolution sensors like Landsat and Sentinel, there has been a dramatic increase in research using satellite data in the last five years [52].

2.2 Literature Review

In this review, we examine recently published manuscripts from landscape ecology that have been made possible through advances in remote sensing. We outline recent developments in remote sensing and landscape ecology, highlighting important developments from each field to illuminate their current and approaching potential. To achieve this, we employed a systematic review of highly cited literature related to landscape ecology and remote sensing for the last five years, from 2014 to 2019. We identified recently published manuscripts that apply remote sensing methods in landscape ecology using Web of Science. We sorted the manuscripts by overall citation count in order to identify the most prominent contributions made within this field. We terminated our exhaustive literature search after identifying all 172 manuscripts meeting the search criteria (e.g., “landscape ecology” & “remote sensing”). The 172 manuscripts were categorized by landscape ecology research themes: landscape structure, landscape change, landscape function. For each landscape ecology theme, we identified remote sensing data sources and analyses most frequently used in landscape ecology by analyzing the author keywords (Table 2.1). Eleven publications were removed that were unrelated to landscape ecology or remote sensing. Additional recently published manuscripts were also incorporated into the review. Once we identified recent contributions of landscape ecology, we projected future research opportunities for landscape ecology by identifying other advances in remote sensing that might also be relevant to landscape ecology, as determined from the most frequently cited manuscripts from remote sensing in Web of Science from 2014 to 2019.

Table 2.1 The thematic coding structure of this literature review. Each manuscript was categorized by landscape ecology theme and example keywords were extracted that related to remote sensing data sources and methods. In this table, the keywords are ordered by most frequently used for each landscape ecology theme. Landscape structure is the spatial arrangement of landscape elements, such as land cover types and forest patches. Landscape change refers to the changes in the landscape structure over time and space. Landscape function is the interactions between landscape structural elements, whether through ecological processes or energy flows, such as the interactions between animal migration routes and forest connectivity.

Theme ***(# of manuscripts)***	**Data Sources** ***(# of manuscripts)***	**Remote Sensing Methods** ***(# of manuscripts)***
Structure *(88)*	lidar *(15)* Landsat *(14)* citizen science *(6)* airborne laser scanning (ALS) *(4)* hyperspectral data *(4)* Unmanned aerial vehicle (UAV) *(4)* aerial photography *(2)* airborne remote sensing *(2)* AVIRIS *(2)* GeoEye-1 *(2)* Google Street View *(2)* high-resolution satellite data *(2)* historical imagery *(2)* IKONOS *(2)* land surface temperature *(2)* MODIS *(2)* PhenoCam dataset *(2)* RapidEye *(2)* participatory science *(2)* TerraSAR-X *(2)* Shuttle Radar Topography Mission (SRTM) *(1)*	canopy-height model *(8)* classification and regression tree *(8)* digital elevation model *(6)* normalized difference vegetation index (NDVI) *(6)* clustering *(4)* random forest machine learning *(4)* segmentation *(4)* spatiotemporal *(4)* support vector machine (SVM) *(4)* 3D urban form *(2)* aggregation *(2)* image processing *(2)* land cover classification *(2)* maximum entropy classifier *(2)* multi-scale *(2)* object-based image analysis (OBIA) *(2)* spectral unmixing *(2)* spectral variable selection *(2)* structure-from-motion (SFM) *(2)* tree species classification *(2)*
Change (*42*)	Landsat *(7)* MODIS *(2)* participatory mapping *(2)* historical map *(1)* lidar *(1)* multi-source satellite images *(1)* PhenoCam *(1)* time series *(1)*	spatiotemporal *(3)* change detection *(1)* landscape accuracy metric *(1)* NDVI *(1)* OBIA *(1)* random forest machine learning *(1)* segmentation *(1)*

Function (*46*)	lidar *(4)*	enhanced vegetation index (EVI) *(2)*
	land surface temperature *(2)*	NDVI *(2)*
	airborne remote sensing *(1)*	change detection *(1)*
	AVIRIS *(1)*	differenced normalized burn ratio *(1)*
	citizen science *(1)*	digital elevation model *(1)*
	microsatellites *(1)*	downscaling *(1)*
	MODIS *(1)*	maximum entropy classifier *(1)*
	National Land Cover Dataset (NLCD) *(1)*	random forest machine learning *(1)*
	participatory mapping *(1)*	radar *(1)*
	WorldView-2 *(1)*	VIIRS *(1)*

2.3 Recent advances in remote sensing

2.3.1 Explosion of data diversity and availability

The first decades of landscape ecology were characterized by a relatively data-poor setting, with only a few satellites potentially providing data and practical limits to analysis. For example, early studies in the 1970-80s typically analyzed only one Landsat image at a time because they were expensive, had to be shipped on tapes from receiving stations, and took weeks to analyze on computers of the time period. In the last ten years, this framework has been overturned, with hundreds of thousands of images freely available for analysis from multiple public and free remote sensing platforms [49, 51–55, 56•, 57•, 58]. These new or improved platforms include those on large satellites like Landsat-8 and Sentinel-2, on airplanes, on unmanned aerial vehicles (UAVs), via small/micro/nanosatellites, and through ground-based sensor systems. Some example sensors include passive multispectral optical (i.e., collecting ground reflectance along the optical light spectrum divided into three to ten segments), actively collected synthetic aperture radar (SAR) (collecting return rates of wavelengths from multiple, pulsating microwave beams), thermal sensors (i.e., heat detection), hyperspectral sensors (i.e., collecting ground reflectance of the sun at ten or more segments of the light spectrum), and actively collected lidar (i.e., collecting return rates of wavelengths from a single, pulsating laser)

[59–59]. Meanwhile, atmospheric noise in data is decreasing. For example, “analysis-ready” imagery and data cubes are now available for Landsat imagery, which enables users to spend less time preprocessing imagery [70, 71]. Whether launched by private companies or public agencies, remote sensing sources are increasing in spatial, spectral, and temporal resolutions of the observations [72, 73].

2.3.2 Emergence of massive-throughput analysis platforms

Open and free high-capacity analysis software and programs have greatly altered the potential for accessing and analyzing time series of imagery and combining data from different remote sensing sources to better understand landscape structure [51, 52, 56•, 57•]. Most notably, the cloud-based storage and processing platform, Google Earth Engine, was first released in 2010 to increase accessibility to remote sensing and geospatial data using Google servers. Prior to this, the only option for many landscape ecologists wishing to use remotely sensed data was to download individual images and analyze them on local computers or networked clusters [54••, 56•]. Cloud-based platforms facilitate aggregation of remotely sensed observations of a landscape collected on different dates into a temporally ordered data “stack” or “cube”. Changes in landscape structures due to natural and human disturbances can then be quantified over time [74–78]. Combining remote sensing observations from different sensors can also provide multi-scale views (i.e., varying spatial and temporal resolutions and extents in time and space) (Table 2.2) [54••, 56•, 79–81]. Recent studies have combined observations from multiple remote sensing sources such as the USGS’s Landsat satellite and NASA’s MODIS satellite [82–85]; Landsat and synthetic aperture radar (SAR) [86]; airborne laser scanning (e.g., lidar) and digital aerial photogrammetric data (e.g., aerial photographs) [87, 88]; unmanned aerial vehicles

(UAVs) and digital aerial photogrammetric data [89]; UAV, aerial, and satellite [90]; lidar and Landsat [91, 92].

Table 2.2 In the first column, we identified possible scale requirements (both spatial and temporal grain and extents) for landscape ecology research. In the second column, we named presently available remote-sensing sources that meet those scale requirements. In the third column, we present example studies that use those sources in their analyses. Landsat is a satellite mission from the USGS consisting of multiple sensors that have been launched since 1972, including the Multispectral Scanner System (MSS), Thematic Mapper (TM), Enhanced Thematic Mapper Plus (ETM+) and Operational Land Imager (OLI). MODIS (Moderate Resolution Imaging Spectroradiometer) is a sensor from NASA that is mounted on two satellites, Terra and Aqua. Sentinel-2 is a European Space Agency mission consisting of two satellites, Sentinel-2A and Sentinel-2B. Planet Labs is a satellite company that has multiple satellites in orbit, including Dove, RapidEye, and SkySat. Unmanned aerial vehicles (UAVs or drones) are useful for mapping small extents at a fine resolution with a mounted sensor on board.

Scale required	**Best sensors at required scale**	**Example studies**
Fine spatial grain	10cm-1m (“Planet Labs” satellites, UAV, airplane)	[38, 45, 48, 93, 183]
Fine temporal grain	Every ~5 days at 10-60m (Sentinel-2), and daily at 250m (MODIS)	[67, 69, 78, 95, 112]
Large spatial extent	Global and daily at 250m (MODIS)	[69, 78, 83, 95]
Long temporal extent	1972 to present, every 16 days at 30-60m (Landsat MSS, TM, ETM+, OLI)	[53, 91, 106, 122, 132]

2.3.3 Development of algorithms for large-scale image classifications

A primary focus of remote sensing research is to develop methods for converting remotely sensed data into a meaningful description or picture of what is actually on the ground. This is referred to as "classification" of the remotely sensed data. Several recent advances have greatly improved algorithms used in classification [54••, 56•, 93]. For example, object-based image classifications group neighboring pixels into objects and classify the objects based on their shape, size, color, texture (spatial variation), and context (neighboring or ancillary information) [94, 95]. Machine/deep learning approaches (e.g., convolutional neural networks, random forests) are automated classification algorithms that rely on minimal user interference when classifying imagery [59, 63, 72, 96–101]. Additionally, time-series analyses have been used to map land cover changes by stacking images from multiple sources and identifying disturbance patterns and deviations from expected values [69, 74, 102–113]. This allows the rapid detection of landscape change and disturbances like forest loss and fires. Time-series analyses have created reliable global-scale landscape change datasets that are freely available for subsequent analyses [114–118]. For example, a regularly updated forest cover dataset including landscape changes and drivers of changes is available annually for the entire globe [119, 120]. Additionally, the World Resources Institute's Global Forest Watch initiative detects forest changes globally in near-real time [121]. Other recent studies have used time-series analyses, machine learning, and object-based image analyses to analyze land surface temperatures and identify urban heat islands [122], to provide increased data to support forest inventory efforts [66], to map landscape changes related to climate change [123], to inform precision agriculture [124], to monitor air pollution [125], to quantify colored dissolved organic matter in lakes [126], to quantify aboveground biomass [127], and to track urbanization [128].

2.4 Advances in landscape ecology using remote sensing

Landscape ecologists use remote sensing for three principal reasons: (1) to quantify landscape **structure** based on classified imagery; (2) to identify landscape **change** and its impact and make future predictions using statistical models; and (3) to quantify landscape **function**. Landscape structure is the spatial arrangement of landscape elements, such as land cover types and forest patches. Landscape change refers to the changes in the landscape structure over time and space. Landscape function is the interactions between landscape structural elements, whether through ecological processes or energy flows, such as the interactions between animal migration routes and forest connectivity.

2.4.1 Quantifying landscape structure

Remote sensing observations provide the potential to map and analyze landscape structure at a variety of spatial and temporal grains and extents. Landscape ecologists analyze both raw remote sensing data and remote sensing-derived maps to quantify landscape structure. For example, by harmonizing airborne lidar and satellite imagery, researchers were able to quantify structural connectivity and identify patches that were most important for landscape-level conservation in Alberta, Canada [129]. Landscape ecologists have extracted landscape-based information using a variety of remote sensing spectral vegetation indices (e.g., tasselled cap, leaf area index, normalized-difference of vegetation index NDVI) [130–132]. In Finland, researchers combined data collected by citizen scientists (e.g., landowners, students, recreationalists) with lidar-derived forest measurements to quantify landscape structure [133]. Additionally, landscape structure has frequently been quantified using open-source toolboxes designed to process remote sensing data [134–137]. The wide range of applications employing landscape-scale analyses has been made possible from the increasing availability of remote sensing sources and advances in imagery analyses (Table 2.3).

Table 2.3 A review of novel remote sensing techniques that were applied in landscape ecology studies and some results that contributed to the field of landscape ecology.

Remote Sensing Advance	Use in Landscape Ecology	Research Finding	Reference
Regional airborne lidar data	Quantified structural habitat connectivity and simulate changes	Identified most important patches for landscape conservation in Alberta, Canada	[129]
Multiple data sources with varying spatial and thematic resolution	Predicted seasonal land surface temperatures	Determined strong predictors of land surface temperatures to include percent of impervious surfaces, percent of tree canopy from spring to fall, and vegetative-based indices from summer to fall	[131]
Multiple data sources from ground observations and airborne lidar	Quantified above-ground forest biomass and vegetation structure	Identified spatially explicit biodiversity indicators for bird habitats for 41 different species in boreal forest regions	[133]
Refining spatial resolution from remote sensing sources	Examined landscape surface metrics at a higher spatial resolution to assess scale-dependent relationships	Found that map accuracy for data aggregation of sub-pixel remote sensing classifications were dependent on spatial heterogeneity of the landscape	[136]
Synthetic Aperture Radar (SAR) data sources	Calculated resistance maps for habitat connectivity	Found that SAR-based maps explained more of the species abundance for forest beetles than aerial photograph-based maps	[141]
Active (lidar) and passive (AVIRIS) aerial sensors	Modeled vegetation structure and historical land use	Determined that topography and substrate type impacted vegetation distribution, and grazing intensity/ranges predicted vegetation patterns on Santa Cruz Island, USA	[142]

2.4.1.1 Future Prospects

Advances in methods for quantifying landscape structure will mirror advances made in remote sensing for image classification due to the direct relationship between a landscape's surface cover and its structure. As data diversity and availability continue to grow, information from remote sensing data seems poised to make novel advances within landscape ecology in the near future. For example, opportunities exist for increasing landscape-scale analyses focusing on biomass analyses and vegetation structure using data from the recently launched and future active-sensors (e.g., NISAR, GEDI, BIOMASS, MOLI, SAOCOM1A, ICESat-2, ALOS-4, TanDEM-L, RADARSAT Constellation Mission) [138]. Additional opportunities will be created to use the finer spatial and temporal resolutions that will be provided by future optical satellites that are being built (e.g., Landsat 9, Sentinel constellation). While many landscape ecology studies take advantage of remote sensing observations collected by aerial and satellite sources, future studies can use observations from novel data sources like UAVs and microsatellites (i.e., small satellites from companies like DigitalGlobe and Planet) for very-high spatial resolution observations of fine-scale landscape features [139], hyperspectral sensors for greater spectral sensitivity when using raw remote sensing values in landscape ecology models [140], and synthetic aperture radar (SAR) sensors and lidar sensors for reconstructing three-dimensional landscape structure and analyzing connectivity [141–143]. Landscape structure can be quantified by using feature extraction techniques and machine-learning classifiers to improve the accuracy of image classifications [80, 144, 145]. By quantifying landscape structure on a cloud-based processing platform like Google Earth Engine [57•], large-area landscape ecology structural analyses become more tenable and it will no longer be necessary to download new imagery to personal computers.

2.4.2 Quantifying landscape change

Landscape ecology studies use remote sensing images from multiple collection dates to identify landscape change, to analyze their impacts on populations, and to predict future landscape change. Satellite-based time-series data (whether from one sensor or many) provide observations spanning multiple decades of landscape change such as cumulative forest cover decline, recovery of forest species from disturbances, degradation of forest patches, and land-use change [130, 132, 146–152]. Researchers applied a temporal-trend analysis of Landsat TM time-series imagery and vegetation indices from 1987 to 2010 to map gradual and abrupt forest decline and regrowth in Québec, Canada and inform land management policy [132]. Another study integrated multi-source imagery from NASA's Landsat MSS, TM, ETM+, the Russian KATE-200 satellite camera, and satellite Keyhole imagery to identify regions for management by evaluating the relationship between oasis changes and landscape structure in an arid region of China from 1963 to 2010 [148]. Remote sensing data has also been incorporated into existing landscape ecology simulations to model stochastic dynamics of landscape structure elements, and in turn, landscape function. For example, landscape ecologists have used remote sensing-based data to predict rates and patterns of urban expansion over time [153], to quantify landscape structure and ecosystem service changes in urban areas [154, 155], and to simulate changes in soil organic carbon due to changing climate [156]. Observations from remote sensing platforms enable landscape ecologists to reconstruct landscape history for analyzing landscape changes and to inform predictive models for landscape changes.

2.4.2.1 Future Prospects

As the temporal revisit rate of satellite image observations gets shorter, landscape ecologists will be able to see landscape changes as they happen in near-real time, whether they are persistent (e.g., fire), ephemeral (e.g., floods), or gradual (e.g., forest degradation) [157–159]. Increased data frequency will be useful for analyzing landscape changes at daily or monthly resolutions rather than only annual resolutions. Additionally, by accessing publicly available near-real-time global datasets that map land cover changes using cloud-based platforms like Google Earth Engine, landscape ecologists will be able to perform their own analyses more rapidly without developing their own image classification protocols. Multi-temporal landscape analyses of the same landscape or analyses comparing different landscapes will become increasingly accessible by employing data fusion methods to combine observations from multiple sensors and weighing the evidence from each classification [54••, 129, 160–162]. Such analyses have been previously difficult for landscape ecology due to data collection limitations and financial costs of imagery. However, open-access satellites provide multi-scale views for free [37, 163]. Robust predictive models that are able to include remote sensing classifications derived from multiple sources or classifications with continuous values (e.g., forest quality on a continuous scale rather than discrete classes) will be useful for incorporating future data sources more readily into existing landscape ecology models.

2.4.3 Understanding landscape function

Landscape ecologists can analyze landscape function of the study area by combining information derived from remote sensing with information from other sources into landscape ecology models. For example, satellite-derived ecosystem service indicators (e.g., water quality, soil moisture, and soil erosion) can be analyzed in combination with land cover information (e.g., wetland area) to estimate ecosystem service provisioning [164, 165]. Habitat classifications identifying population preferences and vulnerability related to landscape change, and primary productivity related to spatial distributions of species have been assessed using object-based classifications and random forest machine learning algorithms of satellite data, vegetation structural observations provided by lidar data, and gross primary productivity values derived from the enhanced vegetation index [139, 143, 145, 166, 167]. By fusing spectral indices like NDVI with vegetative structural information provided by lidar and topographical information derived from SAR observations, human impacts on vegetation patterns and environmental gradients can be analyzed [142]. Research focusing on urban landscape ecology has analyzed remote sensing data like land surface temperature products to examine the relationship between land surface temperature and land cover/use [168–170]. By incorporating remote sensing data like the National Land Cover Database, NDVI, and Landsat 7 ETM+ observations with land surface temperatures, the urban heat island effect can be analyzed and used to predict future land surface temperatures [131].

2.4.3.1 Future Prospects

For analyzing landscape function, advances will be made in landscape ecology by using new remote sensing data sources and analyses to quantify interactions between landscape structure and ecological processes (e.g., land cover type and population movement). Calls have been made to shift habitat assessments from categorical indices (e.g., low, medium, and high) to continuous values (e.g., 0-100) to better evaluate impacts of landscape change on biodiversity and incorporate error quantification into landscape ecology models [115, 171•, 172]. This shift towards continuous values would capitalize on advances made in remote sensing for classifying gradients of sub-pixel land cover and forest quality, per-pixel confidences in classification, and data uncertainty measurements [147, 171•, 172–174]. New sensors like GEDI and continuous data such as forest quality can provide more functional information about the landscape in terms of species distribution, resource distribution, and three-dimensional habitat connectivity [175].

Landscape ecology studies that incorporate remote sensing images can also incorporate data from non-remote sensing sources like crowdsourcing, participatory research, and other existing geospatial datasets [54••, 56•, 176–178]. For example, landscape ecologists can incorporate geolocations of bird sightings collected by citizen scientists in eBird (eBird.org) in combination with vertical vegetative structure data from lidar to improve models analyzing species distribution or biodiversity. Additionally, the fusion of data and imagery from multiple sources can increase spatial, temporal, and spectral resolutions by updating the data cube with the finest resolution data available to better analyze landscape processes [54••, 112, 179–181]. For example, often genetic and metapopulation studies examine landscape changes that occur at scales finer than landscape changes captured by medium-resolution satellites like Landsat. Therefore, there is an opportunity to assimilate very-high spatial resolution remote sensing data from microsatellites and UAVs or temporally fine-scale satellite time series to analyze metapopulation dynamics [182].

2.5 Conclusions

The advances that have been made in landscape ecology using remote sensing can inform future opportunities for integrating remote sensing in landscape ecology studies. Landscape ecology has made advances in quantifying landscape connectivity, using genetics to analyze metapopulation dynamics, examining multi-functional and social-ecological systems, simulating future landscape changes, and establishing landscape histories to inform and model future landscape changes. These advances have been made possible in part due to remote sensing including the production of reliable land cover datasets that use new data sources, time series of remotely sensed data and three-dimensional data, machine-learning classification techniques, and free data accessibility. Within landscape ecology, remote sensing images and analyses have been applied to construct multi-scale, multi-temporal, and multi-source landscape-scale analyses. Upcoming data sources will be used to estimate functional attributes of a landscape such as interactions between landscape elements and ecological processes, which can then be integrated into existing landscape ecology models that relate landscape structure or landscape change to ecological responses like species diversity. Remote sensing derived data can either inform the landscape structure and landscape change or the ecological responses, depending on research objectives and data availability. The fusion of remote sensing observations from multiple sources into data cubes can increase temporal and spatial resolutions without trading off spatial extent coverage. Near-real-time monitoring provided by open-access satellite sensors can provide landscapes pre- and post-change at the time steps necessary to evaluate impacts on ecosystem processes. Ultimately, these advances in data sources at varying scales and resolutions from very high resolution to large area coverage enable landscape ecology analyses that can be produced more rapidly, for larger study regions, and for longer study periods.

2.6 Acknowledgements

Many thanks to Sara Pancheri for annotating the first set of papers reviewed. M.C. designed and organized the literature review, J.C. honed review topics; the authors discussed the findings and contributed to writing the final manuscript.

Compliance with Ethical Standards

Morgan Crowley and Jeffrey Cardille declare that they have no conflict of interest. This article does not contain any studies with human or animal subjects performed by any of the authors.

Funding

Funding for this research was provided by a Natural Sciences and Engineering Research Council (NSERC) Discovery Grant awarded to Cardille, and an NSERC Alexander Graham Bell Canada Graduate Scholarships-Doctoral Award (CGS-D) to Crowley.

2.7 References

Papers of particular interest, published recently, have been highlighted as:

• Important

•• Very Important

1. Turner MG, O'Neill RV, Gardner RH, Milne BT (1989) Effects of changing spatial scale on the analysis of landscape pattern. Landsc Ecol 3:153–162.
2. Lausch A, Blaschke T, Haase D, Herzog F, Syrbe R-U, Tischendorf L, Walz U (2015) Understanding and quantifying landscape structure – A review on relevant process characteristics, data models and landscape metrics. Ecol Modell 295:31–41.
3. Asgarian A, Amiri BJ, Sakieh Y (2015) Assessing the effect of green cover spatial patterns on urban land surface temperature using landscape metrics approach. Urban Ecosyst 18:209–222.
4. Wu J, Zhang Q, Li A (2015) Historical landscape dynamics of Inner Mongolia: patterns, drivers, and impacts. Landsc Ecol 30:1579–1598.
5. Martínez Pastur G, Peri PL, Lencinas MV, García-Llorente M, Martín-López B (2016) Spatial patterns of cultural ecosystem services provision in Southern Patagonia. Landsc Ecol 31:383–399.

6. Vanderhoof MK, Alexander LC, Todd MJ (2016) Temporal and spatial patterns of wetland extent influence variability of surface water connectivity in the Prairie Pothole Region, United States. Landsc Ecol 31:805–824.
7. Arroyo-Rodríguez V, Melo FPL, Martínez-Ramos M, Bongers F, Chazdon RL, Meave JA, Norden N, Santos BA, Leal IR, Tabarelli M (2017) Multiple successional pathways in human-modified tropical landscapes: new insights from forest succession, forest fragmentation and landscape ecology research. Biol Rev Camb Philos Soc 92:326–340.
8. Sponsler DB, Johnson RM (2015) Honey bee success predicted by landscape composition in Ohio, USA. PeerJ 3:e838.
9. Janda P, Trotsiuk V, Mikoláš M, et al (2017) The historical disturbance regime of mountain Norway spruce forests in the Western Carpathians and its influence on current forest structure and composition. For Ecol Manage 388:67–78.
10. Lemessa D, Hambäck PA, Hylander K (2015) The effect of local and landscape level land-use composition on predatory arthropods in a tropical agricultural landscape. Landsc Ecol 30:167–180.
11. Zhou W, Pickett STA, Cadenasso ML (2017) Shifting concepts of urban spatial heterogeneity and their implications for sustainability. Landsc Ecol 32:15–30.
12. Qiu J, Turner MG (2015) Importance of landscape heterogeneity in sustaining hydrologic ecosystem services in an agricultural watershed. doi: 10.1890/ES15-00312.1.
13. Bertrand C, Burel F, Baudry J (2016) Spatial and temporal heterogeneity of the crop mosaic influences carabid beetles in agricultural landscapes. Landsc Ecol 31:451–466.

14. Hiron M, Berg Å, Eggers S, Berggren Å, Josefsson J, Pärt T (2015) The relationship of bird diversity to crop and non-crop heterogeneity in agricultural landscapes. Landsc Ecol 30:2001–2013.

15. Street GM, Fieberg J, Rodgers AR, Carstensen M, Moen R, Moore SA, Windels SK, Forester JD (2016) Habitat functional response mitigates reduced foraging opportunity: implications for animal fitness and space use. Landsc Ecol 31:1939–1953.

16. Moriarty KM, Epps CW, Betts MG, Hance DJ, Bailey JD, Zielinski WJ (2015) Experimental evidence that simplified forest structure interacts with snow cover to influence functional connectivity for Pacific martens. Landsc Ecol 30:1865–1877.

17. Azam C, Le Viol I, Julien J-F, Bas Y, Kerbiriou C (2016) Disentangling the relative effect of light pollution, impervious surfaces and intensive agriculture on bat activity with a national-scale monitoring program. Landsc Ecol 31:2471–2483.

18. McGarigal K, Wan HY, Zeller KA, Timm BC, Cushman SA (2016) Multi-scale habitat selection modeling: a review and outlook. Landsc Ecol 31:1161–1175.

19. Riitters K, Wickham J, Costanza JK, Vogt P (2016) A global evaluation of forest interior area dynamics using tree cover data from 2000 to 2012. Landsc Ecol 31:137–148.

20. Cusser S, Neff JL, Jha S (2016) Natural land cover drives pollinator abundance and richness, leading to reductions in pollen limitation in cotton agroecosystems. Agric Ecosyst Environ 226:33–42.

21. Baudron F, Schultner J, Duriaux J-Y, Gergel SE, Sunderland T (2019) Agriculturally productive yet biodiverse: human benefits and conservation values along a forest-agriculture gradient in Southern Ethiopia. Landsc Ecol 34:341–356.

22. Castillo MG, Hernández HJ, Estades CF (2018) Effect of connectivity and habitat availability on the occurrence of the Chestnut-throated Huet-Huet (Pteroptochos castaneus, Rhinocryptidae) in fragmented landscapes of central Chile. Landsc Ecol 33:1061–1068.

23. Dupras J, Marull J, Parcerisas L, Coll F, Gonzalez A, Girard M, Tello E (2016) The impacts of urban sprawl on ecological connectivity in the Montreal Metropolitan Region. Environ Sci Policy 58:61–73.

24. Krosby M, Breckheimer I, John Pierce D, et al (2015) Focal species and landscape “naturalness” corridor models offer complementary approaches for connectivity conservation planning. Landsc Ecol 30:2121–2132.

25. McClure ML, Hansen AJ, Inman RM (2016) Connecting models to movements: testing connectivity model predictions against empirical migration and dispersal data. Landsc Ecol 31:1419–1432.

26. Ziolkowska E, Ostapowicz K, Radeloff VC (2016) Assessing differences in connectivity based on habitat versus movement models for brown bears in the Carpathians. Landsc Ecol 31:1863–1882.

27. Wan HY, Cushman SA, Ganey JL (2019) Improving habitat and connectivity model predictions with multi-scale resource selection functions from two geographic areas. Landsc Ecol 34:503–519.

28. Dyer RJ (2015) Is there such a thing as landscape genetics? Mol Ecol 24:3518–3528

29. Jackson ND, Fahrig L (2016) Habitat amount, not habitat configuration, best predicts population genetic structure in fragmented landscapes. Landsc Ecol 31:951–968.

30. Cushman SA (2016) Calculating the configurational entropy of a landscape mosaic. Landsc Ecol 31:481–489.

31. Frock CF, Turner MG (2018) Microhabitat conditions and landscape pattern explain nocturnal rodent activity, but not seed removal, in burned and unburned lodgepole pine forests. Landsc Ecol 33:1895–1909.

32. Seidl R, Donato DC, Raffa KF, Turner MG (2016) Spatial variability in tree regeneration after wildfire delays and dampens future bark beetle outbreaks. Proc Natl Acad Sci U S A 113:13075–13080.

33. Harvey BJ, Donato DC, Turner MG (2016) Drivers and trends in landscape patterns of stand-replacing fire in forests of the US Northern Rocky Mountains (1984–2010). Landsc Ecol 31:2367–2383.

34. Bürgi M, Silbernagel J, Wu J, Kienast F (2015) Linking ecosystem services with landscape history. Landsc Ecol 30:11–20.

35. Wiersma YF, McMullin RT (2018) Is it common to be rare on the landscape? A test using a novel model system. Landsc Ecol 33:183–195.

36. Steen-Adams MM, Langston N, Adams M, Mladenoff DJ (2015) Historical framework to explain long-term coupled human and natural system feedbacks: application to a multiple-ownership forest landscape in the northern Great Lakes region, USA. Ecol Soc 20.

37. Wu W, Li Y, Hu Y, Xiu C, Yan X (2018) Impacts of changing forest management areas on forest landscapes and habitat patterns in northeastern China. Sustain Sci Pract Policy 10:1211.

38. Colomina I, Molina P (2014) Unmanned aerial systems for photogrammetry and remote sensing: A review. ISPRS J Photogramm Remote Sens 92:79–97.

39. Lefsky MA, Cohen WB, Parker GG, Harding DJ (2002) Lidar remote sensing for ecosystem studies: Lidar, an emerging remote sensing technology that directly measures the three-dimensional distribution of plant canopies, can accurately estimate vegetation structural attributes and should be of particular interest to forest, landscape, and global ecologists. BioScience 52:19–30.

40. Herold M, Scepan J, Clarke KC (2002) The use of remote sensing and landscape metrics to describe structures and changes in urban land uses. Environ Plan A 34:1443–1458.

41. Ollinger SV, Smith M-L (2005) Net primary production and canopy nitrogen in a temperate forest landscape: An analysis using imaging spectroscopy, modeling and field data. Ecosystems 8:760–778.

42. Vogelmann JE, Helder D, Morfitt R, Choate MJ, Merchant JW, Bulley H (2001) Effects of Landsat 5 Thematic Mapper and Landsat 7 Enhanced Thematic Mapper Plus radiometric and geometric calibrations and corrections on landscape characterization. Remote Sens Environ 78:55–70.

43. Roy DP, Wulder MA, Loveland TR, et al (2014) Landsat-8: Science and product vision for terrestrial global change research. Remote Sens Environ 145:154–172.

44. Franklin SE, Wulder MA (2002) Remote sensing methods in medium spatial resolution satellite data land cover classification of large areas. Prog Phys Geogr: Earth and Environment 26:173–205.

45. Lausch A, Pause M, Merbach I, Zacharias S, Doktor D, Volk M, Seppelt R (2013) A new multiscale approach for monitoring vegetation using remote sensing-based indicators in laboratory, field, and landscape. Environ Monit Assess 185:1215–1235.

46. Turner DP, Ollinger SV, Kimball JS (2004) Integrating remote sensing and ecosystem process models for landscape- to regional-scale analysis of the carbon cycle. BioScience 54:573–584.

47. Wulder M (1998) Optical remote-sensing techniques for the assessment of forest inventory and biophysical parameters. Progress in Physical Geography 22:449–476.

48. Lefsky MA, Cohen WB, Spies TA (2001) An evaluation of alternate remote sensing products for forest inventory, monitoring, and mapping of Douglas-fir forests in western Oregon. Can J For Res 31:78–87.

49. Wulder MA, Masek JG, Cohen WB, Loveland TR, Woodcock CE (2012) Opening the archive: How free data has enabled the science and monitoring promise of Landsat. Remote Sens Environ 122:2–10.

50. Wulder MA, Coops NC (2014) Satellites: Make Earth observations open access. Nature 513:30–31.

51. Wulder MA, White JC, Loveland TR, Woodcock CE, Belward AS, Cohen WB, Fosnight EA, Shaw J, Masek JG, Roy DP (2016) The global Landsat archive: Status, consolidation, and direction. Remote Sens Environ 185:271–283.

52. Zhu Z, Wulder MA, Roy DP, et al (2019) Benefits of the free and open Landsat data policy. Remote Sens Environ 224:382–385.

53. Wulder MA, Loveland TR, Roy DP, et al (2019) Current status of Landsat program, science, and applications. Remote Sens Environ 225:127–147.

54. Wulder MA, Coops NC, Roy DP, White JC, Hermosilla T (2018) Land cover 2.0. Int J Remote Sens 39:4254–4284. **A comprehensive review of the current state of remote sensing for land cover and land cover change mapping, including advances made in the open-access data era for computational, institutional and theoretical approaches.**

55. Woodcock CE, Allen R, Anderson M, et al (2008) Free access to Landsat imagery. Science 320:1011.

56. Dong J, Metternicht G, Hostert P, Fensholt R, Chowdhury RR (2019) Remote sensing and geospatial technologies in support of a normative land system science: status and prospects. Curr Opin Environ Sustain 38:44–52. **A review of remote sensing and data structure and algorithm advances related to land system science targeted for both research and policy.**

57. Gorelick N, Hancher M, Dixon M, Ilyushchenko S, Thau D, Moore R (2017) Google Earth Engine: Planetary-scale geospatial analysis for everyone. Remote Sens Environ 202:18–27. **Overview of Google Earth Engine, the cloud-based platform that uses Google's servers for remote sensing and geospatial data storage and analysis at user-defined scales. Presents example features provided by the platform, including freely available datasets, algorithms and analyses functions, and global-scale datasets that have employed Google Earth Engine.**

58. Wulder MA, Hilker T, White JC, Coops NC, Masek JG, Pflugmacher D, Crevier Y (2015) Virtual constellations for global terrestrial monitoring. Remote Sens Environ 170:62–76. doi: 10.1016/j.rse.2015.09.001.

59. Chen Y, Jiang H, Li C, Jia X, Ghamisi P (2016) Deep feature extraction and classification of hyperspectral images based on convolutional neural networks. IEEE Trans Geosci Remote Sens 54:6232–6251.

60. Chen S, Wang H, Xu F, Jin Y (2016) Target classification using the deep convolutional networks for SAR images. IEEE Trans Geosci Remote Sens 54:4806–4817.

61. Deledalle C, Denis L, Tupin F, Reigber A, Jäger M (2015) NL-SAR: A unified nonlocal framework for resolution-preserving (Pol)(In)SAR denoising. IEEE Trans Geosci Remote Sens 53:2021–2038.

62. Shean DE, Alexandrov O, Moratto ZM, Smith BE, Joughin IR, Porter C, Morin P (2016) An automated, open-source pipeline for mass production of digital elevation models (DEMs) from very-high-resolution commercial stereo satellite imagery. ISPRS J Photogramm Remote Sens 116:101–117.

63. Chen Y, Zhao X, Jia X (2015) Spectral–spatial classification of hyperspectral data based on deep belief network. IEEE J Sel Top Appl Earth Obs Remote Sens 8:2381–2392.

64. Vermote E, Justice C, Claverie M, Franch B (2016) Preliminary analysis of the performance of the Landsat 8/OLI land surface reflectance product. Remote Sens Environ 185:46–56.

65. Pajares G (2015) Overview and current status of remote sensing applications based on unmanned aerial vehicles (UAVs). Photogramm Eng Remote Sensing 81:281–330.

66. Puliti S, Ørka HO, Gobakken T, Næsset E (2015) Inventory of small forest areas using an unmanned aerial system. Remote Sens 7:9632–9654.

67. Immitzer M, Vuolo F, Atzberger C (2016) First experience with Sentinel-2 data for crop and tree species classifications in Central Europe. Remote Sens 8:166.

68. Asner GP, Martin RE, Anderson CB, Knapp DE (2015) Quantifying forest canopy traits: Imaging spectroscopy versus field survey. Remote Sens Environ 158:15–27.

69. Estel S, Kuemmerle T, Alcántara C, Levers C, Prishchepov A, Hostert P (2015) Mapping farmland abandonment and recultivation across Europe using MODIS NDVI time series. Remote Sens Environ 163:312–325.

70. Dwyer J, Roy D, Sauer B, Jenkerson C, Zhang H, Lymburner L (2018) Analysis ready data: Enabling analysis of the Landsat archive. Remote Sens 10(9):1363.

71. Egorov AV, Roy DP, Zhang HK, Hansen MC, Kommareddy A (2018) Demonstration of percent tree cover mapping using Landsat analysis ready data (ARD) and sensitivity with respect to Landsat ARD processing level. Remote Sens 10:209.

72. Hu F, Xia G-S, Hu J, Zhang L (2015) Transferring deep convolutional neural networks for the scene classification of high-resolution remote sensing imagery. Remote Sens 7:14680–14707.

73. Chen S, Tian Y (2015) Pyramid of spatial relatons for scene-level land use classification. IEEE Trans Geosci Remote Sens 53:1947–1957.

74. Hermosilla T, Wulder MA, White JC, Coops NC, Hobart GW, Campbell LB (2016) Mass data processing of time series Landsat imagery: pixels to data products for forest monitoring. Int J Digit Earth 9:1035–1054.

75. Kennedy RE, Yang Z, Cohen WB (2010) Detecting trends in forest disturbance and recovery using yearly Landsat time series: 1. LandTrendr — Temporal segmentation algorithms. Remote Sens Environ 114:2897–2910.

76. Schroeder TA, Wulder MA, Healey SP, Moisen GG (2011) Mapping wildfire and clearcut harvest disturbances in boreal forests with Landsat time series data. Remote Sens Environ 115:1421–1433.

77. Cohen WB, Yang Z, Kennedy R (2010) Detecting trends in forest disturbance and recovery using yearly Landsat time series: 2. TimeSync—Tools for calibration and validation. Remote Sens Environ 114:2911–2924.

78. Jin S, Sader SA (2005) MODIS time-series imagery for forest disturbance detection and quantification of patch size effects. Remote Sens Environ 99:462–470.

79. Zhu X, Helmer EH, Gao F, Liu D, Chen J, Lefsky MA (2016) A flexible spatiotemporal method for fusing satellite images with different resolutions. Remote Sens Environ 172:165–177.

80. Chen X, Long D, Liang S, He L, Zeng C, Hao X, Hong Y (2018) Developing a composite daily snow cover extent record over the Tibetan Plateau from 1981 to 2016 using multisource data. Remote Sens Environ 215:284–299.

81. Zhao Y, Huang B, Song H (2018) A robust adaptive spatial and temporal image fusion model for complex land surface changes. Remote Sens Environ 208:42–62.

82. Gevaert CM, García-Haro FJ (2015) A comparison of STARFM and an unmixing-based algorithm for Landsat and MODIS data fusion. Remote Sens Environ 156:34–44.

83. Gao F, Hilker T, Zhu X, Anderson M, Masek J, Wang P, Yang Y (2015) Fusing Landsat and MODIS data for vegetation monitoring. IEEE Geosci Remote Sens Mag 3:47–60.

84. Gao F, Anderson MC, Zhang X, Yang Z, Alfieri JG, Kustas WP, Mueller R, Johnson DM, Prueger JH (2017) Toward mapping crop progress at field scales through fusion of Landsat and MODIS imagery. Remote Sens Environ 188:9–25.

85. Kwan C, Budavari B, Gao F, Zhu X (2018) A hybrid color mapping approach to fusing MODIS and Landsat images for forward prediction. Remote Sens 10:520.

86. Reiche J, Verbesselt J, Hoekman D, Herold M (2015) Fusing Landsat and SAR time series to detect deforestation in the tropics. Remote Sens Environ 156:276–293.

87. Tompalski P, Coops NC, Marshall PL, White JC, Wulder MA, Bailey T (2018) Combining multi-date airborne laser scanning and digital aerial photogrammetric data for forest growth and yield modelling. Remote Sens 10:347.

88. White JC, Tompalski P, Coops NC, Wulder MA (2018) Comparison of airborne laser scanning and digital stereo imagery for characterizing forest canopy gaps in coastal temperate rainforests. Remote Sens Environ 208:1–14.

89. Goodbody TRH, Coops NC, Hermosilla T, Tompalski P, Crawford P (2018) Assessing the status of forest regeneration using digital aerial photogrammetry and unmanned aerial systems. Int J Remote Sens 39:5246–5264.

90. Matese A, Toscano P, Di Gennaro SF, Genesio L, Vaccari FP, Primicerio J, Belli C, Zaldei A, Bianconi R, Gioli B (2015) Intercomparison of UAV, aircraft and satellite remote sensing platforms for precision viticulture. Remote Sens 7:2971–2990.

91. Matasci G, Hermosilla T, Wulder MA, White JC, Coops NC, Hobart GW, Bolton DK, Tompalski P, Bater CW (2018) Three decades of forest structural dynamics over Canada’s forested ecosystems using Landsat time-series and lidar plots. Remote Sens Environ 216:697–714.

92. Matasci G, Hermosilla T, Wulder MA, White JC, Coops NC, Hobart GW, Zald HSJ (2018) Large-area mapping of Canadian boreal forest cover, height, biomass and other

structural attributes using Landsat composites and lidar plots. Remote Sens Environ 209:90–106.

93. Wulder MA, Hall RJ, Coops NC, Franklin SE (2004) high spatial resolution remotely sensed data for ecosystem characterization. BioScience 54:511–521.

94. Cheng G, Han J (2016) A survey on object detection in optical remote sensing images. ISPRS J Photogramm Remote Sens 117:11–28.

95. Zhai D, Dong J, Cadisch G, Wang M, Kou W, Xu J, Xiao X, Abbas S (2017) Comparison of pixel- and object-based approaches in phenology-based rubber plantation mapping in fragmented landscapes. Remote Sens 10:44.

96. Zhang L, Zhang L, Du B (2016) Deep learning for remote sensing data: A technical tutorial on the state of the art. IEEE Geosci Remote Sens Mag 4:22–40.

97. Zhu XX, Tuia D, Mou L, Xia G, Zhang L, Xu F, Fraundorfer F (2017) Deep learning in remote sensing: A comprehensive review and list of resources. IEEE Geosci Remote Sens Mag 5:8–36.

98. Zhang F, Du B, Zhang L (2015) Saliency-guided unsupervised feature learning for scene classification. IEEE Trans Geosci Remote Sens 53:2175–2184.

99. Zhao W, Du S (2016) Spectral–spatial feature extraction for hyperspectral image classification: A dimension reduction and deep learning approach. IEEE Trans Geosci Remote Sens 54:4544–4554.

100. Ghamisi P, Dalla Mura M, Benediktsson JA (2015) A survey on spectral–spatial classification techniques based on attribute profiles. IEEE Trans Geosci Remote Sens 53:2335–2353.

101. Romero A, Gatta C, Camps-Valls G (2016) Unsupervised deep feature extraction for remote sensing image classification. IEEE Trans Geosci Remote Sens 54:1349–1362.

102. Turner D, Lucieer A, De Jong SM (2015) Time series analysis of landslide dynamics using an unmanned aerial vehicle (UAV). Remote Sens 7:1736–1757.

103. Hermosilla T, Wulder MA, White JC, Coops NC, Hobart GW (2015) Regional detection, characterization, and attribution of annual forest change from 1984 to 2012 using Landsat-derived time-series metrics. Remote Sens Environ 170:121–132.

104. Hermosilla T, Wulder MA, White JC, Coops NC, Hobart GW (2018) Disturbance-informed annual land cover classification maps of Canada's forested ecosystems for a 29-year Landsat time series. Can J Remote Sens 44:67–87.

105. Hermosilla T, Wulder MA, White JC, Coops NC, Hobart GW (2015) An integrated Landsat time series protocol for change detection and generation of annual gap-free surface reflectance composites. Remote Sens Environ 158:220–234.

106. Frazier RJ, Coops NC, Wulder MA, Hermosilla T, White JC (2018) Analyzing spatial and temporal variability in short-term rates of post-fire vegetation return from Landsat time series. Remote Sens Environ 205:32–45.

107. Healey SP, Cohen WB, Yang Z, et al (2018) Mapping forest change using stacked generalization: An ensemble approach. Remote Sens Environ 204:717–728.

108. Cohen WB, Yang Z, Healey SP, Kennedy RE, Gorelick N (2018) A LandTrendr multispectral ensemble for forest disturbance detection. Remote Sens Environ 205:131–140.

109. Zhu Z, Zhang J, Yang Z, Aljaddani AH, Cohen WB, Qiu S, Zhou C (2019) Continuous monitoring of land disturbance based on Landsat time series. Remote Sens Environ 111116.

110. Lee J, Cardille JA, Coe MT (2018) BULC-U: sharpening resolution and improving accuracy of land-use/land-cover classifications in Google Earth Engine. Remote Sens 10:1455.

111. Cardille JA, Fortin JA (2016) Bayesian updating of land-cover estimates in a data-rich environment. Remote Sens Environ 186:234–249.

112. Crowley MA, Cardille JA, White JC, Wulder MA (2019) Multi-sensor, multi-scale, Bayesian data synthesis for mapping within-year wildfire progression. Remote Sens Lett 10:302–311.

113. Crowley MA, Cardille JA, White JC, Wulder MA (2019) Generating intra-year metrics of wildfire progression using multiple open-access data streams. Remote Sens Environ 232:111295.

114. Potapov PV, Turubanova SA, Tyukavina A, Krylov AM, McCarty JL, Radeloff VC, Hansen MC (2015) Eastern Europe’s forest cover dynamics from 1985 to 2012 quantified from the full Landsat archive. Remote Sens Environ 159:28–43.

115. Hansen MC, Loveland TR (2012) A review of large area monitoring of land cover change using Landsat data. Remote Sens Enviro122:66–74.

116. Han J, Zhang D, Cheng G, Guo L, Ren J (2015) Object detection in optical remote sensing images based on weakly supervised learning and high-level feature learning. IEEE Trans Geosci Remote Sens 53:3325–3337.

117. Giglio L, Schroeder W, Justice CO (2016) The collection 6 MODIS active fire detection algorithm and fire products. Remote Sens Environ 178:31–41.

118. Humber ML, Boschetti L, Giglio L, Justice CO (2018) Spatial and temporal intercomparison of four global burned area products. Int J Digit Earth. doi: 10.1080/17538947.2018.1433727.

119. Hansen MC, Potapov PV, Moore R, et al (2013) High-resolution global maps of 21st-century forest cover change. Science 342:850–853.

120. Curtis PG, Slay CM, Harris NL, Tyukavina A, Hansen MC (2018) Classifying drivers of global forest loss. Science 361:1108–1111.

121. World Resources Institute (2014) Global Forest Watch. http://www.globalforestwatch.org. Accessed 31 May 2019.

122. Shen H, Huang L, Zhang L, Wu P, Zeng C (2016) Long-term and fine-scale satellite monitoring of the urban heat island effect by the fusion of multi-temporal and multi-sensor remote sensed data: A 26-year case study of the city of Wuhan in China. Remote Sens Environ 172:109–125.

123. Paul F, Bolch T, Kääb A, et al (2015) The glaciers climate change initiative: Methods for creating glacier area, elevation change and velocity products. Remote Sens Environ 162:408–426.

124. Candiago S, Remondino F, De Giglio M, Dubbini M, Gattelli M (2015) Evaluating multispectral images and vegetation indices for precision farming applications from UAV images. Remote Sensing 7:4026–4047.

125. Peng J, Chen S, Lü H, Liu Y, Wu J (2016) Spatiotemporal patterns of remotely sensed PM2.5 concentration in China from 1999 to 2011. Remote Sens Environ 174:109–121.

126. Brezonik PL, Olmanson LG, Finlay JC, Bauer ME (2015) Factors affecting the measurement of CDOM by remote sensing of optically complex inland waters. Remote Sens Environ 157:199–215.

127. Lu D, Chen Q, Wang G, Liu L, Li G, Moran E (2016) A survey of remote sensing-based aboveground biomass estimation methods in forest ecosystems. Int J Digit Earth 9:63–105.

128. Fu P, Weng Q (2016) A time series analysis of urbanization induced land use and land cover change and its impact on land surface temperature with Landsat imagery. Remote Sens Environ 175:205–214.

129. Guo X, Coops NC, Gergel SE (2018) Integrating airborne lidar and satellite imagery to model habitat connectivity dynamics for spatial conservation prioritization. Landsc Ecol 33:491–511.

130. Biudes MS, Machado NG, de Morais Danelichen VH (2014) Ground and remote sensing-based measurements of leaf area index in a transitional forest and seasonal flooded forest in Brazil. Int J Biometeorol 58:1181–1193.

131. Zhou W, Qian Y, Li X (2014) Relationships between land cover and the surface urban heat island: seasonal variability and effects of spatial and thematic resolution of land cover data on predicting land surface temperatures. Landsc Ecol 29:153–167.

132. Czerwinski CJ, King DJ, Mitchell SW (2014) Mapping forest growth and decline in a temperate mixed forest using temporal trend analysis of Landsat imagery, 1987-2010. Remote Sens Environ 141:188–200.

133. Vihervaara P, Mononen L, Auvinen A-P (2015) How to integrate remotely sensed data and biodiversity for ecosystem assessments at landscape scale. Landsc Ecol 30:501–516.

134. Jung M (2016) LecoS - A python plugin for automated landscape ecology analysis. Ecol Inform 31:18–21.

135. Vogt P, Riitters K (2017) GuidosToolbox: universal digital image object analysis. Eur J Remote Sens 50:352–361.

136. Frazier AE (2014) A new data aggregation technique to improve landscape metric downscaling. Landsc Ecol 29:1261–1276.

137. Frazier AE (2016) Surface metrics: scaling relationships and downscaling behavior. Landsc Ecol 31:351–363.

138. Duncanson L, Armston J, Disney M, et al (2019) The importance of consistent global forest aboveground biomass product validation. Surv Geophys. doi: 10.1007/s10712-019-09538-8.

139. Sillero N, Goncalves-Seco L (2014) Spatial structure analysis of a reptile community with airborne LiDAR data. Int J Geogr Inf Sci 28:1709–1722.

140. Schmidt J, Fassnacht FE, Neff C (2017) Adapting a Natura 2000 field guideline for a remote sensing-based assessment of heathland conservation status. Int J Appl Earth Obs Geoinf 60:61–71.

141. Betbeder J, Laslier M, Hubert-Moy L (2017) Synthetic Aperture Radar (SAR) images improve habitat suitability models. Landsc Ecol 32:1867–1879

142. Dahlin KM, Asner GP, Field CB (2014) Linking vegetation patterns to environmental gradients and human impacts in a Mediterranean-type island ecosystem. Landsc Ecol 29:1571–1585.

143. Barbosa JM, Asner GP (2017) Prioritizing landscapes for restoration based on spatial patterns of ecosystem controls and plant-plant interactions. J Appl Ecol 54:1459–1468.

144. Maclaurin GJ, Leyk S (2016) Extending the geographic extent of existing land cover data using active machine learning and covariate shift corrective sampling. Int J Remote Sens 37:5213–5233.

145. Mishra NB, Crews KA (2014) Mapping vegetation morphology types in a dry savanna ecosystem: integrating hierarchical object-based image analysis with Random Forest. Int J Remote Sens 35:1175–1198.

146. Stark SC, Breshears DD, Garcia ES (2016) Toward accounting for ecoclimate teleconnections: intra- and inter-continental consequences of altered energy balance after vegetation change. Landsc Ecol 31:181–194.

147. Martinez del Castillo E, Garcia-Martin A, Longares Aladren LA (2015) Evaluation of forest cover change using remote sensing techniques and landscape metrics in Moncayo Natural Park (Spain). Appl Geogr 62:247–255.

148. Xie Y, Gong J, Sun P (2014) Oasis dynamics change and its influence on landscape pattern on Jinta oasis in arid China from 1963a to 2010a: Integration of multi-source satellite images. Int J Appl Earth Obs Geoinf 33:181–191.

149. Li Y, Li Y, Qureshi S (2015) On the relationship between landscape ecological patterns and water quality across gradient zones of rapid urbanization in coastal China. Ecol Modell 318:100–108.

150. Li L, Fassnacht FE, Storch I (2017) Land-use regime shift triggered the recent degradation of alpine pastures in Nyanpo Yutse of the eastern Qinghai-Tibetan Plateau. Landsc Ecol 32:2187–2203.

151. Cannon JB, Hepinstall-Cymerman J, Godfrey CM, Peterson CJ (2016) Landscape-scale characteristics of forest tornado damage in mountainous terrain. Landsc Ecol 31:2097–2114

152. Maynard JJ, Karl JW, Browning DM (2016) Effect of spatial image support in detecting long-term vegetation change from satellite time-series. Landsc Ecol 31:2045–2062.

153. Zhao S, Zhou D, Zhu C (2015) Rates and patterns of urban expansion in China's 32 major cities over the past three decades. Landsc Ecol 30:1541–1559.

154. Estoque RC, Murayama Y (2016) Quantifying landscape pattern and ecosystem service value changes in four rapidly urbanizing hill stations of Southeast Asia. Landsc Ecol 31:1481–1507.

155. Liu Y, Peng J, Wang Y (2018) Application of partial least squares regression in detecting the important landscape indicators determining urban land surface temperature variation. Landsc Ecol 33:1133–1145.

156. Wu X, Akujarvi A, Lu N (2015) Dynamics of soil organic carbon stock in a typical catchment of the Loess Plateau: comparison of model simulations with measurements. Landsc Ecol 30:381–397.

157. Liu Z, Yang J, Dwomoh F (2016) Mapping recent burned patches in Siberian larch forest using Landsat and MODIS data. Eur J Remote Sens 49:861–887.

158. Hedo J, Rubio E, Dadi T, López-Serrano FR, Alfaro-Sánchez R, Moya D, Heras J de las (2014) Is remote sensing a good method to define forest fire resilience? A particular case in the South-eastern of the Iberian Peninsula. Parte: http://hdl.handle.net/10316.2/34013.

159. Molinier M, Astola H, Räty T, Woodcock C (2018) Timely and semi-automatic detection of forest logging events in boreal forest using all available Landsat data. In: IGARSS

2018 - 2018 IEEE International Geoscience and Remote Sensing Symposium. ieeexplore.ieee.org, pp 1730–1733.

160. LeClerc E, Wiersma YF (2017) Assessing post-industrial land cover change at the Pine Point Mine, NWT, Canada using multi-temporal Landsat analysis and landscape metrics. Environ Monit Assess 189.

161. Molin PG, Gergel SE, Soares-Filho BS, Ferraz SFB (2017) Spatial determinants of Atlantic forest loss and recovery in Brazil. Landsc Ecol 32:857–870.

162. Szabó L, Burai P, Deák B, Dyke GJ, Szabó S (2019) Assessing the efficiency of multispectral satellite and airborne hyperspectral images for land cover mapping in an aquatic environment with emphasis on the water caltrop (Trapa natans). Int J Remote Sensing 40:5192–5215.

163. Bastos R, Monteiro AT, Carvalho D (2016) Integrating land cover structure and functioning to predict biodiversity patterns: a hierarchical modelling framework designed for ecosystem management. Landsc Ecol 31:701–710.

164. Grimaldi M, Oszwald J, Doledec S (2014) Ecosystem services of regulation and support in Amazonian pioneer fronts: searching for landscape drivers. Landsc Ecol 29:311–328.

165. Xu C, Pu L, Zhu M (2016) Ecological security and ecosystem services in response to land use change in the coastal area of Jiangsu, China. Sustain Sci Pract. Policy 8.

166. Requena-Mullor JM, Lopez E, Castro AJ (2014) Modeling spatial distribution of European badger in arid landscapes: an ecosystem functioning approach. Landsc Ecol 29:843–855.

167. Ziolkowska E, Ostapowicz K, Radeloff VC (2014) Effects of different matrix representations and connectivity measures on habitat network assessments. Landsc Ecol 29:1551–1570.

168. Ma Q, Wu J, He C (2016) A hierarchical analysis of the relationship between urban impervious surfaces and land surface temperatures: spatial scale dependence, temporal variations, and bioclimatic modulation. Landsc Ecol 31:1139–1153.

169. Du P, Liu P, Xia J (2014) Remote Sensing image interpretation for urban environment analysis: Methods, system and examples. Remote Sens 6:9458–9474.

170. Hall SJ, Learned J, Ruddell B (2016) Convergence of microclimate in residential landscapes across diverse cities in the United States. Landsc Ecol 31:101–117.

171. Coops NC, Wulder MA (2019) Breaking the Habit(at). Trends Ecol Evol. doi: 10.1016/j.tree.2019.04.013. **A short review of species mapping and essential biodiversity variables derived from remote sensing data and classification techniques. Emphasizes the importance of using dynamic and continuous metrics for habitat mapping and outlines opportunities for using big data approaches.**

172. Sexton JO, Noojipady P, Anand A, Song X-P, McMahon S, Huang C, Feng M, Channan S, Townshend JR (2015) A model for the propagation of uncertainty from continuous estimates of tree cover to categorical forest cover and change. Remote Sens Environ 156:418–425.

173. Olofsson P, Foody GM, Herold M, Stehman SV, Woodcock CE, Wulder MA (2014) Good practices for estimating area and assessing accuracy of land change. Remote Sens Environ. 148:42–57.

174. Olofsson P, Foody GM, Stehman SV, Woodcock CE (2013) Making better use of accuracy data in land change studies: Estimating accuracy and area and quantifying uncertainty using stratified estimation. Remote Sens Environ. 129:122–31.

175. He KS, Bradley BA, Cord AF, Rocchini D, Tuanmu M-N, Schmidtlein S, Turner W, Wegmann M, Pettorelli N (2015) Will remote sensing shape the next generation of species distribution models? Remote Sens Ecol Conserv 1:4–18.

176. Bagan H, Yamagata Y (2015) Analysis of urban growth and estimating population density using satellite images of nighttime lights and land-use and population data. GISci Remote Sens 52:765–780.

177. Singh H, Garg RD, Karnatak HC, Roy A (2018) Spatial landscape model to characterize biological diversity using R statistical computing environment. J Environ Manage 206:1211–1223.

178. Cardille JA, Jackson MM (2017) Citizen science for assessing landscape change. Learning Landscape Ecology 41–42.

179. Dalla Mura M, Prasad S, Pacifici F, Gamba P, Chanussot J, Benediktsson JA (2015) Challenges and opportunities of multimodality and data fusion in remote sensing. Proc IEEE 103:1585–1601.

180. White JC, Coops NC, Wulder MA, Vastaranta M, Hilker T, Tompalski P (2016) Remote sensing technologies for enhancing forest inventories: A review. Can J Remote Sens 42:619–641.

181. Huang B, Zhao B, Song Y (2018) Urban land-use mapping using a deep convolutional neural network with high spatial resolution multispectral remote sensing imagery. Remote Sens Environ 214:73–86.

182. Olah G, Smith AL, Asner GP (2017) Exploring dispersal barriers using landscape genetic resistance modelling in scarlet macaws of the Peruvian Amazon. Landsc Ecol 32:445–456.

183. Haas J, Ban Y (2017) Mapping and monitoring urban ecosystem services using multitemporal high-resolution satellite data. IEEE J Sel Top Appl Earth Obs Remote Sens 10:669–680.

184. Heigl F, Horvath K, Laaha G (2017) Amphibian and reptile road-kills on tertiary roads in relation to landscape structure: using a citizen science approach with open-access land cover data. BMC Ecol. 17(24).

185. Thompson SD, Nelson TA, White JC (2015) Mapping dominant tree species over large forested areas using Landsat Best-Available-Pixel image composites. Can J Remote Sens 41:203–218.

186. Bishop-Taylor R, Tulbure MG, Broich M (2018) Evaluating static and dynamic landscape connectivity modelling using a 25-year remote sensing time series. Landsc Ecol 33:625–640.

Preface to Chapter 3

In Chapter 2, I identified core methodologies from both landscape ecology and remote sensing for analyzing landscape change and disturbances over space and time. Chapter 3 examines one aspect of landscape change and disturbance mapping by creating a prototype for reconstructing fire progression maps for a single large fire over space and time.

By reviewing approaches for mapping disturbances over time in Chapter 2, I can integrate remote sensing and computational landscape ecology methodologies in Chapter 3 to track fires using multi-source, open-access Earth observations. Chapter 3 advances the fields of remote sensing and landscape ecology by illustrating the opportunities for using multi-source data fusion to reconstruct burned-area progressions in geospatial data time series.

Chapter 3 was published in 2019 in *Remote Sensing Letters* and uses the Chicago (author-date) citation style.

3. Multi-sensor, multi-scale, Bayesian data synthesis for mapping within-year wildfire progression

Authors:

Morgan A. Crowley[a*]

Jeffrey A. Cardille[a]

Joanne C. White[b]

Michael A. Wulder[b]

[a]*Department of Natural Resource Sciences*

McGill University

21,111 Lakeshore Road

Ste.-Anne-de-Bellevue, Québec, Canada

[b]*Canadian Forest Service (Pacific Forestry Centre)*

Natural Resources Canada

506 Burnside Road West

Victoria, British Columbia, Canada

*Corresponding Author: morgan.crowley@mail.mcgill.ca

Journal: Remote Sensing Letters

Publication date: 2019

Full citation: Morgan A. Crowley, Jeffrey A. Cardille, Joanne C. White & Michael A. Wulder (2019) Multi-sensor, multi-scale, Bayesian data synthesis for mapping within-year wildfire progression, Remote Sensing Letters, 10:3, 302-311, DOI: 10.1080/2150704X.2018.1536300

Keywords: fire mapping, disturbance, multi source, data fusion, British Columbia, Landsat, Sentinel-2, MODIS, Google Earth Engine, BULC

Abstract

As freely available remotely sensed data sources proliferate, the ability to combine imagery with high spatial and temporal resolutions enables applications aimed at near-term disturbance detection. In this case study, we present methods for synthesizing burned-area information from multiple sources to map the active phase of the Elephant Hill fire from the 2017 fire season in British Columbia. We used the Bayesian Updating of Land Cover (BULC) algorithm to merge burned-area classifications from a range of remote-sensing sources such as Landsat-8, Sentinel-2, and MODIS. We created provisional classifications by comparing the post-fire Normalized Burn Ratio against pre-fire image composite within the fire boundary provided by the Province of British Columbia. BULC fused the classifications in Google Earth Engine, producing a cohesive time-series stack with updated burned areas for 19 distinct days. The fire burned unevenly throughout its lifespan: a rapid burn phase of 53,097 ha in two weeks by late July, a steady burn phase to 60,000 ha until late August, an accelerated burn phase of 95,766 ha until mid-September, and containment at 203,560 ha in October. The highly automated methods presented herein can synthesize multi-source fire classifications for active phase monitoring both retrospectively and in near-real-time.

3.1 Introduction

Forest disturbance mapping has been made possible for Canada through the Composite-to-Change (C2C) protocol, which uses annual proxy best-available-pixel (BAP) composites across the 30 m Landsat record (Hermosilla et al. 2016; 2017; White et al. 2017). BAP composites enable cloud and gap-free observations while ensuring that similar illumination and growing conditions (August 1 ± 30 days) are represented across years (White et al. 2014). Using these data, the average area burned annually by wildfire in Canada (1985-2010) is estimated to be 1.6 Mha (σ =1.1 Mha, where σ denotes the standard deviation). Operationally, annual data is acquired by provincial and territorial fire management agencies to track the location, size, and cause of wildfires, among other attributes. These jurisdictional data are compiled with other sources to produce the Canadian National Fire Database (CNFDB; Amiro et al. 2001; Stocks et al. 2003; Parisien et al. 2006; Burton et al. 2008). The CNFDB, which typically does not exclude unburned islands and water bodies from its fire perimeters, estimates an average annual area burned of 2.3 Mha (σ =1.9 Mha; White et al. 2017). While both C2C and CNFDB provide estimates of burned area, there are opportunities to augment and further refine burned-area estimates using data from multiple earth observing satellites.

Individual sensors have been used to detect characteristics of forest fires, creating retrospective maps of burned area at a variety of spatial resolutions. For example, the MODIS Collection 6 MCD64A1 global burned area product provides geographic locations and timing of fires at 500 m spatial resolution derived using a burn-sensitive vegetation index (Giglio et al. 2015; Humber et al. 2018). MODIS-derived products provide high temporal but low spatial resolution for monitoring fires, and spatial interpolation techniques have been used to downscale its coarse resolution for fire analyses across North American forests (de Groot et al. 2007; de Groot, Pritchard, and Lynham 2009; Parisien et al. 2011; Parks, Parisien, and Miller 2012; Parks 2014). For Canadian boreal forests, the Normalized Burn Ratios (NBR) and the differenced pre-disturbance and post-disturbance NBRs (dNBR) are reliable estimators of burned areas (Key and Benson 2006; Hall et al. 2008; Soverel, Perrakis, and Coops 2010, Soverel et al. 2011; Hermosilla et al. 2016, 2017; White et al. 2017; Frazier et al. 2018). The NBR and dNBR have been used with fine-scale Landsat time series to detect stand-replacing fires in Canadian forested ecosystems at annual time steps (e.g., Schroeder et al. 2011; Hermosilla et al. 2016; 2017; San-Miguel, Andison and Coops 2017; White et al. 2017; Frazier et al. 2018; San-Miguel, Andison and Coops 2018). In a few cases, observations from multiple sensors have been combined to enable retrospective mapping. For example, the dNBR can be calculated from pre-fire Landsat-8 and post-fire Sentinel-2 observations (Quintano, Fernández-Manso, and Fernández-Manso 2018). These retrospective maps of extinguished fires are useful for managers (Roy et al. 2005; Lentile et al. 2006; San-Miguel, Andison and Coops 2017), but the rapid spread and associated smoky conditions render near-term classification of a fire's rapidly changing extent difficult.

Recent developments suggest that information from multiple satellites can be combined at greater temporal resolution not only for retrospective mapping but also for estimating fire growth while the fire is still active. Until very recently, the density of available data was such that fine-scale near-real-time monitoring of fires was impractical due to high costs and sparse frequencies of observations. Fusing observations from multiple sources advance the possibility of monitoring in near-real-time (Li and Roy 2017; Wulder et al. 2018), such as during the active phase of fires. The Bayesian Updating of Land Cover (BULC) algorithm synthesizes classifications of individual images through time by weighing evidence from multiple classifications to produce a time series of land undergoing rapid change (Cardille and Fortin 2016). BULC records the land-use land-cover (LULC) history for each class of stability and change across large areas, allowing users to view the trajectory and probability of any pixel in the image calculated using Bayes' Theorem. In this letter, we demonstrate how combining observations from multiple sensors can facilitate the mapping of active fires. This fusion takes advantage of the growing frequency and quality of sensors with different spectral and spatial characteristics, capturing near-real-time growth patterns of long-lived fires to inform managers and planners interested in fire risk, spread, and impact.

3.2 Materials and Methods

3.2.1 Study Area

The 2017 fire season was the largest on record for British Columbia (BC) and mapping these fires is important for monitoring forest-disturbance impacts, with considerations related to timber supply, carbon consequences, and animal habitat. One of the largest fires was the Elephant Hill fire, also known as the Ashcroft fire (K20637). This fire started on July 11, 2017, north of Ashcroft, British Columbia and was contained by October 2. The Elephant Hill fire's eventual perimeter grew to 511 km, based upon data shared by the British Columbia Wildfire Service. The final burned area within this perimeter was reported to be 192,016 ha, damaging infrastructure in addition to forested lands (BC Wildfire Service 2017a; BC Wildfire Service 2017b). For context, the final burned area of this individual fire was two-thirds of the cumulative burned area for the entire 2015 fire season (280,738 ha burned by 1,858 fires), and double that of the total area burned in the 2016 fire season (102,019 ha burned by 1,050 fires; BC Wildfire Service 2017c).

3.2.2 Provisional classifications using Landsat-8 OLI, Sentinel-2 and MODIS

Images intersecting the Elephant Hill fire perimeter from summer and autumn 2017 were identified for classification in Google Earth Engine, a cloud-based platform for accessing and processing satellite imagery and geospatial datasets (Gorelick et al. 2017). Differences over the dNBR threshold outlined in Hall et al. (2008) were classified as 'Burned/Burning'; those below the threshold were classified as ‘Unburned’ at that time step (e.g., Frazier et al. 2018). The treatment of each of the relevant sensors—Landsat-8, Sentinel-2, and MODIS—differed slightly and are described below.

Landsat-8: We computed the pre-fire NBR using a 2016 BAP gap-free reflectance composite that was generated following the C2C approach (e.g., White et al. 2014; 2017; Hermosilla et al. 2016; 2017). To compare with the pre-fire status, we identified 10 Landsat-8 surface reflectance images from six different dates, with each image having less than 10% cloud cover. We masked clouds and haze before classification using the pixel-level Quality Assurance (QA) band (Zhu 2017; Egorov et al. 2018; USGS 2018). We differenced the NBR of each image with the pre-fire NBR to produce six dated provisional classifications for use in BULC.

Sentinel-2: We identified 33 Sentinel-2 (A and B) images with less than 10% cloud cover on 11 distinct dates, for classification and use in BULC. In Earth Engine, we generated a pre-fire best-available-pixel image using similar pixel selection criteria as used in C2C. We then calculated the pre-fire NBR values for each pixel for comparison to each image's post-fire NBR values. Because observations from Sentinel-2 are provided in UTM tiles smaller than the study area, we mosaicked the Sentinel-2 images for each distinct day before classification then masked clouds and haze using the QA band of Sentinel-2 observations. The result was 11 date-specific classifications that were used as inputs in BULC.

MODIS: We identified monthly summaries of burned areas from the MODIS Collection 6 MCD64A1 burned area product, for classification and use in BULC (Giglio et al. 2015; Humber et al. 2018). This raster data product detects day-of-burning globally at 500 m resolution with an average uncertainty of 4.3 days and a processing delay between 1.5 to 3 months for the Elephant Hill fire. Because the burned-area product contains the detected burn date in each of the three monthly images, we reclassified these MODIS burned-area products into Burned/Burning and Unburned layers in 15-day summaries. The result was six date-specific summary classifications that were used as inputs to BULC.

Across the three sources, there were 23 provisional classifications of burned area from 19 distinct imaging dates during the study period. Using observations from multiple remote sensing sources greatly reduced the revised interval considered across the portfolio of sensors., we were able to increase the frequency of observations to reduce the temporal revisit intervals provided by the sensors (e.g., Li and Roy 2017). The six Landsat-8 surface reflectance classifications, eleven Sentinel-2 classifications, and six MODIS bi-weekly classifications were ordered by date and used as provisional classification inputs in the BULC algorithm for the Elephant Hill fire study area, outlined in Table 3.1. The combined sensors imaged each pixel an average of 19.5 times between July 5 and October 30, with the entire study area having been imaged at least once in 13 of the 15 weeks that the fire burned.

Table 3.1 Satellite source and acquisition dates for Elephant Hill fire observations, whether MODIS, Landsat-8, or Sentinel-2, that were used as inputs in BULC.

	July				August						September					October			
	5	14	20	30	4	6	11	19	22	26	3	15	16	18	28	3	5	10	30
Landsat-8	×	×		×		×			×				×						
Sentinel-2					×	×	×			×		×			×	×	×	×	×
MODIS	×		×		×			×			×			×					

3.2.3 BULC

To synthesize the information from these three different sensors, we used the BULC algorithm (Cardille and Fortin 2016). BULC applies Bayes' Theorem to interpret a series of time-ordered provisional classifications, synthesizing a time series that shows change and stability in the study area at the per-pixel level. To gauge the reliability of a given provisional classification to the construction of the time series, BULC compares each new classification—from any data source—against the previous classification in the time stack. Using the Producer's Accuracy as the conditional probabilities in Bayes' Theorem, BULC traces the probability of both classes through time. As detailed in Cardille and Fortin (2016), BULC can synthesize moderate-quality classifications over short time intervals to track rapidly changing landscapes. BULC tolerates occasional errors (i.e., resulting from smoke, clouds), and is thereby an ideal fusion algorithm for active-phase fire classification. BULC is able to quantify the burned and burning area of a fire at intermediate time steps between the beginning and end of individual fire events utilizing the dense stack of relatively clear provisional classifications from Landsat-8, Sentinel-2, and MODIS in Google Earth Engine.

3.3 Results

The Elephant Hill fire burned unevenly throughout its active phase: rapid escalation in late July, slow and steady growth until late August, an accelerated phase until mid-September, and containment by October (Figure 3.1).

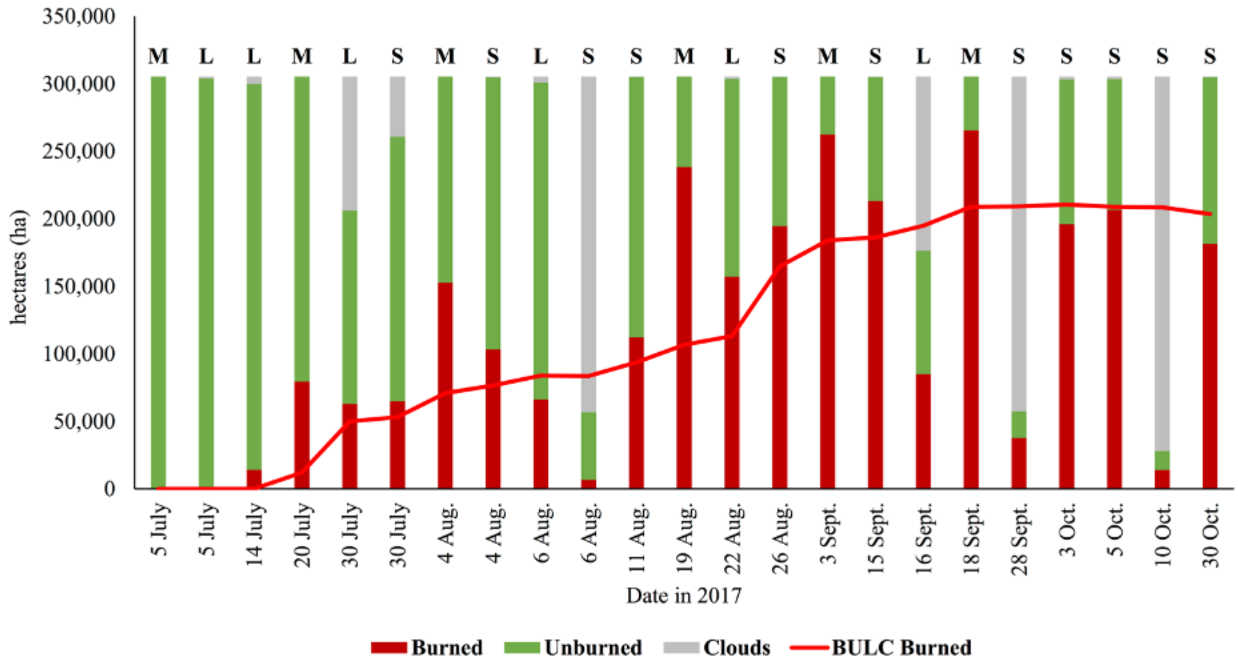

Figure 3.1 Growth in Elephant Hill burned area through time as synthesized in BULC from Landsat-8 (L), Sentinel-2 (S), and MODIS (M). The line indicates BULC estimated Burned/Burning area through time, while bars show the high variability among provisional classifications from each sensor.

BULC synthesizes provisional input classifications from the active phase of the fire, which allows per-pixel burn detection within the British Columbia fire-event perimeter at the collection date of each event. Figure 3.2 shows the final fire perimeter delineated by the British Columbia Wildfire Service superimposed on the BULC burned-area estimates for the Elephant Hill fire at the following time steps: July 5 (*a*), July 30 (*b*), August 26 (*c*), and October 30 following 100% containment (*d*). Figure 3.2(*b*) is the product of five images over 3.5 weeks and shows fire growth from 461 ha on July 20 to 50,122 ha on July 30. Figure 3.2(*c*) shows the BULC classification that results in 14 images over 7.5 weeks, showing a fire growth from 113,103 ha on August 22 to 164,738 ha on August 26. Figure 3.2(*d*) shows the final BULC classification of Burned/Burning pixels within the BC polygon after the fire had been 100% contained. The BULC Burned/Burning area covers 67% of the British Columbia fire agency polygon, amounting to 203,560 burned ha, 6% higher than the estimated 192,016 burned ha (BC Wildfire Service 2017a; BC Wildfire Service 2017b).

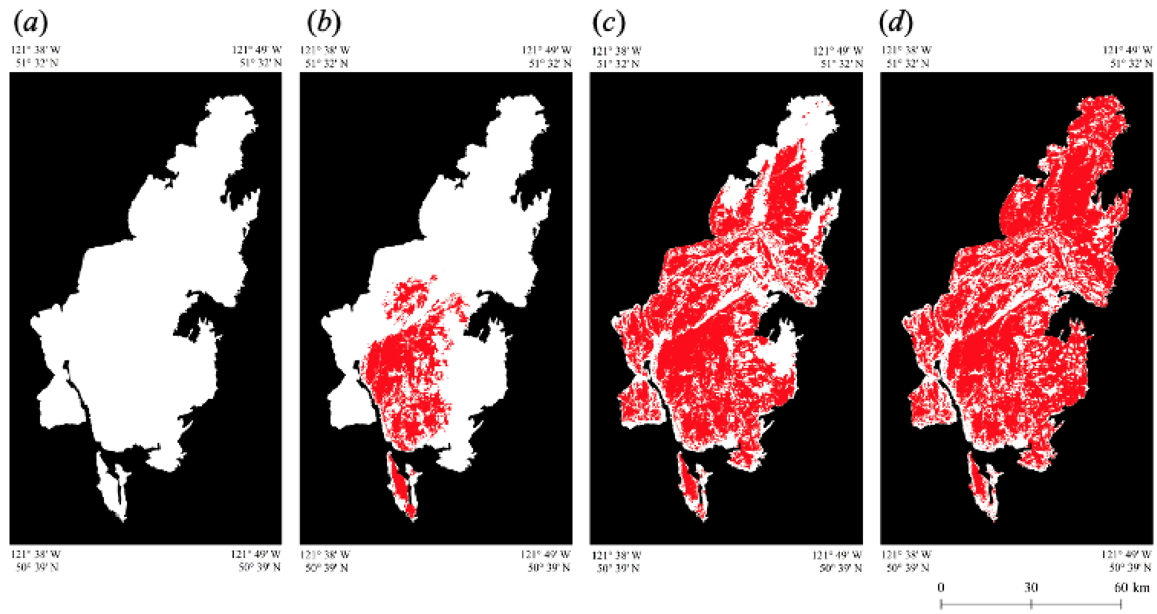

Figure 3.2 BULC burned-area classification estimates in red within the BC Elephant Hill fire perimeter on dates July 5 (a), July 30 (b), August 26 (c), October 30 (d).

The BULC fire classifications detect unburned pixels within the BC fire perimeter. Figure 3.3 compares zoomed regions of the final MODIS burned-area summary with the final BULC classifications for the Elephant Hill fire. The MODIS burned area shown in Figure 3.3(*a*) compared with the final BULC classification shown in Figure 3.3(*b*) emphasizes the unburned pixels within the fire-event perimeter. Additionally, based upon inputs from Landsat and Sentinel-2, BULC identifies Burned/Burning pixels at a finer spatial resolution than the MODIS dataset. The MODIS burned area, shown in Figure 3.3(*c*), detects unburned pixels with a coarser resolution than the fine spatial resolution of the final BULC classification in Figure 3.3*(d*).

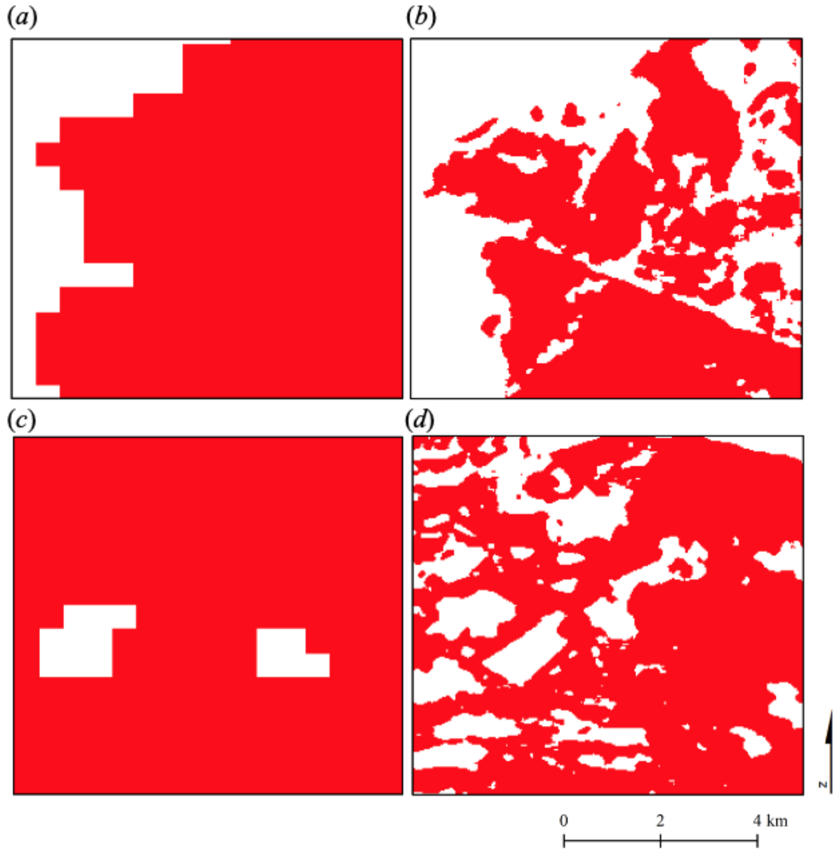

Figure 3.3 Post-fire, final MODIS Collection 6 MCD64A1 burned pixels zoomed to 500 m following October 30, 2017 centred on 121° 29' W, 50° 55' N (a) compared with the final BULC classification (b); post-fire, final MODIS Collection 6 MCD64A1 burned pixels centred on 121° 9' W, 51° 0' N (c) compared with the final BULC classification (d). The multi-sensor approach of the final BULC classification refines the edges of both burned and unburned objects present in the coarser MODIS Collection 6 MCD64A1 dataset.

As BULC processed provisional input classifications, the new information contained therein updated the synthesized classification of the burned area, as shown in Figure 3.4. As the fire progressed through the area surrounding -120.933, 51.286, MODIS-based provisional classification from September 3 changed the probability of fire from around 38% to 62%, high enough to tip the estimated LULC to Burned/Burning in Figure 3.4(*a*). The next view of the area, Sentinel-based provisional classification from September 15 confirmed most of the September 3 classification and changed the probabilities of many of the pixels to be 70% in Figure 3.4(*b*), which classified the LULC to Burned/Burning in those corresponding pixels. The subsequent view of the area (imperfect Landsat-based provisional classification from September 16) refined the BULC classification further. The newly burned pixels in the northwest had a probability of being Burned/Burning around 58% and therefore were captured as Burned/Burning in the BULC classification, and the nearby pixels in the southwest that had not been classified as Burned/Burning were between 24% and 44% probability in Figure 3.4(*c*).

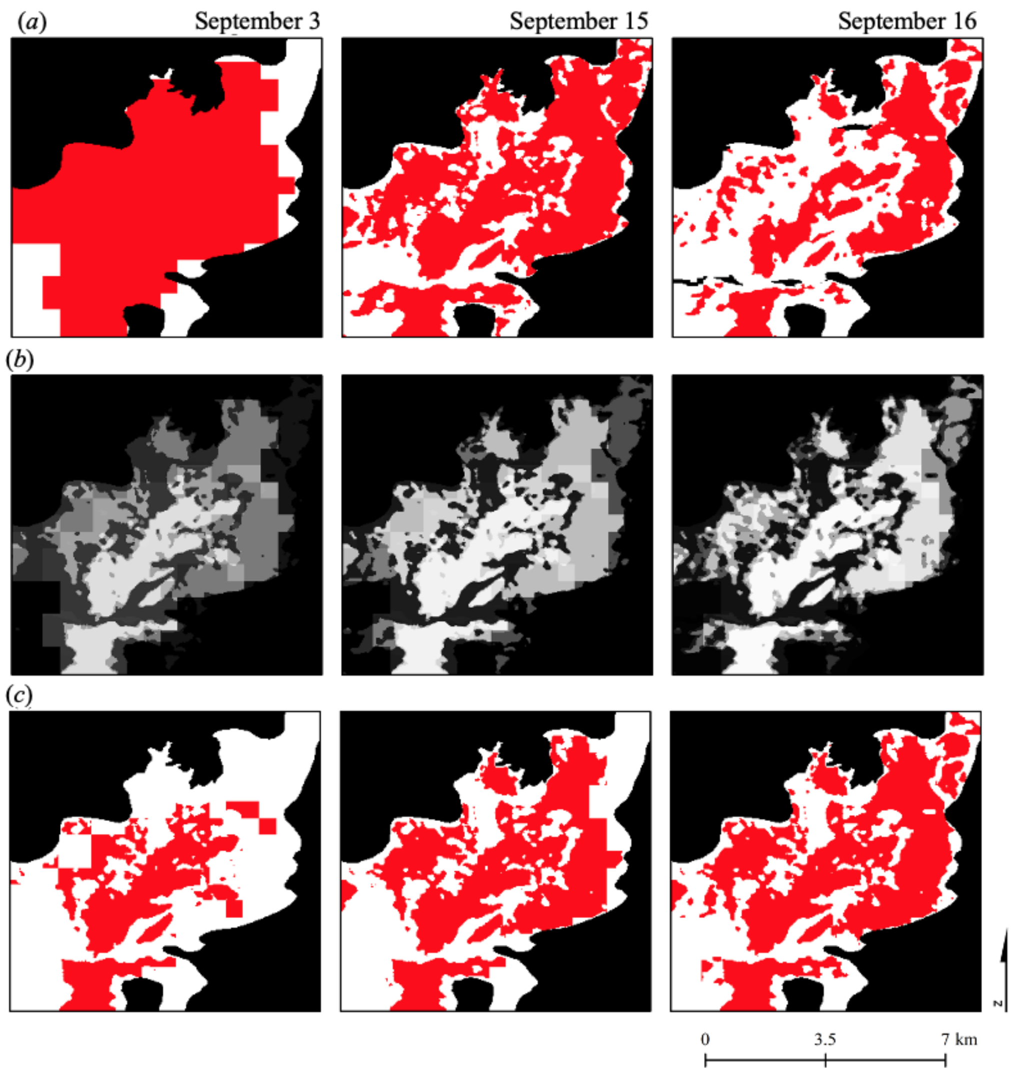

Figure 3.4 As the fire progresses in this region (zoomed on 120° 59' W, 51° 17' N) from September 3 to September 16, the imperfect provisional classifications in row (a) provide evidence of Burned/Burning to influence the per-pixel probabilities in row (b) (lighter gradient depicts larger probabilities), and the updated probabilities classify the pixels as Burned/Burning in the BULC classification in row (c).

3.4 Discussion

In this study, we have demonstrated a highly automated approach for combining accessible data products for active fire monitoring. The application of the BULC algorithm on dNBR and other burned-area classifications provides a seamless and multi-sensor method for synthesis of burned-area observations. This method combines observations from disparate data sources to increase the frequency of usable images to work towards near-real-time detection of burned areas during the fire's active phase. Additional methodological novelty is demonstrated by the capacity to increase temporal revisit rates supporting the reconstruction of active fire lifespans to better understand fire growth and underlying drivers with high temporal frequency and fine spatial resolution.

In this case study, we found that observations from each sensor contributed to the time series tracking the growth of the Elephant Hill fire, thus supporting the fusion of multi-sensor observations to expand near-real-time burned-area detection (Hilker et al. 2009a; 2009b; Wulder et al. 2010; Li and Roy 2017; Wulder et al. 2018). Relying exclusively on Landsat-8 input classifications, our fire time series would be limited to burn detection primarily early in the active fire phase. Similarly, using only input classifications from Sentinel-2, the fire time step would be limited to burn detection after the first major growth in late July. Lastly, utilizing only MODIS burned area data would have caused over-classification of burned areas with coarse pixel resolution (Fraser et al. 2004; White et al. 2017). Even though BULC was able to create a credible time series using these sources, it was not quite real-time mapping: the density of data limited the BULC classification of the fire's burned area to about a 1-week delay. Because BULC is not limited to any set of sensors, as additional imagery becomes available the time series can become more narrowly timed, perhaps to a sub-weekly time series.

The findings of this research provide a method for synthesizing burned-area classifications from multiple sources with varying scales and resolutions, including single-date remote sensing, burned-area detection algorithms, and jurisdictionally produced fire perimeters. For reconstructing the British Columbia 2017 fire season, there are observations available from other platforms (e.g., Landsat-7, Sentinel-3) that BULC could also incorporate imagery to create a sub-weekly time series. Due to the portability of the post-classification synthesis approach presented, future studies can apply these methods to create temporally dense fire-classification stacks for burned-area detection whether analysing fires in near-real-time or retrospectively.

Acknowledgments

This research was undertaken as part of the 'Earth Observation to Inform Canada's Climate Change Agenda (EO3C)' project jointly funded by the Canadian Space Agency (CSA), Government Related Initiatives Program (GRIP), and the Canadian Forest Service (CFS) of Natural Resources Canada. This research was enabled in part by support provided by WestGrid (www.westgrid.ca) and Compute Canada (www.computecanada.ca).

Declaration of interest statement

No potential conflict of interest was reported by the authors

3.5 References

Amiro, B. D., J. B. Todd, B. M. Wotton, K. A. Logan, M. D. Flannigan, B. J. Stocks, J. A. Mason, D. L. Martell, and K. G. Hirsch. 2001. "Direct carbon emissions from Canadian forest fires, 1959 to 1999." *Canadian Journal of Forest Research* 31: 512–525.

BC Wildfire Service. 2017a. “Wildfires of note - Elephant Hill (K20637)." http://bcfireinfo.for.gov.bc.ca/hprScripts/WildfireNews/OneFire.asp?ID=620

BC Wildfire Service. 2017b. “PROT_CURRENT_FIRE_POLYS_SP” (dataset). Ministry of Forests, Lands, Natural Resource Operations and Rural Development. Accessed January 25, 2018. https://catalogue.data.gov.bc.ca/dataset/fire-perimeters-current

BC Wildfire Service. 2017c. “Wildfire season summary." https://www2.gov.bc.ca/gov/content/safety/wildfire-status/about-bcws/wildfire-history/wildfire-season-summary

Burton, P. J., M. A. Parisien, J. A. Hicke, R. J. Hall, and J. T. Freeburn. 2008. “Large fires as agents of ecological diversity in the North American boreal forest.” *International Journal of Wildland Fire* 17(6): 754–767.

Cardille, J. A., and J. Fortin. 2016. “Bayesian updating of land cover estimates in a data-rich environment.” *Remote Sensing of Environment* 186: 234–249.

de Groot, W. J., J. M. Pritchard, and T. J. Lynham. 2009. "Forest floor fuel consumption and carbon emissions in Canadian boreal forest fires." *Canadian Journal of Forest Research* 39: 367–382. doi:10.1139/X08-192

de Groot, W. J., R. Landry, W. A. Kurz, K. R. Anderson, P. Englefield, R. H. Fraser, R. J. Hall, E. Banfield, D. A. Raymond, V. Decker, T. J. Lynham, and J. M. Pritchard. 2007. "Estimating direct carbon emissions from Canadian wildland fires." *International Journal of Wildland Fire* 16: 593–606. doi:10.1071/ WF06150

Egorov, A. V., D. P. Roy, H. K. Zhang, M. C. Hansen, and A. Kommareddy. 2018. “Demonstration of percent tree cover mapping using Landsat Analysis Ready Data

(ARD) and sensitivity with respect to Landsat ARD processing level." *Remote Sensing* 10(2): 209.

Fraser, R. H., R. J. Hall, R. Landry, T. Lynham, D. Raymond, B. Lee, and Z. Li. 2004. "Validation and calibration of Canada-wide coarse resolution satellite burned-area maps." *Photogrammetric Engineering & Remote Sensing* 70: 451–460.

Frazier, R. J., N. C. Coops, M. A. Wulder, T. Hermosilla, and J. C. White. 2018. "Analyzing spatial and temporal variability in short-term rates of post-fire vegetation return from Landsat time series." *Remote Sensing of Environment* 205: 32–45.

Giglio, L., C. Justice, L. Boschetti, and D. Roy. 2015. "MCD64A1 MODIS/Terra+Aqua Burned Area Monthly L3 Global 500m SIN Grid V006" (dataset). NASA EOSDIS Land Processes DAAC. Accessed March 1, 2018. https://doi.org/10.5067/MODIS/MCD64A1.006

Gorelick, N., M. Hancher, M. Dixon, S. Ilyushchenko, D. Thau, and R. Moore. 2017. "Google Earth Engine: Planetary-scale geospatial analysis for everyone." *Remote Sensing of Environment* 202: 18–27.

Hall, R. J., J. T. Freeburn, W. J. de Groot, J. M. Pritchard, T. J. Lynham, and R. Landry. 2008. "Remote sensing of burn severity: experience from western Canada boreal fires." *International Journal of Wildland Fire* 17(4): 476–489.

Hermosilla, T., M. A. Wulder, J. C. White, N. C. Coops, G. W. Hobart, and L. B. Campbell. 2016. "Mass data processing of time series Landsat imagery: pixels to data products for forest monitoring." *International Journal of Digital Earth* 9(11): 1035–1054.

Hermosilla, T., M. A. Wulder, J. C. White, N. C. Coops, and G. W. Hobart. 2017. "Updating Landsat time series of surface-reflectance composites and forest change products with new observations." *International Journal of Applied Earth Observation and Geoinformation* 63: 104–111.

Hilker, T., M. A. Wulder, N. C. Coops, J. Linke, G. McDermid, J. G. Masek, F. Gao, and J. C. White. 2009a. "A new data fusion model for high spatial-and temporal-resolution mapping of forest disturbance based on Landsat and MODIS." *Remote Sensing of Environment* 113(8): 1613–1627.

Hilker, T., M. A. Wulder, N. C. Coops, N. Seitz, J. C. White, F. Gao, J. G. Masek, and G. Stenhouse. 2009b. "Generation of dense time series synthetic Landsat data through data blending with MODIS using a spatial and temporal adaptive reflectance fusion model." *Remote Sensing of Environment* 113(9): 1988–1999.

Humber, M. L., L. Boschetti, L. Giglio, and C. O. Justice. 2018. "Spatial and temporal intercomparison of four global burned area products." *International Journal of Digital Earth* 1–25.

Key, C. H., and N. C. Benson. 2006. *Landscape assessment: sampling and analysis methods.* General Technical Report RMRS-GTR-164-CD, Fort Collins, CO: US Department of Agriculture, Forest Service, Rocky Mountain Research Station.

Lentile, L. B., Z. A. Holden, A. M. Smith, M. J. Falkowski, A. T. Hudak, P. Morgan, S. A. Lewis, P. E. Gessler, and N. C. Benson. 2006. "Remote sensing techniques to assess active fire characteristics and post-fire effects." *International Journal of Wildland Fire* 15(3): 319–345.

Li, J., and D. P. Roy. 2017. "A global analysis of Sentinel-2A, Sentinel-2B and Landsat-8 data revisit intervals and implications for terrestrial monitoring." *Remote Sensing* 9(9): 902.

Parisien M. A., S. A. Parks, C. Miller, M. A. Krawchuk, M. Heathcott, and M. A. Moritz. 2011. "Contributions of ignitions, fuels, and weather to the burn probability of a boreal landscape." *Ecosystems* 14: 1141–1155. doi:10.1007/S10021-011-9474-2

Parisien, M. A., V. S. Peters, Y. Wang, J. M. Little, E. M. Bosch, and B. J. Stocks. 2006. "Spatial patterns of forest fires in Canada 1980–1999." *International Journal of Wildland Fire* 15: 361–374.

Parks, S. A. 2014. "Mapping day-of-burning with coarse-resolution satellite fire-detection data." International Journal of Wildland Fire 23: 215–223.

Parks, S. A., M. A. Parisien, and C. Miller. 2012. "Spatial bottom-up controls on fire likelihood vary across western North America." *Ecosphere* 3(12). doi:10.1890/ES11-00298.1

Quintano, C., A. Fernández-Manso, and O. Fernández-Manso. 2018. "Combination of Landsat and Sentinel-2 MSI data for initial assessing of burn severity." *International Journal of Applied Earth Observation and Geoinformation* 64: 221–225.

Roy, D. P., Y. Jin, P. E. Lewis, and C. O. Justice. 2005. "Prototyping a global algorithm for systematic fire-affected area mapping using MODIS time series data." *Remote Sensing of Environment* 97(2):137–162.

San-Miguel, I., D. W. Andison, and N. C. Coops. 2017. "Characterizing historical fire patterns as a guide for harvesting planning using landscape metrics derived from long term satellite imagery." *Forest Ecology and Management* 399: 155–165. doi:10.1016/j.foreco.2017.05.021.

San-Miguel, I., D. W. Andison, and N. C. Coops. 2018. "Quantifying local fire regimes using the Landsat data-archive: a conceptual framework to derive detailed fire pattern metrics from pixel-level information.” *International Journal of Digital Earth* doi:10.1080/17538947.2018.1464072

Schroeder, T. A., M. A. Wulder, S. P. Healey, and G. G. Moisen. 2011. "Mapping wildfire and clearcut harvest disturbances in boreal forests with Landsat time series data." *Remote Sensing of Environment.* 115(6): 1421–1433.

Soverel, N. O., D. D. Perrakis, and N. C. Coops. 2010. “Estimating burn severity from Landsat dNBR and RdNBR indices across western Canada.” *Remote Sensing of Environment* 114(9): 1896–1909.

Soverel, N. O., N. C. Coops, D. D. Perrakis, L. D. Daniels, and S. E. Gergel. 2011. “The transferability of a dNBR-derived model to predict burn severity across 10 wildland fires in western Canada.” *International Journal of Wildland Fire* 20(4): 518–531.

Stocks, B. J., J. A. Mason, J. B. Todd, E. M. Bosch, B. M. Wotton, B. D. Amiro, M. D. Flannigan, K. G. Hirsch, K. A. Logan, D. L. Martell, and W. R. Skinner. 2003. “Large forest fires in Canada, 1959–1997.” *Journal of Geophysical Research* 108(D1: FFR5): 1–12. doi:10.1029/2001 JD000484

U. S. Geological Survey. 2018. *U.S. Landsat Analysis Ready Data (ARD) Data Format Control Book (DFCB*). LSDS-809, Sioux Falls, SD: US Department of Interior, Earth Resources Observation and Science (EROS) Center. Accessed April 15, 2018. https://landsat.usgs.gov/sites/default/files/documents/LSDS-1873_US_Landsat_ARD_DFCB.pdf

White, J. C., M. A. Wulder, G. W. Hobart, J. E. Luther, T. Hermosilla, P. Griffiths, N. C. Coops, R. J. Hall, P. Hostert, A. Dyk, and L. Guindon. 2014. "Pixel-based image compositing for large-area dense time series applications and science." *Canadian Journal of Remote Sensing* 40(3): 192–212.

White, J. C., M. A. Wulder, T. Hermosilla, N. C. Coops, and G. W. Hobart. 2017. "A nationwide annual characterization of 25-years of forest disturbance and recovery for Canada using Landsat time series." *Remote Sensing of Environment* 194: 303–321.

Wulder, M. A., J. C. White, M. D. Gillis, N. Walsworth, M. C. Hansen, and P. Potapov. 2010. "Multiscale satellite and spatial information and analysis framework in support of a large-area forest monitoring and inventory update." *Environmental Monitoring and Assessment* 170(1–4): 417–433.

Wulder, M. A., N. C. Coops, D. P. Roy, J. C. White, and T. Hermosilla. 2018. "Land cover 2.0." *International Journal of Remote Sensing* 39(12): 4254–4284. doi:10.1080/01431161.2018.1452075

Zhu, Z. 2017. "Change detection using Landsat time series: A review of frequencies, preprocessing, algorithms, and applications." *ISPRS Journal of Photogrammetry and Remote Sensing* 130: 370–384.

Preface to Chapter 4

In Chapter 3, I prototyped a method for reconstructing the Elephant Hill fire's progression using multi-source, open-access satellite data with a Bayesian synthesis algorithm in Google Earth Engine. Chapter 3 was a novel contribution to the field because it used both multi-source data and a cloud-based processing platform to support future wildfire monitoring with all available open-access data. Chapter 3 served as a prototype for Chapter 4, where this approach will be used to reconstruct burn progressions for 89 stand-replacing fires from the 2017 British Columbia fire season.

Building upon the methods presented in Chapter 3, I apply the Bayesian synthesis algorithm on over 1500 observations from four satellite sensors with a sub-weekly temporal resolution. I employ an image segmentation approach in the provisional burned classification creation before Bayesian fusion, thus illustrating future opportunities for working in an object-based rather than pixel-based burned-area mapping framework. I also use these fire progressions to create fire and fire season progression metrics, making Chapter 4 a novel contribution to the field of remote sensing and fire science.

Chapter 4 was published in 2019 in *Remote Sensing of Environment* and uses the Harvard citation style.

4. Generating intra-year metrics of wildfire progression using multiple open-access satellite data streams

Authors:

Morgan A. Crowley[a*]

Jeffrey A. Cardille[a]

Joanne C. White[b]

Michael A. Wulder[b]

[a]*Department of Natural Resource Sciences*

McGill University

21,111 Lakeshore Road

Ste.-Anne-de-Bellevue, Québec, Canada

[b]*Canadian Forest Service (Pacific Forestry Centre)*

Natural Resources Canada

506 Burnside Road West

Victoria, British Columbia, Canada

*Corresponding Author: morgan.crowley@mail.mcgill.ca

Journal: Remote Sensing of Environment

Special Issue: Remote sensing of land change science with Google Earth Engine

Publication date: 2019

Full citation: Crowley, M. A., Cardille, J. A., White, J. C., & Wulder, M. A. (2019). Generating intra-year metrics of wildfire progression using multiple open-access satellite data streams. *Remote Sensing of Environment*, 232, 111295. https://doi.org/10.1016/j.rse.2019.111295.

Keywords: fire mapping, disturbance, multi source, data fusion, British Columbia, Landsat, Sentinel-2, MODIS, Google Earth Engine, BULC

Highlights

- Retrospective and near real-time wildfire maps using data from multiple sensors
- Bayesian-synthesized Earth observation data for mapping wildfire progression
- Daily and weekly fire progression metrics to quantify and characterize fire behaviour
- 35-week time series provided updated weekly burned areas for 89 fires in 2017.
- Each pixel within a fire perimeter observed an average of 34 times April–December.

Abstract

The 2017 fire season was one of the largest on record for British Columbia (BC), Canada, in terms of total area burned (estimated 1.2 million hectares), affecting the safety and air quality of numerous communities. Moreover, fires of this number and extent alter the wood supply for harvesting, the nature of habitat for wildlife, and can affect regional and national carbon budgets. As a result, it is important to map these fires accurately and to monitor within-year fire progression in order to quantify the resulting forest-disturbance impacts fully. The Bayesian Updating of Land Cover (BULC) algorithm was used to merge burned-area classifications of individual fires from a range of remote sensing sources such as Landsat-7, Landsat-8, Sentinel-2, and MODIS (MCD64A1) burned-area dataset. Together, these provisional classifications imaged each pixel within a known fire perimeter an average of 33.8 times between April 1 and December 1. The resulting 35-week time-series stack had updated weekly burned areas for each of the 89 fires in BC in 2017. Province-wide fire progression was variable throughout the period analyzed, characterized by a steady burn phase of 41,437 ha (5% of total area burned) over a two-week period in early July, an accelerated burn phase of 149,422 ha (17%) from mid-July to early August, another steady burn phase of 218,079 ha (24%) for one month until early

September, and a second accelerated burn phase of 301,931 ha (34%) over two weeks in late September with subsequent steady growth of 180,119 ha (20%) over 1.5 months until containment in late October. Herein, we demonstrate how such temporally dense fire classification stacks can be used to analyze fire progression over the course of a fire season (both retrospectively and in near-real time) providing useful metrics to characterize and compare fire events. End-of-season burned-area estimates correspond with estimates derived from the National Burned Area Composite (NBAC) product that is generated retrospectively from fire best-available mapping approaches. This rapid interpretation of information enables the analysis of suppression success and potential drivers of fires spread while facilitating analyses of carbon budget consequences as well as impacts to communities and timber supply.

4.1 Introduction

In 2017, British Columbia (BC), Canada, faced its most severe fire season to date in terms of total area burned. Due to the severity of the wildfires, BC was in an official State of Emergency from July 7 to September 15, the longest-running State of Emergency in the history of the province (British Columbia, 2018). Single fires such as the Plateau fire grew to be quadruple the size of the total area burned in the 2016 BC fire season and a quarter of the long-term annual mean burned area for all of Canada (BC Wildfire Service, 2017a; Natural Resources Canada, 2018a). The number, size, duration, and intensity of BC's wildfires have large-scale impacts on communities, surrounding ecosystems, industries, carbon balances, and more. Reflecting upon this extreme fire season, the BC government issued a report describing the 2017 fire season as "the new normal" for wildfire conditions and vulnerability for future fire seasons within the province (Abbott and Chapman, 2018). As part of the report, recommendations were made to increase real-time, near-term, and consistent mapping approaches for monitoring the fire disturbances to aid in planning and emergency responses (Abbott and Chapman, 2018). Thus, it is vital for highly systematic and rapid large-scale disaster mapping and near-term monitoring of wildfires to better aid communities and understand fire ecology and underlying factors that contribute to their behavior in these wildfire-prone areas. This recent increase in burned area and wildfire occurrence is not unique to BC, however. Longer-term trends indicate a greater fire season length at the global (Jolly et al., 2015) and increasing fuel loads and fire activity related to a changing climate in western North America (Abatzoglou and Williams, 2016), further underscoring a need for systematic monitoring efforts in Canada (Bowman, 2018).

Several national datasets capture annual area burned information for Canada. First, each jurisdiction (i.e., province or territory) maps the final perimeters of major fires; each jurisdictions' dataset is then combined to produce the Canadian National Fire Database (CNFDB; Amiro et al., 2001; Burton et al., 2009; Parisien et al., 2006; Stocks et al., 2003). An aspatial database of burned area is also maintained by the Canadian Council of Forest Ministers (CCFM; Canadian Council of Forest Ministers, 2018). The Carbon Accounting Program for Canada's forest sector requires more detailed fire boundaries and estimates of burned area, which led to the development of the Canadian National Burned Area Composite (NBAC; Stinson et al. 2011). NBAC uses a compilation of data sources, including jurisdictional data (as per CNFDB) and satellite data such as Landsat, to capture refined fire perimeters by excluding large, unburned islands and waterbodies (de Groot et al., 2007; Fraser et al., 2000). Lastly, the Composite-to-Change (C2C) protocol provides a fully automated remote-sensing-based methodology for mapping forest disturbances including burned areas, using the annual proxy best-available-pixel (BAP) composites across the 30m Landsat record (Hermosilla et al., 2016, 2017; White et al., 2017). The cloud and gap-free BAP composites allow for similar growing conditions inter-annually, to enable long-term forest disturbance monitoring and inventorying (White et al., 2014). Each of these products provides post-hoc estimates of total national annual burned area, but there is further opportunity to map and refine near-term burned-area estimates using data from multiple Earth-observing satellites across large regions such as BC.

Several remote-sensing platforms can be used to estimate burning and burned areas at a variety of spatial resolutions for forest disturbances in Canada. The Canadian Forest Service uses data from AVHRR, MODIS, and VIIRS for its Fire Monitoring, Mapping, and Modeling (Fire M3) daily hotspot map that is publicly available and utilized by fire agencies across Canada to assess near-real-time fire activities (Fraser et al., 2000). The daily, coarser-resolution MODIS Collection 6 MCD64A1 global burned area product provides geographic locations and timing of fires at 500m spatial resolution (Giglio et al., 2015; Humber et al., 2018). For finer scale disturbance analyses in Canadian and North American forests, spatial interpolation techniques or fusion with Landsat imagery have been used to downscale the coarse resolution of the MODIS, while at the same time leveraging the high temporal frequency of MODIS imagery and data products (de Groot et al., 2007, 2009; Hilker et al., 2009a, 2009b; Parisien et al., 2011; Parks et al., 2012; Parks, 2014). For Landsat-8 and Sentinel-2, the Normalized Burn Ratio (NBR) and its subtractive change from a pre-fire value (dNBR) provide reliable, fine-scale annual estimates of burned areas from stand-replacing fires for Canadian boreal forests (Frazier et al., 2018; Hall et al., 2008; Hermosilla et al., 2016, 2017; Key and Benson, 2006; San-Miguel et al., 2017, 2018; Schroeder, et al. 2011; Soverel et al., 2010; 2011; White et al., 2017). However, the final maps created from these pixel-based burned-area mapping techniques can be heavily impacted by on-the-ground haze, smoke, and flare fire conditions that cause low-quality or missing data.

There is an opportunity for near-real-time monitoring of disturbances such as fire through data-synthesis of observations from numerous sources (Li and Roy, 2017; Wulder et al., 2018). Within-year fire progression can be constructed by fusing observations from multiple data sources into a synthesized time series, however three main limitations that remain. First, the smoke and haze from fires can obscure active fire visibility in observations from optical sources, creating difficulties for the classification of an active fire’s mid-burn extent from a single-date image. Second, due to the coarse resolution of MODIS imagery, daily products detect only the largest unburned islands within fire perimeters and can result in overestimation of cumulative burned areas. Third, the processing requirements (e.g., download, correction, normalization, and interpretation) of multiple data streams over large areas for near-daily observations create a challenging image analysis environment and data processing load. Despite these challenges, there are complementary strengths of these data streams (e.g., temporal frequency of MODIS, temporal frequency and spatial resolution of Sentinel, high-accuracies for boreal forest disturbance detection of Landsat) that could potentially be combined for mapping of fires in near-real-time (e.g., Boschetti et al., 2015; Hilker et al., 2009a, 2009b; Korhonen et al., 2017; Mora et al., 2013; Roy et al., 2014; Wulder et al., 2010). Crowley et al. (2019) adapted the BULC algorithm (Cardille and Fortin, 2016; Lee et al., 2018) to map the growth and extinction of a single fire event (Elephant Hill fire) at a near-weekly frequency for a small area (<200,000 ha). That research explored the opportunity for combining multi-source satellite image fusion for reconstructing a high-resolution burn progression time series for a single fire.

This research analyzes fire progressions for a given fire season over the entire province of British Columbia, Canada, with a forest area of approximately 60 million ha. We are able to examine the cumulative fire season trends as well as individual fire behaviors throughout the fire season. Our objectives are four-fold. First, we present a methodology for weighing multi-scale, multi-source burned-area evidence incorporating many fires over a 245-day study period using a singular, statistically driven post-classification fusion algorithm (BULC). Second, we apply a newly available segmentation algorithm in Google Earth Engine and a multi-source dNBR technique. Third, we present an automated approach that employs the provisional classification and synthesis entirely using data and functionality made available in Google Earth Engine. Fourth, we demonstrate how the derived information outputs can be used to characterize the spatio-temporal development of the fires over the course of the fire season, introducing novel metrics enabled by the applied methods. In sum, the objective of this work is to track detailed fire progressions over an extremely large area for an entire fire season using observations from multiple sources of imagery with differing spatial, temporal, and spectral characteristics.

4.2 Materials and Methods

4.2.1 Study Area

The 2017 British Columbia fire season began in April, with an exceptional increase in the burned area following a series of extreme thunderstorms between July 6 to July 8, and a second surge in fire activity in August due to sustained hot and dry weather and heightened build-up of fuels (BC Wildfire Service, 2017a). The BC Wildfire Service estimated a total of 1.2 million hectares burned throughout the fire season, resulting in $568 million in fire suppression costs (BC Wildfire Service, 2017a).

The four largest wildfires from the 2017 fire season comprised an estimated 80% of the total burned-area from the 2017 fire season in BC (Figure 4.1). The largest fire of the season, the Plateau fire (C10784), was identified on July 7 within the Itcha Ilgachuz Provincial Park, west of

Quesnel and northwest of Williams Lake (BC Wildfire Service, 2017c). This massive interface fire grew to an estimated 520,885 ha from multiple smaller fires merging (BC Wildfire Service, 2017c). The second largest fire of the 2017 fire season in terms of area burned, the Hanceville-Creek fire (C50647), was an interface fire located southwest of Williams Lake (BC Wildfire Service, 2017d). Hanceville-Creek fire was discovered on July 8 and grew to an estimated size of 239,339 ha (BC Wildfire Service, 2017d). The third fire examined, the Elephant Hill fire (K20637), was an interface fire located near Ashcroft and was used as the prototype study area in Crowley et al. (2019). It was detected on July 6 and grew to an estimated size of 192,016 ha (BC Wildfire Service, 2017e). The fourth-largest fire, the White River fire (N21628), grew to an estimated size of 26,399 ha after its identification on July 29 northeast of Canal Flats (BC Wildfire Service, 2017f).

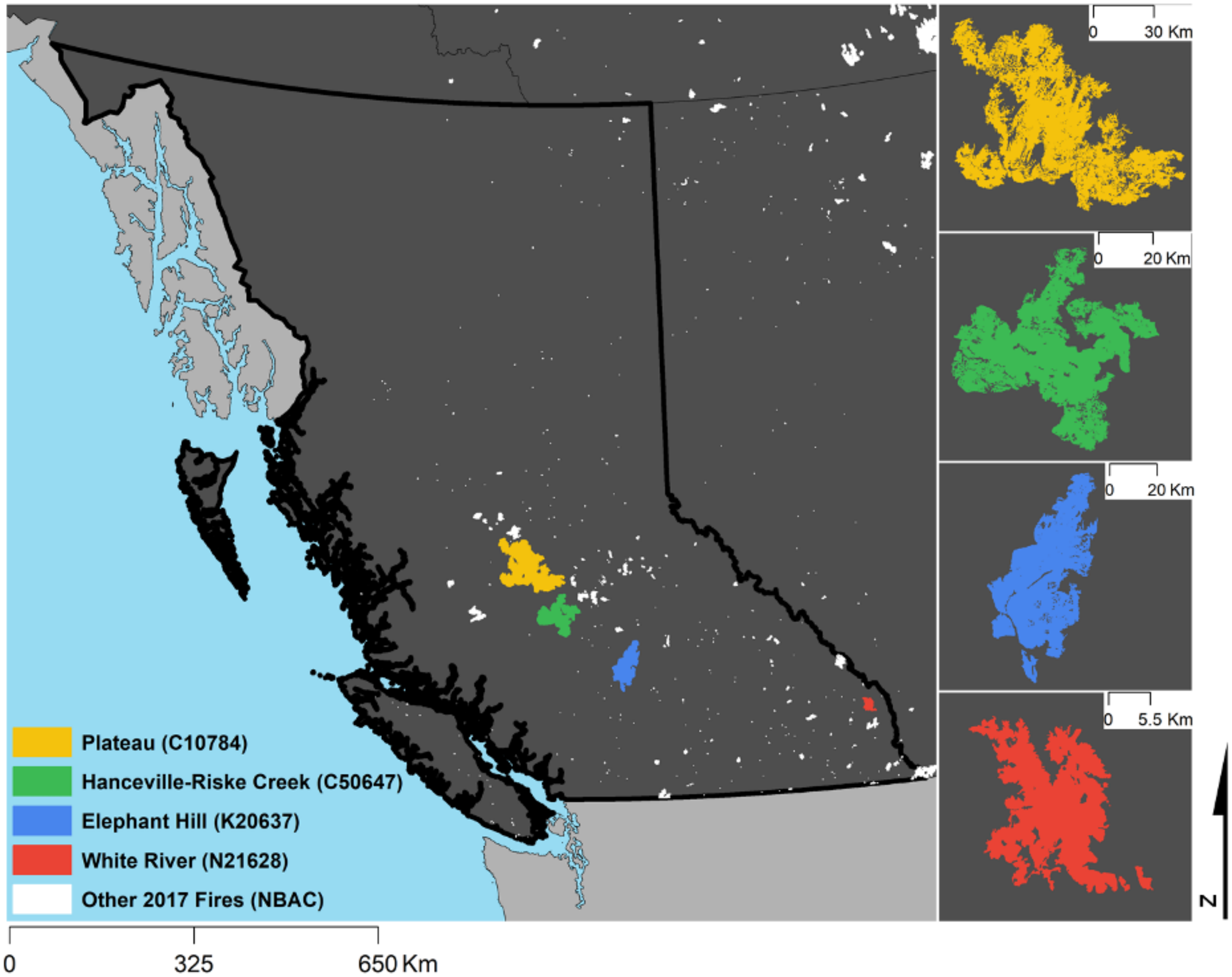

Figure 4.1 The locations of the 2017 British Columbia fires, which comprise the study area, shown as NBAC polygons inside the provincial boundary. The four largest fires can be viewed individually in the panels on the right.

4.2.2 Google Earth Engine implementation

We implemented our burned-area dataset creation and analysis using a series of four stages in Google Earth Engine (Gorelick et al., 2017) shown in Figure 4.2 with each stage's inputs and outputs. First, we created provisional classifications using observations from April to December 2017 within each fire's CNFDB perimeter (section 4.2.3). Second, we synthesized the provisional classifications together using the BULC algorithm (section 4.2.4). Third, we compared the end-of-season mapped fire areas to the corresponding interpretations in the NBAC dataset (section 4.2.5). Lastly, we produced whole-season and whole-province analyses of changing fire behaviors and patterns through time in the 2017 BC fire season. Data are described in greater detail within each subsequent methods section.

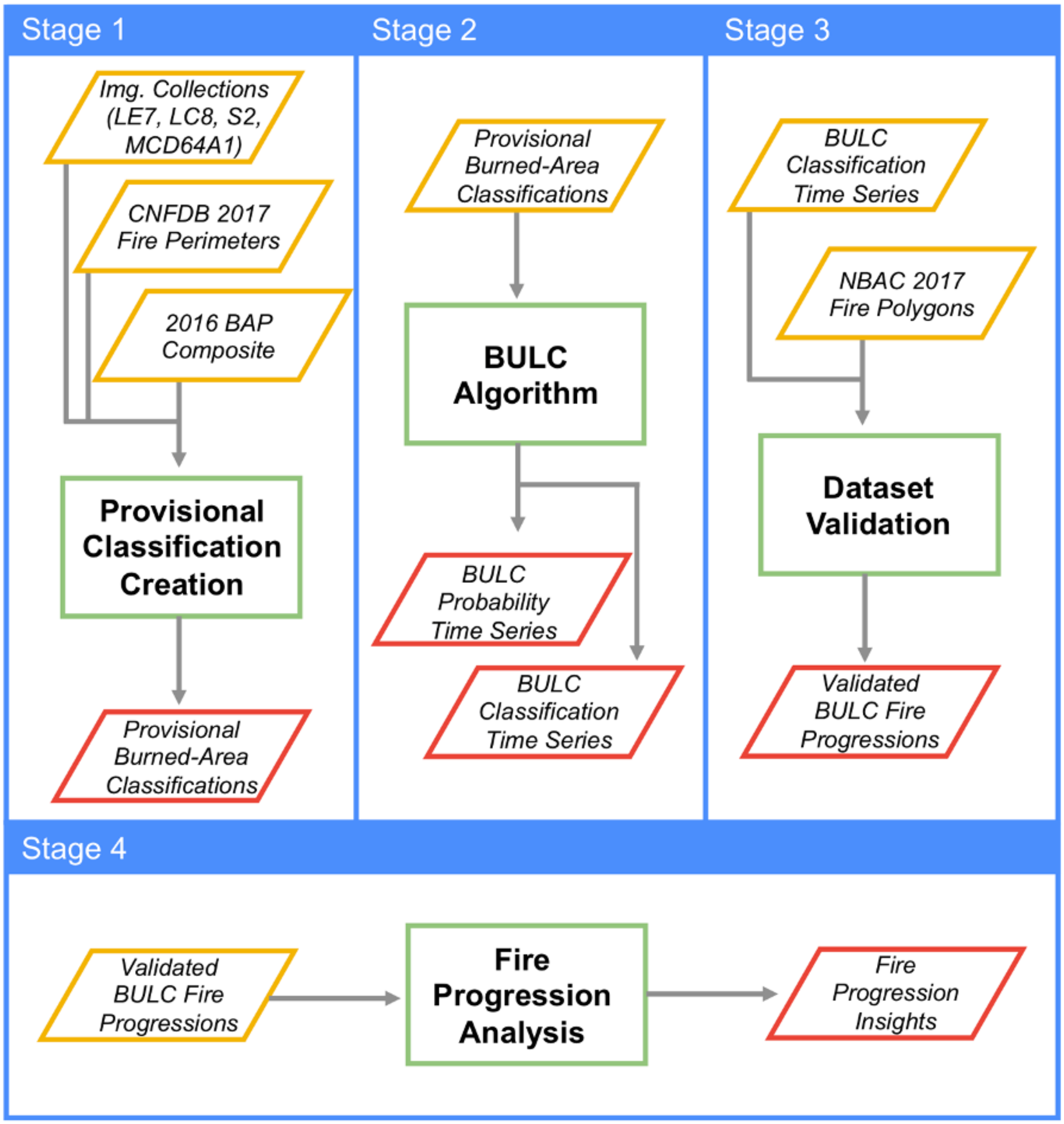

Figure 4.2 Outline of the four stages of analysis for this research, shown in a simplified flow chart (yellow represents inputs, green represents processes, and red represents outputs). Stage 1 (left) created provisional classifications that were then used in the BULC algorithm in Stage 2 (center). The output from Stage 2 was used in the validation in Stage 3 (right). The validated outputs from Stage 3 were then analyzed further in Stage 4 (bottom).

4.2.3 Provisional classifications using Landsat-8, Landsat-7, Sentinel-2, and MODIS

We identified 207 Landsat-8 OLI/TIRS Collection 1 Level-2 surface reflectance images, 200 Landsat-7 ETM+ Collection 1 Level-2 surface reflectance images, and 1094 Sentinel-2 MSI Level-1C images with less than 20% cloud cover between April 1 and December 1, 2017, intersecting with the fire perimeters. We masked all clouds and haze before classification using the pixel-level Quality Assurance (QA) band for Landsat and Sentinel-based imagery (Egorov et al., 2018; USGS, 2018; Zhu, 2017).

We implemented the differenced Normalized Burn Ratio (dNBR; Key and Benson, 1999, 2006) on the Landsat and Sentinel imagery to create provisional classifications of burned area for each fire in each image. First, we calculated the Normalized Burn Ratio (NBR) (Key and Benson, 1999, 2006), which captures the variation between healthy vegetation and burned areas detected in the near-infrared (NIR) and shortwave infrared (SWIR) wavelengths. The ratio is calculated per-pixel for each image by dividing the NIR minus SWIR reflectance values by the NIR plus SWIR reflectance values. Low NBR values correspond with bare and burned areas and high values correspond with vegetation.

Each active-fire NBR image was segmented into median-NBR objects using the Simple Non-Iterative Clustering (SNIC) segmentation algorithm available in Google Earth Engine (Achanta and Süsstrunk, 2017). Segmentation algorithms like SNIC create pixel clusters using imagery information such as texture, color or pixel values, shape, and size and are especially useful for forest disturbances (Blaschke, 2010; Wulder et al., 2004). Many fire-detection methods rely on pixel-based approaches, but image segmentation offers advances for the refinement of burned-area imagery (Gitas et al., 2004; Veraverbeke et al., 2012). In particular, SNIC is a bottom-up, seed-based segmentation approach that groups neighboring pixels together into clusters based on input data and parameters such as compactness, connectivity, and neighborhood size. To segment each active-fire NBR image, we set the SNIC parameters as follows: compactness was set to 0.1 to enable larger clusters, connectivity was set to 8, the neighbourhood size was set to 8 pixels to avoid tile boundary artifacts, and the seeds were created in a hexagonal pattern using a superpixel seed spacing of 4 pixels.

Using the 2016 BAP composite a pre-fire expected NBR; we calculated the differenced Normalized Burn Ratio (dNBR) using each segmented active-fire NBR image. The dNBR is calculated by subtracting the post-fire NBR from the pre-fire NBR, where negative and lower values correspond with regrowth and unburned vegetation and higher values correspond with fire severity (Key and Benson, 2006). The dNBR index is often calculated using single-source imagery, however, observations from pre-fire Landsat-8 and post-fire Sentinel-2 can be combined to enable retrospective mapping without impact on stand-replacing fire map accuracy (Quintano et al., 2018). For this reason, we utilized the 2016 BAP gap-free surface reflectance composite that was generated following the C2C approach to calculate the pre-fire NBR to compare with Landsat-7, Landsat-8, and Sentinel-2 observations (e.g., Hermosilla et al., 2016, 2017; White et al., 2014, 2017). We differenced the segmented active-fire NBR of each image with the pre-fire NBR to produce 259 dated provisional classifications from Landsat-7, -8 and Sentinel-2 for use in BULC, from 157 distinct dates during the study period. This approach pre-processed each dNBR image with temporal contextualization from the BAP protocol and spatial normalization from the segmentation. Differences over the stand-replacing fire dNBR threshold (dNBR > 0.284) for moderate to high severity, as outlined in Hall et al. (2008), were classified as ‘Burned/Burning’; those below the threshold were classified as ‘Unburned’ at that time step (e.g., Crowley et al., 2019; Frazier et al., 2018).

To create the MODIS provisional classifications, we summarized 15-day burned areas from the MODIS Collection 6 MCD64A1 burned area product as classifications (Giglio et al., 2015; Humber et al., 2018). This raster data product detects day-of-burning globally at 500m resolution with an average uncertainty of 5.3 days and a processing delay between 1.5 to 2.5 months for the 2017 BC fires. Each monthly MODIS burned-area raster contains the detected day-of-burn for pixels, we reclassified these MODIS burned-area products into Burned/Burning and Unburned layers in 15-day summaries. The result was 17 date-specific summary classifications that were used as inputs to BULC.

In total, we classified 276 provisional classifications spanning 167 distinct imaging dates during the study period. The 83 Landsat-8 surface reflectance classifications, 76 Landsat-7 surface reflectance classifications, 100 Sentinel-2 classifications, and 17 MODIS bi-weekly classifications were ordered by date and used as provisional classification inputs in the BULC algorithm. Combined, these sensors imaged each pixel within the fire perimeters an average of 33.8 times between April 1 and December 1, with the entire study area imaged approximately once in each of the 35 weeks of the fire season.

4.2.4 Bayesian Updating of Land Cover (BULC) algorithm

We used the BULC algorithm to fuse the burned-area information from the four sources for the 2017 fires (Cardille and Fortin, 2016; Crowley et al., 2019). BULC applies Bayes' Theorem to each pixel within each time-ordered provisional classification. The provisional input classifications are used as the prior knowledge in Bayes’ Theorem and contribute to the synthesized time series summarizing evidence-based change and stability for each pixel. First, provisional classifications are ordered temporally and compared pixel-by-pixel to calculate their correspondence in an agreement matrix. This agreement matrix serves as conditional probabilities in Bayes' formula, which are then tracked for each class in each pixel for the duration of the time series. BULC traces the probability of two classes, burned and unburned, corresponding to the two classes from the dNBR classifications. Probabilities are updated through time using new evidence provided by each new provisional classification in the stack. The most-likely class per pixel is evaluated to create the BULC classification at each time step in the series.

BULC can be used to fuse varying-quality classifications over fine temporal scales to track rapidly changing landscapes, as detailed in the context of a 2013 wildfire in Quebec in Cardille and Fortin (2016). Like other burned-area classifying algorithms (Padilla et al., 2014, 2015), BULC's burned-area estimations correspond with the availability of images from a given provisional classification source. For example, if clear observations from a single source are only available monthly, this can cause a delay in the temporal burn date given by BULC. As BULC is sensor-independent (Cardille and Fortin, 2016), data acquired by more sensors can be considered by the algorithm to improve the frequency and accuracy of the fire sequence to rectify any temporal gaps in imagery availability from a single source. Additionally, BULC can accommodate occasional errors such as from smoke, clouds, haze by relying on the input classifications from multiple data sources to fill temporal and quality gaps in imagery.

A previous study has demonstrated the ability for BULC to fuse information from multiple data sources into a singular, consistent fire progression dataset in British Columbia for a large fire event (203,560 ha; Crowley et al., 2019). Fusing images from Sentinel-2, Landsat-8, and MODIS, BULC leveraged the temporal and spatial resolution strengths of data from each sensor to produce a spatially explicit time series that documented the fire's changing patterns at sub-weekly time scales and at the 30m spatial resolution of Landsat. Therefore, BULC is able to estimate the burned area of an active fire at intermediate time steps relying on a dense stack of relatively clear provisional classifications from multiple sources in Google Earth Engine.

4.2.5 Agency data for fire perimeters and burned-area estimates

4.2.5.1 Canadian National Fire Database (CNFDB)

At the end of the fire season, the BC Wildfire Service digitizes official fire perimeters for each fire available in a vectorized dataset that is then used in the CNFDB compilation of fire perimeters across Canada. For the 2017 fire season, the most commonly used methods for delineating BC fire perimeters were ground/airborne GPS, manual sketches from observers in aircraft, and remote sensing image digitization (e.g., satellite, aerial, digital camera). The 2017 fire season dataset had 379 distinct fire perimeters for BC, capturing the final extent and estimated burned area for each fire as determined by the various provincial fire agencies (BC Wildfire Service, 2017b). Of the 379 fire polygons included in the CNFDB database, there were 290 fire polygons that were either duplicate polygons or grew to be less than <100ha in provincially calculated burned area. As these fires typically burned for a limited period (i.e., only a few days), they were removed for consideration. This dataset provides the estimated burned area for the province each year, and these estimates are further refined following the fire season by the remote sensing supported NBAC dataset.

4.2.5.2 National Burned Area Composite (NBAC)

The NBAC is created in the year following each fire season to provide a more spatially refined, vectorized burned area dataset for Canada’s Carbon Accounting Program (Stinson et al. 2011). For the 89 fires from the 2017 fire season, the most commonly used method for delineating the NBAC burned area polygons was using the Canadian Forest Service/Canadian

Center for Remote Sensing fine spatial resolution derived products from Single Acquisition Fire Mapping System (SAFiMS) or Multi Acquisition Fire Mapping Systems (MAFiMS) software on Landsat-based satellite imagery (Table 4.1). For NBAC, SAFiMS and MAFiMS satellite mapping is done manually for each fire using pre- and post-fire images, assessed in areas of the country with sufficient levels of fire activity. The final NBAC product is generated using a rule-based algorithm to select the best-available data source for each fire event, considering the quality of the data source and the methods used for mapping. For the 89 fires from the 2017 BC fire season, 57 NBAC fire events were created from SAFiMS/MAFiMS processing of Landsat imagery, including the four largest fires: Plateau, Hanceville-Riske Creek, Elephant Hill, and White River. The remaining 32 NBAC fire polygons were based on fire agency polygons (e.g., CNFDB), created either from manual sketches or ground/aerial GPS data.

Table 4.1 NBAC Dataset metadata for 89 2017 BC fires including data provider and fire mapping method and source.

Data provider	Fire mapping method and source	Total fires mapped
NRCan Remote Sensing	SAFiMS/MAFiMS on Landsat imagery	57
Provincial Fire Agency	Aerial Survey GPS	18
	Field Survey GPS	9
	Hand Sketch	3
	Undefined	2

4.2.6 Comparison of burned-area estimates

The NBAC was used for comparison against the end-of-season BULC burned area maps to assess the degree of correspondence in burned area estimates. First, we cross-tabulated the pixels of the NBAC data and BULC at each time step. Using these cross-tabulations, we calculated the Dice Coefficient for each date and bias in terms of proportion of burned area between the NBAC data with the BULC end-of-series burned-area map, following the validation methods employed in Padilla et al. (2015). In particular, the Dice Coefficient in this scenario estimates the spatial overlap between the BULC fire-progression dataset and the NBAC dataset, ranging from 0 (no agreement) to 1 (complete agreement) (Padilla et al., 2014, 2015).

4.2.7 Fire progression metrics

Availing upon the unique information provided by the BULC fire progression data, we generated a number of metrics to characterize the 2017 fires in BC (Table 4.2). These metrics quantify the spatio-temporal characteristics of the fires in both summary and comparison values that can be used to describe and compare the fire season and individual fire behaviors. Fire metrics can be calculated at various temporal scales, including daily, weekly, and entire fire season. Additionally, these metrics can be calculated relative to the fire season's calendar days/weeks to examine fire season features or relative to the individual fire's day of fire to examine fire-specific features.

Table 4.2 Definition and purpose for each fire progression metric, where n is the burned area on a given day (d) or week (w).

Fire Progression Metric	Definition	Purpose
Cumulative burned area	Total burned area at each time step per fire or per fire season in hectares (n_t)	Summary metric for burned area over time
Cumulative area relative to max area	Proportion of cumulative burned area divided by maximum burned area per fire (n_t / n_{max})	Comparison metric for burned area over time
Daily burned area	Burned area growth from prior time step to current time step per fire in hectares ($n_d – n_{d-1}$)	Summary metric for daily burned area change
Daily burned area relative to max area	Proportion of daily burned area divided by maximum burned area per fire $(n_d – n_{d-1})/(n_{max})$	Comparison metric for daily burned area changes
Number of active fires	Count of total fires actively burning at each time step	Summary metric indicating combined fire season activity
Number of fires at peak burn week	Count of fires per week that have their maximum *Weekly relative change in burned area*	Summary metric indicating fire season activity per fire
Weekly observation rate	Average number of observations per fire per week during its active phase and across entire fire season	Summary metric for data availability per fire
Weekly relative change in burned area	Proportion of burned area growth from the past week divided by previous week's burned area amount $(n_w – n_{w-1})/(n_{w-1})$	Comparison metric for relative weekly burned area changes per week

4.3 Results

4.3.1 Correspondence of BULC burned area dataset for BC

We calculated the Dice Coefficient, bias, relative bias, and relative difference to quantify agreement between the NBAC and BULC dataset (Table 4.3). The average relative difference in burned area was -7.5% for larger fires with an average Dice Coefficient of 0.76 (e.g., Plateau, Hanceville-Riske Creek, Elephant Hill), and -16.0% for smaller fires that had lower average Dice Coefficient of 0.61 (e.g., White River). The bias and relative bias for all BC fires pointed towards the BULC dataset estimated the burned area as lower compared to the NBAC dataset (i.e., bias of -0.34, relative bias of -0.41). The lower estimation of burned area in the BULC-derived dataset is most evident on the edges of burned objects when comparing the BULC and NBAC datasets (Figure 4.3). Both datasets have strong agreement (i.e., ~99% on average) in the clearly unburned and much of the burned area (Figure 4.3D, 4.3H, 4.3L, 4.3P), and the BULC dataset tends to provide a lower estimate of burned areas corresponding with the satellite imagery. The level of correspondence between the BULC burned area estimate with the NBAC dataset builds confidence in the BULC outputs.

Table 4.3 Dataset validation using the National Burned Area Composite (NBAC), the relative difference and the Dice coefficient was calculated using the correspondence between the BULC final dataset against individual fire polygons from the NBAC dataset.

Fire Region	BULC (ha)	NBAC (ha)	Relative difference (%)	Dice Coefficient
All BC Fires	890,988	1,057,998	-15.79	0.73
Plateau (C10784)	381,168	410,382	-7.12	0.75
Hanceville-Riske Creek (C50647)	199,075	214,293	-7.10	0.76
Elephant Hill (K20637)	165,894	180,867	-8.27	0.76
White River (N21628)	16,164	23,153	-30.19	0.66

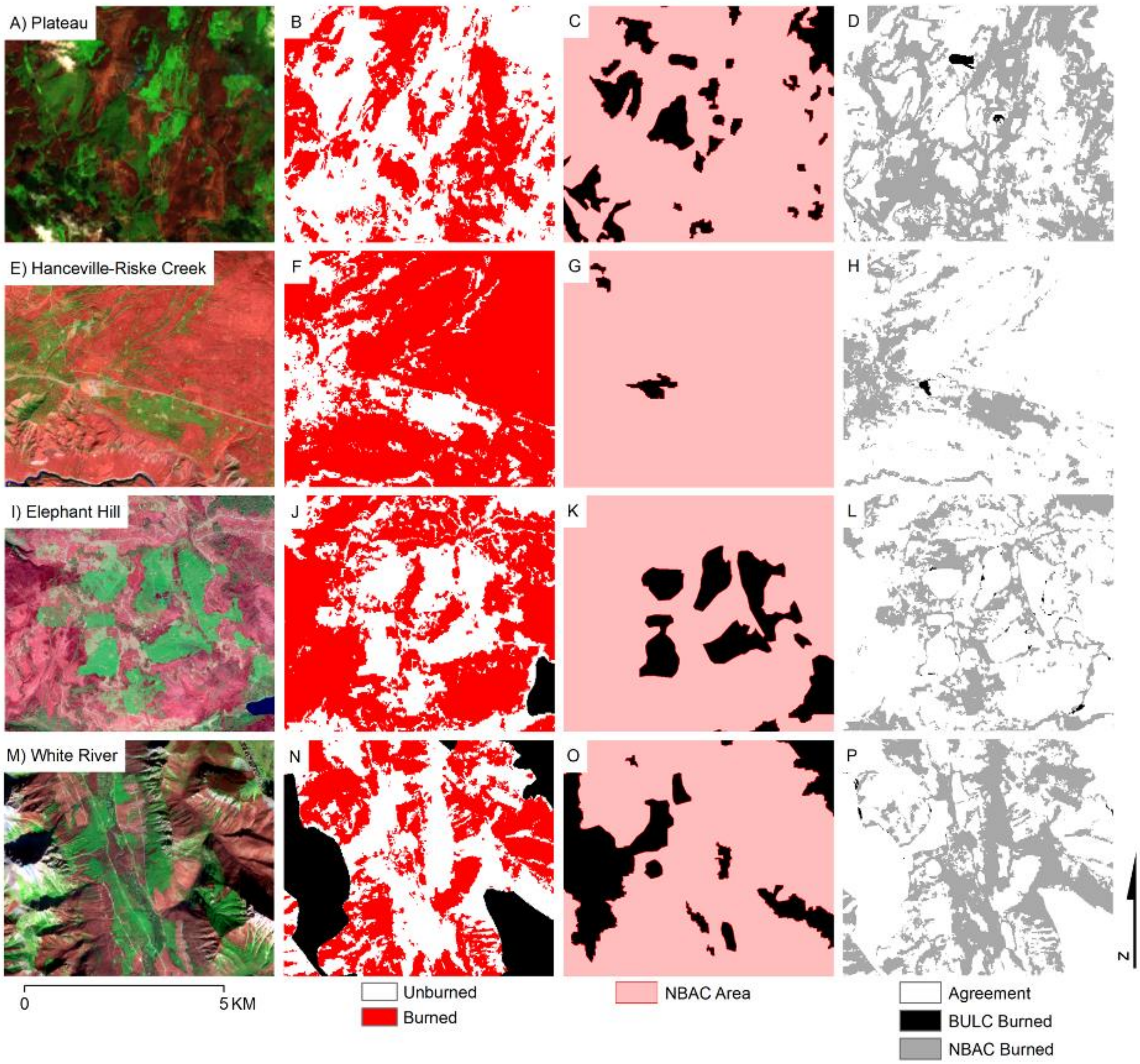

Figure 4.3 For each fire (rows), zoomed final burned area Landsat-8/Sentinel-2 composite in column 1 (A, E, I, M), corresponding BULC final classification in column 2 (B, F, J, N), corresponding NBAC burned area polygon in column 3 (C, G, K, O) and fire agreement between burned area from the BULC fire progression dataset and the burned area from the NBAC dataset in column 4 (D, H, L, P). In the Landsat-8 and Sentinel-2 composites in column 1, red areas correspond with burned area.

In Figure 4.4, we compare the datasets in terms of their refined capabilities, showing the final BULC classification for Elephant Hill fire against the raw Sentinel-2 image for the fire, the polygons marking the CNFDB fire perimeter and NBAC burned area, and the final MODIS burned area dataset for this fire on October 4, 2017 (following its containment). Evident refinement has been made in burned-area detection to Landsat resolution with this BULC burned area dataset with burned-area agreement with the existing refined datasets, while also creating fire progression details that will be further examined in the subsequent sections.

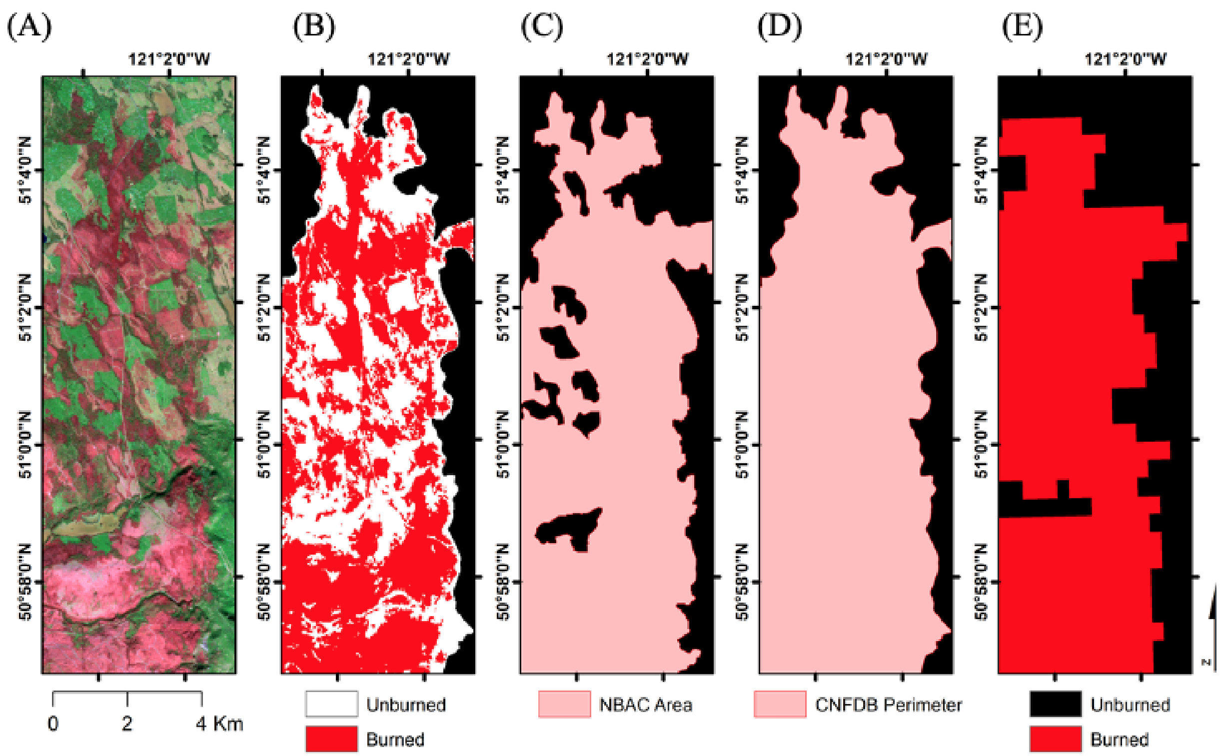

Figure 4.4 Burned-area dataset comparisons against final burned area Sentinel-2 image from October 3 in (A) for the Elephant Hill fire zoomed in at fire edge at 51°10' N, 121°2'W. The resulting October 3 BULC classification within the CNFDB fire boundary is shown in (B), highlighting the fine spatial resolution. The NBAC burned area polygon dataset is shown in (C), the CNFDB polygon perimeter dataset is shown in (D), and the final MODIS burned area is shown in (E).

4.3.2 Fire progression metrics

BULC synthesized provisional input classifications from the fire season, which allows per-pixel burn progressions within the British Columbia fire-event perimeters at the collection date of each provisional classification. Considered together, the 89 fires of the 2017 fire season burned unevenly temporally through the summer and autumn (Figure 4.5). The cumulative area burned through the fire season was irregular and was characterized by a steady burn phase of 41,437 ha for two weeks from its start in early July to mid-month, an accelerated burn phase by 149,422 ha for two weeks from mid-July to early August, a steady burn phase of 218,079 ha for one month from early August to early September, and a second accelerated burn phase of 301,931 ha for two weeks from early September to mid-September, and subsequent steady growth by 180,119 ha for 1.5 months from mid-September until containment in late October.

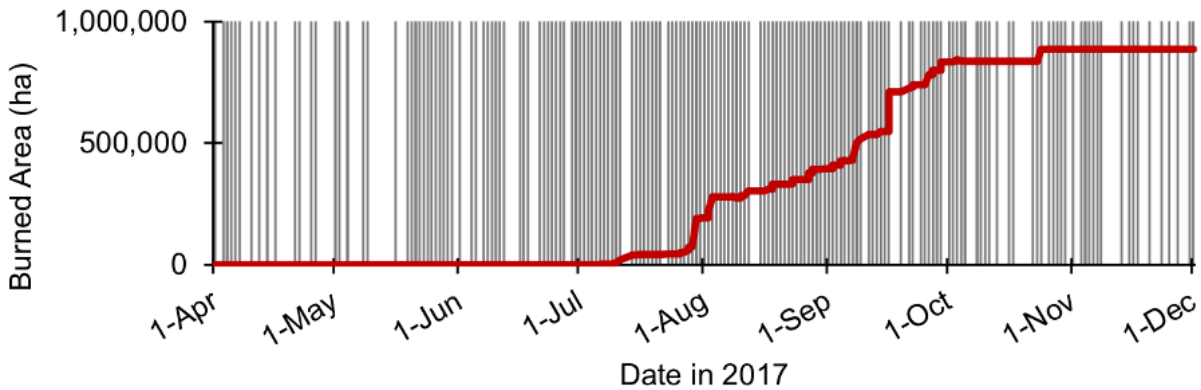

Figure 4.5 Cumulative burned-area progression for the 89 fires in 2017 in British Columbia, Canada, from the beginning of the fire season in April to December 1, with provisional classification frequency denoted by grey bars.

Provisional, burned-area classifications were synthesized together in the same time series stack by BULC, and using that dataset, individual fire progressions for each fire polygon can be examined in greater detail. The four largest fires of 2017 (Figure 4.6A) accounted for 86% of the total 2017 burned area in BC. Individual fires varied in the timing of their burned area and burn rates, with many smaller fires burning quickly to their final size (Figure 4.6B) while the larger fires experienced longer burn periods. Many smaller fires grow to their final burned area within a single day (Figure 4.6B, 4.6C), indicating these fires were extinguished quickly and contained to a smaller area. The largest fires grew to their final burned areas more gradually (4.6B), but with spikes in daily burned area following a widespread lightning storm that caused many ignitions across BC (Figure 6D).

By examining the maximum size and burned-area growth rates of the individual fires (Figure 4.6), we developed a heuristic to characterize the 2017 fires, characterizing them according to size (small versus large) and their rate of spread (slow versus fast). Large fires grew to be greater than 20,000 hectares in total burned area, while small fires were smaller than 20,000 hectares. Fast fires grew more than 40% of their burned area in a single week, while slow fires did not. Of the 89 fires we analyzed, 13 were small and slow fires growing to their final extent of less than 20,000 hectares steadily across the fire season. These small and slow fires accounted for 3% of the total burned area of the 2017 fire season. By contrast, small and fast fires (n =72) were less than 20,000 ha in size and had rapid growth periods over their actively burning period (e.g., growing to over 40% of their burned area within a single week like the White River). Small and fast fires accounted for 13% of the cumulative burned area for the 2017 fire season. Two fires were large fires (>20,000 ha) and had dispersed growth periods throughout their active phase (e.g., Hanceville-Riske Creek, Elephant Hill). These two large and slow fires accounted for 41% of the cumulative burned area for the fire season. One fire, the Plateau fire, was a large and fast-moving fire that had rapid growth weeks over 40% of its final burned area. This single large and fast developing fire event accounted for 43% of the cumulative burned area for the 2017 fire season

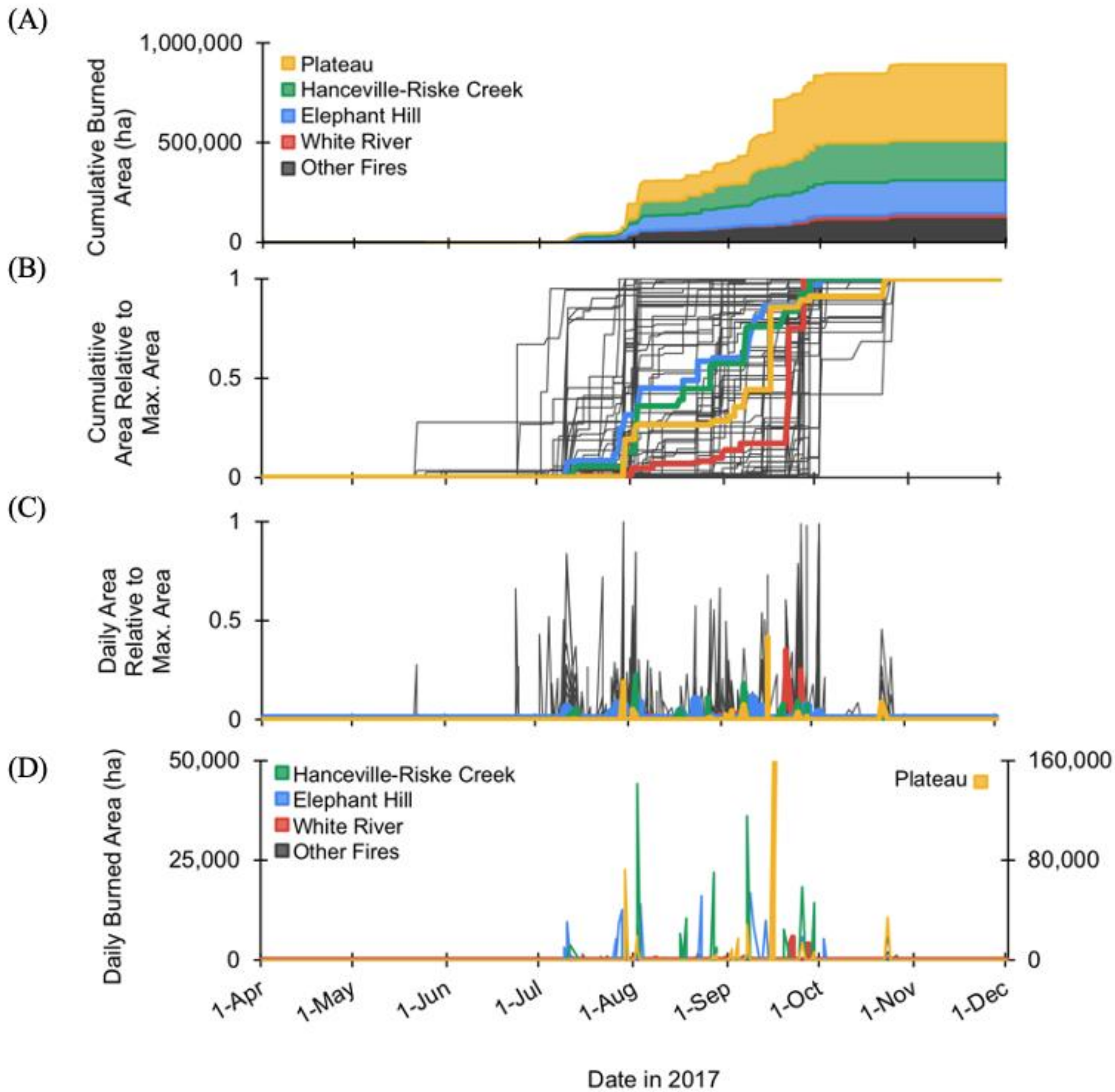

Figure 4.6 Individual fire (A) cumulative burned-area progression in ha, (B) cumulative burned-area progression relative to maximum area, (C) daily burned area relative to maximum burned area, (D) daily burned area in ha for each of the 89 fires in 2017 in British Columbia, Canada, from the beginning of the fire season in April to December 1, with the four fires presented in greater depth in the following sections colored uniquely.

Fire progressions and corresponding metrics can be summarized to weekly attributes to better identify key periods of the fire season. For fires of all sizes, there were two key periods of individual fire growths compared to previous weekly burned areas, occurring in week 18 (end of July) and week 26 (mid-September) of the fire season (Figure 4.7A). The number of fires actively burning increased notably by 33% between July 16 and July 27, corresponding with a widespread lightning storm on July 17 that caused many ignitions across BC (Figure 4.7B). 22 fires had their peak burn weeks in week 18 (July 29) following the lightning storm, and 21 additional fires had their peak burn week during week 26 beginning on September 23 (Figure 4.7C). BC fire agencies employed many resources to contain all of these growing fires during their peak burn weeks in July (Figure 4.7B, 4.7C; Abbott and Chapman, 2018). However, the four largest fires steadily grew out of control following that period to contribute the largest areas to the cumulative burned area and the largest daily burned areas (Figures 4.6A, 4.6D, 4.7A). Following the second peak burn week in mid-September, 67% of the fires were extinguished between September 23 and October 7 as shown by the decreasing total count of active fires after week 26 (Figure 4.7B).

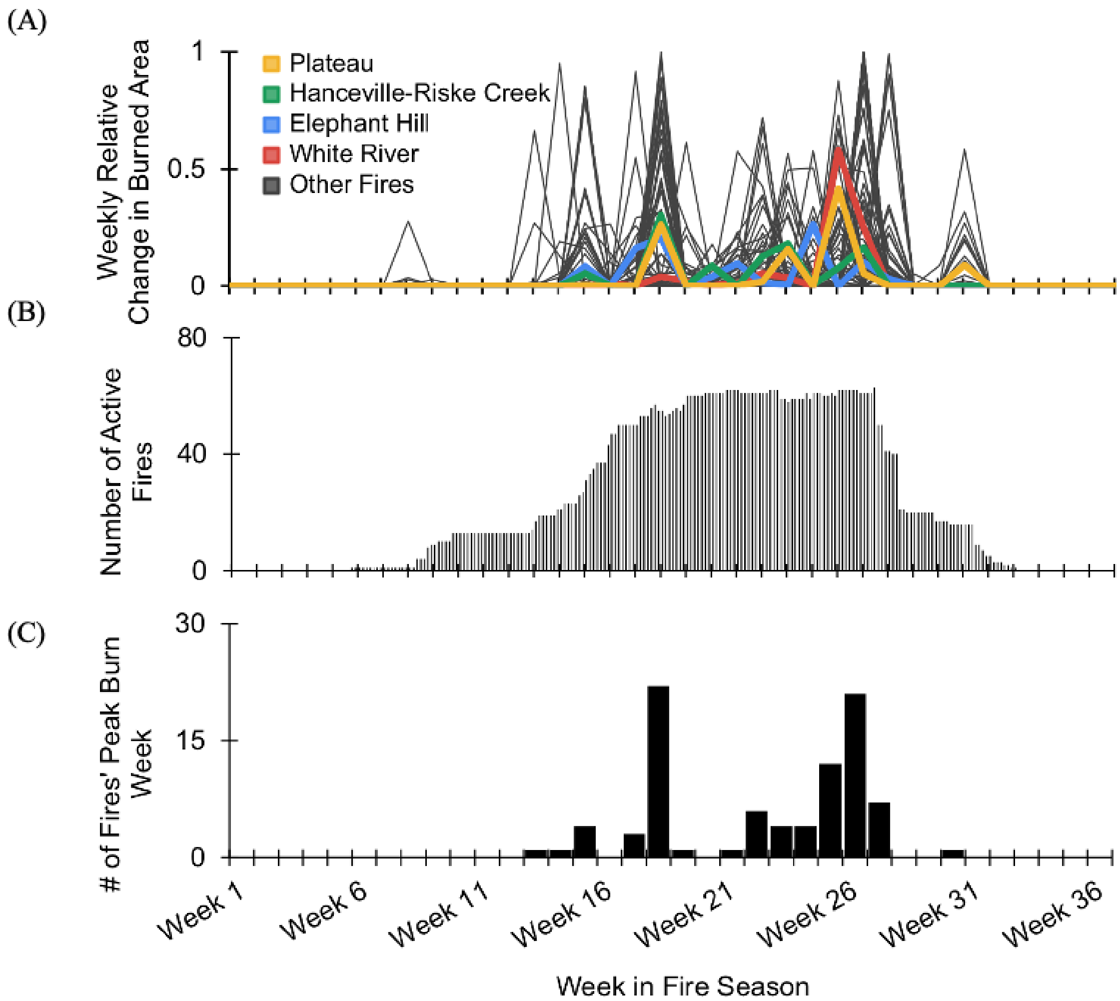

Figure 4.7 Weekly fire season attributes, including (A) weekly relative change in burned area for each fire, (B) number of active fires, (C) number of fires' peak burn weeks, from the beginning of the fire season in April to December 1, with the four fires presented in greater depth in the following sections colored uniquely.

4.3.3 Individual fire attributes

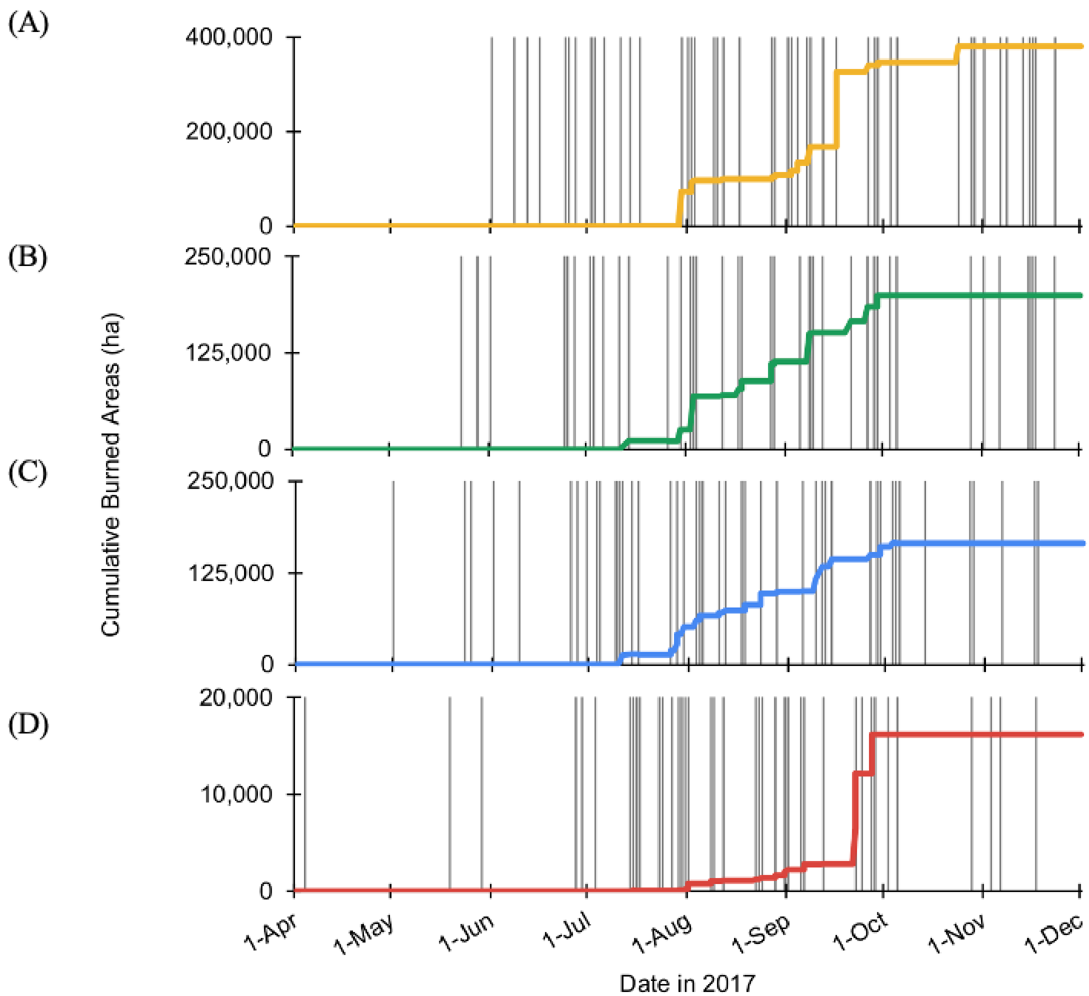

Figure 4.8 Burned-area progression tables for individual fires, including (A) Plateau, (B) Hanceville-Riske Creek, (C) Elephant Hill, (D) White River, from the beginning of the fire season in April to December 1, with observation frequency denoted by grey bars. The denser the grey bars in the figure, the more observations included in BULC as provisional classifications.

There were consistent observations throughout each fire's active phase that helped delineate their individual burn progressions (Figure 4.8). The Plateau Fire was the largest fire from the 2017 BC fire season and was a large and fast-moving fire that grew in distinct burn phases over the duration of its long actively burning period of 10 weeks (Figure 4.8a). The burn progressions for the Plateau fire for the entire fire season highlights these large increases in burned areas at the end of July and middle of September. The Hanceville-Riske Creek Fire was the second-largest fire from the 2017 BC fire season and was a large and steady growing fire over the duration of its 11-week burning period (Figure 4.8B). The burn progression for the Hanceville-Riske Creek depicts steady increases in burned areas throughout the fire's active phase. The Elephant Hill fire was a large and steady 12-week burning period, with two larger increases in burned area of the fire at the end of July and during the middle of September (Figure 4.8C). The fourth largest 2017 BC fire, the White River fire, was a small and fast burning fire during its 9-week burning period and had a rapid jump in size at the end of September following a steady increase in burned/burning area (Figure 4.8D).

Each of these fires had distinct peak burn weeks that contributed to a majority of their total burned areas, and we can view the pre-peak week and post-peak week BULC classifications to better visualize the fire behaviors (Figure 4.9). Prior to its peak burn week in mid-September, the Plateau fire had already burned nearly 120,000 ha (30% of total burned area) by September 2 in distinct, separate smaller fires that were joined together in its peak burn phase (Figure 4.9A, 4.9B). The Hanceville-Riske Creek fire had a peak burn week in the end of July following its growth to 68,636 ha (34% of total burned area) on August 3 after its ignition in early July (Figure 4.9C, 4.9D). The Elephant Hill fire grew to 66,767 ha (40% of total burned area) on August 4 after its ignition in early July and prior to its peak burn week at the end of July (Figure 4.9E, 4.9F). Lastly, the White River fire had its peak burn week in mid-September after growing to 2,236 ha (14% of final burned area) on September 1 (Figure 4.9G, 4.9H). BULC classifications for distinct dates of interest can be mapped individually in addition to being summarized in date-of-burned-observation maps.

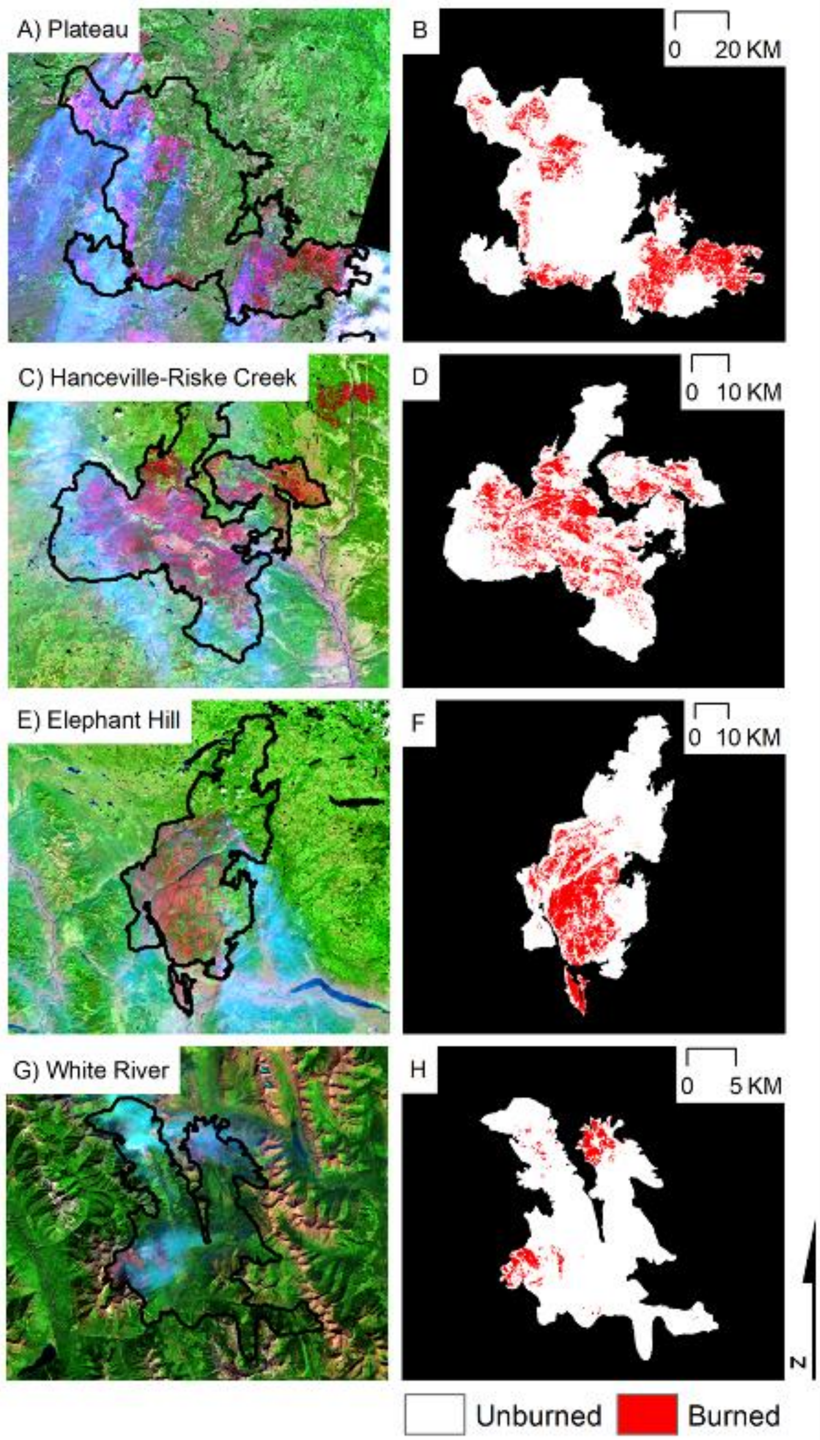

Figure 4.9 For each fire (rows), intermediate burned area Landsat-8/Sentinel-2 composite in column 1 using the least-cloudy imagery from the nearest-in-time date from Landsat-8 or Sentinel-2 shown in Bands 7/12, 5/8, 3 (A, C, E, G) and intermediate BULC burned area dataset within the official CNFDB fire boundary zoomed on each fire in column 2 on September 2 (B), August 3 (D), August 4 (E), and September 1 (F).

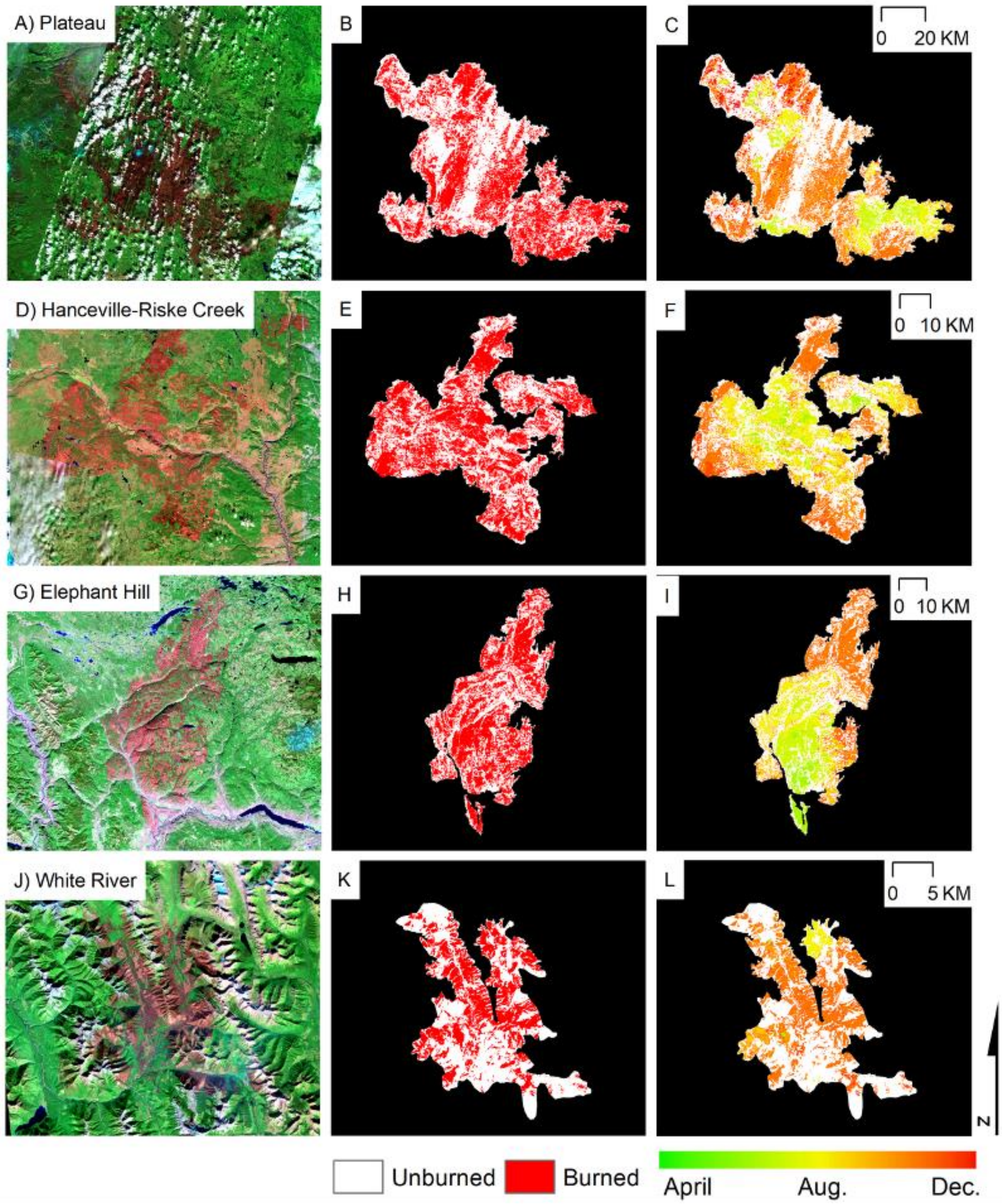

Figure 4.10 For each fire (rows), final burned area Landsat-8/Sentinel-2 composite in column 1 for Bands 7,5,3/12,8,3 (A, D, G, J), final BULC burned area dataset within the official CNFDB fire boundary zoomed on each fire in column 2 (B, E, H, K), and fire-progression dataset shown from April to December in column 3 (C, E, I, L). In the Landsat-8 and Sentinel-2 composites in column 1, red areas correspond with burned area. The scale bar in column 3 is the same for all images in columns 1 and 2.

When the burn history presented by BULC can be charted for each large fire (e.g., Figure 4.8), it is possible to also map the spatio-temporal dynamics of each fire as it progressed (Figure 4.10). For the Plateau fire, the fire had grown to its maximum extent near October 24 at 381,168 burned ha (Figure 4.10A 4.10B) from several smaller fires that grew together rapidly late in the fire season (Figure 4.10C). The Hanceville-Riske Creek fire grew to its final extent by September 29 at 199,075 burned ha (Figure 4.10D, 4.10E) steadily outward from its central ignition location (Figure 4.10F). The similarly sized Elephant Hill fire grew to its final extent by October 3 at 165,894 burned ha (Figure 4.10G, 4.10H) in two distinct growth phases that expanded northward from its initial ignition source (Figure 4.10I). The small but fast burning White River fire, had a final burned extent of 16,164 burned ha (Figure 4.10J, 4.10K) that grew southward from its initial ignition source in a mountainous region (Figure 4.10L).

In addition, fire progressions can also be compared using the elapsed fire duration, from ignition to completion, to better compare fire-level behaviors and attributes (Figure 4.11). The temporal window for days of fire was determined by the final day of growth to the final maximum fire size. For the Plateau fire, it was active for 122 days, with distinct burn periods throughout the active phase most notably on day 87 when relative burned area grew by 42% (Figure 4.11A). The Plateau fire had a weekly observation rate of 1.72 observations per week during its actively burning period and 1.22 observations per week throughout the entire fire season. The Hanceville-Riske Creek fire had more dispersed burn periods throughout its 126-day actively burning period, with 23% relative growth on day 5 and 18% relative growth on day 101 (Figure 4.11B). The Hanceville-Riske Creek fire had a weekly observation rate of 1.00 during its burning period and 1.5 throughout the entire fire season. The Elephant Hill fire had more steady burn periods without any distinct jumps of relative burned area growth greater than 10%

throughout its 96-day burn period (Figure 4.11C). The Elephant Hill fire had a weekly observation rate of 2.09 observations per week during its actively burning period and 1.22 observations per week throughout the entire fire season. The White River fire had very low burn periods until large spikes of relative growths of 23% on day 69 and 34% on day 71 in its 74-day actively burning periods (Figure 4.11D). The White River fire had a weekly observation rate of 1.03 during its burning period and 2.27 throughout the entire fire season. The average relative weekly burn rate for each of the four fires throughout their actively burning weeks were between 8-11%. The 2017 fire season average for relative weekly burn rate was 26.6% with a range from 8.3% to 100%.

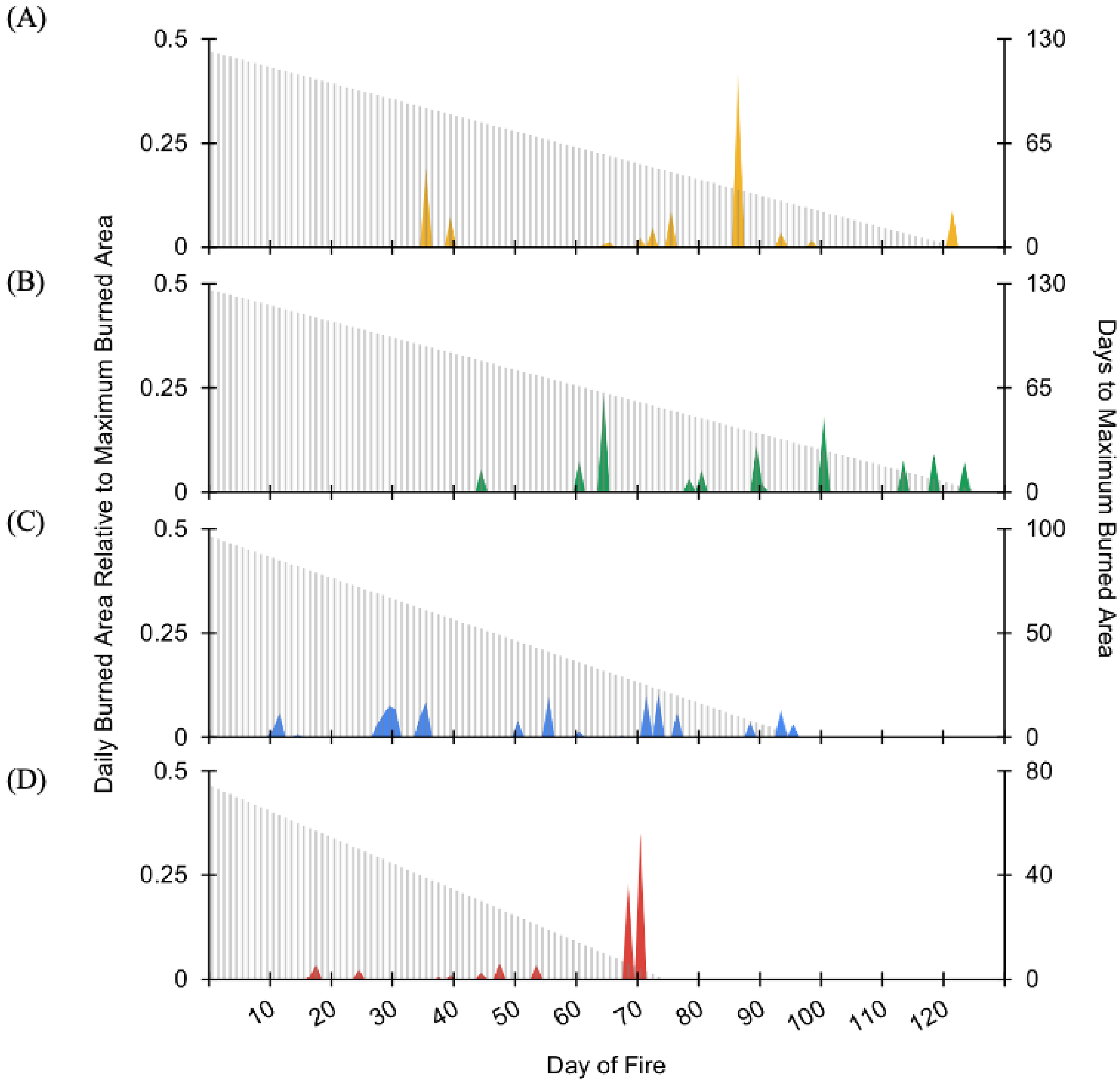

Figure 4.11 Daily burned area relative to maximum burned areas for each of the (A) Plateau, (B) Hanceville-Riske Creek, (C) Elephant Hill, (D) White River fires, from normalized to days of fire rather than calendar date, with number of days until maximum burned date denoted in gray (secondary axis).

4.4 Discussion

Burned-area progression analyses were created for each of the 2017 fires in BC and created a large-area methodological approach for mapping the growth of fires throughout their active phases using data from multiple sources. Observation rate varied from fire to fire when creating this dataset over the extensive, BC-wide area for all 89 unique fires. The four largest fires from the study area shared characteristics as interface fires that were discovered in July. The largest and smallest fires presented, the Plateau and White River, both experienced two periods of large growth rates in August and September with fast burning characteristics. While both large fires, Elephant Hill and Hanceville-Riske Creek fires had more constant growth rates throughout their active phases. This work builds upon existing fire progression mapping methods outside of Canada that utilize the MO(Y)D14 active fire dataset to interpolate day-of-burn values for vectorized fire perimeters (e.g., Benali et al., 2016; Veraverbeke et al. 2014). The BULC approach advances fire progression methods by synthesizing fine-scale observations from multiple sensors to utilize the fine temporal resolution of coarse sensors like MODIS alongside the fine spatial scale resolution of sensors like Landsat and Sentinel-2. This enables weekly date-of-burn values derived for each pixel within the final fire perimeters at the spatial resolution of the input observations.

As presented in Figures 4.3 and 4.4, the BULC product refines the burned/burning maps spatially compared with the existing datasets such as the CNFDB and NBAC burned-area dataset for mapping burned areas in British Columbia for the 2017 fire season. The spatial refinement of the BULC burned-area dataset relied heavily on Landsat and Sentinel-2 observations, which made up 94% of the total observations used as provisional classifications. Depending on the targeted use of burned-area datasets, the spatial scale and refinement necessary for analysis may vary. For example, the NBAC burned-area dataset provides burned area estimates that are more spatially generalized relative to the BULC fire-progression dataset, which may be preferable for providing less conservative estimates of carbon losses at the end of each season. However, if the burn-progression dataset is being used for targeting harvesting after the wildfires, then a more spatially refined approach such as is provided by BULC may be preferred.

Near-real-time monitoring of disturbances is made possible through data-synthesis advancements for fusing observations from multiple sources (Li and Roy, 2017; Wulder et al., 2018). Although this approach does not currently provide real-time monitoring capacity, our long-term goal is to extend the approach to include a fire detection component by integrating active fire perimeters from provincial fire agencies. This would allow BULC to proceed mostly as described here, refining burned areas as new imagery arrived. By using active fire observations from multiple remote sensing sources, we were able to reduce the revisit interval provided by the sensors. BULC is a spectrally independent algorithm, which allows for the integration of data from multiple sources. In the case of mapping burned-area datasets, this allows for using the most reliable burned-area classification protocol to classify imagery from varying sensors while also integrating information provided by previously created burned-area datasets.

In a practical context, the highly automated approach to mapping provides a refined, spatially explicit estimate of burned area that is available when the fire season concludes or at any time throughout the fire season. For all BC fires, the burned-area estimate generated from this approach was within 16% of burned area estimates derived from a best-available composite mapping product that is typically generated retrospectively. The three largest fires have the greatest consequences for carbon loss and forest management and the burned-area estimates achieved with BULC were within 7.5% on average of NBAC burned-area estimates. Note that while correspondence to NBAC builds confidence in the generated BULC outputs, both products represent an estimate, and neither are truth. The approach demonstrated herein provides opportunities for actively mapping wildfires through the fire season to have running total of refined burned areas also highlighting locations of interest regarding carbon consequences and forest management and planning.

By increasing the number of data sources availed upon for mapping, such as using imagery from Landsat-7 in addition to Landsat-8, Sentinel-2, and MODIS, and by raising the cloud-cover threshold, we were able to retrospectively create fire observations at a sub-weekly scale. One challenge of using observations from cloudy, coarse, and scan line corrector-off (SLC-off; Wulder et al. 2011) imagery with no data is that there is a risk of causing temporal or spatial gaps in imaging. Temporal gaps occur when the fire grows, but there is a lack of clear observations to update the map. Additionally, spatial gaps arise when there are clear observations with partial coverage that update portions of the fire. The benefit of using the observations from Landsat-7 is that its observations fill temporal gaps in the time series. The risk, however, is that its usage may propagate further spatial gaps and partial-image updates due to systematically missing data. For example, some of the Plateau Fire intermediary BULC-classifications contain strips of missing data in burned areas as the mapping relied largely on Landsat-7 imagery to provide temporal coverage. The benefit of including MODIS data is that its observations fill both temporal and spatial gaps in the time series. One trade-off is that production and release of the MODIS burned-area dataset takes approximately 4 months to deliver burned areas related to a given month. Another risk, however, is a coarsening of the final data product, whether in intermediary time steps or the dataset's duration. For example, a lack of data for several days for the Hanceville-Riske Creek and Elephant Hill fires caused anomalous spikes in burned-area estimations.

The impact of these temporal and spatial gaps in observations can be reduced in two ways; that is, using object-based knowledge to fill data gaps and increasing observations from non-optical sources. First, future methods can use segmentation to fill in spatial gaps within Landsat-7 provisional classifications (e.g., Wulder et al. 2004). Alternatively, BULC could update a series of pre-defined burned-area objects using evidence from partial observations to reduce spatial gaps. Second, there are opportunities to utilize observations from Synthetic-Aperture Radar (SAR) sensors such as Sentinel-1 to increase both temporal and spatial gaps from optical-sensor observations (Chuvieco et al., 2019). There are fewer algorithms for burned-area detection in Sentinel-1 imagery (e.g., Engelbrecht et al., 2017; Lohberger et al., 2018; Verhegghen et al., 2016), but even moderately reliable provisional classifications would provide gap-filling evidence for burned/burning pixels in the BULC algorithm.

The province-wide analysis opens new opportunities for understanding fire at regional, national, and continental scales. For example, comparisons can be made using this data source to relate characteristics of growing fires and act as validation for pre-existing forecasted fire weather datasets, fire behavior datasets, and existing wildland fire growth simulation models for Canada's boreal forest (Natural Resources Canada, 2018b; Fire Growth Model, 2018). Additional analyses can be performed to evaluate the relationship between underlying drivers of fire behavior (e.g., land cover, disturbance history) with the resulting fine-scale, patch-level fire progressions (e.g., Nogueira et al., 2016; Parks et al., 2018). Ultimately, the analysis area is not limited by the common constraints of disk space and processing speed because the provisional classification protocol and BULC algorithm are both programmed in Google Earth Engine.

Information regarding fire progression through time, within a given year, offers insights regarding suppression success and enables linkages to potential drivers of fire spread.

4.5 Conclusion

In this study, we created and analyzed a fire-progression time series for all 89 fires in the historically large 2017 BC fire season using freely available data from multiple sensors and BULC. Working within the 2017 fire perimeters created by the BC Wildfire Service, we used over 1500 raw scenes from Landsat-7, Landsat-8, Sentinel-2, and MODIS to create 276 provisional input classifications. BULC was then used to merge the provisional classifications in Google Earth Engine, producing a synthesized time-series stack with updated weekly burned areas for the 2017 fire season for each fire in BC. This approach estimated burned areas for the 2017 fire season to within 16% of the estimates developed by the Canadian federal government in cooperation with provincial authorities for this fire season while uniquely also mapping fire progressions throughout the entire fire season.

By reconstructing fire progressions for actively burning fires using a multi-source satellite time series approach, we are able to examine burned-area attributes for the fire season and individual fires at varying temporal windows. Fires from the same fire season have varying attributes, whether small or large and quickly or slowly burning. A majority of the fires in the 2017 fire season were small and had rapid growth periods but accounted for less than 13% of the cumulative fire area. Small and slow-growing fires accounted for only 3% of burned areas. Of the three largest fires investigated (e.g., Plateau, Hanceville-Riske, Elephant Hill), collectively representing 83% of the cumulative burned area for the 2017 fire season, burning was widespread but progressed at variable rates (both slow and rapid). Most of the behaviours and peak burn periods for the fire season were associated with weather events such as lightning and windstorms that occurred in early July and mid-September. Individual fires have varying burn progressions and different spatial patterns. By examining the daily burned areas of fires relative to total burned areas, we can quantify, compare, and contrast fire characteristics and the length of active burning phase.

This study reveals the potential for classifying multi-source, fire-progression stacks in other fire-prone regions and fire seasons utilizing our approach. Opportunities exist for increasing sources for fire observations for retrospective progression reconstruction and for implementing this approach for near-real-time fire monitoring to better inform fire agencies and forest managers. By implementing this approach using open-source satellite sources and remote sensing platforms, it can be applied on other historical fire seasons in Canada and tested for applicability internationally. Retrospective and near-term fire-classification stacks like these for historical and future fire seasons can be used to analyze underlying fire ecology and inform future disaster management.

Acknowledgements

This research was undertaken as part of the 'Earth Observation to Inform Canada's Climate Change Agenda (EO3C)' project jointly funded by the Canadian Space Agency (CSA), Government Related Initiatives Program (GRIP), and the Canadian Forest Service (CFS) of Natural Resources Canada. This research was enabled in part by support provided by WestGrid (www.westgrid.ca) and Compute Canada (www.computecanada.ca). Many thanks to Nicolas Rivarola, Sara Pancheri, and Eric Davies. This manuscript benefited from the insights of three anonymous reviewers.

4.6 References

Abatzoglou, J.T., Williams, A.P., 2016. Impact of anthropogenic climate change on wildfire across western US forests. Proceedings of the National Academy of Sciences. 113(42), 11770-11775.

Abbott, G., Chapman, M., 2018. Addressing the new normal: 21st century disaster management in British Columbia. British Columbia Government Report. 1–140. https://www2.gov.bc.ca/assets/gov/public-safety-and-emergency-services/emergency-preparedness-response-recovery/embc/bc-flood-and-wildfire-review-addressing-the-new-normal-21st-century-disaster-management-in-bc-web.pdf

Achanta, R., and Süsstrunk, S., 2017. Superpixels and polygons using simple non-iterative clustering. 2017 IEEE Conference Computer Vision and Pattern Recognition (CVPR). 4895–4904.

Amiro, B.D., Todd, J.B., Wotton, B.M., Logan, K.A., Flannigan, M.D., Stocks, B.J., Mason, J.A., Martell, D.L. Hirsch, K.G., 2001. Direct carbon emissions from Canadian forest fires, 1959-1999. Canadian Journal of Forest Research. 31(3), 512–525.

Blaschke, T., 2010. Object based image analysis for remote sensing. ISPRS Journal of Photogrammetry and Remote Sensing. 65(1), 2–16.

BC Wildfire Service, 2017a. Wildfire season summary. https://www2.gov.bc.ca/gov/content/safety/wildfire-status/about-bcws/wildfire-history/wildfire-season-summary (accessed 28 October 2018).

[dataset] BC Wildfire Service, 2017b. PROT_CURRENT_FIRE_POLYS_SP Ministry of Forests, Lands, Natural Resource Operations and Rural Development. https://catalogue.data.gov.bc.ca/dataset/fire-perimeters-current (accessed 25 January 2018)

BC Wildfire Service, 2017c. Wildfires of note - Plateau Fire (C0784). http://bcfireinfo.for.gov.bc.ca/hprScripts/WildfireNews/OneFire.asp?ID=645 (accessed 28 October 2018).

BC Wildfire Service, 2017d. Wildfires of note – Hanceville-Riske Creek (C50647). http://bcfireinfo.for.gov.bc.ca/hprScripts/WildfireNews/OneFire.asp?ID=666 (accessed 28 October 2018).

BC Wildfire Service, 2017e. Wildfires of note - Elephant Hill (K20637). http://bcfireinfo.for.gov.bc.ca/hprScripts/WildfireNews/OneFire.asp?ID=620 (accessed 28 October 2018).

BC Wildfire Service, 2017f. Wildfires of note – White River Fire (N1628). http://bcfireinfo.for.gov.bc.ca/hprScripts/WildfireNews/OneFire.asp?ID=678 (accessed 28 October 2018).

Benali, A., Russo, A., Sá, A.C., Pinto, R., Price, O., Koutsias, N., Pereira, J., 2016. Determining fire dates and locating ignition points with satellite data. Remote Sensing. 8(4), 326.

Boschetti, L., Roy, D.P., Justice, C.O., Humber, M.L., 2015. MODIS–Landsat fusion for large area 30m burned area mapping. Remote Sensing of Environment. 161, 27–42.

Bowman, D. 2018. Wildfire science is at a loss for comprehensive data. Nature. 560(7). doi: 10.1038/d41586-018-05840-4

British Columbia, 2018. Remembering 2017: Looking back a year later at the start of the 2017 wildfire season for the Cariboo Fire Centre. https://www2.gov.bc.ca/gov/content/safety/wildfire-status/about-bcws/wildfire-history/remembering-2017 (accessed 28 October 2018).

Burton, P.J., Parisien, M.A., Hicke, J.A., Hall, R.J., Freeburn, J.T., 2009. Large fires as agents of ecological diversity in the North American boreal forest. International Journal of Wildland Fire. 17(6), 754–767.

Canadian Council of Forest Ministers, 2018. Forest Fires. http://nfdp.ccfm.org/en/data/fires.php (accessed 30 October 2018).

Cardille, J.A., Fortin, J.A., 2016. Bayesian updating of land-cover estimates in a data-rich environment. Remote Sensing of Environment. 186, 234–249.

Chuvieco, E., Mouillot, F., van der Werf, G.R., San Miguel, J., Tanasse, M., Koutsias, N., García, M., Yebra, M., Padilla, M., Gitas, I., Heil, A., 2019. Historical background and current developments for mapping burned area from satellite Earth observation. Remote Sensing of Environment. 225, 45-64.

Crowley, M.A., Cardille, J.A., White, J.C., Wulder, M.A., 2019. Multi-sensor, multi-scale, Bayesian data synthesis for mapping within-year wildfire progression. Remote Sensing Letters. 10.3(2019), 302–311. doi: 10.1080/2150704X.2018.1536300

de Groot, W.J., Pritchard, J.M., Lynham, T.J., 2009. Forest floor fuel consumption and carbon emissions in Canadian boreal forest fires. Canadian Journal of Forest Research. 39(2), 367–382. doi:10.1139/X08-192

de Groot, W.J., Landry, R., Kurz, W.A., Anderson, K.R., Englefield, P., Fraser, R.H., Hall, R.J., Banfield, E., Raymond, D.A., Decker, V., Lynham, T.J., 2007. Estimating direct carbon emissions from Canadian wildland fires. International Journal of Wildland Fire. 16(5), 593–606. doi:10.1071/ WF06150

Egorov, A.V., Roy, D.P., Zhang, H.K., Hansen, M.C., Kommareddy, A., 2018. Demonstration of percent tree cover mapping using Landsat Analysis Ready Data (ARD) and sensitivity with respect to Landsat ARD processing level. Remote Sensing. 10(2), 209.

Engelbrecht, J., Theron, A., Vhengani, L., Kemp, J., 2017. A simple normalized difference approach to burnt area mapping using multi-polarisation C-Band SAR. Remote Sensing. 9(8), 764.

Fire Growth Model, 2018. Prometheus - Overview. http://www.firegrowthmodel.ca/prometheus/overview_e.php (accessed 28 October 2018).

Fraser, R.H., Li, Z., Cihlar, J., 2000. Hotspot and NDVI differencing synergy (HANDS): A new technique for burned area mapping over boreal forest. Remote Sensing of Environment. 74(3), 362-376.

Fraser, R.H., Hall, R.J., Landry, R., Lynham, T., Raymond, D., Lee, B., Li, Z., 2004. Validation and calibration of Canada-wide coarse-resolution satellite burned-area maps. Photogrammetric Engineering and Remote Sensing. 70(4), 451–460.

Frazier, R.J., Coops, N.C., Wulder, M.A., Hermosilla, T., White, J.C., 2018. Analyzing spatial and temporal variability in short-term rates of post-fire vegetation return from Landsat time series. Remote Sensing of Environment. 205, 32–45.

[dataset] Giglio, L., Justice, C., Boschetti, L., Roy, D., 2015. MCD64A1 MODIS/Terra+Aqua Burned Area Monthly L3 Global 500m SIN Grid V006. NASA EOSDIS Land Processes DAAC. https://doi.org/10.5067/MODIS/MCD64A1.006 (accessed 1 March 2018).

Gitas, I.Z., Mitri, G.H., Ventura, G., 2004. Object-based image classification for burned area mapping of Creus Cape, Spain, using NOAA-AVHRR imagery. Remote Sensing of Environment. 92(3), 409–413.

Gorelick, N., Hancher, M., Dixon, M., Ilyushchenko, S., Thau, D., Moore, R., 2017. Google Earth Engine: Planetary-scale geospatial analysis for everyone. Remote Sensing of Environment. 202, 18–27.

Hall, R.J., Freeburn, J.T., de Groot, W.J., Pritchard, J.M., Lynham, T.J., Landry, R., 2008. Remote sensing of burn severity: experience from western Canada boreal fires. International Journal of Wildland Fire. 17(4), 476–489.

Hermosilla, T., Wulder, M.A., White, J.C., Coops, N.C., Hobart, G.W., Campbell, L.B., 2016. Mass data processing of time series Landsat imagery: pixels to data products for forest monitoring. International Journal of Digital Earth. 9(11), 1035–1054.

Hermosilla, T., Wulder, M.A., White, J.C., Coops, N.C., Hobart, G.W., 2017. Updating Landsat time series of surface-reflectance composites and forest change products with new observations. International Journal of Applied Earth Observation and Geoinformation. 63, 104–111.

Hilker, T., Wulder, M.A., Coops, N.C., Linke, J., McDermid, G., Masek, J.G., Gao, F., White, J.C., 2009a. A new data fusion model for high spatial-and temporal-resolution mapping of forest disturbance based on Landsat and MODIS. Remote Sensing of Environment. 113(8), 1613–1627.

Hilker, T., Wulder, M.A., Coops, N.C., Seitz, N., White, J.C., Gao, F., Masek, J.G., Stenhouse, G., 2009b. Generation of dense time series synthetic Landsat data through data blending with MODIS using a spatial and temporal adaptive reflectance fusion model. Remote Sensing of Environment. 113(9), 1988–1999.

Humber, M.L., Boschetti, L., Giglio, L., Justice, C.O., 2018. Spatial and temporal intercomparison of four global burned area products. International Journal of Digital Earth. 1–25.

Jolly, W.M., Cochrane, M.A., Freeborn, P.H., Holden, Z.A., Brown, T.J., Williamson, G.J., Bowman, D.M., 2015. Climate-induced variations in global wildfire danger from 1979 to 2013. Nature Communications. 6, 7537.

Key, C.H., Benson, N.C., 1999. Measuring and remote sensing of burn severity. In L. F. Neuenschwander, & K. C. Ryan (Eds.), Proceedings Joint Fire Science Conference and Workshop, vol. II (p. 284). Moscow, ID: University of Idaho and International Association of Wildland Fire.

Key, C.H., Benson, N.C., 2006. Landscape Assessment (LA). FIREMON: Fire effects monitoring and inventory system. In: Lutes, D.C., Keane, R.E., Carati, J.F., Key, C.H., Benson, N.C., Gangi, L.J. (Eds.), General technical report RMRS-GTR-164-CD (pp. LA−1-55). USDA Forest Service, Rocky Mountains Research Station, Fort Collins, CO. https://doi.org/10.2737/RMRS-GTR-164

Korhonen, L., Hadi, Packalen, P., Rautiainen, M., 2017. Comparison of Sentinel-2 and Landsat 8 in the estimation of boreal forest canopy cover and leaf area index. Remote Sensing of Environment. 195, 259–274.

Lee, J., Cardille, J., Coe, M., 2018. BULC-U: Sharpening resolution and improving accuracy of land-use/land-cover classifications in Google Earth Engine. Remote Sensing. 10(9), 1455.

Li, J., Roy, D.P., 2017. A global analysis of sentinel-2A, sentinel-2B and Landsat-8 data revisit intervals and implications for terrestrial monitoring. Remote Sensing. 9(9), 902.

Lohberger, S., Stängel, M., Atwood, E.C., Siegert, F., 2018. Spatial evaluation of Indonesia's 2015 fire-affected area and estimated carbon emissions using Sentinel-1. Global Change Biology. 24(2), 644-654.

Mora, B., Wulder, M.A., White, J.C., Hobart, G., 2013. Modeling stand height, volume, and biomass from very high spatial resolution satellite imagery and samples of airborne LiDAR. Remote Sensing. 5(5), 2308–2326.

[dataset] Natural Resources Canada, 2018a. nbac_2017_r2_20180725_1603.zip Canadian National Fire Database - National Burned Area Composite. http://cwfis.cfs.nrcan.gc.ca/downloads/nbac/ (accessed 10 September 2018).

Natural Resources Canada, 2018b. Monthly and Seasonal Forecasts - Canadian Wildland Fire Information System. http://cwfis.cfs.nrcan.gc.ca/maps/forecasts (accessed 28 October 2018).

Nogueira, J.M., Ruffault, J., Chuvieco, E., Mouillot, F., 2016. Can we go beyond burned area in the assessment of global remote sensing products with fire patch metrics? Remote Sensing. 9(1), 7.

Padilla, M., Stehman, S.V. Chuvieco, E., 2014. Validation of the 2008 MODIS-MCD45 global burned area product using stratified random sampling. Remote Sensing of Environment. 144, 187-196.

Padilla, M., Stehman, S.V., Ramo, R., Corti, D., Hantson, S., Oliva, P., Alonso-Canas, I., Bradley, A.V., Tansey, K., Mota, B., Pereira, J.M., 2015. Comparing the accuracies of remote sensing global burned area products using stratified random sampling and estimation. Remote Sensing of Environment. 160, 114-121.

Parisien, M.A., Parks, S.A., Miller, C., Krawchuk, M.A., Heathcott, M., Moritz, M.A., 2011. Contributions of ignitions, fuels, and weather to the spatial patterns of burn probability of a boreal landscape. Ecosystems. 14(7), 1141–1155. doi:10.1007/S10021-011-9474-2

Parisien, M.A., Peters, V.S., Wang, Y., Little, J.M., Bosch, E.M., Stocks, B.J., 2006. Spatial patterns of forest fires in Canada, 1980–1999. International Journal of Wildland Fire. 15(3), 361–374.

Parks, S.A., Parisien, M.A., Miller, C., 2012. Spatial bottom-up controls on fire likelihood vary across western North America. Ecosphere. 3(1), 1–20. doi:10.1890/ES11-00298.1

Parks, S.A., 2014. Mapping day-of-burning with coarse-resolution satellite fire-detection data. International Journal of Wildland Fire. 23(2), 215–223.

Parks, S.A., Holsinger, L.M., Panunto, M.H., Jolly, W.M., Dobrowski, S.Z., Dillon, G.K., 2018. High-severity fire: evaluating its key drivers and mapping its probability across western US forests. Environmental Research Letters. 13(4), 044037.

Quintano, C., Fernández-Manso, A., Fernández-Manso, O., 2018. Combination of Landsat and Sentinel-2 MSI data for initial assessing of burn severity. International Journal of Applied Earth Observation and Geoinformation. 64, 221–225.

Roy, D.P., Wulder, M.A., Loveland, T.R., Woodcock, C.E., Allen, R.G., Anderson, M.C., Helder, D., Irons, J.R., Johnson, D.M., Kennedy, R., Scambos, T.A., 2014. Landsat-8: Science and product vision for terrestrial global change research. Remote Sensing of Environment. 145, 154–172.

San-Miguel, I., Andison, D.W., Coops, N.C., 2017. Characterizing historical fire patterns as a guide for harvesting planning using landscape metrics derived from long term satellite imagery. Forest Ecology and Management. 399, 155–165. doi:10.1016/j.foreco.2017.05.021.

San-Miguel, I., Andison, D.W., Coops, N.C., 2018. Quantifying local fire regimes using the Landsat data-archive: a conceptual framework to derive detailed fire pattern metrics from pixel-level information. International Journal of Digital Earth. 1–22. doi:10.1080/17538947.2018.1464072

Schroeder, T.A., Wulder, M.A., Healey, S.P., Moisen, G.G., 2011. Mapping wildfire and clearcut harvest disturbances in boreal forests with Landsat time series data. Remote Sensing of Environment. 115(6), 1421–1433.

Soverel, N.O., Perrakis, D.D., Coops, N.C., 2010. Estimating burn severity from Landsat dNBR and RdNBR indices across western Canada. Remote Sensing of Environment. 114(9), 1896–1909.

Soverel, N.O., Coops, N.C., Perrakis, D.D., Daniels, L.D., Gergel, S.E., 2011. The transferability of a dNBR-derived model to predict burn severity across 10 wildland fires in western Canada. International Journal of Wildland Fire. 20(4), 518–531.

Stinson, G., Kurz, W.A., Smyth, C.E., Neilson, E.T., Dymond, C.C., Metsaranta, J.M., Boisvenue, C., Rampley, G.J., Li, Q., White, T.M., Blain, D., 2011. An inventory-based analysis of Canada's managed forest carbon dynamics, 1990 to 2008. Global Change Biology. 17(6), 2227-2244.

Stocks, B.J., Mason, J.A., Todd, J.B., Bosch, E.M., Wotton, B.M., Amiro, B.D., Flannigan, M.D., Hirsch, K.G., Logan, K.A., Martell, D.L., Skinner, W.R., 2003. Large forest fires in Canada, 1959–1997. Journal of Geophysical Research: Atmospheres. 108(D1: FFR5): 1–12. doi:10.1029/2001 JD000484

U. S. Geological Survey, 2018. U.S. Landsat Analysis Ready Data (ARD) Data Format Control Book (DFCB). LSDS-809, Sioux Falls, SD: US Department of Interior, Earth Resources

Observation and Science (EROS) Center. https://landsat.usgs.gov/sites/default/files/documents/LSDS-1873_US_Landsat_ARD_DFCB.pdf (accessed 15 April 2018).

Veraverbeke, S., Somers, B., Gitas, I., Katagis, T., Polychronaki, A., Goossens, R., 2012. Spectral mixture analysis to assess post-fire vegetation regeneration using Landsat Thematic Mapper imagery: Accounting for soil brightness variation. International Journal of Applied Earth Observation and Geoinformation. 14(1), 1–11.

Veraverbeke, S., Sedano, F., Hook, S.J., Randerson, J.T., Jin, Y., Rogers, B.M., 2014. Mapping the daily progression of large wildland fires using MODIS active fire data. International Journal of Wildland Fire. 23(5), 655–667.

Verhegghen, A., Eva, H., Ceccherini, G., Achard, F., Gond, V., Gourlet-Fleury, S., Cerutti, P., 2016. The potential of Sentinel satellites for burnt area mapping and monitoring in the Congo Basin forests. Remote Sensing. 8(12), 986.

White, J.C., Wulder, M.A., Hobart, G.W., Luther, J.E., Hermosilla, T., Griffiths, P., Coops, N.C., Hall, R.J., Hostert, P., Dyk, A., Guindon, L., 2014. Pixel-based image compositing for large-area dense time series applications and science. Canadian Journal of Remote Sensing. 40(3), 192–212.

White, J.C., Wulder, M.A., Hermosilla, T., Coops, N.C., Hobart, G.W., 2017. A nationwide annual characterization of 25 years of forest disturbance and recovery for Canada using Landsat time series. Remote Sensing of Environment. 194, 303–321.

Wulder, M.A., Skakun, R.S., Kurz, W.A., White, J.C., 2004. Estimating time since forest harvest using segmented Landsat ETM+ imagery. Remote Sensing of Environment. 93(1–2), 179–187.

Wulder, M.A., White, J.C., Gillis, M.D., Walsworth, N., Hansen, M.C., Potapov, P., 2010. Multiscale satellite and spatial information and analysis framework in support of a large-area forest monitoring and inventory update. Environmental Monitoring and Assessment. 170(1–4), 417–433.

Wulder, M.A., White, J.C., Masek, J.G., Dwyer, J., Roy, D.P., 2011. Continuity of Landsat observations: Short term considerations. Remote Sensing of Environment. 115(2), 747–751.

Wulder, M.A., Coops, N.C., Roy, D.P., White, J.C., Hermosilla, T., 2018. Land cover 2.0. International Journal of Remote Sensing. 39(12), 4254–4284. doi:10.1080/01431161.2018.1452075

Zhu, Z., 2017. Change detection using Landsat time series: A review of frequencies, preprocessing, algorithms, and applications. ISPRS Journal of Photogrammetry and Remote Sensing. 130, 370–384.

Preface to Chapter 5

Chapter 4 presented a large-area data fusion approach for mapping and analyzing active wildfire progressions with novel fire progression metrics for individual and cumulative fire season scales. Chapter 4 advanced the field of remote sensing and fire science by mapping a synthesized fire progression time series for all stand-replacing BC fires in 2017 and using fire progression metrics to compare fire characteristics. I often contextualized the fire progression metrics with fire drivers describing fire season conditions throughout Chapter 4's analysis, highlighting future research opportunities to integrate fire drivers into fire season progressions. Chapter 5 builds upon Chapters 2, 3 and 4 to apply a whole-systems lens to fire monitoring and management using Earth observations.

Chapter 5 identifies information needs for each fire monitoring and management stage to clarify stakeholder priorities for future research and management interventions. Chapter 5 advances the field of wildfire remote sensing by conceptually connecting all stages of the fire research cycle, identifying future data needs and opportunities, and working collaboratively with stakeholders from each stage of the fire research cycle. This last research chapter is an important contribution to the broader fields of fire sciences and remote sensing because it applies a whole-systems approach to research design, which is less frequently used in the nexus of these fields. Additionally, Chapter 5 outlines future research opportunities that will guide me as I progress in my fire remote sensing career.

Chapter 5 will be submitted for review in 2022 and uses the American Psychological Association (APA) citation style.

5. Towards a whole-system framework for wildfire monitoring using Earth observations

Authors:

Morgan A. Crowley[a*], Christopher Stockdale[b], Joshua M. Johnston[c], Michael A. Wulder[d], Tianjia Liu[e], Jessica L. McCarty[f], Jesse T. Rieb[g], Jeffrey A. Cardille[a], Joanne C. White[d]

[a]*Department of Natural Resource Sciences, McGill University, Sainte-Anne-de-Bellevue, Québec, Canada*

[b]*Canadian Forest Service (Northern Forestry Centre), Natural Resources Canada, Edmonton, Alberta, Canada*

[c]*Canadian Forest Service (Great Lakes Forestry Centre), Natural Resources Canada, Sault Sainte Marie, Ontario, Canada*

[d]*Canadian Forest Service (Pacific Forestry Centre), Natural Resources Canada, Victoria, British Columbia, Canada*

[e]*Department of Earth and Planetary Sciences, Harvard University, Cambridge, Massachusetts, USA*

[f]*Department of Geography, Miami University, Oxford, Ohio, USA*

[g]*Department of Geography, McGill University, Montréal, Québec, Canada*

*Corresponding Author: morgan.crowley@mail.mcgill.ca

Intended submission date: April 2022

Keywords: Earth observations, complex systems, wildfires, fire monitoring, remote sensing

Abstract

Fire seasons have become increasingly variable and extreme due to changing climatological, ecological and social conditions. Earth observation data are critical for monitoring fires and their impacts. Herein, we present a whole-system framework for identifying and synthesizing fire monitoring objectives and data needs throughout the life cycle of a fire event. The four stages of fire monitoring informed using Earth observation data include: 1) pre-fire vegetation inventories, 2) active-fire monitoring, 3) post-fire assessment, and 4) multi-scale synthesis. We identify the challenges and opportunities associated with current approaches to fire monitoring, highlighting four case studies from North America. The field of remote sensing is experiencing a rapid proliferation of new data sources, providing observations that can inform all aspects of our fire monitoring framework; however, significant challenges for meeting fire monitoring objectives remain. We identify future opportunities for data sharing and rapid co-development of information products like fire dashboards using cloud computing that benefit from open-access Earth observation and other geospatial data layers.

5.1 Introduction

Around the world, the impacts of a warming climate on fire activity are clear, from lengthening fire seasons to increased variability in the number, extent, and severity of fires. These changes correspond with more extreme ecological factors and shifting human populations that contribute to a complex, interrelated cycle of forest fires and associated impacts (Jolly et al., 2015; Wooster et al., 2021). Communities in these fire-prone regions try to reduce the negative impacts of wildfires through prevention and suppression but face challenges due to increased, unpredictable ignition locations in remote forests with heavy fuel loads that are vulnerable to uncontrolled and less predictable spread (Coogan et al., 2019, 2020; Flannigan et al., 2009; McFayden et al., 2019). Through a broad lens, fire monitoring should not be limited to the time of active fire. Pre-fire monitoring is essential to community preparedness, while active and post-fire monitoring are critical for characterizing impacts and understanding the effectiveness of management interventions (and assessment of post-fire damages). To monitor conditions and changes in vast fire-prone landscapes in Canada and the United States, communities often rely on Earth observation data collected by sensors mounted on satellites, airplanes, unoccupied aerial and high-altitude systems, balloons, and ground-based systems (Chuvieco et al., 2019, 2020; Giglio et al., 2016; Johnston et al., 2020; O'Connor, 2021; Schroeder et al., 2008; Wooster et al., 2021). However, each of these remote-sensing data sources provides a specific type of information at a specific spatial scale, and each has associated advantages and limitations, such as financial costs for data collection on demand, delayed revisit rates for freely available data sources, mismatched provincial or fire-agency focused data collection, and no existing fire-focused satellite sensors for cross-boundary data collection (Chuvieco et al., 2019; Crowley & Cardille, 2020; Johnston et al., 2020). While these disparate data sources fulfill specific fire monitoring information needs, they are rarely brought together or used synergistically to produce new information products or enable new insights.

A whole-systems fire monitoring approach, whereby multi-stage objectives are synthesized using Earth observations, can help stakeholders harmonize wildfire response and management objectives to better respond to the complex ecological and social conditions of the wildfire system. Whole-systems approaches are already used in fire ecology to unite multiple scientific fields, methodologies, and spatial and temporal scales (Bowman & Murphy, 2011; McWethy et al., 2019; Tedim et al., 2018). For example, pyrogeography is a disciplinarian framework that combines biological, atmospheric, and social approaches to better understand the multiple direct and indirect factors of fire activity in the past, present, and future (Bowman et al., 2013; Bowman & Murphy, 2011; Krawchuk et al., 2009; Roos et al., 2014). Given this context, herein, we propose a whole-system fire monitoring framework using Earth observation data as an opportunity to address the varying objectives associated with forest monitoring and management before, during, and after a wildfire occurs. Four main stages of fire monitoring have been identified (Chuvieco et al., 2019, 2020; Wooster et al., 2021): (1) pre-fire inventory, (2) active-fire monitoring: (3) post-fire analysis, and (4) multi-scale synthesis. The information, needs, data sources, and tools required vary at each stage; as observation abilities increase, the opportunities and constraints increase. Our objectives are to outline the information needs associated with each stage of our fire monitoring framework, describe how the stages relate to each other, and define how Earth observation data can be used to meet objectives within our holistic framework. We then consider this whole-systems fire monitoring framework in the context of four case studies from western North America to demonstrate how the proposed framework could address some of the identified challenges when similar conditions are experienced in the future.

5.2 Fire monitoring: growing opportunities for Earth observations at each stage

Each fire monitoring stage has unique information needs that are met by specific data sources matching their priority spatial and temporal scales. Spatial and temporal characteristics of a given sensor also link to image extent and revisit time. Very-high and high spatial resolution sensors typically have a smaller spatial extent, which can result in longer revisit times if consistent viewing geometry is required. Requirements for rapid revisit times necessitate trade-offs in spatial resolution, favouring coarse spatial resolution data (i.e., > 500 m2) and resulting in less spatial detail for mapped features. For example, many remote sensing and fire community members use data sources such as the Geostationary Operational Environmental Satellite (GOES-R), Moderate Resolution Imaging Spectroradiometer (MODIS) or Visible Infrared Imaging Radiometer Suite (VIIRS) for active fire monitoring because they have a frequent revisit, are readily available, pre-processed, and open-access. Other stakeholders who prioritize spatially fine-scale mapping and monitoring, and do not need the information as rapidly, use Landsat, Sentinel-2, or joint Landsat and Sentinel-2 based workflows that calculate band ratios or use training-data-informed classification algorithms to map pre-fire vegetative conditions or post-fire fire burned areas and severity. Often in these instances, the nuances in differing fire monitoring objectives vary drastically (J. M. Johnston et al., 2020) al., 2020), and mismatches in temporal and spatial scales and resolutions create gaps and limitations in research findings and emergency decision-making. Fire monitoring objectives can be categorized into four major stages outlined in Figure 5.1 and Table 5.1 including, 1) pre-fire inventories (Arroyo et al., 2008; Chuvieco et al., 2020; Gale et al., 2021; White et al., 2016), 2) active-fire monitoring (Chuvieco et al., 2020; Johnston et al., 2020; Wooster et al., 2021), 3) post-fire assessment (Bartels et al., 2016; Chuvieco et al., 2019, 2020; Frolking et al., 2009; White et al., 2016), 4) multi-scale synthesis (Roos et al., 2014). The fire monitoring stages over have commonalities of data inputs and outputs, the intersections of which can be categorized into three sub-stages, including fire behaviour prediction analyses (1A), impact assessments (2A), and recovery and successional trajectory (3A).

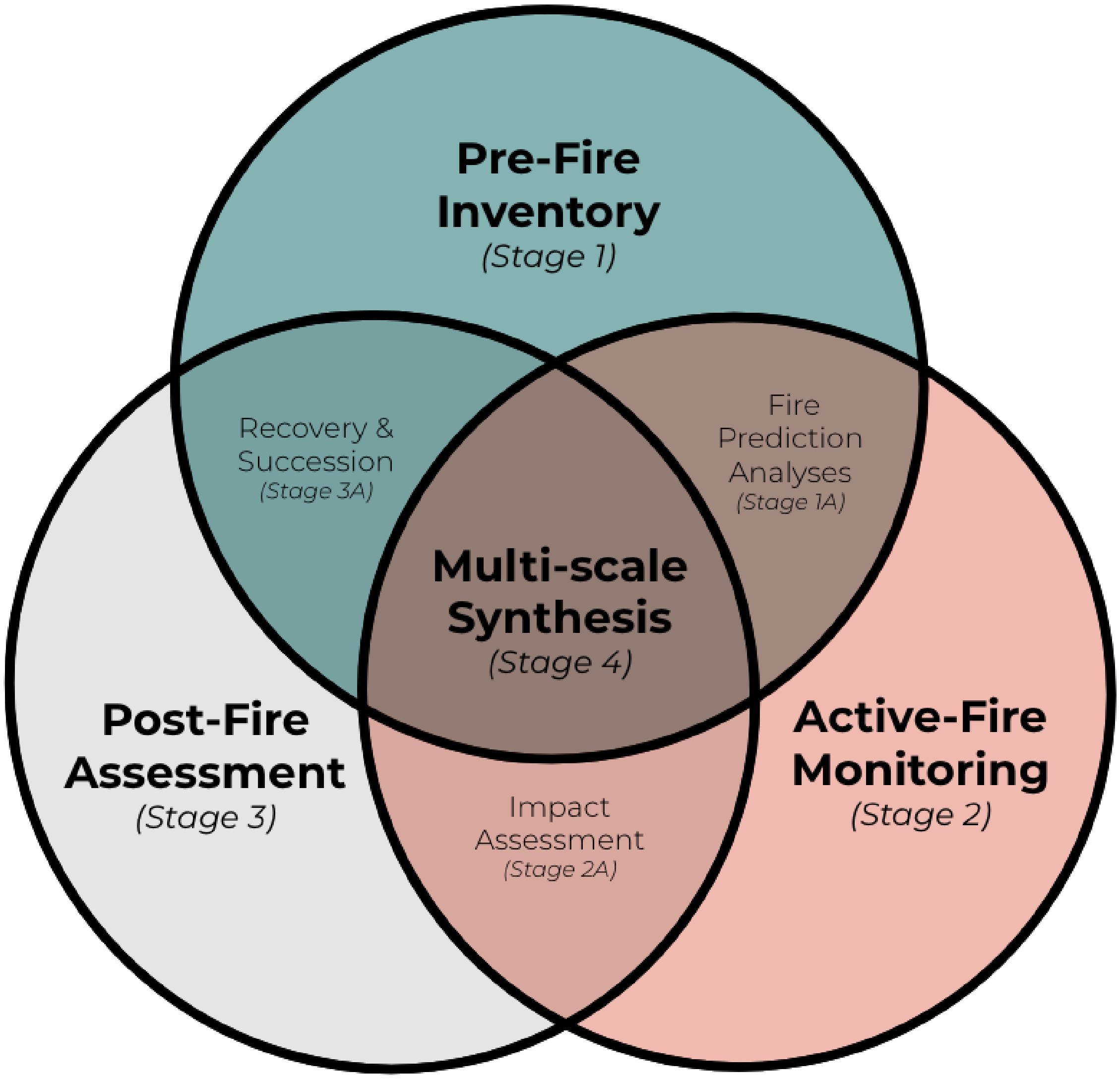

Figure 5.1 The four-stage, whole-systems fire monitoring framework that mirrors the life cycle of a fire event from before, during, and after the fire. Starting from the left, Stage 1 is pre-fire inventory, overlapping in 1A with fire prediction analyses with Stage 2, active-fire monitoring. The objectives of Stage 2 intersect with Stage 3, post-fire assessment, in Stage 2A, impact assessments. Stage 3 objectives intersect with Stage 1 objectives in Stage 3A, recovery and succession. The three major Stages 1-3 intersect together to match the objectives of Stage 4, multi-scale synthesis.

Table 5.1 Summary of objectives and primary information needs for each fire monitoring stage and substage as described in Section 5.2.

Stage	Description	Objective	Primary information needs and data sources/additional information requirements
1	Pre-Fire Inventory	*What can burn?*	• Detailed, annual observations of forest structure (e.g., forest type, height stem density), vegetation/fuel conditions, and important infrastructure (e.g., roads, power lines, pipelines, municipal facilities) • Analysis-ready, medium spatial resolution RS data
1A	Fire Behaviour and Prediction Analysis	*Where and how could it burn?*	• Annual inventory maps from Stage 1 • Additional information on forest vertical structure (e.g., crown base height) from airborne lidar
2	Active-Fire Monitoring	*Where is the fire and what is it doing?*	• Near-real time detection (sub-daily) • Rapid download (e.g., minimal latency) • High-to-medium spatial resolution RS data • On-demand data collection
2A	Impact Assessment	*Where and how did it burn?*	• Fire characteristics data from Stage 2 • Burn characteristics from active remote sensing
3	Post-Fire Assessment	*What burned and how did it burn?*	• Open-access data • High-to-medium spatial resolution RS data (e.g., Landsat, Sentinel-2) or fine temporal resolution (e.g., MODIS, VIIRS, GOES) • Data fusion algorithms (e.g., machine learning, Bayesian synthesis)
3A	Recovery & Succession	*Where and how will it regrow?*	• Burned area maps from Stage 3 • Regrowth characteristics from active remote sensing or retrospectively from time series optical EO data
4	Multi-scale Synthesis	*What has and can burn in the past, present, and future?*	• Pre-, active, post-fire information • Social and ecological data • Cloud-based platforms and dashboards

5.2.1 Stage 1: Pre-fire Inventory

In Stage 1, stakeholders answer "what can burn?" on a landscape before a fire occurs. Pre-fire information needs relate to the vegetation available on the landscape to burn and the associated risks to communities, wildlife, and critical infrastructure. There are a variety of pre-fire inventorying objectives that must be met before a fire happens to identify what could be vulnerable to impacts when a fire is ignited and spreads. Using geospatial technologies and remotely sensed data, managers and scientists will inventory landscape resources, forested areas, vegetation types, infrastructure, fuel types, and fuel moisture conditions. Sometimes inventories will rely on historical data to identify locations impacted by past disturbances (Shang et al., 2020). Vegetation inventory maps are often used to support forest and landscape management efforts to mitigate the impacts of future fires (O'Connor, 2021). In Stage 1A (Figure 5.1), fire behaviour and prediction analyses use pre-fire inventories for pre-season planning or to model potential active fire characteristics in fuel growth models (Chuvieco et al., 2020; Wotton et al., 2009). This stage often informs active-fire characterization by providing information from fire growth models using parameters gathered from controlled burns, vegetation inventories, and other landscape condition data (e.g., Jolly and Freeborn 2017). By relying on information provided from pre-fire inventories, fire behaviour prediction analyses support Stage 2, active-fire monitoring, by helping to predict what could happen and plan future response if a fire begins in a particular location under specific weather conditions.

The characteristics of remotely sensed data sources used to create landscape inventory maps vary based on the objectives for their usage, for example, for forest inventory or fire growth modelling. In the case of fuel and vegetation inventory maps, many existing datasets do not use Earth observations in their creation, thus rendering them outdated. Fuel and vegetation inventory maps typically rely on sources with a medium spatial resolution (10m to 30m). Remote sensing-based fuel loads and vegetation maps are primarily derived from optical sensors (such as Landsat or Sentinel-2) and updated monthly or annually (Chuvieco et al., 2020; Gale et al., 2021). Some data sources such as MODIS-derived vegetation datasets are updated with higher temporal frequency but at the expense of having a coarser spatial resolution. Fuel and vegetation condition maps are often outdated from current landscape conditions due to the tradeoffs between spatial extent, spatial resolution, and revisit rates relative to the rate of disturbances in the region. Additionally, these vegetation maps lack vertical information due to the limitations of optical data sources for estimating vegetation structure. Census and GIS-based infrastructure datasets are typically updated at 5- to 10-year cycles. Infrastructure can also be estimated from imagery-based classifications that identify impervious surfaces or built-up features (Xian et al., 2009).

The minimum mapping unit for Stage 1 to inform pre-fire inventorying is the object of interest on the landscape, whether vegetation-related (e.g., forest stand) or infrastructure (e.g., houses, cabins, pipelines, powerlines). A primary data need for Stage 1 is Earth observations collected with a medium temporal resolution to regularly update fuel, vegetation and infrastructure inventories and medium spatial resolution to support operational response (Chuvieco et al., 2020). To properly inform fire prediction models in Stage 1A, annual inventory maps that provide vertical structure can refine estimates of standing fuel loads and their condition. To work towards near-real-time fuel condition maps, satellite missions with short revisit rates (e.g., less than one week) will be particularly useful to update fuel inventory maps at more frequent intervals. There is often a tradeoff in download latency for near-real-time observations between accessing the data rapidly and the time it takes to pre-process and classify the imagery. Analysis-ready data can help streamline data processing latencies when updating fuel inventories by reducing the number of steps in the analysis process. There are opportunities for these inventory maps to benefit from airborne LiDAR data and recently or soon-to-be-launched SAR and LiDAR satellite missions (e.g., ICESat-2, ALOS-4, NISAR, BIOMASS, GEDI, RADARSAT Constellation Mission) to inform vertical components of fuel inventories (Chuvieco et al., 2020; García et al., 2012; O'Connor, 2021; White et al., 2016).

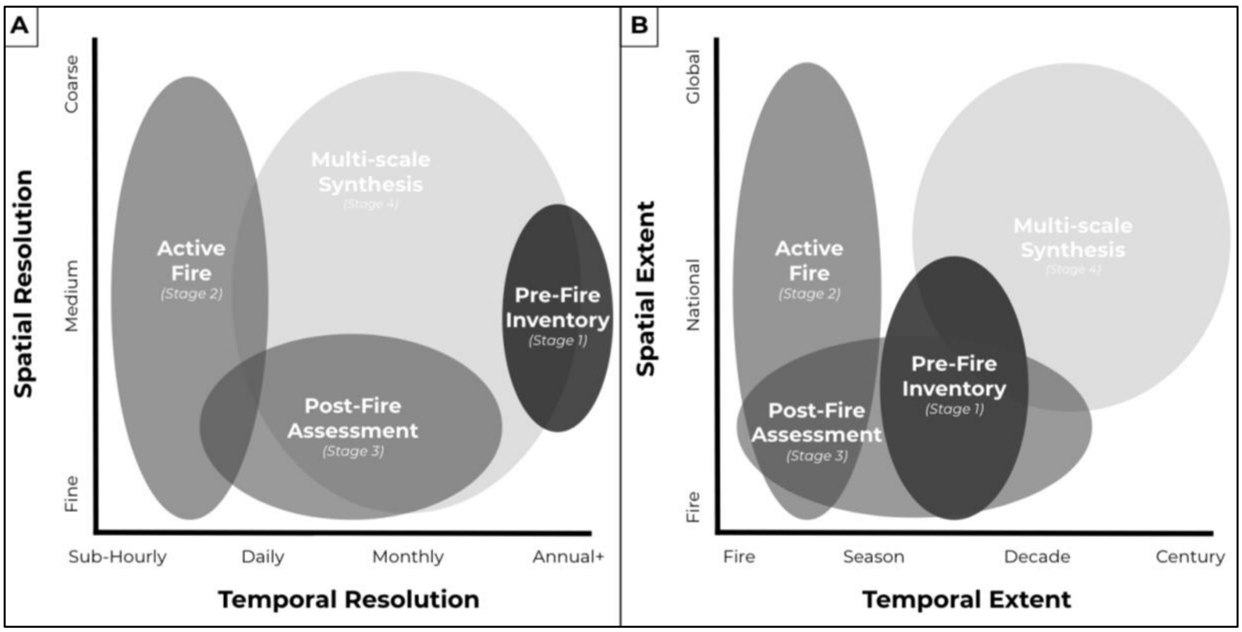

Figure 5.2 What information is needed for each fire monitoring stage to meet their mapping objectives? Each stage's information needs in terms of Earth observation scalar characteristics are plotted as shaded circles in A) for ideal spatial and temporal resolution and in B) for spatial and temporal extent/coverage.

5.2.2 Stage 2: Active-fire monitoring

In the event of an active fire, the main objective in Stage 2 is to answer, "where is the fire?" on a landscape and "what is it doing?". Active-fire monitoring in Stage 2 relies on remote-sensing data collected with reduced latency so that stakeholders can make emergency suppression decisions in a timely manner (Johnston et al., 2020; Wooster et al., 2021). Satellite systems like GOES, VIIRS, MODIS and SLSTR, provide large-area imagery with a moderate spatial resolution (375m to 2km) and sub-daily collection rates, beneficial for detecting ignitions across large regions (Roy et al., 2005). However, analyses using these sources can be impacted by atmospheric interferences and sub-optimal collecting rates (Chuvieco et al., 2020; Johnston et al., 2020; Wooster et al., 2021).

Detailed, near-real-time active fire monitoring focuses on helping control and limit active fire spread through fire detection, delineation, and characterization. Active fire monitoring uses Earth observations to detect actively burning fires, estimate fire radiative power, and derive or delineate fire characterizations like perimeters, sub-pixel conditions, intensity, rate of spread, fuel consumption, and real-time emissions (Wooster et al., 2021). Optical sensors that collect data with infrared bands are useful for fire detection and characterization, however, can be vulnerable to false positives due to similarities between fire and other infrared-emitting features like sunglints, volcanoes, and more (Johnston et al., 2020; Wooster et al., 2021). Detected fire hotspots and characteristics, in conjunction with knowledge of available fuels (pre-fire stage), are used in fire growth models to inform evacuation decisions for nearby communities and prevention and immediate fire suppression operations. These models have to be updated with real-time information on fire perimeters to make short-term fire predictions that estimate where and when a fire will move in a particular direction based on where it is currently burning (Johnston et al., 2020). On-demand data collection is particularly useful for this type of active fire monitoring and is made possible with commercial satellites (e.g., DigitalGlobe's Worldview-3, DLR FireBIRD), solar-powered high-altitude systems (e.g., Airbus Zephyr unoccupied aerial vehicle), aerial surveys (Allison et al., 2016), or handheld cameras. However, these systems are costly and cover smaller spatial extents than satellite data sources.

Stage 2A occurs either immediately after the fire has been extinguished or using data collected directly after the fire has burned to assess its near-term impacts (Chuvieco et al., 2019, 2020). In this stage, remotely sensed data are used to estimate how the fire burned, its severity, and the burn depth relative to the active fire and burned areas. By analyzing active-fire data collected with reduced latency in Stage 2, the fire impact assessments of Stage 2A are often used to inform post-fire analyses further explored in Stage 3. Synthetic Aperture Radar (SAR) satellites like RADARSAT and Sentinel-1 that employ active remote sensing approaches are particularly useful for estimating these types of fire characteristics because they can be used to penetrate smoke/haze and map burned areas (Chuvieco et al., 2019). However, SAR satellite imagery often has longer revisit rates and pre-processing times. Tradeoffs between data collection characteristics and availability time create difficulty for rapid active-fire detection, delineation, and characterization.

A crucial characteristic of remote-sensing sources for future active fire monitoring is rapid download latency, ideally less than 30 minutes between data collection and availability to the user (Johnston et al., 2020). High-to-medium spatial resolution observations are valuable contributions for delineating precise active-fire boundaries, Figure 5.2, however easily accessible sub-daily observations are even more critical to support fast updates of these maps for decision-making (Johnston et al., 2020). Rapid data access and processing is vital for fire detection and emergency response; therefore, there are significant opportunities to utilize machine learning algorithms to quickly map active fire boundaries on the fly to reduce classification latency (Jain et al., 2020). Dedicated fire monitoring satellite programs like the proposed WildFireSat missions will advance fire delineation and characterization because they have been designed to meet the user needs in the active-fire monitoring stage with frequent revisit rates, medium spatial resolution, large area coverage, and reduced latency for data collection (Johnston et al., 2020).

5.2.3 Stage 3: Post-fire assessment

Stage 3 focuses on post-fire assessments to answer the question "what burned and how did it burn?" and analyses the impacts of the fire itself, management strategies, and suppression efforts. Burned area mapping is the primary objective to map the final disturbance extent and understand what burned and how it burned when a fire passed through (Chuvieco et al., 2019). In this stage, post-fire analyses of fire behaviour and spread are reconstructed in relation to underlying ecological conditions. The results from these analyses are helpful for refining fire prediction models and better understanding future fire drivers. Stage 3A uses post-fire assessments that identify burned regions to monitor fuel recovery and successional trajectories (Bartels et al., 2016; Chu & Guo, 2013). Inventory maps created in Stage 1 are informed by Stage 3A analyses that can identify the post-fire changes to underlying landscape conditions to identify what burned and what can burn next. Post-fire studies focus on how vegetation regrows in burned areas that experienced different fire severities.

Current post-fire assessments presently rely on readily available, open-access data that have either high-to-medium spatial resolution (e.g., Landsat, Sentinel-2) or fine temporal resolution (e.g., MODIS, VIIRS, GOES) (Andela et al., 2019; Chuvieco et al., 2016, 2020; Frazier et al., 2018; Hawbaker et al., 2017). Very-high and high spatial resolution data are available from commercial satellites from companies like Planet and DigitalGlobe; however, these imagery sources can be cost-prohibitive for broadscale applications, cover small spatial extents, or lack temporal revisits rates ideal for post-fire successional assessments. Additionally, LiDAR and SAR data are useful for mapping changes in vegetation structure and recovery after a fire disturbance (Bright et al., 2017; Chu & Guo, 2013; Frolking et al., 2009; Lefsky et al., 2001; White et al., 2017).

Much like the other stages of fire monitoring analyses, tradeoffs must be made to prioritize different post-fire analysis objectives, Figure 5.2. Data fusion algorithms could help leverage benefits from various Earth observation sources by informing post-fire analyses with fused data about burned and unburned regions (Johnston et al., 2020). Opportunities exist to fuse fine temporal resolution observations with the high-to-medium spatial resolution data from optical, SAR, and LiDAR sources to create large-area datasets. There are existing data fusion algorithms that assimilate some of these data sources on the fly or provide analysis-ready data for further post-fire analyses (Boschetti et al., 2015; Chuvieco et al., 2020; Crowley et al., 2019a, 2019b; Hilker, Wulder, Coops, Linke, et al., 2009; Hilker, Wulder, Coops, Seitz, et al., 2009). But additional data fusion algorithms will be necessary to leverage input data sources' unique and informative characteristics into one unified, seamless analysis.

5.2.4 Stage 4: Multi-scale synthesis

At Stage 4 of the framework presented in Figure 1, multi-scale synthesis and pyrogeography analyses use data and results from all of the other stages (Bowman et al., 2013; Bowman & Murphy, 2011; Krawchuk et al., 2009; Roos et al., 2014). These assessments, which are central to the fire system monitoring framework, explore complex, large-scale concepts like classifying ecosystem trajectories, fire regimes, firesheds, and fire risk (McFayden et al., 2019). In this interrelated stage of fire monitoring, social and ecological data are often integrated together to better understand the complex wildfire system (Chuvieco et al., 2020). Broad-scale, pyrogeography-based fire monitoring analyses that utilize Earth observations assimilate data and findings from pre, active, and post-fire analyses as well as long and short-term historical geospatial data, Figure 5.2.

To support multi-scale analyses like these in Stage 4, individual fire monitoring Stages 1, 2 and 3 must meet their fire monitoring objectives and achieve their primary information needs. To synthesize the findings from the multiple stages, cloud-based data processing and storage platforms are beneficial for creating fire dashboards (e.g., Pyregence, Technosylva) that increase open data accessibility and rapid analyses (Lanclos, 2021; Saah, 2021). By using existing multi-source Earth observations, dashboards like these can support end-to-end user applications between the different fire monitoring stages by providing analysis-ready data and emergency alerts. Multi-scale fire monitoring analyses are also being incorporated into mission plans before the satellite launch and data collection. For example, dedicated fire monitoring satellite missions would be more readily able to assist these analyses because the different user groups from each fire monitoring stage are involved in the planning from the start of the satellite design to the data processing algorithm creation to designing the data-sharing platforms.

5.3 Applying the whole fire system monitoring framework to historical fires

The whole-systems framework can be applied to historical fires to assess mismatches between monitoring objectives, information needs, and available data. This section will use four historical fires, fire seasons, and regions as case studies representing each stage of the whole fire monitoring framework, Table 5.2. The 2016 Horse River Fire in Alberta, Canada highlights the important impacts that inaccurate pre-fire information in Stage 1 can have on all subsequent fire monitoring stages. The 2021 White Rock Lake Fire, in British Columbia, Canada, demonstrates how a paucity of data and a failure to meet the information needs in Stage 2 can adversely impact active fire response. The 1988 Yellowstone Fires in Wyoming, USA highlights the importance of satellite data sources for supporting post-fire, retrospective analyses in Stage 3. Lastly, the numerous pyrogeographical studies assessing the fire-prone Northern Rockies region in the conterminous USA illustrate the benefits of Stage 4 multi-scale analyses to analyze fire regimes, legacies, resiliency, and ecological shifts. For each case study, our objective is to describe the context associated with the particular fire and indicate how Earth observation data could have been used to support the objectives and information needs associated with that stage. In so doing we also make recommendations for how Earth observations could be used to better support fire monitoring under similar future conditions.

Table 5.2 Characteristics overview for each case study corresponding with fire monitoring stages 1 through 4.

Stage	Case Study	Location	Scope	Total Area Burned (ha)	Start/held dates or study period	Suspected Cause
1	Horse River Fire	Alberta, Canada	Incident	585,000	May 1 to July 4, 2016	Human
2	White Rock Lake Fire	British Columbia, Canada	Incident	83,342	July 13 to September 10, 2021	Lightning
3	Yellowstone Fires	Wyoming, USA	Fire Season	485,600	June to September 1988	Lightning and human
4	Northern Rocky Mountains	Conterminous, USA	Fire Atlas	~100,000	Various dates between 1900 to 2007	Lightning

5.3.1 Stage 1: Horse River Fire, Alberta, Canada

The 2016 Horse River Fire occurred near Fort McMurray, Alberta and burned over 585,000 hectares. It is one of the costliest wildfires in Canadian history, with nearly $9 billion in damages and over 2400 structures destroyed (Malbeuf, 2021). In the week leading up to the fire ignition on May 1, fire behaviour models had successfully predicted extreme conditions despite needing improvements to weather forecasting to include longer-term dryness of past seasons (Ahmed et al., 2019; Nash et al., 2017). However, the existing vegetation inventory was too coarse in spatial resolution and missed more explosive understory fuel types and dryer ground fuels, and the infrastructure inventory around the community was outdated and lacked up-to-date information about valuable structures and assets (Nash et al., 2017). The response agencies only learned about the significance of critical infrastructure (e.g., electricity and pumping stations) once they were already at risk of being destroyed by the fire.

In the case of the Horse River Fire, pre-fire information did not fully characterize the risk of explosive vegetation fuel conditions and critical infrastructure for Stage 1. This challenge had cascading impacts on subsequent stages because the existing infrastructure inventory created in Stage 1 differed from the information needs of the fire predictions made in Stage 1A and the emergency respondents in Stage 2. Similar to other historical fires like California's Camp Fire in 2018 (Griffin, 2021), if the fire agencies of Fort McMurray had had access to fine-scale, near-real-time landscape inventories identifying significant infrastructure and fuel conditions, they could have planned accordingly to mitigate some of the severe impacts on the high-risk and vulnerable community. The post-fire report for the Horse River Fire (Nash et al., 2017) recommended a unified response from provincial and local fire agencies. We would extend this recommendation to the generation of Stage 1 information products that multi-scale jurisdictional fire agencies (e.g., local, provincial, federal) should coordinate inventory and mapping efforts. The Horse River Fire exemplifies how inaccurate pre-fire data products can severely impact response and ultimately outcomes of catastrophic wildfires in the vicinity of communities. This example also illustrates the importance of involving different end-users throughout the fire monitoring system when objectives and creating near-real-time updating inventory maps.

5.3.2 Stage 2: White Rock Lake Fire, British Columbia, Canada

British Columbia experienced its third-worst fire season in 2021 in terms of area burned, just behind the historic 2018 and 2017 seasons (Kulkarni, 2021). Record-breaking temperatures due to a series of heatwaves combined with drought conditions culminated in a disastrous fire season for the southern interior region of the province (BC Wildfire Service, 2021). One fire of note was the White Rock Lake Fire near Falkland, BC, which caused significant damage to nearly 80 properties. During the White Rock Lake Fire, the intense smoky conditions and high winds limited airborne response (MacPherson & Dickson, 2021), which is a challenge commonly faced in active-fire monitoring as illustrated by the 2017 Kenow Fire in Alberta, Canada (Rumbolt, 2017). The smoky conditions also limited the availability of clear optical Earth observation data for monitoring White Rock Lake Fire conditions, which further contributed to data sparsity.

The lack of data available for monitoring the White Rock Lake Fire resulted in delays in meeting the information needs for Stage 2 active fire mapping and decision-making. Social media served as a leading source of communication to update community members about evacuation alerts and fire location statuses (MacPherson & Dickson, 2021). While the lack of contemporaneous reconnaissance data throughout the fire event in Stage 2 hindered operational response, remotely sensed data will be instrumental in supporting Stage 2A and 3 analyses. For example, when examining the subsequent research that followed the data sparsity throughout the 2017 Kenow Fire, Landsat observations were used to estimate fire severity (Whitman et al., 2020), ground-based LiDAR data was collected to quantify carbon dioxide release (Gerrand et al., 2021), and mixed-methods of satellite and ground-based observations were used to identify vegetation recovery and successional trajectories (Eisenberg et al., 2019). In the case of the

White Rock Lake Fire, Earth observation satellites with short-wave infrared or infrared sensors and short temporal imaging latency could have helped image the active wildfire as it spread and was clouded in smoke. Proposed missions such as WildFireSat, which house sensors specifically designed for imaging wildfires, would be useful for increasing the likelihood of clear observations to support Stage 2 mapping objectives.

5.3.3 Stage 3: Yellowstone Fires, Wyoming, USA

From June to September 1988, Yellowstone National Park experienced catastrophic wildfires that burned nearly 1.2 million acres in the region (Hansen & Krantz, 2008; Kwak-Hefferan, 2021). The fires were ignited by natural and human sources in a region experiencing severe drought, extreme weather conditions and increased fuel loads (Turner & The Conversation US, 2018). Aerial surveys with infrared sensors were conducted throughout the fire season to calculate daily burned area and map fire perimeters (Rothermel et al., 1994). Following the conclusion of the fire season, scientists analyzed the impacts of the fires on the Yellowstone National Park landscape using available optical imagery from Landsat Thematic Mapper (TM) sensor from the following fire season to classify burn severity using estimates of biomass loss (Turner et al., 1994, 1997). Post-fire analyses revealed relationships between daily fire size and pattern, fire severity and early vegetation succession (Turner et al., 1994, 1997).

For the Yellowstone Fires of 1988, the information available for post-fire analyses in Stage 3 was limited by the technologies and data accessibility of the time. These post-fire analyses of the Yellowstone Fires relied on a single, cloud-free Landsat TM image from August 2, 1989, and aerial surveys for daily burned areas and patterns (Rothermel et al., 1994; Turner et al., 1994, 1997). The analyses of fire impacts, pattern, and early succession were performed prior to the open-access data policy being enacted in 2008 (Woodcock et al., 2008; Zhu et al., 2019), thus limiting the availability of satellite-based information for post-fire analyses before this date. In the case of the Yellowstone Fires of 1988, successional data was collected from field-based samples from the following summer. For a similar fire season today, opportunities exist to use data from open-access, satellite-based LiDAR, SAR, and optical sensors to map near-term, early vegetation succession data across large areas (Bartels et al., 2016; Bolton et al., 2017; Hermosilla et al., 2018). Technological and policy advancements have increased data types and accessibility, and data fusion algorithms can be used to synthesize information from these new data sources for comprehensive post-fire analyses (Boschetti et al., 2015; Chuvieco et al., 2020; Crowley et al., 2019a, 2019b; Hilker, Wulder, Coops, Linke, et al., 2009; Hilker, Wulder, Coops, Seitz, et al., 2009). These types of retrospective analyses or forensic audits enable greater understanding of fire behaviour and efficacy of response and control strategies. Moreover, information derived from these investigations can in turn refine parameterizations of fire spread models. The feedback and interplay among the various stages of the framework represented in Figure 5.1 are key to maximizing investments in data, infrastructures, and systems to better manage and integrate information.

5.3.4 Stage 4: Northern Rocky Mountains, Conterminous USA

The fire regime and system of the Northern Rockies region of the United States have been analyzed extensively through multi-scale and pyrogeography studies using combined satellite-based data sources and previously created satellite-derived products. For example, LANDFIRE vegetation and fire regime products have been combined with multi-decadal burn severity products from Monitoring Trends in Burn Severity (MTBS) to analyze regional forest resilience to wildfires, fire legacies, and ecological shifts over future conditions (Kemp et al., 2016, 2019). Digitized polygon fire perimeters from local national forests and parks have been used to create a fire atlas for the region (Morgan et al., 2014). By combining the region's fire atlas with LANDFIRE vegetation data, scientists characterized pyrogeography and multi-season climate drivers for the twentieth century (Gibson et al., 2014; Morgan et al., 2008, 2014). Other studies in this region analyzed the impact of forest management practices on fire severity for past fires in the US Northern Rockies by combining satellite-derived burn severity from MTBS and fuel characteristics from LANDFIRE (Wimberly et al., 2009).

In the case of the US Northern Rockies region and multi-scale analyses of Stage 4, it is more difficult to perform large-scale, cross-boundary analyses because existing pre-processed fire products like fire atlases, LANDFIRE, and MTBS have been created at regional or national extents. Multi-scale analyses that rely on these satellite-derived products are limited to the spatial and temporal scale characteristics of the input remotely sensed data or the algorithms used to create the datasets. Data fusion algorithms, open-access workflows, and cloud-based fire dashboards can support future multi-scale analyses that synthesize information from multiple sources (Boschetti et al., 2015; Chuvieco et al., 2020; Crowley et al., 2019a, 2019b; Hilker, Wulder, Coops, Linke, et al., 2009). In particular, fire dashboards can integrate data developed in the first three fire monitoring stages to contextualize present-day fires with historical fire patterns, behaviours, and risk across multiple temporal and spatial scales (Lanclos, 2021; Saah, 2021). By integrating information outcomes from all the stages of the framework, Stage 4 syntheses provide social-ecological systems findings that can inform future response, policy, and planning.

5.4 Discussion and Conclusions

In this study, we present a holistic framework for Earth observation analysis that identifies the multiple stages of monitoring during the life cycle of the wildfire system. By identifying and synthesizing objectives and information needs for each fire monitoring stage using this framework, Earth observation-based fire monitoring can be better positioned to support future fire suppression and management. We identified fire monitoring stage priorities to assemble, facilitate, and expedite the accessibility of Earth observations to inform near-real-time modeling and management, further supporting downstream fire mapping and analyses. In the case of wildland fires, as illustrated by the four case studies presented, failure to information needs and fire monitoring objectives can result in catastrophe, whether loss of life, infrastructure, ecosystems, and more. Whole-systems frameworks like the one presented herein can be used to navigate the complexities of fire monitoring by understanding information needs at each stage, identifying existing data sources, and conceptualizing measures to advance fire monitoring capacity in the future.

By applying this framework to four North American fire case studies, we show how a holistic framework can help identify gaps between data acquisition, supply, analysis, and desires for stakeholders. The case studies illustrate the importance of having access to the right information for the right scale at the right time to meet fire monitoring objectives for each stage. For example, the 2021 White Rock Lake Fire illustrated that there can be significant challenges in acquiring the data necessary to support the information needs associated with a given stage, and moreover that delays in processing that data into the required information products and getting those products into the hands of decision-makers can have downstream consequences for response and management. Fire analysis dashboards like Pyregence show promise for making fire monitoring data and alerts publicly available as soon as they can be processed. Additionally, fire dashboards can support multi-scale analyses and multi-stage data synthesis to contextualize current fire events with historical conditions, disturbances, and succession. Fire dashboards, however, must be designed in consultation with all stakeholders (e.g., provincial and federal fire agencies, First Nations communities, local governments, landowners, residents) to help prioritize the information needs of a broad range of end-users while also building trust and awareness of the resource.

In recent years, we have seen the launch of multiple Earth observation satellites that will be particularly useful for meeting fire monitoring objectives outlined in the whole-systems framework. Recently launched Landsat-9, GEDI, ICESAT-2, RADARSAT Constellation Mission, and others will provide perspectives of pre, active, and post-fire landscapes with cutting-edge data characteristics like frequent revisit rates, capacity to characterize vertical structure and distribution of vegetation, and smoke and haze penetrating wavelengths. Proposed missions like WildFireSat will be designed with fire monitoring objectives at the forefront. Together, all these data sources will advance forest fire monitoring capacity due to the increased volume of data and the complementary nature of the observations. By fusing these sources with historical data from the long-term, open-access Landsat program, multi-decadal pyrogeographical analyses using Earth observations will provide additional insights into the fire system from the past fifty years.

A significant contribution of this whole-systems approach is increasing the understanding of fire systems and multiple objectives for remote sensing scientists. There is often a challenge to find the right balance between validation of information products generated from Earth observation data and providing timely outputs to meet the needs of decision-makers. Fire dashboards co-designed with representatives from multiple stakeholder groups can be particularly powerful to ensure that future fire monitoring approaches prioritize the needs of the whole fire system. This framework can be applied to future fire case studies to identify mismatches between fire monitoring objectives and data needs. By identifying these inconsistencies, users from similar fire systems will be able to identify challenges and opportunities for paths forwards using Earth observations to support fire monitoring and management of future fires.

5.5 References

Ahmed, M. R., Hassan, Q. K., Abdollahi, M., & Gupta, A. (2019). Introducing a New Remote Sensing-Based Model for Forecasting Forest Fire Danger Conditions at a Four-Day Scale. Remote Sensing, 11(18), 2101.

Allison, R. S., Johnston, J. M., Craig, G., & Jennings, S. (2016). Airborne Optical and Thermal Remote Sensing for Wildfire Detection and Monitoring. Sensors , 16(8). https://doi.org/10.3390/s16081310

Andela, N., Morton, D. C., Giglio, L., Paugam, R., Chen, Y., Hantson, S., van der Werf, G. R., & Randerson, J. T. (2019). The Global Fire Atlas of individual fire size, duration, speed and direction. Earth System Science Data, 11(2), 529–552.

Arroyo, L. A., Pascual, C., & Manzanera, J. A. (2008). Fire models and methods to map fuel types: The role of remote sensing. Forest Ecology and Management, 256(6), 1239–1252.

Bartels, S. F., Chen, H. Y. H., Wulder, M. A., & White, J. C. (2016). Trends in post-disturbance recovery rates of Canada’s forests following wildfire and harvest. Forest Ecology and Management, 361, 194–207.

BC Wildfire Service. (2021). 2021 Wildfire Season Summary. Retrieved October 15, 2021, from https://www2.gov.bc.ca/gov/content/safety/wildfire-status/about-bcws/wildfire-history/wildfire-season-summary

Bolton, D. K., Coops, N. C., Hermosilla, T., Wulder, M. A., & White, J. C. (2017). Assessing variability in post-fire forest structure along gradients of productivity in the Canadian boreal using multi-source remote sensing. Journal of Biogeography, 44(6), 1294–1305.

Boschetti, L., Roy, D. P., Justice, C. O., & Humber, M. L. (2015). MODIS–Landsat fusion for large area 30m burned area mapping. Remote Sensing of Environment, 161, 27–42.

Bowman, D. M. J. S., & Murphy, B. P. (2011). Australia—A Model System for the Development of Pyrogeography. Fire Ecology, 7(1), 5–12.

Bowman, D. M. J. S., O'Brien, J. A., & Goldammer, J. G. (2013). Pyrogeography and the Global Quest for Sustainable Fire Management. Annual Review of Environment and Resources, 38(1), 57–80.

Bright, B. C., Hudak, A. T., Meddens, A. J. H., Hawbaker, T. J., Briggs, J. S., & Kennedy, R. E. (2017). Prediction of Forest Canopy and Surface Fuels from Lidar and Satellite Time Series Data in a Bark Beetle-Affected Forest. Forests, Trees and Livelihoods, 8(9), 322.

Chu, T., & Guo, X. (2013). Remote Sensing Techniques in Monitoring Post-Fire Effects and Patterns of Forest Recovery in Boreal Forest Regions: A Review. Remote Sensing, 6(1), 470–520.

Chuvieco, E., Aguado, I., Salas, J., García, M., Yebra, M., & Oliva, P. (2020). Satellite Remote Sensing Contributions to Wildland Fire Science and Management. Current Forestry Reports, 6(2), 81–96.

Chuvieco, E., Mouillot, F., van der Werf, G. R., San Miguel, J., Tanasse, M., Koutsias, N., García, M., Yebra, M., Padilla, M., Gitas, I., Heil, A., Hawbaker, T. J., & Giglio, L. (2019). Historical background and current developments for mapping burned area from satellite Earth observation. Remote Sensing of Environment, 225, 45–64.

Chuvieco, E., Yue, C., Heil, A., Mouillot, F., Alonso-Canas, I., Padilla, M., Pereira, J. M., Oom, D., & Tansey, K. (2016). A new global burned area product for climate assessment of fire impacts. Global Ecology and Biogeography: A Journal of Macroecology, 25(5), 619–629.

Coogan, S. C. P., Daniels, L. D., Boychuk, D., Burton, P. J., Flannigan, M. D., Gauthier, S., Kafka, V., Park, J. S., & Mike Wotton, B. (2020). Fifty years of wildland fire science in Canada. Canadian Journal of Forest Research. Journal Canadien de La Recherche Forestiere. https://cdnsciencepub.com/doi/10.1139/cjfr-2020-0314

Coogan, S. C. P., Robinne, F.-N., Jain, P., & Flannigan, M. D. (2019). Scientists' warning on wildfire — a Canadian perspective. Canadian Journal of Forest Research. Journal Canadien de La Recherche Forestiere, 49(9), 1015–1023.

Crowley, M. A., & Cardille, J. A. (2020). Remote sensing's recent and future contributions to landscape ecology. Current Landscape Ecology Reports, 5(3), 45–57.

Crowley, M. A., Cardille, J. A., White, J. C., & Wulder, M. A. (2019a). Large-area synthesis of multiple remotely sensed data sources for mapping within-year wildfire progression. Remote Sensing of Environment.

Crowley, M. A., Cardille, J. A., White, J. C., & Wulder, M. A. (2019b). Multi-sensor, multi-scale, Bayesian data synthesis for mapping within-year wildfire progression. Remote Sensing Letters , 10(3), 302–311.

Eisenberg, C., Anderson, C. L., Collingwood, A., Sissons, R., Dunn, C. J., Meigs, G. W., Hibbs, D. E., Murphy, S., Kuiper, S. D., SpearChief-Morris, J., Little Bear, L., Johnston, B., &

Edson, C. B. (2019). Out of the Ashes: Ecological Resilience to Extreme Wildfire, Prescribed Burns, and Indigenous Burning in Ecosystems. Frontiers in Ecology and Evolution, 7, 436.

Flannigan, M. D., Krawchuk, M. A., de Groot, W. J., Mike Wotton, B., & Gowman, L. M. (2009). Implications of changing climate for global wildland fire. International Journal of Wildland Fire, 18(5), 483–507.

Frazier, R. J., Coops, N. C., Wulder, M. A., Hermosilla, T., & White, J. C. (2018). Analyzing spatial and temporal variability in short-term rates of post-fire vegetation return from Landsat time series. Remote Sensing of Environment, 205, 32–45.

Frolking, S., Palace, M. W., Clark, D. B., Chambers, J. Q., Shugart, H. H., & Hurtt, G. C. (2009). Forest disturbance and recovery: A general review in the context of spaceborne remote sensing of impacts on aboveground biomass and canopy structure. Journal of Geophysical Research, 114(G2). https://doi.org/10.1029/2008jg000911

Gale, M. G., Cary, G. J., Van Dijk, A. I. J. M., & Yebra, M. (2021). Forest fire fuel through the lens of remote sensing: Review of approaches, challenges and future directions in the remote sensing of biotic determinants of fire behaviour. Remote Sensing of Environment, 255, 112282.

García, M., Popescu, S., Riaño, D., Zhao, K., Neuenschwander, A., Agca, M., & Chuvieco, E. (2012). Characterization of canopy fuels using ICESat/GLAS data. Remote Sensing of Environment, 123, 81–89.

Gerrand, S., Aspinall, J., Jensen, T., Hopkinson, C., Collingwood, A., & Chasmer, L. (2021). Partitioning carbon losses from fire combustion in a montane Valley, Alberta Canada. Forest Ecology and Management, 496, 119435.

Gibson, C. E., Morgan, P., & Wilson, A. M. (2014). Atlas of digital polygon fire extents for Idaho and western Montana. 2nd Edition [Data set]. Fort Collins, CO: Forest Service Research Data Archive. https://doi.org/10.2737/RDS-2009-0006-2

Giglio, L., Schroeder, W., & Justice, C. O. (2016). The collection 6 MODIS active fire detection algorithm and fire products. Remote Sensing of the Environment, 178, 31–41.

Hansen, L., & Krantz, L. (2008, August 29). Remembering The 1988 Yellowstone Fires. NPR. https://www.npr.org/templates/story/story.php?storyId=94126845

Hawbaker, T. J., Vanderhoof, M. K., Beal, Y.-J., Takacs, J. D., Schmidt, G. L., Falgout, J. T., Williams, B., Fairaux, N. M., Caldwell, M. K., Picotte, J. J., Howard, S. M., Stitt, S., & Dwyer, J. L. (2017). Mapping burned areas using dense time-series of Landsat data. Remote Sensing of Environment, 198, 504–522.

Hermosilla, T., Wulder, M. A., White, J. C., Coops, N. C., & Hobart, G. W. (2018). Disturbance-Informed Annual Land Cover Classification Maps of Canada’s Forested Ecosystems for a 29-Year Landsat Time Series. Canadian Journal of Remote Sensing, 44(1), 67–87.

Hilker, T., Wulder, M. A., Coops, N. C., Linke, J., McDermid, G., Masek, J. G., Gao, F., & White, J. C. (2009). A new data fusion model for high spatial- and temporal-resolution mapping of forest disturbance based on Landsat and MODIS. Remote Sensing of Environment, 113(8), 1613–1627.

Hilker, T., Wulder, M. A., Coops, N. C., Seitz, N., White, J. C., Gao, F., Masek, J. G., & Stenhouse, G. (2009). Generation of dense time series synthetic Landsat data through data blending with MODIS using a spatial and temporal adaptive reflectance fusion model. Remote Sensing of Environment, 113(9), 1988–1999.

Jain, P., Coogan, S. C. P., Subramanian, S. G., Crowley, M., Taylor, S., & Flannigan, M. D. (2020). A review of machine learning applications in wildfire science and management. In arXiv [cs.LG]. arXiv. http://arxiv.org/abs/2003.00646

Johnston, J. M., Jackson, N., McFayden, C., Ngo Phong, L., Lawrence, B., Davignon, D., Wooster, M. J., van Mierlo, H., Thompson, D. K., Cantin, A. S., Johnston, D., Johnston, L. M., Sloane, M., Ramos, R., & Lynham, T. J. (2020). Development of the User Requirements for the Canadian WildFireSat Satellite Mission. Sensors , 20(18). https://doi.org/10.3390/s20185081

Jolly, W. M., Cochrane, M. A., Freeborn, P. H., Holden, Z. A., Brown, T. J., Williamson, G. J., & Bowman, D. M. J. S. (2015). Climate-induced variations in global wildfire danger from 1979 to 2013. Nature Communications, 6, 7537.

Kemp, K. B., Higuera, P. E., & Morgan, P. (2016). Fire legacies impact conifer regeneration across environmental gradients in the U.S. northern Rockies. Landscape Ecology, 31(3), 619–636.

Kemp, K. B., Higuera, P. E., Morgan, P., & Abatzoglou, J. T. (2019). Climate will increasingly determine post-fire tree regeneration success in low-elevation forests, Northern Rockies, USA. Ecosphere , 10(1), e02568.

Krawchuk, M. A., Moritz, M. A., Parisien, M.-A., Van Dorn, J., & Hayhoe, K. (2009). Global pyrogeography: the current and future distribution of wildfire. PloS One, 4(4), e5102.

Kulkarni, A. (2021, October 4). A look back at the 2021 B.C. wildfire season. CBC News. https://www.cbc.ca/news/canada/british-columbia/bc-wildfires-2021-timeline-1.6197751

Kwak-Hefferan, E. (2021, June 20). The Summer Yellowstone Burned. What Went Wrong in 1988? https://www.yellowstonepark.com/park/history/1988-fires-yellowstone/

Lanclos, R. (2021, October 18). CAL FIRE Applies New Predictive and Tactical Tools to Fight Ferocious Fires. https://www.esri.com/about/newsroom/blog/cal-fire-puts-entire-team-on-same-map/

Lefsky, M. A., Cohen, W. B., & Spies, T. A. (2001). An evaluation of alternate remote sensing products for forest inventory, monitoring, and mapping of Douglas-fir forests in western Oregon. Canadian Journal of Forest Research. Journal Canadien de La Recherche Forestiere, 31(1), 78–87.

MacPherson, M., & Dickson, C. (2021, September 15). Paradise lost. CBC News. https://newsinteractives.cbc.ca/longform/white-rock-lake-fire

Malbeuf, J. (2021, May 3). Forged by fire: Fort McMurray 5 years after the disaster. CBC News. https://newsinteractives.cbc.ca/longform/fort-mcmurray-five-years-on-from-disaster

McFayden, C. B., Boychuk, D., Woolford, D. G., Wheatley, M. J., & Johnston, L. (2019). Impacts of wildland fire effects on resources and assets through expert elicitation to support fire response decisions. International Journal of Wildland Fire, 28(11), 885–900.

McWethy, D. B., Schoennagel, T., Higuera, P. E., Krawchuk, M., Harvey, B. J., Metcalf, E. C., Schultz, C., Miller, C., Metcalf, A. L., Buma, B., Virapongse, A., Kulig, J. C., Stedman, R. C., Ratajczak, Z., Nelson, C. R., & Kolden, C. (2019). Rethinking resilience to wildfire. Nature Sustainability, 2(9), 797–804.

Morgan, P., Heyerdahl, E. K., & Gibson, C. E. (2008). Multi-season climate synchronized forest fires throughout the 20th century, northern Rockies, USA. Ecology, 89(3), 717–728.

Morgan, P., Heyerdahl, E. K., Miller, C., Wilson, A. M., & Gibson, C. E. (2014). Northern Rockies Pyrogeography: an Example of Fire Atlas Utility. Fire Ecology, 10(1), 14–30.

Nash, T., St. Arnaud, L., Tithecott, A., Simpson, B., & Stocks, B. (2017). A Review of the 2016

Horse River Wildfire. MNP LLP. https://www.alberta.ca/assets/documents/Wildfire-MNP-Report.pdf

O'Connor, A. (2021, July 8). Effective Wildfire Management Using Remote Sensing Technology. L3Harris Geospatial. https://www.l3harrisgeospatial.com/Learn/Whitepapers/Whitepaper-Detail/ArtMID/17811/ArticleID/24063/Effective-Wildfire-Management-Using-Remote-Sensing-Technology?utm_source=twitter&utm_medium=wildfire_management_whitepaper

Roos, C. I., Bowman, D. M. J. S., Balch, J. K., Artaxo, P., Bond, W. J., Cochrane, M., D'Antonio, C. M., DeFries, R., Mack, M., Johnston, F. H., Krawchuk, M. A., Kull, C. A., Moritz, M. A., Pyne, S., Scott, A. C., & Swetnam, T. W. (2014). Pyrogeography, historical ecology, and the human dimensions of fire regimes. Journal of Biogeography, 41(4), 833–836.

Rothermel, R. C., Hartford, R. A., & Chase, C. H. (1994). Fire growth maps for the 1988 Greater Yellowstone Area Fires. U.S. Department of Agriculture, Forest Service, Intermountain Research Station. https://doi.org/10.2737/int-gtr-304

Roy, D. P., Jin, Y., Lewis, P. E., & Justice, C. O. (2005). Prototyping a global algorithm for systematic fire-affected area mapping using MODIS time series data. Remote Sensing of Environment, 97(2), 137–162.

Rumbolt, R. (2017, September 13). Water bombers back in the skies fighting "Goliath of a fire" in Waterton Lakes National Park. CBC News. https://www.cbc.ca/news/canada/calgary/waterton-fire-water-bomber-aircraft-fight-fire-1.4285571

Saah, D. (2021, May 2). Close to Home: Fighting wildfires with better science. Press Democrat. https://www.pressdemocrat.com/article/opinion/close-to-home-fighting-wildfires-with-better-science/

Schroeder, W., Prins, E., Giglio, L., Csiszar, I., Schmidt, C., Morisette, J., & Morton, D. (2008). Validation of GOES and MODIS active fire detection products using ASTER and ETM+ data. Remote Sensing of Environment, 112(5), 2711–2726.

Shang, C., Wulder, M. A., Coops, N. C., White, J. C., & Hermosilla, T. (2020). Spatially-Explicit Prediction of Wildfire Burn Probability Using Remotely-Sensed and Ancillary Data. Canadian Journal of Remote Sensing, 46(3), 313–329.

Tedim, F., Leone, V., Amraoui, M., Bouillon, C., Coughlan, M. R., Delogu, G. M., Fernandes, P. M., Ferreira, C., McCaffrey, S., McGee, T. K., & Others. (2018). Defining Extreme Wildfire Events: Difficulties, Challenges, and Impacts, Fire, 1, 9.

Turner, M. G., Hargrove, W. W., Gardner, R. H., & Romme, W. H. (1994). Effects of fire on landscape heterogeneity in Yellowstone National Park, Wyoming. Journal of Vegetation Science: Official Organ of the International Association for Vegetation Science, 5(5), 731–742.

Turner, M. G., Romme, W. H., Gardner, R. H., & Hargrove, W. W. (1997). Effects of fire size and pattern on early succession in Yellowstone National Park. Ecological Monographs, 67(4), 411–433.

Turner, M. G., & The Conversation US. (2018, August 28). Yellowstone Rebounded from an Epic 1988 Fire—That May Be Harder in Future. Scientific American. https://www.scientificamerican.com/article/yellowstone-rebounded-from-an-epic-1988-fire-that-may-be-harder-in-future/

White, J. C., Coops, N. C., Wulder, M. A., Vastaranta, M., Hilker, T., & Tompalski, P. (2016). Remote Sensing Technologies for Enhancing Forest Inventories: A Review. Canadian Journal of Remote Sensing, 42(5), 619–641.

White, J. C., Wulder, M. A., Hermosilla, T., Coops, N. C., & Hobart, G. W. (2017). A nationwide annual characterization of 25 years of forest disturbance and recovery for Canada using Landsat time series. Remote Sensing of Environment, 194, 303–321.

Whitman, E., Parisien, M.-A., Holsinger, L. M., Park, J., & Parks, S. A. (2020). A method for creating a burn severity atlas: an example from Alberta, Canada. International Journal of Wildland Fire, 29(11), 995–1008.

Wimberly, M. C., Cochrane, M. A., Baer, A. D., & Pabst, K. (2009). Assessing fuel treatment effectiveness using satellite imagery and spatial statistics. Ecological Applications: A Publication of the Ecological Society of America, 19(6), 1377–1384.

Woodcock, C. E., Allen, R., Anderson, M., Belward, A., Bindschadler, R., Cohen, W., Gao, F., Goward, S. N., Helder, D., Helmer, E., Nemani, R., Oreopoulos, L., Schott, J.,

Thenkabail, P. S., Vermote, E. F., Vogelmann, J., Wulder, M. A., & Wynne, R. (2008). Free access to Landsat imagery. Science, 320(5879), 1011.

Wooster, M. J., Roberts, G. J., Giglio, L., Roy, D., Freeborn, P., Boschetti, L., Justice, C., Ichoku, C., Schroeder, W., Davies, D., Smith, A., Setzer, A., Csiszar, I., Strydom, T., Frost, P., Zhang, T., Xu, W., de Jong, M., Johnston, J., … San-Miguel, J. (2021). Satellite remote sensing of active fires: History and current status, applications and future requirements. Remote Sensing of Environment, 267, 112694.

Wotton, B. M., Alexander, M. E., & Taylor, S. W. (2009). Updates and revisions to the 1992

Canadian Forest Fire Behavior Prediction System. Natural Resources Canada. https://www.researchgate.net/publication/274383139

Xian, G., Homer, C., & Fry, J. (2009). Updating the 2001 National Land Cover Database land cover classification to 2006 by using Landsat imagery change detection methods. Remote Sensing of Environment, 113(6), 1133–1147.

Zhu, Z., Wulder, M. A., Roy, D. P., Woodcock, C. E., Hansen, M. C., Radeloff, V. C., Healey, S. P., Schaaf, C., Hostert, P., Strobl, P., Pekel, J.-F., Lymburner, L., Pahlevan, N., & Scambos, T. A. (2019). Benefits of the free and open Landsat data policy. Remote Sensing of Environment, 224, 382–385.

6. Discussion and synthesis

In this dissertation, I explored opportunities for using multi-scale, open-access Earth observations and cloud-based processing for monitoring environmental change, such as wildfires. The field of remote sensing will continue to have significant advances for environmental change monitoring as new satellites with new data characteristics are launched and made more readily accessible to stakeholders and scientists. New cloud-based and cyberinfrastructure platforms like Google Earth Engine, Microsoft Planetary Computer, and Open Data Cube enable easy access and processing of new Earth observation data sources without needing a supercomputer. These dramatic advances support rapid environmental monitoring for hazards and disasters like forest fires.

Remote sensing is both a scientific field and a powerful methodological tool that can enable achievements in other research fields through raw imagery, analysis-ready data, pre-processed datasets, or processing platforms. Chapter 2 illustrated the importance of integrating methods and data from remote sensing into landscape ecology by examining the historical contributions of the Earth observation approaches to landscape ecology research. By doing so, I showed how remote sensing data and methodological approaches can continue to support advancing multi-scale landscape ecology research examining landscape function, structure, and change. As remote sensing data sources continue to proliferate, landscape ecologists will continue to tackle large-scale, synthesis-based questions using Earth observation techniques. This chapter examined recently published research from 2015 to 2019 and can serve as a baseline for future evaluations of remote sensing's contributions to landscape ecology research as both fields continue to benefit from open-source data and technological advances.

Remote-region fire monitoring is made possible with increased data availability, accessibility, and processing platforms, especially multi-source, multi-scale wildfire progression mapping with data fusion techniques. In Chapters 3 and 4, I made use of these advances in remote sensing to create a novel prototype for synthesizing fire classifications from multiple satellite sources to reconstruct near-term fire progressions in British Columbia, Canada. As we prepare for future satellite missions, including some that focus exclusively on mapping fires, novel data fusion techniques will be integral to synthesize data and leverage the strengths of each Earth observation source to improve fire monitoring. Because of its cloud-based approach, my method for fire classification synthesis can be used to reconstruct historic fires or track future wildfire progressions, cross-validate fire behaviour models, and compare fire progression metrics between historic fires and fire seasons. There are opportunities for this method to be applied in larger geographic areas, spanning longer periods, integrating active synthetic aperture radar (SAR) data sources (Engelbrecht et al., 2017), and using other commercial optical remote sensing data sources. Additionally, by using the output fire progression dataset generated with the approach illustrated in Chapters 3 and 4, these methods can provide information about active wildland fire progressions to improve our understanding of fire growth and associated drivers over space and time.

The whole-systems fire monitoring framework presented in Chapter 5 was developed as a result of the lessons learned from analyzing remote sensing contributions to landscape ecology in Chapter 2 and creating and applying a prototype for fire progression mapping using data fusion in Chapters 3 and 4. In particular, when presenting my research at scientific conferences throughout my Ph.D. program, I was often asked if my prototype would work in different fire scenarios that had different monitoring objectives. It was clear that while the other researchers were all looking at the same landscape phenomena, they had different information needs and priorities that could be achieved with adjustments to the spatial and temporal resolutions of the input Earth observation sources. By examining the fire monitoring system together as a whole, we can better understand and meet objectives by including all the stakeholders from every fire monitoring stage together in one framework. Like the wildfire system that is impacted by interrelated social and ecological fire drivers occurring on the same landscape, each fire monitoring stage is related to the prior stage's data products and research findings and then impacts the subsequent stage. This chapter advances opportunities for whole-systems approaches using Earth observations to support fire and environmental change monitoring.

This research opens doors for overcoming additional challenges in environmental change monitoring. The BULC algorithm could be used to synthesize incidence, burned area, day-of-burn, and burn severity classifications from both optical and radar sensors to analyze wildfire behaviours and fire season archetypes throughout Canadian history. Other opportunities exist by using deep learning or automated machine learning to integrate fire drivers into fire progression and occurrence mapping protocols (Jain et al., 2020; Reichstein et al., 2019) and to analyze the relationship between wildfire progressions and fire drivers over time. Ultimately, this research advances multi-scale, multi-source fire monitoring and identifies opportunities for Earth observation sciences to aid in wildfire planning and response.

6.1 References

Engelbrecht, J., Theron, A., Vhengani, L., Kemp, J., 2017. A Simple Normalized Difference Approach to Burnt Area Mapping Using Multi-Polarisation C-Band SAR. Remote Sensing 9, 764.

Jain, P., Coogan, S.C.P., Subramanian, S.G., Crowley, M., Taylor, S., Flannigan, M.D., 2020. A review of machine learning applications in wildfire science and management. arXiv [cs.LG].

Reichstein, M., Camps-Valls, G., Stevens, B., Jung, M., Denzler, J., Carvalhais, N., Prabhat, 2019. Deep learning and process understanding for data-driven Earth system science. Nature 566, 195–204.

7. Conclusion

This thesis contributes to fire disturbance monitoring by producing and analyzing fire progressions using multi-scale approaches that draw upon landscape ecology and remote sensing theory, as identified in Chapter 2. In Chapters 3 and 4, I present and apply a new data-fusion protocol for reconstructing fire progressions in British Columbia using multi-sensor, multi-scale Earth observations and analyze the resulting fire progressions for large fires using novel fire progression metrics. This research advances the field of remote sensing by implementing systematic methods for synthesizing multi-source data to improve near-term fire disturbance monitoring, thus illustrating opportunities for future multi-source Earth observation data fusion using Bayesian approaches. Chapter 5 presents a whole-systems fire monitoring framework that can be used to identify and harmonize fire monitoring objectives and data needs throughout the life cycle of a fire event using Earth observations. Overall, my thesis highlights the current and future opportunities using cloud computing and open-access Earth observations to advance environmental change monitoring.

Complete list of references

Abatzoglou, J.T., Williams, A.P., 2016. Impact of anthropogenic climate change on wildfire across western US forests. Proceedings of the National Academy of Sciences. 113(42), 11770-11775.

Abbott, G., Chapman, M., 2018. Addressing the new normal: 21st century disaster management in British Columbia. British Columbia Government Report. 1–140. https://www2.gov.bc.ca/assets/gov/public-safety-and-emergency-services/emergency-preparedness-response-recovery/embc/bc-flood-and-wildfire-review-addressing-the-new-normal-21st-century-disaster-management-in-bc-web.pdf

Achanta, R., and Süsstrunk, S., 2017. Superpixels and polygons using simple non-iterative clustering. 2017 IEEE Conference Computer Vision and Pattern Recognition (CVPR). 4895–4904.

Agee, J.K., 1999. Fire effects on landscape fragmentation in interior west forests. Forest fragmentation: wildlife and management implications. (Eds JA Rochelle, LA Lehmann, J Wisniewski) pp 43–60.

Ahmed, M.R., Hassan, Q.K., Abdollahi, M., Gupta, A., 2019. Introducing a New Remote Sensing-Based Model for Forecasting Forest Fire Danger Conditions at a Four-Day Scale. Remote Sensing 11, 2101.

Aldersley, A., Murray, S.J., Cornell, S.E., 2011. Global and regional analysis of climate and human drivers of wildfire. Sci. Total Environ. 409, 3472–3481.

Allison, R.S., Johnston, J.M., Craig, G., Jennings, S., 2016. Airborne Optical and Thermal Remote Sensing for Wildfire Detection and Monitoring. Sensors 16. https://doi.org/10.3390/s16081310

Amiro, B.D., Todd, J.B., Wotton, B.M., Logan, K.A., Flannigan, M.D., Stocks, B.J., Mason, J.A., Martell, D.L., Hirsch, K.G., 2001. Direct carbon emissions from Canadian forest fires, 1959-1999. Can. J. For. Res. 31, 512–525.

Andela, N., Morton, D.C., Giglio, L., Chen, Y., van der Werf, G.R., Kasibhatla, P.S., DeFries, R.S., Collatz, G.J., Hantson, S., Kloster, S., Bachelet, D., Forrest, M., Lasslop, G., Li, F., Mangeon, S., Melton, J.R., Yue, C., Randerson, J.T., 2017. A human-driven decline in global burned area. Science 356, 1356–1362.

Andela, N., Morton, D.C., Giglio, L., Paugam, R., Chen, Y., Hantson, S., van der Werf, G.R., Randerson, J.T., 2019. The Global Fire Atlas of individual fire size, duration, speed and direction. Earth Syst. Sci. Data 11, 529–552.

Arora, V.K., Melton, J.R., 2018. Reduction in global area burned and wildfire emissions since 1930s enhances carbon uptake by land. Nat. Commun. 9, 1326.

Arroyo-Rodríguez, V., Melo, F.P.L., Martínez-Ramos, M., Bongers, F., Chazdon, R.L., Meave, J.A., Norden, N., Santos, B.A., Leal, I.R., Tabarelli, M., 2017. Multiple successional pathways in human-modified tropical landscapes: new insights from forest succession, forest fragmentation and landscape ecology research. Biol. Rev. Camb. Philos. Soc. 92, 326–340.

Arroyo, L.A., Pascual, C., Manzanera, J.A., 2008. Fire models and methods to map fuel types: The role of remote sensing. For. Ecol. Manage. 256, 1239–1252.

Asgarian, A., Amiri, B.J., Sakieh, Y., 2015. Assessing the effect of green cover spatial patterns on urban land surface temperature using landscape metrics approach. Urban Ecosyst. 18, 209–222.

Asner, G.P., Martin, R.E., Anderson, C.B., Knapp, D.E., 2015. Quantifying forest canopy traits:

Imaging spectroscopy versus field survey. Remote Sens. Environ. 158, 15–27.

Asner, G.P., Townsend, A.R., Braswell, B.H., 2000. Satellite observation of El Niño effects on Amazon Forest phenology and productivity. Geophys. Res. Lett. 27, 981–984.

Asner, G.P., Warner, A.S., 2003. Canopy shadow in IKONOS satellite observations of tropical forests and savannas. Remote Sens. Environ. 87, 521–533.

Azam, C., Le Viol, I., Julien, J.-F., Bas, Y., Kerbiriou, C., 2016. Disentangling the relative effect of light pollution, impervious surfaces and intensive agriculture on bat activity with a national-scale monitoring program. Landsc. Ecol. 31, 2471–2483.

Bagan, H., Yamagata, Y., 2015. Analysis of urban growth and estimating population density using satellite images of nighttime lights and land-use and population data. GISci Remote Sens. 52, 765–780.

Barbosa, J.M., Asner, G.P., 2017. Prioritizing landscapes for restoration based on spatial patterns of ecosystem controls and plant-plant interactions. J. Appl. Ecol. 54, 1459–1468.

Bartels, S.F., Chen, H.Y.H., Wulder, M.A., White, J.C., 2016. Trends in post-disturbance recovery rates of Canada's forests following wildfire and harvest. For. Ecol. Manage. 361, 194–207.

Bastos, R., Monteiro, A.T., Carvalho, D., 2016. Integrating land cover structure and functioning to predict biodiversity patterns: a hierarchical modelling framework designed for ecosystem management. Landsc. Ecol. 31, 701–710.

Baudron, F., Schultner, J., Duriaux, J.-Y., Gergel, S.E., Sunderland, T., 2019. Agriculturally productive yet biodiverse: human benefits and conservation values along a forest-agriculture gradient in Southern Ethiopia. Landsc. Ecol. 34, 341–356.

BC Wildfire Service, 2017a. Wildfire season summary.

https://www2.gov.bc.ca/gov/content/safety/wildfire-status/about-bcws/wildfire-history/wildfire-season-summary (accessed 28 October 2018).

[dataset] BC Wildfire Service, 2017b. PROT_CURRENT_FIRE_POLYS_SP Ministry of Forests, Lands, Natural Resource Operations and Rural Development. https://catalogue.data.gov.bc.ca/dataset/fire-perimeters-current (accessed 25 January 2018)

BC Wildfire Service, 2017c. Wildfires of note - Plateau Fire (C0784). http://bcfireinfo.for.gov.bc.ca/hprScripts/WildfireNews/OneFire.asp?ID=645 (accessed 28 October 2018).

BC Wildfire Service, 2017d. Wildfires of note – Hanceville-Riske Creek (C50647). http://bcfireinfo.for.gov.bc.ca/hprScripts/WildfireNews/OneFire.asp?ID=666 (accessed 28 October 2018).

BC Wildfire Service, 2017e. Wildfires of note - Elephant Hill (K20637). http://bcfireinfo.for.gov.bc.ca/hprScripts/WildfireNews/OneFire.asp?ID=620 (accessed 28 October 2018).

BC Wildfire Service, 2017f. Wildfires of note – White River Fire (N1628). http://bcfireinfo.for.gov.bc.ca/hprScripts/WildfireNews/OneFire.asp?ID=678 (accessed 28 October 2018).

BC Wildfire Service, 2017g. Remembering 2017: Looking back a year later at the start of the 2017 wildfire season for the Cariboo Fire Centre [WWW Document]. Province of British Columbia. URL https://www2.gov.bc.ca/gov/content/safety/wildfire-status/about-bcws/wildfire-history/remembering-2017 (accessed 2.15.19).

BC Wildfire Service, 2021. 2021 Wildfire Season Summary [WWW Document]. URL https://www2.gov.bc.ca/gov/content/safety/wildfire-status/about-bcws/wildfire-history/wildfire-season-summary (accessed 10.15.21).

Benali, A., Russo, A., Sá, A.C., Pinto, R., Price, O., Koutsias, N., Pereira, J., 2016. Determining fire dates and locating ignition points with satellite data. Remote Sensing. 8(4), 326.

Bernier, P.Y., Gauthier, S., Jean, P.-O., Manka, F., Boulanger, Y., Beaudoin, A., Guindon, L., 2016. Mapping Local Effects of Forest Properties on Fire Risk across Canada. For. Trees Livelihoods 7, 157.

Bertrand, C., Burel, F., Baudry, J., 2016 Spatial and temporal heterogeneity of the crop mosaic influences carabid beetles in agricultural landscapes. Landsc. Ecol. 31, 451–466.

Bessie, W.C., Johnson, E.A., 1995. The Relative Importance of Fuels and Weather on Fire Behavior in Subalpine Forests. Ecology 76, 747–762.

Betbeder, J., Laslier, M., Hubert-Moy, L., 2017. Synthetic Aperture Radar (SAR) images improve habitat suitability models. Landsc. Ecol. 32, 1867–1879

Bishop-Taylor, R., Tulbure, M.G., Broich, M., 2018. Evaluating static and dynamic landscape connectivity modelling using a 25-year remote sensing time series. Landsc. Ecol. 33, 625–640.

Biudes, M.S., Machado, N.G., de Morais Danelichen, V.H., 2014. Ground and remote sensing-based measurements of leaf area index in a transitional forest and seasonal flooded forest in Brazil. Int. J. Biometeorol 58, 1181–1193.

Blaschke, T., 2010. Object based image analysis for remote sensing. ISPRS Journal of Photogrammetry and Remote Sensing. 65(1), 2–16.

Bolton, D.K., Coops, N.C., Hermosilla, T., Wulder, M.A., White, J.C., 2017. Assessing variability in post-fire forest structure along gradients of productivity in the Canadian boreal using multi-source remote sensing. J. Biogeogr. 44, 1294–1305.

Boschetti, L., Roy, D.P., Justice, C.O., Humber, M.L., 2015. MODIS–Landsat fusion for large area 30m burned area mapping. Remote Sens. Environ. 161, 27–42.

Bowman, D., 2018. Wildfire science is at a loss for comprehensive data. Nature. 560(7). doi: 10.1038/d41586-018-05840-4

Bowman, D.M.J.S., Murphy, B.P., 2011. Australia—A Model System for the Development of Pyrogeography. Fire Ecology 7, 5–12.

Bowman, D.M.J.S., O'Brien, J.A., Goldammer, J.G., 2013. Pyrogeography and the Global Quest for Sustainable Fire Management. Annu. Rev. Environ. Resour. 38, 57–80.

Boyd, D.S., Danson, F.M., 2005. Satellite remote sensing of forest resources: three decades of research development. Progress in Physical Geography: Earth and Environment. https://doi.org/10.1191/0309133305pp432ra

Brezonik, P.L., Olmanson, L.G., Finlay, J.C., Bauer, M.E., 2015. Factors affecting the measurement of CDOM by remote sensing of optically complex inland waters. Remote Sens. Environ. 157, 199–215.

Bright, B.C., Hudak, A.T., Meddens, A.J.H., Hawbaker, T.J., Briggs, J.S., Kennedy, R.E., 2017. Prediction of Forest Canopy and Surface Fuels from Lidar and Satellite Time Series Data in a Bark Beetle-Affected Forest. For. Trees Livelihoods 8, 322.

British Columbia, 2018. Remembering 2017: Looking back a year later at the start of the 2017 wildfire season for the Cariboo Fire Centre. https://www2.gov.bc.ca/gov/content/safety/wildfire-status/about-bcws/wildfire-history/remembering-2017 (accessed 28 October 2018).

Bürgi, M., Silbernagel, J., Wu, J., Kienast, F., 2015. Linking ecosystem services with landscape history. Landsc. Ecol. 30, 11–20.

Burton, P.J., Parisien, M.-A., Hicke, J.A., Hall, R.J., Freeburn, J.T., 2009. Large fires as agents of ecological diversity in the North American boreal forest. Int. J. Wildland Fire 17, 754–767.

Canadian Council of Forest Ministers, 2018. Forest Fires. http://nfdp.ccfm.org/en/data/fires.php (accessed 30 October 2018).

Candiago, S., Remondino, F., De Giglio, M., Dubbini, M., Gattelli, M., 2015. Evaluating multispectral images and vegetation indices for precision farming applications from UAV images. Remote Sensing 7, 4026–4047.

Cannon, J.B., Hepinstall-Cymerman, J., Godfrey, C.M., Peterson, C.J., 2016. Landscape-scale characteristics of forest tornado damage in mountainous terrain. Landsc. Ecol. 31, 2097–2114

Cardille, J.A., Fortin, J.A., 2016. Bayesian updating of land-cover estimates in a data-rich environment. Remote Sens. Environ. 186, 234–249.

Cardille, J.A., Jackson, M.M., 2017. Citizen science for assessing landscape change. Learning Landscape Ecology 41–42.

Cardille, J.A., Perez, E., Crowley, M.A., Wulder, M.A., White, J.C., Hermosilla, T., 2022. Multi-sensor change detection for within-year capture and labelling of forest disturbance. Remote Sensing of Environment. https://doi.org/10.1016/j.rse.2021.112741

Castillo, M.G., Hernández, H.J., Estades, C.F., 2018. Effect of connectivity and habitat availability on the occurrence of the Chestnut-throated Huet-Huet (Pteroptochos castaneus, Rhinocryptidae) in fragmented landscapes of central Chile. Landsc. Ecol. 33, 1061–1068.

Chen, S., Tian, Y., 2015. Pyramid of spatial relatons for scene-level land use classification. IEEE Trans. Geosci. Remote Sens. 53, 1947–1957.

Chen, S., Wang, H., Xu, F., Jin, Y., 2016. Target classification using the deep convolutional networks for SAR images. IEEE Trans. Geosci. Remote Sens. 54, 4806–4817.

Chen, X., Long, D., Liang, S., He, L., Zeng, C., Hao, X., Hong, Y., 2018. Developing a composite daily snow cover extent record over the Tibetan Plateau from 1981 to 2016 using multisource data. Remote Sens. Environ. 215, 284–299.

Chen, Y., Jiang, H., Li, C., Jia, X., Ghamisi, P., 2016. Deep feature extraction and classification of hyperspectral images based on convolutional neural networks. IEEE Trans. Geosci. Remote Sens. 54, 6232–6251.

Chen, Y., Li, L., Lu, D., Li, D., 2018. Exploring Bamboo Forest Aboveground Biomass Estimation Using Sentinel-2 Data. Remote Sensing 11, 7.

Chen, Y., Zhao, X., Jia, X., 2015. Spectral–spatial classification of hyperspectral data based on deep belief network. IEEE J. Sel. Top. Appl. Earth Obs. Remote Sens. 8, 2381–2392.

Cheng, G., Han, J., 2016. A survey on object detection in optical remote sensing images. ISPRS J. Photogramm. Remote Sens. 117, 11–28.

Chu, T., Guo, X., 2013. Remote Sensing Techniques in Monitoring Post-Fire Effects and Patterns of Forest Recovery in Boreal Forest Regions: A Review. Remote Sensing 6, 470–520.

Chuvieco, E., Aguado, I., Salas, J., García, M., Yebra, M., Oliva, P., 2020. Satellite Remote Sensing Contributions to Wildland Fire Science and Management. Current Forestry Reports 6, 81–96.

Chuvieco, E., Mouillot, F., van der Werf, G.R., San Miguel, J., Tanasse, M., Koutsias, N., García, M., Yebra, M., Padilla, M., Gitas, I., Heil, A., Hawbaker, T.J., Giglio, L., 2019. Historical background and current developments for mapping burned area from satellite Earth observation. Remote Sens. Environ. 225, 45–64.

Chuvieco, E., Yue, C., Heil, A., Mouillot, F., Alonso-Canas, I., Padilla, M., Pereira, J.M., Oom, D., Tansey, K., 2016. A new global burned area product for climate assessment of fire impacts. Glob. Ecol. Biogeogr. 25, 619–629.

Cohen, W.B., Goward, S.N., 2004. Landsat's Role in Ecological Applications of Remote Sensing. Bioscience 54, 535–545.

Cohen, W.B., Maiersperger, T.K., Spies, T.A., Oetter, D.R., 2001. Modelling forest cover attributes as continuous variables in a regional context with Thematic Mapper data. Int. J. Remote Sens. 22, 2279–2310.

Cohen, W.B., Spies, T.A., Fiorella, M., 1995. Estimating the age and structure of forests in a multi-ownership landscape of western Oregon, U.S.A. Int. J. Remote Sens. 16, 721–746.

Cohen, W.B., Yang, Z., Healey, S.P., Kennedy, R.E., Gorelick, N., 2018. A LandTrendr multispectral ensemble for forest disturbance detection. Remote Sens. Environ. 205, 131–140.

Cohen, W.B., Yang, Z., Kennedy, R.E., 2010. Detecting trends in forest disturbance and recovery using yearly Landsat time series: 2. TimeSync—Tools for calibration and validation. Remote Sens. Environ. 114, 2911–2924.

Collins, B.M., Miller, J.D., Thode, A.E., Kelly, M., van Wagtendonk, J.W., Stephens, S.L., 2009. Interactions Among Wildland Fires in a Long-Established Sierra Nevada Natural Fire Area. Ecosystems 12, 114–128.

Colomina, I., Molina, P., 2014. Unmanned aerial systems for photogrammetry and remote sensing: A review. ISPRS J. Photogramm. Remote Sens. 92, 79–97.

Coogan, S.C.P., Daniels, L.D., Boychuk, D., Burton, P.J., Flannigan, M.D., Gauthier, S., Kafka, V., Park, J.S., Mike Wotton, B., 2020. Fifty years of wildland fire science in Canada. Canadian Journal Forest Research.

Coogan, S.C.P., Robinne, F.-N., Jain, P., Flannigan, M.D., 2019. Scientists' warning on wildfire — a Canadian perspective. Can. J. For. Res. 49, 1015–1023.

Coops, N.C., Wulder, M.A., 2019. Breaking the Habit(at). Trends. Ecol. Evol. doi: 10.1016/j.tree.2019.04.013

Coughlan, M.R., Magi, B.I., Derr, K.M., 2018. A Global Analysis of Hunter-Gatherers, Broadcast Fire Use, and Lightning-Fire-Prone Landscapes. Fire 1, 41.

Crowley, M.A., Cardille, J.A., 2020. Remote sensing's recent and future contributions to landscape ecology. Curr. Landsc. Ecol. Rep. 5, 45–57.

Crowley, M.A., Cardille, J.A., White, J.C., Wulder, M.A., 2019a. Large-area synthesis of multiple remotely sensed data sources for mapping within-year wildfire progression. Remote Sens. Environ. 232, 111295.

Crowley, M.A., Cardille, J.A., White, J.C., Wulder, M.A., 2019b. Multi-sensor, multi-scale, Bayesian data synthesis for mapping within-year wildfire progression. Remote Sens. Lett. 10, 302–311.

Curran, P., 1980. Multispectral remote sensing of vegetation amount. Progress in Physical Geography: Earth and Environment 4, 315–341.

Curtis, P.G., Slay, C.M., Harris, N.L., Tyukavina, A., Hansen, M.C., 2018. Classifying drivers of global forest loss. Science 361, 1108–1111.

Cushman, S.A., 2016. Calculating the configurational entropy of a landscape mosaic. Landsc.

Ecol. 31, 481–489.

Cusser, S., Neff, J.L., Jha. S., 2016. Natural land cover drives pollinator abundance and richness, leading to reductions in pollen limitation in cotton agroecosystems. Agric. Ecosyst. Environ. 226, 33–42.

Czerwinski, C.J., King, D.J., Mitchell, S.W., 2014. Mapping forest growth and decline in a temperate mixed forest using temporal trend analysis of Landsat imagery, 1987-2010. Remote Sens. Environ. 141, 188–200.

Dahlin, K.M., Asner, G.P., Field, C.B., 2014. Linking vegetation patterns to environmental gradients and human impacts in a Mediterranean-type island ecosystem. Landsc. Ecol. 29, 1571–1585.

Dalla Mura, M., Prasad, S., Pacifici, F., Gamba, P., Chanussot, J., Benediktsson, J.A., 2015. Challenges and opportunities of multimodality and data fusion in remote sensing. Proc. IEEE 103, 1585–1601.

Danson, F.M., Plummer, S.E., Briggs, S.A., 1995. Remote sensing and the information extraction problem.

de Groot, W.J., Cantin, A.S., Flannigan, Soja, A.J., Gowman, L.M., Newbery, A., 2013a. A comparison of Canadian and Russian boreal forest fire regimes. For. Ecol. Manage. 294, 23–34.

de Groot, W.J., Flannigan, Cantin, A.S., 2013b. Climate change impacts on future boreal fire regimes. For. Ecol. Manage. 294, 35–44.

de Groot, W.J., Landry, R., Kurz, W.A., Anderson, K.R., Englefield, P., Fraser, R.H., Hall, R.J., Banfield, E., Raymond, D.A., Decker, V., Lynham, T.J., 2007. Estimating direct carbon emissions from Canadian wildland fires. International Journal of Wildland Fire. 16(5), 593–606. doi:10.1071/ WF06150

de Groot, W.J., Pritchard, J.M., Lynham, T.J., 2009. Forest floor fuel consumption and carbon emissions in Canadian boreal forest fires. Can. J. For. Res. 39, 367–382.

Deines, J.M., Kendall, A.D., Crowley, M.A., Rapp, J., Cardille, J.A., Hyndman, D.W., 2019. Mapping three decades of irrigation across the US High Plains Aquifer with Landsat. Remote Sensing of Environment 233, 111400.

Deledalle, C., Denis, L., Tupin, F., Reigber, A., Jäger, M., 2015. NL-SAR: A unified nonlocal framework for resolution-preserving (Pol)(In)SAR denoising. IEEE Trans. Geosci. Remote Sens. 53, 2021–2038.

Dong, J., Metternicht, G., Hostert, P., Fensholt, R., Chowdhury, R.R., 2019. Remote sensing and geospatial technologies in support of a normative land system science: status and prospects. Curr. Opin. Environ. Sustain. 38, 44–52.

Du, P., Liu, P., Xia J., 2014. Remote Sensing image interpretation for urban environment analysis: Methods, system and examples. Remote Sens. 6, 9458–9474.

Duncanson, L., Armston, J., Disney, M., et al., 2019. The importance of consistent global forest aboveground biomass product validation. Surv. Geophys. doi: 10.1007/s10712-019-09538-8.

Dupras, J., Marull, J., Parcerisas, L., Coll, F., Gonzalez, A., Girard, M., Tello, E., 2016. The impacts of urban sprawl on ecological connectivity in the Montreal Metropolitan Region. Environ. Sci. Policy 58, 61–73.

Dwyer, J., Roy, D., Sauer, B., Jenkerson, C., Zhang, H., Lymburner, L., 2018. Analysis ready data: Enabling analysis of the Landsat archive. Remote Sens. 10(9), 1363.

Dyer, R.J., 2015. Is there such a thing as landscape genetics? Mol. Ecol. 24, 3518–3528.

Egorov, AV., Roy, D.P., Zhang, HK., Hansen, MC., Kommareddy, A., 2018. Demonstration of percent tree cover mapping using Landsat analysis ready data (ARD) and sensitivity with respect to Landsat ARD processing level. Remote Sens. 10, 209.

Eisenberg, C., Anderson, C.L., Collingwood, A., Sissons, R., Dunn, C.J., Meigs, G.W., Hibbs, D.E., Murphy, S., Kuiper, S.D., SpearChief-Morris, J., Little Bear, L., Johnston, B., Edson, C.B., 2019. Out of the Ashes: Ecological Resilience to Extreme Wildfire, Prescribed Burns, and Indigenous Burning in Ecosystems. Frontiers in Ecology and Evolution 7, 436.

Eklundh, L., Harrie, L., Kuusk, A., 2001. Investigating relationships between Landsat ETM+ sensor data and leaf area index in a boreal conifer forest. Remote Sens. Environ. 78, 239–251.

Engelbrecht, J., Theron, A., Vhengani, L., Kemp, J., 2017. A Simple Normalized Difference Approach to Burnt Area Mapping Using Multi-Polarisation C-Band SAR. Remote Sensing 9, 764.

Estel, S., Kuemmerle, T., Alcántara, C., Levers, C., Prishchepov, A., Hostert, P., 2015. Mapping farmland abandonment and recultivation across Europe using MODIS NDVI time series. Remote Sens. Environ. 163, 312–325.

Estoque, RC., Murayama, Y., 2016. Quantifying landscape pattern and ecosystem service value changes in four rapidly urbanizing hill stations of Southeast Asia. Landsc. Ecol. 31, 1481–1507.

Fiore, A.M., Naik, V., Leibensperger, E.M., 2015. Air quality and climate connections. J. Air Waste Manag. Assoc. 65, 645–685.

Fire Growth Model, 2018. Prometheus - Overview.

http://www.firegrowthmodel.ca/prometheus/overview_e.php (accessed 28 October 2018).

Flannigan, M.D., Harrington, J.B., 1988. A Study of the Relation of Meteorological Variables to Monthly Provincial Area Burned by Wildfire in Canada (1953–80). J. Appl. Meteorol. 27, 441–452.

Flannigan, M.D., Krawchuk, M.A., de Groot, W.J., Mike Wotton, B., Gowman, L.M., 2009. Implications of changing climate for global wildland fire. Int. J. Wildland Fire 18, 483–507.

Flannigan, M.D., Logan, K.A., Amiro, B.D., Skinner, W.R., Stocks, B.J., 2005. Future Area Burned in Canada. Clim. Change 72, 1–16.

Flannigan, M.D., Stocks, B.J., Wotton, B.M., 2000. Climate change and forest fires. Sci. Total Environ. 262, 221–229.

Fortin, J.A., Cardille, J.A., Perez, E., 2020. Multi-sensor detection of forest-cover change across 45 years in Mato Grosso, Brazil. Remote Sensing of Environment. https://doi.org/10.1016/j.rse.2019.111266

Franklin, S.E., Wulder, M.A., 2002. Remote sensing methods in medium spatial resolution satellite data land cover classification of large areas. Prog Phys Geogr: Earth and Environment 26, 173–205.

Franklin, S.E., Wulder, M.A., Gerylo, G.R., 2001. Texture analysis of IKONOS panchromatic data for Douglas-fir forest age class separability in British Columbia. Int. J. Remote Sens. 22, 2627–2632.

Fraser, R.H., Hall, R.J., Landry, R., Lynham, T., Raymond, D., Lee, B., Li, Z., 2004. Validation and Calibration of Canada-Wide Coarse-Resolution Satellite Burned-Area Maps. Photogrammetric Engineering & Remote Sensing 70, 451–460.

Fraser, R.H., Li, Z., Cihlar, J., 2000. Hotspot and NDVI Differencing Synergy (HANDS): A New Technique for Burned Area Mapping over Boreal Forest. Remote Sens. Environ. 74, 362–376.

Frazier, A.E., 2014. A new data aggregation technique to improve landscape metric downscaling. Landsc. Ecol. 29, 1261–1276.

Frazier, A.E., 2016. Surface metrics: scaling relationships and downscaling behavior. Landsc. Ecol. 31, 351–363.

Frazier, R.J., Coops, N.C., Wulder, M.A., Hermosilla, T., White, J.C., 2018. Analyzing spatial and temporal variability in short-term rates of post-fire vegetation return from Landsat time series. Remote Sens. Environ. 205, 32–45.

Frock, C.F., Turner, M.G., 2018. Microhabitat conditions and landscape pattern explain nocturnal rodent activity, but not seed removal, in burned and unburned lodgepole pine forests. Landsc. Ecol. 33, 1895–1909.

Frolking, S., Palace, M.W., Clark, D.B., Chambers, J.Q., Shugart, H.H., Hurtt, G.C., 2009. Forest disturbance and recovery: A general review in the context of spaceborne remote sensing of impacts on aboveground biomass and canopy structure. J. Geophys. Res. 114. https://doi.org/10.1029/2008jg000911

Fu, P., Weng, Q., 2016. A time series analysis of urbanization induced land use and land cover change and its impact on land surface temperature with Landsat imagery. Remote Sens. Environ. 175, 205–214.

Gale, M.G., Cary, G.J., Van Dijk, A.I.J.M., Yebra, M., 2021. Forest fire fuel through the lens of remote sensing: Review of approaches, challenges and future directions in the remote sensing of biotic determinants of fire behaviour. Remote Sens. Environ. 255, 112282.

Gamon, J.A., Field, C.B., Goulden, M.L., Griffin, K.L., Hartley, A.E., Joel, G., Penuelas, J., Valentini, R., 1995. Relationships between NDVI, canopy structure, and photosynthesis in three Californian vegetation types. Ecol. Appl. 5, 28–41.

Gao, F., Anderson, M.C., Zhang, X., Yang, Z., Alfieri, J.G., Kustas, W.P., Mueller, R., Johnson, D.M., Prueger, J.H., 2017. Toward mapping crop progress at field scales through fusion of Landsat and MODIS imagery. Remote Sens. Environ. 188, 9–25.

Gao, F., Hilker, T., Zhu, X., Anderson, M.A., Masek, J., Wang, P., Yang, Y., 2015. Fusing Landsat and MODIS data for vegetation monitoring. IEEE Geosci. Remote. Sens. Mag. 3, 47–60.

Garcia Millan, V., Sanchez-Azofeifa, A., 2018. Quantifying Changes on Forest Succession in a Dry Tropical Forest Using Angular-Hyperspectral Remote Sensing. Remote Sensing 10, 1865.

García, M., Popescu, S., Riaño, D., Zhao, K., Neuenschwander, A., Agca, M., Chuvieco, E., 2012. Characterization of canopy fuels using ICESat/GLAS data. Remote Sens. Environ. 123, 81–89.

Gerrand, S., Aspinall, J., Jensen, T., Hopkinson, C., Collingwood, A., Chasmer, L., 2021. Partitioning carbon losses from fire combustion in a montane Valley, Alberta Canada. For. Ecol. Manage. 496, 119435.

Gevaert, C.M., García-Haro, F.J., 2015. A comparison of STARFM and an unmixing-based algorithm for Landsat and MODIS data fusion. Remote Sens. Environ. 156, 34–44.

Ghamisi, P., Dalla Mura, M., Benediktsson, J.A., 2015. A survey on spectral–spatial classification techniques based on attribute profiles. IEEE Trans. Geosci. Remote Sens. 53, 2335–2353.

Gibson, C.E., Morgan, P., Wilson, A.M., 2014. Atlas of digital polygon fire extents for Idaho and western Montana. 2nd Edition. https://doi.org/10.2737/RDS-2009-0006-2

Giglio, L., Boschetti, L., Roy, D.P., Humber, M.L., Justice, C.O., 2018. The Collection 6 MODIS burned area mapping algorithm and product. Remote Sens. Environ. 217, 72–85.

[dataset] Giglio, L., Justice, C., Boschetti, L., Roy, D., 2015. MCD64A1 MODIS/Terra+Aqua Burned Area Monthly L3 Global 500m SIN Grid V006. NASA EOSDIS Land Processes DAAC. https://doi.org/10.5067/MODIS/MCD64A1.006 (accessed 1 March 2018).

Giglio, L., Schroeder, W., Justice, C.O., 2016. The collection 6 MODIS active fire detection algorithm and fire products. Remote Sens. Environ. 178, 31–41.

Gitas, I.Z., Mitri, G.H., Ventura, G., 2004. Object-based image classification for burned area mapping of Creus Cape, Spain, using NOAA-AVHRR imagery. Remote Sensing of Environment. 92(3), 409–413.

Goodbody, T.R.H., Coops, N.C., Hermosilla, T., Tompalski, P., Crawford, P., 2018. Assessing the status of forest regeneration using digital aerial photogrammetry and unmanned aerial systems. Int. J. Remote Sens. 39, 5246–5264.

Gorelick, N., Hancher, M., Dixon, M., Ilyushchenko, S., Thau, D., Moore, R., 2017. Google Earth Engine: Planetary-scale geospatial analysis for everyone. Remote Sens. Environ., 202, 18–27.

Gralewicz, N.J., Nelson, T.A., Wulder, M.A., 2012a. Spatial and temporal patterns of wildfire ignitions in Canada from 1980 to 2006. Int. J. Wildland Fire 21, 230–242.

Gralewicz, N.J., Nelson, T.A., Wulder, M.A., 2012b. Factors influencing national scale wildfire susceptibility in Canada. For. Ecol. Manage. 265, 20–29.

Grimaldi, M., Oszwald, J., Doledec, S., 2014. Ecosystem services of regulation and support in

Amazonian pioneer fronts: searching for landscape drivers. Landsc. Ecol. 29, 311–328.

Guo, X., Coops, N.C., Gergel, S.E., 2018. Integrating airborne lidar and satellite imagery to model habitat connectivity dynamics for spatial conservation prioritization. Landsc. Ecol. 33, 491–511.

Haas, J., Ban, Y., 2017. Mapping and monitoring urban ecosystem services using multitemporal high-resolution satellite data. IEEE J. Sel. Top. Appl. Earth Obs. Remote Sens. 10, 669–680.

Hall, F.G., Shimabukuro, Y.E., Huemmrich, K.F., 1995. Remote sensing of forest biophysical structure using mixture decomposition and geometric reflectance models. Ecol. Appl. 5, 993–1013.

Hall, R.J., Freeburn, J.T., de Groot, W.J., Pritchard, J.M., Lynham, T.J., Landry, R., 2008. Remote sensing of burn severity: experience from western Canada boreal fires. International Journal of Wildland Fire. 17(4), 476–489.

Hall, S.J., Learned, J., Ruddell, B., 2016. Convergence of microclimate in residential landscapes across diverse cities in the United States. Landsc. Ecol. 31, 101–117.

Han, J., Zhang, D., Cheng, G., Guo, L., Ren, J., 2015. Object detection in optical remote sensing images based on weakly supervised learning and high-level feature learning. IEEE Trans. Geosci. Remote Sens. 53, 3325–3337.

Hanes, C.C., Wang, X., Jain, P., Parisien, M.-A., Little, J.M., Flannigan, M.D., 2019. Fire-regime changes in Canada over the last half century. Can. J. For. Res. 49, 256–269.

Hansen, L., Krantz, L., 2008. Remembering The 1988 Yellowstone Fires. NPR.

Hansen, M.C., Loveland, T.R., 2012. A review of large area monitoring of land cover change using Landsat data. Remote Sensing of Environment.

https://doi.org/10.1016/j.rse.2011.08.024

Hansen, M.C., Potapov, P.V., Moore, R., Hancher, M., Turubanova, S.A., Tyukavina, A., Thau, D., Stehman, S.V., Goetz, S.J., Loveland, T.R., Kommareddy, A., Egorov, A., Chini, L., Justice, C.O., Townshend, J.R.G., 2013. High-resolution global maps of 21st-century forest cover change. Science 342, 850–853.

Harvey, B.J., Donato, D.C., Turner, M.G., 2016. Drivers and trends in landscape patterns of stand-replacing fire in forests of the US Northern Rocky Mountains (1984–2010). Landsc. Ecol. 31, 2367–2383.

Hawbaker, T.J., Vanderhoof, M.K., Beal, Y.-J., Takacs, J.D., Schmidt, G.L., Falgout, J.T., Williams, B., Fairaux, N.M., Caldwell, M.K., Picotte, J.J., Howard, S.M., Stitt, S., Dwyer, J.L., 2017. Mapping burned areas using dense time-series of Landsat data. Remote Sens. Environ. 198, 504–522.

He, K.S., Bradley, B.A., Cord, A.F., Rocchini, D., Tuanmu, M.-N., Schmidtlein, S., Turner, W., Wegmann, M., Pettorelli, N., 2015. Will remote sensing shape the next generation of species distribution models? Remote Sens. Ecol. Conserv. 1, 4–18.

Healey, S.P., Cohen, W.B., Yang, Z., et al., 2018. Mapping forest change using stacked generalization: An ensemble approach. Remote Sens. Environ. 204, 717–728.

Healey, S.P., Yang, Z., Cohen, W.B., Pierce, D.J., 2006. Application of two regression-based methods to estimate the effects of partial harvest on forest structure using Landsat data. Remote Sens. Environ. 101, 115–126.

Hedo J., Rubio, E., Dadi, T., López-Serrano, F.R., Alfaro-Sánchez, R., Moya, D., de las Heras, J., 2014. Is remote sensing a good method to define forest fire resilience? A particular case in the South-eastern of the Iberian Peninsula. Parte:

http://hdl.handle.net/10316.2/34013.

Heigl, F., Horvath, K., Laaha, G., 2017. Amphibian and reptile road-kills on tertiary roads in relation to landscape structure: using a citizen science approach with open-access land cover data. B.M.C. Ecol. 17(24).

Helbig, M., Pappas, C., Sonnentag, O., 2016. Permafrost thaw and wildfire: Equally important drivers of boreal tree cover changes in the Taiga Plains, Canada. Geophysical Research Letters. https://doi.org/10.1002/2015gl067193

Hermosilla, T., Wulder, M.A., White, J.C., Coops, N.C., Hobart, G.W., 2015. An integrated Landsat time series protocol for change detection and generation of annual gap-free surface reflectance composites. Remote Sens. Environ. 158, 220–234.

Hermosilla, T., Wulder, M.A., White, J.C., Coops, N.C., Hobart, G.W., 2015. Regional detection, characterization, and attribution of annual forest change from 1984 to 2012 using Landsat-derived time-series metrics. Remote Sens. Environ. 170, 121–132.

Hermosilla, T., Wulder, M.A., White, J.C., Coops, N.C., Hobart, G.W., 2018. Disturbance-informed annual land cover classification maps of Canada's forested ecosystems for a 29-year Landsat time series. Can. J. Remote Sens. 44, 67–87.

Hermosilla, T., Wulder, M.A., White, J.C., Coops, N.C., Hobart, G.W., 2017. Updating Landsat time series of surface-reflectance composites and forest change products with new observations. Int. J. Appl. Earth Obs. Geoinf. 63, 104–111.

Hermosilla, T., Wulder, M.A., White, J.C., Coops, N.C., Hobart, G.W., Campbell, L.B., 2016. Mass data processing of time series Landsat imagery: pixels to data products for forest monitoring. International Journal of Digital Earth 9, 1035–1054.

Herold, M., Scepan, J., Clarke, K.C., 2002. The use of remote sensing and landscape metrics to describe structures and changes in urban land uses. Environ. Plan. A 34, 1443–1458.

Hilker, T., Wulder, M.A., Coops, N.C., Linke, J., McDermid, G., Masek, J.G., Gao, F., White, J.C., 2009a. A new data fusion model for high spatial- and temporal-resolution mapping of forest disturbance based on Landsat and MODIS. Remote Sens. Environ. 113, 1613–1627.

Hilker, T., Wulder, M.A., Coops, N.C., Seitz, N., White, J.C., Gao, F., Masek, J.G., Stenhouse, G., 2009b. Generation of dense time series synthetic Landsat data through data blending with MODIS using a spatial and temporal adaptive reflectance fusion model. Remote Sens. Environ. 113, 1988–1999.

Hiron, M., Berg, A., Eggers, S., Berggren, A., Josefsson, J., Pärt, T., 2015. The relationship of bird diversity to crop and non-crop heterogeneity in agricultural landscapes. Landsc. Ecol. 30, 2001–2013.

Horler, D.N.H., Ahern, F.J., 1986. Forestry information content of Thematic Mapper data. Int. J. Remote Sens. 7, 405–428.

Hu, F., Xia, G-S., Hu, J., Zhang, L., 2015. Transferring deep convolutional neural networks for the scene classification of high-resolution remote sensing imagery. Remote Sens. 7, 14680–14707.

Huang, B., Zhao, B., Song, Y., 2018. Urban land-use mapping using a deep convolutional neural network with high spatial resolution multispectral remote sensing imagery. Remote Sens. Environ. 214, 73–86.

Huang, X., Rein, G., 2016. Interactions of Earth's atmospheric oxygen and fuel moisture in smouldering wildfires. Sci. Total Environ. 572, 1440–1446.

Humber, M.L., Boschetti, L., Giglio, L., Justice, C.O., 2018. Spatial and temporal intercomparison of four global burned area products. Int. J. Digit. Earth 2018. https://doi.org/10.1080/17538947.2018.1433727

Immitzer, M., Vuolo, F., Atzberger, C., 2016. First experience with Sentinel-2 data for crop and tree species classifications in Central Europe. Remote Sens. 8, 166.

Iverson, L.R., Graham, R.L., Cook, E.A., 1989. Applications of satellite remote sensing to forested ecosystems. Landsc. Ecol. 3, 131–143.

Jackson, N.D., Fahrig, L., 2016. Habitat amount, not habitat configuration, best predicts population genetic structure in fragmented landscapes. Landsc. Ecol. 31, 951–968.

Jain, P., Coogan, S.C.P., Subramanian, S.G., Crowley, M., Taylor, S., Flannigan, M.D., 2020. A review of machine learning applications in wildfire science and management. arXiv [cs.LG].

Janda, P., Trotsiuk, V., Mikoláš, M., et al., 2017. The historical disturbance regime of mountain Norway spruce forests in the Western Carpathians and its influence on current forest structure and composition. For. Ecol. Manage. 388, 67–78.

Jin, S., Sader, S.A., 2005. MODIS time-series imagery for forest disturbance detection and quantification of patch size effects. Remote Sens. Environ. 99, 462–470.

Johnston, J.M., Jackson, N., McFayden, C., Ngo Phong, L., Lawrence, B., Davignon, D., Wooster, M.J., van Mierlo, H., Thompson, D.K., Cantin, A.S., Johnston, D., Johnston, L.M., Sloane, M., Ramos, R., Lynham, T.J., 2020. Development of the User Requirements for the Canadian WildFireSat Satellite Mission. Sensors 20. https://doi.org/10.3390/s20185081

Johnston, L.M., Wang, X., Erni, S., Taylor, S.W., McFayden, C.B., Oliver, J.A., Stockdale, C., Christianson, A., Boulanger, Y., Gauthier, S., Arseneault, D., Mike Wotton, B., Parisien, M.-A., Flannigan, M.D., 2020. Wildland fire risk research in Canada. Environmental Reviews.

Jolly, W.M., Cochrane, M.A., Freeborn, P.H., Holden, Z.A., Brown, T.J., Williamson, G.J., Bowman, D.M.J.S., 2015. Climate-induced variations in global wildfire danger from 1979 to 2013. Nat. Commun. 6, 7537.

Jung, M., 2016. LecoS - A python plugin for automated landscape ecology analysis. Ecol. Inform. 31, 18–21.

Kayitakire, F., Hamel, C., Defourny, P., 2006. Retrieving forest structure variables based on image texture analysis and IKONOS-2 imagery. Remote Sens. Environ. 102, 390–401.

Keeley, J.E., 2009. Fire intensity, fire severity and burn severity: a brief review and suggested usage. Int. J. Wildland Fire 18, 116.

Kemp, K.B., Higuera, P.E., Morgan, P., 2016. Fire legacies impact conifer regeneration across environmental gradients in the U.S. northern Rockies. Landsc. Ecol. 31, 619–636.

Kemp, K.B., Higuera, P.E., Morgan, P., Abatzoglou, J.T., 2019. Climate will increasingly determine post-fire tree regeneration success in low-elevation forests, Northern Rockies, USA. Ecosphere 10, e02568.

Kennedy, R.E., Yang, Z., Cohen, W.B., 2010. Detecting trends in forest disturbance and recovery using yearly Landsat time series: 1. LandTrendr — Temporal segmentation algorithms. Remote Sens. Environ. 114, 2897–2910.

Key, C.H., Benson, N.C., 1999. Measuring and remote sensing of burn severity. In L. F. Neuenschwander, & K. C. Ryan (Eds.), Proceedings Joint Fire Science Conference and Workshop, vol. II (p. 284). Moscow, ID: University of Idaho and International Association of Wildland Fire.

Key, C.H., Benson, N.C., 2006. Landscape Assessment (LA). FIREMON: Fire effects monitoring and inventory system. In: Lutes, D.C., Keane, R.E., Carati, J.F., Key, C.H., Benson, N.C., Gangi, L.J. (Eds.), General technical report RMRS-GTR-164-CD (pp. LA-1-55). USDA Forest Service, Rocky Mountains Research Station, Fort Collins, CO. https://doi.org/10.2737/RMRS-GTR-164

Korhonen, L., Hadi, Packalen, P., Rautiainen, M., 2017. Comparison of Sentinel-2 and Landsat 8 in the estimation of boreal forest canopy cover and leaf area index. Remote Sens. Environ. 195, 259–274.

Krawchuk, M.A., Moritz, M.A., Parisien, M.-A., Van Dorn, J., Hayhoe, K., 2009. Global pyrogeography: the current and future distribution of wildfire. PLoS One 4, e5102.

Krosby, M., Breckheimer, I., John Pierce, D., et al., 2015. Focal species and landscape “naturalness” corridor models offer complementary approaches for connectivity conservation planning. Landsc. Ecol. 30, 2121–2132.

Kulkarni, A., 2021. A look back at the 2021 B.C. wildfire season. CBC News.

Kwak-Hefferan, E., 2021. The Summer Yellowstone Burned. What Went Wrong in 1988? [WWW Document]. URL https://www.yellowstonepark.com/park/history/1988-fires-yellowstone/ (accessed 11.1.21).

Kwan, C., Budavari, B., Gao, F., Zhu, X., 2018. A hybrid color mapping approach to fusing MODIS and Landsat images for forward prediction. Remote Sens. 10, 520.

Lanclos, R., 2021. CAL FIRE Applies New Predictive and Tactical Tools to Fight Ferocious Fires [WWW Document]. URL https://www.esri.com/about/newsroom/blog/cal-fire-puts-entire-team-on-same-map/ (accessed 10.20.21).

Lausch, A., Blaschke, T., Haase, D., Herzog, F., Syrbe, R.-U., Tischendorf L., Walz U., 2015. Understanding and quantifying landscape structure – A review on relevant process characteristics, data models and landscape metrics. Ecol. Modell. 295, 31–41.

Lausch, A., Pause, M., Merbach, I., Zacharias, S., Doktor, D., Volk, M., Seppelt, R., 2013. A new multiscale approach for monitoring vegetation using remote sensing-based indicators in laboratory, field, and landscape. Environ. Monit. Assess. 185, 1215–1235.

LeClerc, E., Wiersma, Y.F., 2017. Assessing post-industrial land cover change at the Pine Point Mine, NWT., Canada using multi-temporal Landsat analysis and landscape metrics. Environ. Monit. Assess. 189.

Lee, J., Cardille, J.A., Coe, M.T., 2018. BULC-U: Sharpening Resolution and Improving Accuracy of Land-Use/Land-Cover Classifications in Google Earth Engine. Remote Sensing 10, 1455.

Lee, J., Cardille, J.A., Coe, M.T., 2020. Agricultural Expansion in Mato Grosso from 1986–2000: A Bayesian Time Series Approach to Tracking Past Land Cover Change. Remote Sensing. https://doi.org/10.3390/rs12040688

Lefsky, M.A., Cohen, W.B., Parker, G.G., Harding, D.J., 2002. Lidar remote sensing for ecosystem studies: Lidar, an emerging remote sensing technology that directly measures the three-dimensional distribution of plant canopies, can accurately estimate vegetation structural attributes and should be of particular interest to forest, landscape, and global ecologists. BioScience 52, 19–30.

Lefsky, M.A., Cohen, W.B., Spies, T.A., 2001. An evaluation of alternate remote sensing products for forest inventory, monitoring, and mapping of Douglas-fir forests in western Oregon. Can. J. For. Res. 31, 78–87.

Lemessa, D., Hambäck, P.A., Hylander, K., 2015. The effect of local and landscape level land-use composition on predatory arthropods in a tropical agricultural landscape. Landsc. Ecol. 30, 167–180.

Lentile, L.B., Holden, Z.A., Smith, A.M., Falkowski, M.J., Hudak, A.T., Morgan, P., Lewis, S.A., Gessler, P.E., Benson, N.C., 2006. Remote sensing techniques to assess active fire characteristics and post-fire effects. International Journal of Wildland Fire 15(3), 319–345.

Li, J., Roy, D.P., 2017. A Global Analysis of Sentinel-2A, Sentinel-2B and Landsat-8 Data Revisit Intervals and Implications for Terrestrial Monitoring. Remote Sensing 9, 902.

Li, L., Fassnacht, F.E., Storch, I., 2017. Land-use regime shift triggered the recent degradation of alpine pastures in Nyanpo Yutse of the eastern Qinghai-Tibetan Plateau. Landsc. Ecol. 32, 2187–2203.

Li, X., Strahler, A.H., 1985. Geometric-Optical Modeling of a Conifer Forest Canopy. IEEE Trans. Geosci. Remote Sens. GE-23, 705–721.

Li, Y., Li, Y., Qureshi, S., 2015. On the relationship between landscape ecological patterns and water quality across gradient zones of rapid urbanization in coastal China. Ecol. Modell. 318, 100–108.

Liu, Y., Peng, J., Wang, Y., 2018. Application of partial least squares regression in detecting the important landscape indicators determining urban land surface temperature variation. Landsc. Ecol. 33, 1133–1145.

Liu, Z., Yang, J., Dwomoh, F., 2016. Mapping recent burned patches in Siberian larch forest using Landsat and MODIS data. Eur. J. Remote Sens. 49, 861–887.

Lohberger, S., Stängel, M., Atwood, E.C., Siegert, F., 2018. Spatial evaluation of Indonesia's

2015 fire-affected area and estimated carbon emissions using Sentinel-1. Global Change Biology. 24(2), 644-654.

Lu, D., 2006. The potential and challenge of remote sensing-based biomass estimation. Int. J. Remote Sens. 27, 1297–1328.

Lu, D., Chen, Q., Wang, G., Liu, L., Li, G., Moran, E., 2016. A survey of remote sensing-based aboveground biomass estimation methods in forest ecosystems. Int. J. Digit Earth 9, 63–105.

Luther, J.E., Fournier, R.A., Piercey, D.E., Guindon, L., Hall, R.J., 2006. Biomass mapping using forest type and structure derived from Landsat TM imagery. Int. J. Appl. Earth Obs. Geoinf. 8, 173–187.

Ma Q., Wu, J., He, C., 2016. A hierarchical analysis of the relationship between urban impervious surfaces and land surface temperatures: spatial scale dependence, temporal variations, and bioclimatic modulation. Landsc. Ecol. 31, 1139–1153.

Maclaurin, G.J., Leyk, S., 2016. Extending the geographic extent of existing land cover data using active machine learning and covariate shift corrective sampling. Int. J. Remote Sens. 37, 5213–5233.

MacPherson, M., Dickson, C., 2021. Paradise lost. CBC News.

Malamud, B.D., Morein, G., Turcotte, D.L., 2005. Log-periodic behavior in a forest-fire model. Nonlinear Process. Geophys. 12, 575–585.

Malbeuf, J., 2021. Forged by fire: Fort McMurray 5 years after the disaster. CBC News.

Marceau, D.J., Howarth, P.J., Gratton, D.J., 1994. Remote sensing and the measurement of geographical entities in a forested environment. 1. The scale and spatial aggregation problem. Remote Sensing of Environment. https://doi.org/10.1016/0034-4257(94)90046-

9

Martin, M.E., Aber, J.D., 1997. High spectral resolution remote sensing of forest canopy lignin, nitrogen, and ecosystem processes. Ecol. Appl. 7, 431–443.

Martinez del Castillo, E., Garcia-Martin, A., Longares Aladren, L.A., 2015. Evaluation of forest cover change using remote sensing techniques and landscape metrics in Moncayo Natural Park (Spain). Appl. Geogr. 62, 247–255.

Martínez Pastur, G., Peri, P.L., Lencinas, M.V., García-Llorente, M., Martín-López, B., 2016. Spatial patterns of cultural ecosystem services provision in Southern Patagonia. Landsc. Ecol. 31, 383–399.

Matasci, G., Hermosilla, T., Wulder, M.A., White, J.C., Coops, N.C., Hobart, G.W., Bolton, D.K., Tompalski, P., Bater, C.W., 2018. Three decades of forest structural dynamics over Canada's forested ecosystems using Landsat time-series and lidar plots. Remote Sens. Environ. 216, 697–714.

Matasci, G., Hermosilla, T., Wulder, M.A., White, J.C., Coops, N.C., Hobart, G.W., Zald, H.S.J., 2018. Large-area mapping of Canadian boreal forest cover, height, biomass and other structural attributes using Landsat composites and lidar plots. Remote Sens. Environ. 209, 90–106.

Matese, A., Toscano, P., Di Gennaro, S.F., Genesio, L., Vaccari, F.P., Primicerio, J., Belli, C., Zaldei, A., Bianconi, R., Gioli, B., 2015. Intercomparison of UAV., aircraft and satellite remote sensing platforms for precision viticulture. Remote Sens. 7, 2971–2990.

Maynard, J.J., Karl, J.W., Browning, D.M., 2016. Effect of spatial image support in detecting long-term vegetation change from satellite time-series. Landsc. Ecol. 31, 2045–2062.

McCarty, J.L., Aalto, J., Paunu, V.-V., Arnold, S.R., Eckhardt, S., Klimont, Z., Fain, J.J., Evangeliou, N., Venäläinen, A., Tchebakova, N.M., Parfenova, E.I., Kupiainen, K., Soja, A.J., Huang, L., Wilson, S., 2021. Reviews and syntheses: Arctic fire regimes and emissions in the 21st century. Biogeosciences. https://doi.org/10.5194/bg-18-5053-2021

McClure, M.L., Hansen, AJ., Inman, R.M., 2016. Connecting models to movements: testing connectivity model predictions against empirical migration and dispersal data. Landsc. Ecol. 31, 1419–1432.

McFayden, C.B., Boychuk, D., Woolford, D.G., Wheatley, M.J., Johnston, L., 2019. Impacts of wildland fire effects on resources and assets through expert elicitation to support fire response decisions. Int. J. Wildland Fire 28, 885–900.

McGarigal, K., Wan, H.Y., Zeller, K.A., Timm, B.C., Cushman, S.A., 2016. Multi-scale habitat selection modeling: a review and outlook. Landsc. Ecol. 31, 1161–1175.

McKenzie, D., Miller, C., Falk, D.A., 2011. Toward a Theory of Landscape Fire, in: McKenzie, D., Miller, C., Falk, D.A. (Eds.), The Landscape Ecology of Fire. Springer Netherlands, Dordrecht, pp. 3–25.

McRoberts, R.E., Tomppo, E.O., 2007. Remote sensing support for national forest inventories. Remote Sens. Environ. 110, 412–419.

McWethy, D.B., Schoennagel, T., Higuera, P.E., Krawchuk, M., Harvey, B.J., Metcalf, E.C., Schultz, C., Miller, C., Metcalf, A.L., Buma, B., Virapongse, A., Kulig, J.C., Stedman, R.C., Ratajczak, Z., Nelson, C.R., Kolden, C., 2019. Rethinking resilience to wildfire. Nature Sustainability 2, 797–804.

Meyn, A., White, P.S., Buhk, C., Jentsch, A., 2007. Environmental drivers of large, infrequent wildfires: the emerging conceptual model. Progress in Physical Geography: Earth and Environment 31, 287–312.

Mishra, N.B., Crews, K.A., 2014. Mapping vegetation morphology types in a dry savanna ecosystem: integrating hierarchical object-based image analysis with Random Forest. Int. J. Remote Sens. 35, 1175–1198.

Molin, P.G., Gergel, S.E., Soares-Filho, B.S., Ferraz, S.F.B., 2017. Spatial determinants of Atlantic forest loss and recovery in Brazil. Landsc. Ecol. 32, 857–870.

Molinier, M., Astola, H., Räty, T., Woodcock, C.E., 2018. Timely and semi-automatic detection of forest logging events in boreal forest using all available Landsat data. In: IGARSS 2018 - 2018 IEEE International Geoscience and Remote Sensing Symposium. ieeexplore.ieee.org, pp 1730–1733.

Mora, B., Wulder, M.A., White, J.C., Hobart, G., 2013. Modeling Stand Height, Volume, and Biomass from Very High Spatial Resolution Satellite Imagery and Samples of Airborne LiDAR. Remote Sensing 5, 2308–2326.

Morgan, P., Hardy, C.C., Swetnam, T.W., Rollins, M.G., Long, D.G., 2001. Mapping fire regimes across time and space: Understanding coarse and fine-scale fire patterns. International Journal of Wildland Fire. https://doi.org/10.1071/wf01032

Morgan, P., Heyerdahl, E.K., Gibson, C.E., 2008. Multi-season climate synchronized forest fires throughout the 20th century, northern Rockies, USA. Ecology 89, 717–728.

Morgan, P., Heyerdahl, E.K., Miller, C., Wilson, A.M., Gibson, C.E., 2014. Northern Rockies Pyrogeography: an Example of Fire Atlas Utility. Fire Ecology 10, 14–30.

Moriarty, K.M., Epps, C.W., Betts, M.G., Hance, D.J., Bailey, J.D., Zielinski, W.J., 2015. Experimental evidence that simplified forest structure interacts with snow cover to influence functional connectivity for Pacific martens. Landsc. Ecol. 30, 1865–1877.

Nash, T., St. Arnaud, L., Tithecott, A., Simpson, B., Stocks, B., 2017. A Review of the 2016

Horse River Wildfire. MNP LLP.

National Academies of Sciences, Engineering, and Medicine, Division on Earth and Life Studies, Board on Agriculture and Natural Resources, Board on Earth Sciences and Resources, Committee on Increasing Resilience to Wildland Fire: A Century of Wildland Fire Research, 2017. A Century of Wildland Fire Research: Contributions to Long-term Approaches for Wildland Fire Management: Proceedings of a Workshop. National Academies Press.

[dataset] Natural Resources Canada, 2018a. nbac_2017_r2_20180725_1603.zip Canadian National Fire Database - National Burned Area Composite. http://cwfis.cfs.nrcan.gc.ca/downloads/nbac/ (accessed 10 September 2018).

Natural Resources Canada, 2018b. Monthly and Seasonal Forecasts - Canadian Wildland Fire Information System. http://cwfis.cfs.nrcan.gc.ca/maps/forecasts (accessed 28 October 2018).

Nelson, T., Niemann, K.O., Wulder, M.A., 2002. Spatial statistical techniques for aggregating point objects extracted from high spatial resolution remotely sensed imagery. J. Geogr. Syst. 4, 423–433.

Nogueira, J.M., Ruffault, J., Chuvieco, E., Mouillot, F., 2016. Can we go beyond burned area in the assessment of global remote sensing products with fire patch metrics? Remote Sensing. 9(1), 7.

O'Connor, A., 2021. Effective Wildfire Management Using Remote Sensing Technology [WWW Document]. L3Harris Geospatial. URL https://www.l3harrisgeospatial.com/Learn/Whitepapers/Whitepaper-Detail/ArtMID/17811/ArticleID/24063/Effective-Wildfire-Management-Using-Remote-

Sensing-Technology?utm_source=twitter&utm_medium=wildfire_management_whitepaper (accessed 10.18.21).

Olah, G., Smith, A.L., Asner, G.P., 2017. Exploring dispersal barriers using landscape genetic resistance modelling in scarlet macaws of the Peruvian Amazon. Landsc. Ecol. 32, 445–456.

Ollinger, S.V., Smith, M.-L., 2005. Net primary production and canopy nitrogen in a temperate forest landscape: An analysis using imaging spectroscopy, modeling and field data. Ecosystems 8, 760–778.

Olofsson, P., Foody, G.M., Herold, M., Stehman, S.V., Woodcock, C.E., Wulder, M.A., 2014. Good practices for estimating area and assessing accuracy of land change. Remote Sens. Environ. 148, 42–57.

Olofsson, P., Foody, G.M., Stehman, S.V., Woodcock, C.E., 2013. Making better use of accuracy data in land change studies: Estimating accuracy and area and quantifying uncertainty using stratified estimation. Remote Sens. Environ. 129, 122–31.

Padilla, M., Stehman, S.V. Chuvieco, E., 2014. Validation of the 2008 MODIS-MCD45 global burned area product using stratified random sampling. Remote Sensing of Environment. 144, 187-196.

Padilla, M., Stehman, S.V., Ramo, R., Corti, D., Hantson, S., Oliva, P., Alonso-Canas, I., Bradley, A.V., Tansey, K., Mota, B., Pereira, J.M., 2015. Comparing the accuracies of remote sensing global burned area products using stratified random sampling and estimation. Remote Sensing of Environment. 160, 114-121.

Pajares, G., 2015. Overview and current status of remote sensing applications based on unmanned aerial vehicles (UAVs). Photogramm Eng Remote Sensing 81, 281–330.

Palace, M., Keller, M., Asner, G.P., Hagen, S., Braswell, B., 2008. Amazon forest structure from IKONOS satellite data and the automated characterization of forest canopy properties. Biotropica 40, 141–150.

Parisien, M.-A., Parks, S.A., Krawchuk, M.A., Little, J.M., Flannigan, M.D., Gowman, L.M., Moritz, M.A., 2014. An analysis of controls on fire activity in boreal Canada: comparing models built with different temporal resolutions. Ecol. Appl. 24, 1341–1356.

Parisien, M.-A., Peters, V.S., Wang, Y., Little, J.M., Bosch, E.M., Stocks, B.J., 2006. Spatial patterns of forest fires in Canada, 1980–1999. Int. J. Wildland Fire 15, 361–374.

Parisien, M.A., Parks, S.A., Miller, C., Krawchuk, M.A., Heathcott, M., Moritz, M.A., 2011. Contributions of ignitions, fuels, and weather to the spatial patterns of burn probability of a boreal landscape. Ecosystems. 14(7), 1141–1155. doi:10.1007/S10021-011-9474-2

Parks, S.A., 2014. Mapping day-of-burning with coarse-resolution satellite fire-detection data. Int. J. Wildland Fire 23, 215–223.

Parks, S.A., Holsinger, L.M., Miller, C., Nelson, C.R., 2015. Wildland fire as a self-regulating mechanism: the role of previous burns and weather in limiting fire progression. Ecol. Appl. 25, 1478–1492.

Parks, S.A., Holsinger, L.M., Panunto, M.H., Matt Jolly, W., Dobrowski, S.Z., Dillon, G.K., 2018. High-severity fire: evaluating its key drivers and mapping its probability across western US forests. Environ. Res. Lett. 13, 044037.

Parks, S.A., Miller, C., Holsinger, L.M., Scott Baggett, L., Bird, B.J., 2016. Wildland fire limits subsequent fire occurrence. Int. J. Wildland Fire 25, 182–190.

Parks, S.A., Miller, C., Nelson, C.R., Holden, Z.A., 2014. Previous Fires Moderate Burn

Severity of Subsequent Wildland Fires in Two Large Western US Wilderness Areas. Ecosystems 17, 29–42.

Parks, S.A., Parisien, M.-A., Miller, C., 2012. Spatial bottom-up controls on fire likelihood vary across western North America. Ecosphere 3, 1–20.

Paul, F., Bolch, T., Kääb, A., et al., 2015. The glaciers climate change initiative: Methods for creating glacier area, elevation change and velocity products. Remote Sens. Environ. 162, 408–426.

Pausas, J.G., Keeley, J.E., 2019. Wildfires as an ecosystem service. Front. Ecol. Environ. 17, 289–295.

Peng, J., Chen, S., Lu, H., Liu, Y., Wu, J., 2016. Spatiotemporal patterns of remotely sensed PM2.5 concentration in China from 1999 to 2011. Remote Sens. Environ. 174, 109–121.

Peterson, G.D., 2002. Contagious Disturbance, Ecological Memory, and the Emergence of Landscape Pattern. Ecosystems 5, 329–338.

Pohjanmies, T., Triviño, M., Le Tortorec, E., Mazziotta, A., Snäll, T., Mönkkönen, M., 2017. Impacts of forestry on boreal forests: An ecosystem services perspective. Ambio 46, 743–755.

Potapov, P.V., Turubanova, S.A., Tyukavina, A., Krylov, A.M., McCarty, J.L., Radeloff, V.C., Hansen, M.C., 2015. Eastern Europe's forest cover dynamics from 1985 to 2012 quantified from the full Landsat archive. Remote Sens. Environ. 159, 28–43.

Prestemon, J.P., Hawbaker, T.J., Bowden, M., Carpenter, J., Brooks, M.T., Abt, K.L., Sutphen, R., Scranton, S., 2013. Wildfire ignitions: a review of the science and recommendations for empirical modeling. Gen. Tech. Rep. SRS-GTR-171. Asheville, NC: USDA-Forest Service, Southern Research Station., 20 p. 171, 1–20.

Price, O.F., Pausas, J.G., Govender, N., Flannigan, M., Fernandes, P.M., Brooks, M.L., Bird, R.B., 2015. Global patterns in fire leverage: the response of annual area burnt to previous fire. Int. J. Wildland Fire 24, 297–306.

Puliti, S., Ørka, H.O., Gobakken, T., Næsset, E., 2015. Inventory of small forest areas using an unmanned aerial system. Remote Sens. 7, 9632–9654.

Qiu, J., Turner, M.G., 2015. Importance of landscape heterogeneity in sustaining hydrologic ecosystem services in an agricultural watershed. doi: 10.1890/ES15-00312.1.

Quintano, C., Fernández-Manso, A., Fernández-Manso, O., 2018. Combination of Landsat and Sentinel-2 MSI data for initial assessing of burn severity. International Journal of Applied Earth Observation and Geoinformation. 64, 221–225.

Reiche, J., Verbesselt, J., Hoekman, D., Herold, M., 2015. Fusing Landsat and SAR time series to detect deforestation in the tropics. Remote Sens. Environ. 156, 276–293.

Reichstein, M., Camps-Valls, G., Stevens, B., Jung, M., Denzler, J., Carvalhais, N., Prabhat, 2019. Deep learning and process understanding for data-driven Earth system science. Nature 566, 195–204.

Reid, C.E., Brauer, M., Johnston, F.H., Jerrett, M., Balmes, J.R., Elliott, C.T., 2016. Critical Review of Health Impacts of Wildfire Smoke Exposure. Environ. Health Perspect. 124, 1334–1343.

Remy, C.C., Hély, C., Blarquez, O., Magnan, G., Bergeron, Y., Lavoie, M., Ali, A.A., 2017. Different regional climatic drivers of Holocene large wildfires in boreal forests of northeastern America. Environmental Research Letters. https://doi.org/10.1088/1748-9326/aa5aff

Requena-Mullor, J.M., Lopez, E., Castro, A.J., 2014. Modeling spatial distribution of European badger in arid landscapes: an ecosystem functioning approach. Landsc. Ecol. 29, 843–855.

Riitters, K., Wickham, J., Costanza, J.K., Vogt, P., 2016. A global evaluation of forest interior area dynamics using tree cover data from 2000 to 2012. Landsc. Ecol. 31, 137–148.

Rittmaster, R., Adamowicz, W.L., Amiro, B., Pelletier, R.T., 2006. Economic analysis of health effects from forest fires. Can. J. For. Res. 36, 868–877.

Romero, A., Gatta, C., Camps-Valls, G., 2016. Unsupervised deep feature extraction for remote sensing image classification. IEEE Trans. Geosci. Remote Sens. 54, 1349–1362.

Romme, W.H., 1982. Fire and Landscape Diversity in Subalpine Forests of Yellowstone National Park. Ecol. Monogr. 52, 199–221.

Roos, C.I., Bowman, D.M.J.S., Balch, J.K., Artaxo, P., Bond, W.J., Cochrane, M., D'Antonio, C.M., DeFries, R., Mack, M., Johnston, F.H., Krawchuk, M.A., Kull, C.A., Moritz, M.A., Pyne, S., Scott, A.C., Swetnam, T.W., 2014. Pyrogeography, historical ecology, and the human dimensions of fire regimes. J. Biogeogr. 41, 833–836.

Rothermel, R.C., Hartford, R.A., Chase, C.H., 1994. Fire growth maps for the 1988 Greater Yellowstone Area Fires. U.S. Department of Agriculture, Forest Service, Intermountain Research Station, Ogden, UT. https://doi.org/10.2737/int-gtr-304

Roy, D.P., Jin, Y., Lewis, P.E., Justice, C.O., 2005. Prototyping a global algorithm for systematic fire-affected area mapping using MODIS time series data. Remote Sens. Environ. 97, 137–162.

Roy, D.P., Wulder, M.A., Loveland, T.R., C. E., W., Allen, R.G., Anderson, M.C., Helder, D., Irons, J.R., Johnson, D.M., Kennedy, R., Scambos, T.A., Schaaf, C.B., Schott, J.R., Sheng, Y., Vermote, E.F., Belward, A.S., Bindschadler, R., Cohen, W.B., Gao, F., Hipple, J.D., Hostert, P., Huntington, J., Justice, C.O., Kilic, A., Kovalskyy, V., Lee, Z.P., Lymburner, L., Masek, J.G., McCorkel, J., Shuai, Y., Trezza, R., Vogelmann, J., Wynne, R.H., Zhu, Z., 2014. Landsat-8: Science and product vision for terrestrial global change research. Remote Sens. Environ. 145, 154–172.

Rumbolt, R., 2017. Water bombers back in the skies fighting “Goliath of a fire” in Waterton Lakes National Park. CBC News.

Saah, D., 2021. Close to Home: Fighting wildfires with better science. Press Democrat.

San-Miguel, I., Andison, D.W., Coops, N.C., 2017. Characterizing historical fire patterns as a guide for harvesting planning using landscape metrics derived from long term satellite imagery. Forest Ecology and Management. 399, 155–165. doi:10.1016/j.foreco.2017.05.021.

San-Miguel, I., Andison, D.W., Coops, N.C., 2018. Quantifying local fire regimes using the Landsat data-archive: a conceptual framework to derive detailed fire pattern metrics from pixel-level information. International Journal of Digital Earth. 1–22. doi:10.1080/17538947.2018.1464072

Scarth, P., Phinn, S.R., McAlpine, C., 2001. Integrating High and Moderate Spatial Resolution Image Data to Estimate Forest Age Structure. Can. J. Remote Sens. 27, 129–142.

Schmidt, J., Fassnacht, F.E., Neff, C., 2017. Adapting a Natura 2000 field guideline for a remote sensing-based assessment of heathland conservation status. Int. J. Appl. Earth Obs. Geoinf. 60, 61–71.

Schroeder, T.A., Wulder, M.A., Healey, S.P., Moisen, G.G., 2011. Mapping wildfire and clearcut harvest disturbances in boreal forests with Landsat time series data. Remote Sens. Environ. 115, 1421–1433.

Schroeder, W., Prins, E., Giglio, L., Csiszar, I., Schmidt, C., Morisette, J., Morton, D., 2008. Validation of GOES and MODIS active fire detection products using ASTER and ETM+ data. Remote Sens. Environ. 112, 2711–2726.

Seidl, R., Donato, D.C., Raffa, K.F., Turner, M.G., 2016. Spatial variability in tree regeneration after wildfire delays and dampens future bark beetle outbreaks. Proc. Natl. Acad. Sci. U. S. A. 113, 13075–13080.

Sexton, J.O., Noojipady, P., Anand, A., Song, X.-P., McMahon, S., Huang, C., Feng, M., Channan, S., Townshend, J.R., 2015. A model for the propagation of uncertainty from continuous estimates of tree cover to categorical forest cover and change. Remote Sens. Environ. 156, 418–425.

Shang, C., Wulder, M.A., Coops, N.C., White, J.C., Hermosilla, T., 2020. Spatially-Explicit Prediction of Wildfire Burn Probability Using Remotely-Sensed and Ancillary Data. Can. J. Remote Sens. 46, 313–329.

Shean, D.E., Alexandrov, O., Moratto, Z.M., Smith, B.E., Joughin, I.R., Porter, C., Morin, P., 2016. An automated, open-source pipeline for mass production of digital elevation models (DEMs) from very-high-resolution commercial stereo satellite imagery. ISPRS J. Photogramm. Remote Sens. 116, 101–117.

Shen, H., Huang, L., Zhang, L., Wu, P., Zeng, C., 2016. Long-term and fine-scale satellite monitoring of the urban heat island effect by the fusion of multi-temporal and multi-sensor remote sensed data: A 26-year case study of the city of Wuhan in China. Remote Sens. Environ. 172, 109–125.

Sillero, N., Goncalves-Seco, L., 2014. Spatial structure analysis of a reptile community with airborne LiDAR data. Int. J. Geogr Inf Sci 28, 1709–1722.

Singh, H., Garg, R.D., Karnatak, H.C., Roy, A., 2018. Spatial landscape model to characterize biological diversity using R statistical computing environment. J Environ Manage 206, 1211–1223.

Soverel, N.O., Coops, N.C., Perrakis, D.D., Daniels, L.D., Gergel, S.E., 2011. The transferability of a dNBR-derived model to predict burn severity across 10 wildland fires in western Canada. International Journal of Wildland Fire., 20(4), 518–531.

Soverel, N.O., Perrakis, D.D., Coops, N.C., 2010. Estimating burn severity from Landsat dNBR and RdNBR indices across western Canada. Remote Sensing of Environment. 114(9), 1896–1909.

Sponsler, D.B., Johnson, R.M., 2015. Honey bee success predicted by landscape composition in Ohio, USA. PeerJ 3, e838.

Stark, S.C., Breshears, D.D., Garcia, E.S., 2016. Toward accounting for ecoclimate teleconnections: intra- and inter-continental consequences of altered energy balance after vegetation change. Landsc. Ecol. 31, 181–194.

Steen-Adams, M.M., Langston, N., Adams, M., Mladenoff, D.J., 2015. Historical framework to explain long-term coupled human and natural system feedbacks: application to a multiple-ownership forest landscape in the northern Great Lakes region, US.A. Ecol Soc 20.

Steininger, M.K., 2000. Satellite estimation of tropical secondary forest above-ground biomass: Data from Brazil and Bolivia. Int. J. Remote Sens. 21, 1139–1157.

Stinson, G., Kurz, W.A., Smyth, C.E., Neilson, E.T., Dymond, C.C., Metsaranta, J.M., Boisvenue, C., Rampley, G.J., Li, Q., White, T.M., Others, 2011. An inventory-based analysis of Canada's managed forest carbon dynamics, 1990 to 2008. Glob. Chang. Biol.

17, 2227–2244.

Stocks, B.J., Fosberg, M.A., Lynham, T.J., Mearns, L., Wotton, B.M., Yang, Q., Jin, J.Z., Lawrence, K., Hartley, G.R., Mason, J.A., Others, 1998. Climate change and forest fire potential in Russian and Canadian boreal forests. Clim. Change 38, 1–13.

Stocks, B.J., Mason, J.A., Todd, J.B., Bosch, E.M., Wotton, B.M., Amiro, B.D., Flannigan, M.D., Hirsch, K.G., Logan, K.A., Martell, D.L., Skinner, W.R., 2002. Large forest fires in Canada, 1959–1997. J. Geophys. Res. 108, 512.

Street, G.M., Fieberg, J., Rodgers, A.R., Carstensen, M., Moen, R., Moore, S.A., Windels, S.K., Forester, J.D., 2016. Habitat functional response mitigates reduced foraging opportunity: implications for animal fitness and space use. Landsc. Ecol. 31, 1939–1953.

Szabó, L., Burai, P., Deák, B., Dyke, G.J., Szabó, S., 2019. Assessing the efficiency of multispectral satellite and airborne hyperspectral images for land cover mapping in an aquatic environment with emphasis on the water caltrop (Trapa natans). Int. J. Remote Sensing 40, 5192–5215.

Tedim, F., Leone, V., Amraoui, M., Bouillon, C., Coughlan, M.R., Delogu, G.M., Fernandes, P.M., Ferreira, C., McCaffrey, S., McGee, T.K., Others, 2018. Defining Extreme Wildfire Events: Difficulties, Challenges, and Impacts, Fire, 1, 9.

Thom, D., Seidl, R., 2016. Natural disturbance impacts on ecosystem services and biodiversity in temperate and boreal forests. Biol. Rev. Camb. Philos. Soc. 91, 760–781.

Thompson, S.D., Nelson, T.A., White, J.C., 2015. Mapping dominant tree species over large forested areas using Landsat Best-Available-Pixel image composites. Can. J. Remote Sens. 41, 203–218.

Tompalski, P., Coops, N.C., Marshall, P.L., White, J.C., Wulder, M.A., Bailey, T., 2018.

Combining multi-date airborne laser scanning and digital aerial photogrammetric data for forest growth and yield modelling. Remote Sens. 10, 347.

Turner, D., Lucieer, A., De Jong, S.M., 2015. Time series analysis of landslide dynamics using an unmanned aerial vehicle (UAV). Remote Sens. 7, 1736–1757.

Turner, D.P., Ollinger, S.V., Kimball, J.S., 2004. Integrating remote sensing and ecosystem process models for landscape- to regional-scale analysis of the carbon cycle. BioScience 54, 573–584.

Turner, M.G., Hargrove, W.W., Gardner, R.H., Romme, W.H., 1994. Effects of fire on landscape heterogeneity in Yellowstone National Park, Wyoming. J. Veg. Sci. 5, 731–742.

Turner, M.G., O'Neill, R.V., Gardner, R.H., Milne B.T., 1989. Effects of changing spatial scale on the analysis of landscape pattern. Landsc. Ecol. 3, 153–162.

Turner, M.G., Romme, W.H., 1994. Landscape dynamics in crown fire ecosystems. Landsc. Ecol. 9, 59–77.

Turner, M.G., Romme, W.H., Gardner, R.H., Hargrove, W.W., 1997. Effects of fire size and pattern on early succession in Yellowstone National Park. Ecol. Monogr. 67, 411–433.

Turner, M.G., The Conversation US, 2018. Yellowstone Rebounded from an Epic 1988 Fire—That May Be Harder in Future. Scientific American.

U. S. Geological Survey, 2018. U.S. Landsat Analysis Ready Data (ARD) Data Format Control Book (DFCB). LSDS-809, Sioux Falls, SD: US Department of Interior, Earth Resources Observation and Science (EROS) Center. https://landsat.usgs.gov/sites/default/files/documents/LSDS-1873_US_Landsat_ARD_DFCB.pdf (accessed 15 April 2018).

Vanderhoof, M.K., Alexander, L.C., Todd, M.J.., 2016. Temporal and spatial patterns of wetland extent influence variability of surface water connectivity in the Prairie Pothole Region, United States. Landsc. Ecol. 31, 805–824.

Veraverbeke, S., Sedano, F., Hook, S.J., Randerson, J.T., Jin, Y., Rogers, B.M., 2014. Mapping the daily progression of large wildland fires using MODIS active fire data. International Journal of Wildland Fire. 23(5), 655–667.

Veraverbeke, S., Somers, B., Gitas, I., Katagis, T., Polychronaki, A., Goossens, R., 2012. Spectral mixture analysis to assess post-fire vegetation regeneration using Landsat Thematic Mapper imagery: Accounting for soil brightness variation. International Journal of Applied Earth Observation and Geoinformation. 14(1), 1–11.

Verhegghen, A., Eva, H., Ceccherini, G., Achard, F., Gond, V., Gourlet-Fleury, S., Cerutti, P., 2016. The potential of Sentinel satellites for burnt area mapping and monitoring in the Congo Basin forests. Remote Sensing. 8(12), 986.

Vermote, E., Justice, C., Claverie, M., Franch, B., 2016. Preliminary analysis of the performance of the Landsat 8/OLI land surface reflectance product. Remote Sens. Environ. 185, 46–56.

Vihervaara, P., Mononen, L., Auvinen, A.-P., 2015. How to integrate remotely sensed data and biodiversity for ecosystem assessments at landscape scale. Landsc. Ecol. 30, 501–516.

Vogelmann, J.E., Helder, D., Morfitt, R., Choate, M.J., Merchant, J.W., Bulley, H., 2001. Effects of Landsat 5 Thematic Mapper and Landsat 7 Enhanced Thematic Mapper Plus radiometric and geometric calibrations and corrections on landscape characterization. Remote Sens. Environ. 78, 55–70.

Vogt, P., Riitters, K., 2017. GuidosToolbox: universal digital image object analysis. Eur. J. Remote Sens. 50, 352–361.

Wan, H.Y., Cushman, S.A., Ganey, J.L., 2019. Improving habitat and connectivity model predictions with multi-scale resource selection functions from two geographic areas. Landsc. Ecol. 34, 503–519.

Wang, X., Thompson, D.K., Marshall, G.A., Tymstra, C., Carr, R., Flannigan, M.D., 2015. Increasing frequency of extreme fire weather in Canada with climate change. Clim. Change 130, 573–586.

White, J.C., Coops, N.C., Wulder, M.A., Vastaranta, M., Hilker, T., Tompalski, P., 2016. Remote sensing technologies for enhancing forest inventories: A review. Can. J. Remote Sens. 42, 619–641.

White, J.C., Tompalski, P., Coops, N.C., Wulder, M.A., 2018. Comparison of airborne laser scanning and digital stereo imagery for characterizing forest canopy gaps in coastal temperate rainforests. Remote Sens. Environ., 208, 1–14.

White, J.C., Wulder, M.A., Hermosilla, T., Coops, N.C., Hobart, G.W., 2017. A nationwide annual characterization of 25 years of forest disturbance and recovery for Canada using Landsat time series. Remote Sens. Environ. 194, 303–321.

White, J.C., Wulder, M.A., Hobart, G.W., Luther, J.E., Hermosilla, T., Griffiths, P., Coops, N.C., Hall, R.J., Hostert, P., Dyk, A., Guindon, L., 2014. Pixel-Based Image Compositing for Large-Area Dense Time Series Applications and Science. Can. J. Remote Sens. 40, 192–212.

Whitman, E., Parisien, M.-A., Holsinger, L.M., Park, J., Parks, S.A., 2020. A method for creating a burn severity atlas: an example from Alberta, Canada. Int. J. Wildland Fire 29, 995–1008.

Whitman, E., Parisien, M.-A., Thompson, D.K., Hall, R.J., Skakun, R.S., Flannigan, M.D., 2018.

Variability and drivers of burn severity in the northwestern Canadian boreal forest. Ecosphere. https://doi.org/10.1002/ecs2.2128

Wiersma, Y.F., McMullin, R.T., 2018. Is it common to be rare on the landscape? A test using a novel model system. Landsc. Ecol. 33, 183–195.

Wimberly, M.C., Cochrane, M.A., Baer, A.D., Pabst, K., 2009. Assessing fuel treatment effectiveness using satellite imagery and spatial statistics. Ecol. Appl. 19, 1377–1384.

Woodcock, C.E., Allen, R., Anderson, M., Belward, A., Bindschadler, R., Cohen, W., Gao, F., Goward, S.N., Helder, D., Helmer, E., Nemani, R., Oreopoulos, L., Schott, J., Thenkabail, P.S., Vermote, E.F., Vogelmann, J., Wulder, M.A., Wynne, R., 2008. Free access to Landsat imagery. Science 320, 1011.

Wooster, M.J., Roberts, G.J., Giglio, L., Roy, D., Freeborn, P., Boschetti, L., Justice, C., Ichoku, C., Schroeder, W., Davies, D., Smith, A., Setzer, A., Csiszar, I., Strydom, T., Frost, P., Zhang, T., Xu, W., de Jong, M., Johnston, J., Ellison, L., Vadrevu, K., McCarty, J., Tanpipat, V., Schmidt, C., San-Miguel, J., 2021. Satellite remote sensing of active fires: History and current status, applications and future requirements. Remote Sens. Environ. 267, 112694.

World Resources Institute., 2014. Global Forest Watch. http://www.globalforestwatch.org. Accessed 31 May 2019.

Wotton, B.M., Alexander, M.E., Taylor, S.W., 2009. Updates and revisions to the 1992 Canadian Forest Fire Behavior Prediction System. Natural Resources Canada.

Wu, J., Zhang, Q., Li, A., 2015. Historical landscape dynamics of Inner Mongolia: patterns, drivers, and impacts. Landsc. Ecol. 30, 1579–1598.

Wu, W., Li, Y., Hu, Y., Xiu, C., Yan, X., 2018. Impacts of changing forest management areas on forest landscapes and habitat patterns in northeastern China. Sustain Sci. Pract. Policy 10, 1211.

Wu, X., Akujarvi, A., Lu, N., 2015. Dynamics of soil organic carbon stock in a typical catchment of the Loess Plateau: comparison of model simulations with measurements. Landsc. Ecol. 30, 381–397.

Wulder, M.A., 1998. Optical remote-sensing techniques for the assessment of forest inventory and biophysical parameters. Progress in Physical Geography 22, 449–476.

Wulder, M.A., Coops, N.C., 2014. Satellites: Make Earth observations open access. Nature 513, 30–31.

Wulder, M.A., Coops, N.C., Roy, D.P., White, J.C., Hermosilla, T., 2018. Land cover 2.0. Int. J. Remote Sens. 39, 4254–4284.

Wulder, M.A., Hall, R.J., Coops, N.C., Franklin, S.E., 2004. High spatial resolution remotely sensed data for ecosystem characterization. BioScience 54, 511–521.

Wulder, M.A., Hilker, T., White, J.C., Coops, N.C., Masek, J.G., Pflugmacher, D., Crevier, Y., 2015. Virtual constellations for global terrestrial monitoring. Remote Sens. Environ. 170, 62–76. doi: 10.1016/j.rse.2015.09.001.

Wulder, M.A., Loveland, T.R., Roy, D.P., et al., 2019. Current status of Landsat program, science, and applications. Remote Sens. Environ. 225, 127–147.

Wulder, M.A., Masek, J.G., Cohen, W.B., Loveland, T.R., Woodcock, C.E., 2012. Opening the archive: How free data has enabled the science and monitoring promise of Landsat. Remote Sens. Environ. 122, 2–10.

Wulder, M.A., Skakun, R.S., Kurz, W.A., White, J.C., 2004. Estimating time since forest harvest using segmented Landsat ETM+ imagery. Remote Sensing of Environment. 93(1–2), 179–187.

Wulder, M.A., White, J.C., Gillis, M.D., Walsworth, N., Hansen, M.C., Potapov, P., 2010. Multiscale satellite and spatial information and analysis framework in support of a large-area forest monitoring and inventory update. Environmental Monitoring and Assessment. 170(1–4), 417–433.

Wulder, M.A., White, J.C., Loveland, T.R., Woodcock, C.E., Belward, A.S., Cohen, W.B., Fosnight, E.A., Shaw, J., Masek, J.G., Roy, D.P., 2016. The global Landsat archive: Status, consolidation, and direction. Remote Sens. Environ. 185, 271–283.

Wulder, M.A., White, J.C., Masek, J.G., Dwyer, J., Roy, D.P., 2011. Continuity of Landsat observations: Short term considerations. Remote Sensing of Environment. 115(2), 747–751.

Xian, G., Homer, C., Fry, J., 2009. Updating the 2001 National Land Cover Database land cover classification to 2006 by using Landsat imagery change detection methods. Remote Sens. Environ. 113, 1133–1147.

Xie, Y., Gong, J., Sun, P., 2014. Oasis dynamics change and its influence on landscape pattern on Jinta oasis in arid China from 1963a to 2010a: Integration of multi-source satellite images. Int. J. Appl. Earth Obs. Geoinf. 33, 181–191.

Xu, C., Pu, L., Zhu, M., 2016. Ecological security and ecosystem services in response to land use change in the coastal area of Jiangsu, China. Sustain. Sci. Pract. Policy 8.

Zhai, D., Dong, J., Cadisch, G., Wang, M., Kou, W., Xu, J., Xiao, X., Abbas, S., 2017. Comparison of pixel- and object-based approaches in phenology-based rubber plantation mapping in fragmented landscapes. Remote Sens. 10, 44.

Zhang, F., Du, B., Zhang, L., 2015. Saliency-guided unsupervised feature learning for scene classification. IEEE Trans. Geosci. Remote Sens. 53, 2175–2184.

Zhang, L., Zhang, L., Du, B., 2016. Deep learning for remote sensing data: A technical tutorial on the state of the art. IEEE Geosci. Remote. Sens. Mag. 4, 22–40.

Zhao, S., Zhou, D., Zhu, C., 2015. Rates and patterns of urban expansion in China's 32 major cities over the past three decades. Landsc. Ecol. 30, 1541–1559.

Zhao, W., Du, S., 2016. Spectral–spatial feature extraction for hyperspectral image classification: A dimension reduction and deep learning approach. IEEE Trans. Geosci. Remote Sens. 54, 4544–4554.

Zhao, Y., Huang, B., Song, H., 2018. A robust adaptive spatial and temporal image fusion model for complex land surface changes. Remote Sens. Environ. 208, 42–62.

Zhou, W., Pickett, S.T.A., Cadenasso, M.L., 2017. Shifting concepts of urban spatial heterogeneity and their implications for sustainability. Landsc. Ecol. 32, 15–30.

Zhou, W., Qian, Y., Li, X., 2014. Relationships between land cover and the surface urban heat island: seasonal variability and effects of spatial and thematic resolution of land cover data on predicting land surface temperatures. Landsc. Ecol. 29, 153–167.

Zhu, X., Helmer, E.H., Gao, F., Liu, D., Chen, J., Lefsky, M.A., 2016. A flexible spatiotemporal method for fusing satellite images with different resolutions. Remote Sens. Environ. 172, 165–177.

Zhu, X., Tuia, D., Mou, L., Xia, G., Zhang, L., Xu, F., Fraundorfer, F., 2017. Deep learning in remote sensing: A comprehensive review and list of resources. IEEE Geosci. Remote. Sens. Mag. 5, 8–36.

Zhu, Z., 2017. Change detection using Landsat time series: A review of frequencies, preprocessing, algorithms, and applications. ISPRS Journal of Photogrammetry and

Remote Sensing. 130, 370–384.

Zhu, Z., Wulder, M.A., Roy, D.P., Woodcock, C.E., Hansen, M.C., Radeloff, V.C., Healey, S.P., Schaaf, C., Hostert, P., Strobl, P., Pekel, J.-F., Lymburner, L., Pahlevan, N., Scambos, T.A., 2019. Benefits of the free and open Landsat data policy. Remote Sens. Environ. 224, 382–385.

Zhu, Z., Zhang, J., Yang, Z., Aljaddani, A.H., Cohen, W.B., Qiu, S., Zhou, C., 2019. Continuous monitoring of land disturbance based on Landsat time series. Remote Sens. Environ. 111116.

Ziolkowska, E., Ostapowicz, K., Radeloff, V.C., 2014. Effects of different matrix representations and connectivity measures on habitat network assessments. Landsc. Ecol. 29, 1551–1570.

Ziolkowska, E., Ostapowicz, K., Radeloff, V.C., 2016. Assessing differences in connectivity based on habitat versus movement models for brown bears in the Carpathians. Landsc. Ecol. 31, 1863–1882.